ZONGULDAK BÜLENT ECEVİT UNIVERSITY

GRADUATE SCHOOL OF NATURAL AND APPLIED SCIENCES

SEA LEVEL CHANGES IN THE BLACK SEA AND ITS IMPACTS ON THE

COASTAL AREAS

DEPARTMENT OF GEOMATICS ENGINEERING

DOCTOR OF PHILOSOPHY THESIS

NEVİN BETÜL AVŞAR

JUNE 2019

ZONGULDAK BÜLENT ECEVİT UNIVERSITY

GRADUATE SCHOOL OF NATURAL AND APPLIED SCIENCES

SEA LEVEL CHANGES IN THE BLACK SEA AND ITS IMPACTS ON THE

COASTAL AREAS

DEPARTMENT OF GEOMATICS ENGINEERING

DOCTOR OF PHILOSOPHY THESIS

Nevin Betül AVŞAR

ADVISOR : Prof. Şenol Hakan KUTOĞLU

CO-ADVISOR : Prof. Shuanggen JIN

ZONGULDAK

June 2019

APPROVAL OF THE THESIS:

The thesis entitled "Sea Level Changes in The Black Sea and Its Impacts on the Coastal Areas" and submitted by Nevin Betül AVŞAR has been examined and accepted by the jury as a Doctor of Philosophy thesis in Department of Geomatics Engineering, Graduate School of Natural and Applied Sciences, Zonguldak Bülent Ecevit University. 27/06/2019
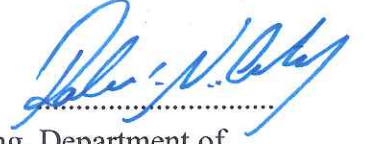
Advisor: Prof. Şenol Hakan KUTOĞLU
Zonguldak Bülent Ecevit University, Faculty of Engineering, Department of Geomatics Engineering
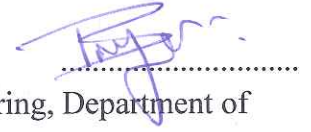
Member: Prof. Çetin MEKİK
Zonguldak Bülent Ecevit University, Faculty of Engineering, Department of Geomatics Engineering

Member: Prof. Rahmi Nurhan ÇELİK
İstanbul Technical University, Faculty of Civil Engineering, Department of Geomatics Engineering

Member: Assoc. Prof. Bihter EROL
İstanbul Technical University, Faculty of Civil Engineering, Department of Geomatics Engineering

Member: Assist. Prof. Eray KÖKSAL
Zonguldak Bülent Ecevit University, Faculty of Engineering, Department of Geomatics Engineering

---

Approved by the Graduate School of Natural and Applied Sciences. …/…/2019

Prof. Ahmet ÖZARSLAN
Director

ii

"With this thesis it is declared that all the information in this thesis is obtained and presented according to academic rules and ethical principles. Also as required by academic rules and ethical principles all works that are not result of this study are cited properly."

Nevin Betül AVŞAR

ABSTRACT

Doctor of Philosophy Thesis

SEA LEVEL CHANGES IN THE BLACK SEA AND ITS IMPACTS ON THE COASTAL AREAS

Nevin Betül AVŞAR

Zonguldak Bülent Ecevit University
Graduate School of Natural and Applied Sciences
Department of Geomatics Engineering

Thesis Advisor: Prof. Şenol Hakan KUTOĞLU
Co-Advisor: Prof. Shuanggen JIN
June 2019, 168 pages

Scientific researches assert that global sea level rise will accelerate during the 21st century in response to increasing ocean thermal expansion and glaciers/ice sheet melting. It means that the sea level rise should consider a serious threat especially for the unprotected coastal regions. Lying between Europe and Asia, the Black Sea is one of the most interesting and unique seas. It has three singular characteristics: (1) The Black Sea is the most isolated from the Atlantic Ocean that is connected to this remote ocean via the Marmara, Aegean, and Mediterranean seas through a chain of narrow straits: Bosporus, Dardanelles, and Gibraltar. Nevertheless, the Black Sea is relatively deep for such a sea. (2) The drainage area of the Black Sea containing major European rivers (Danube, Dnieper, Don, etc.) is roughly 5.5 times size of its surface area. (3) And the Black Sea is the world's largest anoxic basin, nearly 90% of its water volume is anoxic. The Black Sea coastal zone has also a densely populated. Therefore, monitoring of sea level change is significant especially in terms of the social-economic activities and ongoing coastal erosion in the region. In this context, this study aims to clarify present-day sea level changes in the Black Sea from different sea level observations.

ABSTRACT (continued)

Analysis of multi-mission satellite altimetry data revealed that the sea level in the Black Sea rose at a mean rate of 3.2 ± 0.6 mm/year from January 1993 to December 2014. The results show that maximum sea level occurs in May-June, whereas its minimum occurs during the September-November period. Moreover, the relative sea level at 13 tide-gauge stations along the Black Sea coast generally indicated rising trends. The coastal sea level changes were also investigated by satellite altimetry data; especially for Poti and Tuapse stations having long-term data, the results were consistent with tide-gauges. On the other hand, in order to detect the impact of vertical land motion on the coastal sea level change, the vertical movements at 3 Global Positioning System (GPS) stations (SINP, SLEE and TRBN), which were almost co-located with the Sinop, Sile and Trabzon tide-gauge stations, were analysed using GAMIT/GLOBK software. Consequently, at these 3 stations, the trends of absolute coastal sea level had a better agreement between satellite altimetry and tide-gauge + GPS.

For the period of September 1981 – November 2015, it was determined that the Sea Surface Temperature (SST) in the Black Sea rose 0.04 °C per year, and its annual amplitude reached its maximum in August. Until the prior to mid-1999 and after early-2008, good correlations were observed between SST and sea level changes. On the other hand, over the period of 2002–2017, the rate of seawater mass change in the Black Sea from the Gravity Recovery and Climate Experiment (GRACE) mascon solutions was 2.3 ± 1.0 mm/year. Besides, the sum of mass-induced and steric-induced (temperature + salinity) changes showed similar fluctuations with the total sea level changes obtained from altimetry.

Furthermore, in this study, vertical land motion along the Black Sea coast was estimated from combination of satellite altimetry and tide-gauge sea level time series. The obtained velocities were compared with the observations of 20 GPS stations in the region, and the results generally exhibited a good agreement.

Keywords: Black Sea, sea level change, satellite altimetry, tide-gauge, GPS, vertical land motion.

Science Code: 616.01.00

ÖZET

Doktora Tezi

KARADENİZ'DE DENİZ SEVİYESİ DEĞİŞİMLERİ VE KIYI ALANLARI ÜZERİNDEKİ ETKİLERİ

Nevin Betül AVŞAR

Zonguldak Bülent Ecevit Üniversitesi
Fen Bilimleri Enstitüsü
Geomatik Mühendisliği Anabilim Dalı

Tez Danışmanı: Prof. Dr. Şenol Hakan KUTOĞLU
İkinci Danışman: Prof. Dr. Shuanggen JIN
Haziran 2019, 168 sayfa

Bilimsel araştırmalar, küresel deniz seviyesi yükselmesinin 21. yüzyılda hızlanacağını ortaya koymaktadır. Bu durum, özellikle korunmasız kıyı bölgeleri için ciddi bir tehdit anlamına gelmektedir. Karadeniz, dünya denizleri arasında farklı özellikleri ile öne çıkan bir denizdir. Dar bir boğazlar zinciriyle (İstanbul, Çanakkale ve Cebelitarık Boğazları) Atlantik Okyanusu'na bağlanır ve böyle bir iç denize göre derinliği fazladır. Başlıca Avrupa nehirlerini (Tuna, Dinyeper, Don vb.) içeren drenaj alanı, yüzey alanının yaklaşık 5.5 katı büyüklüğündedir. Dünyanın en büyük anoksik havzasıdır; su hacminin yaklaşık %90'ında oksijen bulunmaz. Diğer yandan, kıyı bölgesi yoğun bir nüfusa sahiptir ki; deniz seviyesi değişimlerinin izlenmesi Karadeniz kıyıları için özellikle sosyo-ekonomik faaliyetler ve süregelen kıyı erozyonu açısından önemlidir. Bu doğrultuda, bu çalışmanın esas amacı, Karadeniz'de günümüz deniz seviyesi değişimlerinin araştırılmasıdır.

ÖZET (devam ediyor)

Çok misyonlu uydu altimetre verilerinin analizi, Ocak 1993 – Aralık 2014 döneminde Karadeniz'de deniz seviyesinin 3.2 ± 0.6 mm/yıl hızla yükseldiğini ortaya koymuştur. Sonuçlar maksimum deniz seviyesinin Mayıs-Haziran aylarında, minimum deniz seviyesinin ise Eylül-Kasım döneminde meydana geldiğini göstermiştir. Karadeniz kıyılarındaki 13 mareograf istasyonu verisinin analizi, Karadeniz kıyılarında bağıl deniz seviyesi için de genel olarak yükselme trendleri göstermiştir. Kıyısal deniz seviyesi değişimleri ayrıca uydu altimetre verileri ile araştırılmış; özellikle uzun-dönemli veriye sahip Poti ve Tuapse istasyonları için sonuçlar mareograf verileri ile tutarlı bulunmuştur. Diğer yandan, kıyılarda düşey kara hareketinin deniz seviyesi değişimlerine etkilerini izleyebilmek için Sinop, Sile and Trabzon mareograf istasyonları ile neredeyse eş konumlu olan 3 GPS istasyonundaki (SINP, SLEE and TRBN) düşey hareketler GAMIT/GLOBK yazılımı ile analiz edilmiştir. Bu 3 istasyonda mutlak kıyısal deniz seviyesi değişimleri için, uydu altimetresi ile mareograf ve GPS'den elde edilen sonuçların tutarlılığının arttığı gözlenmiştir.

Eylül 1981 – Kasım 2015 döneminde, Karadeniz'de deniz yüzeyi sıcaklığının yılda 0.04 °C yükseldiği ve yıllık genliğinin Ağustos ayında maksimuma ulaştığı belirlenmiştir. 1999'un ilk yarısına kadar ve 2008 yılından itibaren deniz yüzeyi sıcaklığı değişimleri ile deniz seviyesi değişimleri arasında iyi bir korelasyon bulunmuştur. Diğer yandan 2002–2017 döneminde, GRACE mascon verilerinden Karadeniz'de deniz suyu kütlesi değişimlerinin hızı 2.3 ± 1.0 mm/yıl olarak bulunmuştur. Ayrıca kütle kaynaklı değişimler ile sterik değişimlerin (sıcaklık + tuzluluk) toplamı, altimetreden elde edilen deniz seviyesi değişimleri ile benzer salınımlar göstermiştir.

Bu çalışmada ayrıca, Karadeniz kıyıları boyunca düşey kara hareketi uydu altimetresi ve mareograf deniz seviyesi zaman serilerinin kombinasyonu kullanılarak tahmin edilmiştir. Elde edilen hızlar, bölgedeki 20 GPS istasyonunun gözlemleri ile karşılaştırılmış ve sonuçlar genel olarak iyi bir uyum sergilemiştir.

Anahtar Kelimeler: Karadeniz, deniz seviyesi değişimi, uydu altimetresi, mareograf, GPS, düşey kara hareketi.

Bilim Kodu: 616.01.00.

ACKNOWLEDGEMENTS

"Çalışmak demek, boşuna yorulmak, terlemek değildir. Zamanın gereklerine göre bilim ve teknik ve her türlü uygar buluşlardan azami derecede istifade etmek zorunludur."

Mustafa Kemal ATATÜRK

ACKNOWLEDGEMENTS (continued)

TABLE OF CONTENTS

LIST OF FIGURES

LIST OF FIGURES (continued)

LIST OF FIGURES (continued)

LIST OF TABLES

LIST OF SYMBOLS AND ABBREVIATIONS

SYMBOLS

~	: Tilde
W_0	: Gravity potential of geoid
%	: Per cent
°C	: Centigrade degree
‰	: Per mille
σ_t	: Sigma-t
3D	: Three-dimensional
a	: Equatorial radius (semimajor axis) of a reference ellipsoid
f	: Flattening of a reference ellipsoid
ρ	: Density
S	: Salinity
T	: Temperature
P	: Pressure
2D	: Two-dimensional
3σ	: Three sigma
v	: Linear trend
A	: Amplitude
ω	: Angular frequency
φ	: Phase

ABBREVIATIONS

AATSR	**:** Advanced Along Track Scanning Radiometer
ADT	**:** Absolute Dynamic Topography
ALES	**:** Adaptive Leading Edge Subwaveform
AMR	**:** Advanced Microwave Radiometer

LIST OF SYMBOLS AND ABBREVIATIONS (continued)

AMSR-E : Advanced Microwave Scanning Radiometer for EOS

AOML : Atlantic Oceanographic and Meteorological Laboratory

AUV : Autonomous Underwater Vehicles

AVISO : Archiving, Validation and Interpretation of Satellite Oceanographic

AVHRR : Advanced Very High-Resolution Radiometer

COASTALT : ESA development of COASTal ALTimetry

CCI : Climate Change Initiative

CFOSAT : Chinese-French Oceanic SATellite

CMEMS : Copernicus Marine Environment Monitoring Service

CNES : Centre National d'Etudes Spatiales

CSR : University of Texas Center for Space Research

CTD : Conductivity, Temperature, Depth

CTOH : Center for Topographic studies on the Ocean and Hydrosphere

CSIRO : Commonwealth Scientific and Industrial Research Organisation

DLR : Deutsche Zentrum für Luft- und Raumfahrt

DMSP : Defense Meteorological Satellite Program

DORIS : Doppler Orbitography and Radiopositioning Integrated by Satellite

DT : Delayed Time

DUACS : Data Unification and Altimeter Combination System

ENSO : El Nino/Southern Oscillation

EnviSat : Environmental Satellite

EOF : Empirical Orthogonal Function

EPN : EUREF Permanent Network

ERS : European Remote Sensing

ESA : European Space Agency

EURO-ARGO RI: European Contribution to the Argo Program

EuroGOOS : European Global Ocean Observing System

EWT : Equivalent Water Thickness

FTP : File Transfer Protocol

GDM : General Directorate of Mapping

GEBCO : General Bathymetric Chart of the Oceans

GFO : Geosat Follow-On

LIST OF SYMBOLS AND ABBREVIATIONS (continued)

GFZ	**:**	GeoforschungsZentrum Potsdam
GIA	**:**	Glacial Isostatic Adjustment
GLOSS	**:**	Global Sea Level Observing System
GMSL	**:**	Global Mean Sea Level
GIA	**:**	Glacial Isostatic Adjustment
GLOSS	**:**	Global Sea Level Observing System
GMSL	**:**	Global Mean Sea Level
GNSS	**:**	Global Navigation Satellite System
GOOS	**:**	Global Ocean Observing System
GPS	**:**	Global Positioning System
GPS(t)	:	GPS time series
GRACE	**:**	Gravity Recovery and Climate Experiment
GRACE-FO	**:**	GRACE Follow-On
HY	**:**	HaiYang
IB	**:**	Inverse Barometer
ICESat	**:**	Ice, Cloud, and land Elevation Satellite
IERS	**:**	International Earth Rotation Service
IGS	**:**	International GNSS Service
InSAR	**:**	Interferometric Synthetic Aperture Radar
IOC	**:**	Intergovernmental Oceanographic Commission
IODE	**:**	International Oceanographic Data and Information Exchange
IPCC	**:**	Intergovernmental Panel on Climate Change
IPCC AR5	**:**	IPCC Fifth Assessment Report
ITU	**:**	Istanbul Technical University
JCOMMOPS	**:**	Joint IOC-World Meteorological Organization Technical Commission for Oceanography and Marine Meteorology in situ Observations Programme Support Centre
JMR	**:**	enhanced Jason-1 Microwave Radiometer
JPL	**:**	Jet Propulsion Laboratory
Mascon	**:**	mass concentration blocks
MDT	**:**	Mean Dynamic Topography
Metop	**:**	Meteorological Operational

MIRAS **:** Microwave Imaging Radiometer with Aperture Synthesis

MIT **:** Massachusetts Institute of Technology

MODIS **:** Moderate Resolution Imaging Spectroradiometer

MSL **:** Mean Sea Level

MSS **:** Mean Sea Surface

MWI **:** MicroWave Radiometer

MWR **:** EnviSat Micro-Wave Radiometer

NAO **:** North Atlantic Oscillation

NASA **:** National Aeronautics and Space Administration

NCEI **:** National Centers for Environmental Information

NGL **:** Nevada Geodetic Laboratory

NOAA **:** National Oceanic and Atmospheric Administration

NOC **:** National Oceanography Centre

NRT **:** Near Real Time

OGCM **:** Ocean General Circulation Model

OISST **:** Optimum Interpolation 1/4 degree daily Sea Surface Temperature

OpenADB **:** Open Altimeter Database

OST **:** Ocean Surface Topography

PEACHI **:** Prototype for Expertise on AltiKa for Coastal, Hydrology and Ice

PISTACH **:** Prototype Innovant de Systeme de Traitement pour les Applications Cotieres et l'Hydrologie

PRARE **:** Precise Range And Range-Rate Equipment

PSMSL **:** Permanent Service for Mean Sea Level

PSU **:** Practical Salinity Unit

RADS **:** Radar Altimeter Database System

RLR **:** Revised Local Reference

RMS **:** Root Mean Square

ROV **:** Remotely Operated Underwater Vehicles

SA(t) **:** Satellite Altimetry sea level time series

SAR **:** Synthetic Aperture Radar

SARAL **:** Satellite with ARgos and ALtika

SLA **:** Sea Level Anomaly

SLSTR   **:** Sea and Land Surface Temperature Radiometer

SMAP   **:** Soil Moisture Active/Passive

SMOS   **:** Soil Moisture and Ocean Salinity

SSH   **:** Sea Surface Height

SSM/I   **:** Special Sensor Microwave Imager

SSS   **:** Sea Surface Salinity

SST   **:** Sea Surface Temperature

SWOT   **:** Surface Water and Ocean Topography

T/P   **:** Topex/Poseidon

TG(t)   **:** Tide-Gauge sea level time series

TMR   **:** Topex/Poseidon Microwave Radiometer

TOGA   **:** Tropical Ocean Global Atmosphere

TUDES   **:** Turkish National Sea Level Monitoring System

TUDKA-99   **:** Turkish National Vertical Control Network-1999

TUSAGA-Active: Turkish National Permanent Real-Time Kinematic Network

UHSLC   **:** University of Hawaii Sea Level Center

UNEP-WCMC: United Nations Environment World Conservation Monitoring Centre

UNESCO   **:** United Nations Educational, Scientific and Cultural Organization

XBT   **:** eXpendable BathyThermograph

CHAPTER 1

INTRODUCTION

1.1 PURPOSE OF THESIS

Negative impact of increase in the amount of greenhouse gases on the climate change is an incontestable fact (IPCC 2013, URL-1). High global surface temperatures, which is a direct result of changes in the composition of atmosphere, lead to thermal expansion of oceans and rapid melting of glaciers and ice sheets resulting in sea level rise. Thus, sea level rise is an important parameter for monitoring the progression of climate change. Considering present and future of our world, scientific study of sea level rise is an essential for adapting to sea level extremes. Sea level changes can affect human activities in coastal areas and alter ecosystems (IPCC 2014).

In "Working Group I contribution to the Fifth Assessment Report of the Intergovernmental Panel on Climate Change (IPCC AR5)" (IPCC 2013), it is stated that Global Mean Sea Level (GMSL) has risen by 17–21 cm in the period 1901–2010 due to global warming. According to this report, by depending on different scenarios the range of projected sea level rise is 26 to 82 cm on 1986–2005 levels by the end of the 21st century (the period 2081–2100). It is also considered that the greatest contribution to future sea level rise will be the Antarctic ice sheet melting from global warming, and this effect will not be easily measurable.

Potential sea level rise poses a significant threat to areas with low topography. Today about 600 million people live nearby the sea (mostly concentrated in several of the largest world megacities) (Cazenave et al. 2018) and this number is expected to double by 2060 (Nicholls 2010). Flooding, inundation, storm, erosion, habitat loss, ecosystem damage, contamination of underground water are mostly damaging/catastrophic impacts of sea level rise on coastal zones. The importance of these impacts depends on the character of the coastal environment. Nevertheless, it is clear that some of them can threaten human life and coastal installations (Douglas et al. 2001, Karaca and Nicholls 2008, Nicholls 2010, Nicholls and Cazenave 2010).

In this context, a comprehensive assessment of present-day sea level change and its driving factors is important for adaption to its impacts, and associated socio-economic issues. Accurate estimation of future sea level changes, predetermination of regions which may be affected by sea level rise and taking precautions against possible impacts require regular monitoring of sea level change and its components. No doubt, the temporal evolution of sea level change reflects the changes occurring in the Earth's climate system. In fact, numerous sea level researches include both the implications of ocean movements on climate and vice-versa, i.e., the effects of climate change on the oceans.

From past to present, coastal regions have always attracted high interest in terms of social and economic (Creel 2003). Increasing human migration to these regions brings about thinking over the impacts of sea level rise. As well as preservation of coastal ecosystem, sustainable life in the coastal areas has been one of the major concern of the scientific studies. An effective management and sustainable use of coastal areas need multidisciplinary studies about the reasons and impacts of sea level rise.

According to the scenarios in the final report of the ClimateCost project of European Community (Brown et al. 2011), many people (~ 438,000) may need to move away from coastal zones because of flooding by the 2050s. It is also stated in the same report (basing on Tol et al. 2008) that in the Europe, although some coastal areas are already well protected against rising sea levels (e.g., the low-lying regions of the North Sea coast), the Black Sea coastal zones (such as those of Bulgaria, Romania, Turkey and Ukraine) have far less protection.

Tide-gauge data have been using nearly two century for observing sea level (Douglas 2001, Dusto 2014). Since tide-gauge measures sea level according to a fixed point on land, vertical movement of the point affects sea level measurements. So, at tide-gauge stations it is necessary to perform repeated geodetic measurements to determine sea level changes independent of land movements. Furthermore, a network of tide-gauge stations, having a good global, regional or local distribution, which is always by reference to same datum are needed to monitor long-term sea level changes. The Permanent Service for Mean Sea Level (PSMSL) is a global data centre which is responsible for the collection, publication, analysis and interpretation of sea level data from the global networks like the Global Sea Level Observing System (GLOSS) Core Network. Sea level monitoring in Turkey is carried out by General Directorate of Mapping (GDM) within the Turkish National Sea Level Monitoring System (TUDES) stations that is in accordance with

the GLOSS standards. In many tide-gauge stations (e.g., the TUDES stations), meteorological parameters such as air temperature, air pressure, humidity and wind affecting sea level change are also measured. Moreover, a geodetic datum reference can use a tidal datum as a start point. In national vertical datum of many countries definition, local mean sea level is estimated from annual means of long-term sea level data from tide-gauges.

With development of satellite systems, satellite altimetry technique has been using in sea level measurements since 1970s (URL-2). Since 1993, modern satellite altimetry record has provided accurate measurements of sea surface height with near-global coverage (except for north and south of about 60°). This technique is based on determination of the distance between satellite and sea surface with high accuracy. By combining this distance information with precise satellite position data, sea surface height is achieved. Satellite altimetry provides very useful information for studying of global and regional sea level changes, determination of ocean surface and ocean floor topography, monitoring of ocean currents, geoid determination, tracking of ice thickness and glacier topography, etc., (Fu and Cazaneve 2001, Stammer and Cazenave 2018). A lot of satellite altimetry missions have been launched from past to present (URL-2). Data centres such as French Archiving, Validation and Interpretation of Satellite Oceanographic Data (AVISO), Copernicus Marine Environment Monitoring Service (CMEMS), and Radar Altimeter Database System (RADS) enable free access to altimeter data for scientific studies. Moreover, National Aeronautics and Space Administration (NASA), National Oceanic and Atmospheric Administration (NOAA), European Space Agency (ESA) Climate Change Initiative (CCI) Programme, University of Colorado, and Commonwealth Scientific and Industrial Research Organisation (CSIRO) are currently processing altimetry data and providing various sea level products such as GMSL.

Tide-gauge records show that the 20th century GMSL has been rising at a mean rate of 1.2 to 1.9 mm/y (Church and White 2011, Dangendorf et al. 2017, Hay et al. 2015, Jevrejeva et al. 2014). Recent studies (Ablain et al. 2017, Cazenave et al. 2018, Legeais et al. 2018, Nerem et al. 2018b) state that average rate (~ 3 mm/y) of global sea level rise from the altimetry observations available since the early 1990s has been almost twice as large as the 20th average. These studies also assert the GMSL has accelerated over the altimetry era.

Sea level changes are not geographically uniform. Satellite altimetry observations show that there is a strong regional variability in sea level rates (Cazenave et al. 2018). Regional sea level

changes can deviate substantially from those of the global mean, and even in some regions can reveal a condition opposite to global trend (Stammer et al. 2013). In this sense, this study is focused on sea level changes in the Black Sea, and its relation to global sea level changes. It is aimed to reveal a reliable model of sea level rise by using data of tide-gauge stations along the Black Sea coast and satellite altimetry. Sea level observations from both the techniques are used to infer information on trend of the Black Sea level and its periodicity. Moreover, in order to project the sea level to future, mechanisms driving sea level change in the Black Sea are investigated. The dynamic factors (sea surface temperature, salinity, mass variations, tectonic movements, etc.) which affect the sea level changes are analysed to model the sea level changes correctly depending on time and location. This study also assesses the potential impacts of sea level rise in the Black Sea coast in the light of past studies.

This study aims to observe impacts of climate change in terms of sea level change in the Black Sea by considering its basin dynamics. It is important for sustainability of socio-economic activity of six countries (Bulgaria, Georgia, Romania, Russia, Turkey and Ukraine) surrounding the Black Sea. It is also crucial for protecting of the coastal ecosystem. Since coastal regions are both valuable and vulnerable areas; monitoring of regional sea level change in the Black Sea, which has a trend, in common with global sea level is significant for correct management of coastal environment and living conditions around the Black Sea coast.

Eventually, main purposes of this thesis are stated as follows:

- Investigation of present-day sea level change in the Black Sea from satellite altimetry data,
- Estimation of the mean rate of sea level rise over the Black Sea,
- Determination of relative sea level changes from tide-gauge data along the Black Sea coast,
- Comparison of coastal sea level changes from satellite altimetry and tide-gauges, and detection of vertical land motions along the Black Sea coast,
- Analysis of general impacts of sea level rise over the Black Sea.

Briefly, the main purpose of this study is to clarify the current rate of present-day sea level rise in the Black Sea from available in-situ and satellite data, and to reveal its possible impacts on the coasts.

1.2 LITERATURE REVIEW

From past to present, numerous studies have been carried out to determine seasonal and interannual variability of the Black Sea level. According to Terziev (1991), the Black Sea level increased by 20 cm in the last 100 years (Ginzburg et al. 2011). Ginzburg et al. (2011) also referred to Goryachkin and Ivanov (2006) that the sea level rose with velocity of 1.83 ± 0.7 mm/y from the mid-1920s to about 1985.

Tide-gauge is one of the oldest instruments for measuring sea level changes. The distributed data belonging to tide-gauge along the Black Sea coast date back nearly at the last quarter of 19th century. In this context, in many studies, relative sea level change in the Black Sea has been determined tide-gauge measurements. Boguslavsky et al. (1998) evaluated 47 tide-gauge observations collected before the year 1985, along the Black Sea coast except for the Anatolian coast. By also considering the effect of continental discharge, atmospheric pressure, and density distribution upon the local sea level vacillations, they asserted that the Black Sea mean level rate was 1.6 mm/y during the observation period. Moreover, using tide-gauge records Tsimplis and Baker (2000) showed that the mean sea level in the Black Sea rose at a rate of 2.2 mm/y until 1960, and continued to rise at a similar rate until the 1990s.

Alpar et al. (2000) reported that the mean sea level reaches the highest levels in May-June and the lowest values in October-November in the Black Sea, based on data from tide-gauge stations. They used the annual time series of 7 tide-gauge stations from Bondar (1989). By adding the data of Samsun tide-gauge station, they indicated that the rate of sea level rise varies from coast the coast; the highest change was recorded at Poti station (8.2 mm/y) and the lowest change was recorded at Kerci station (1.3 mm/y) between 1860 and 1990. While at Varna, Constanta, Sulina, Odessa and Sevastopol stations, the sea level rise is of 3.3, 2.7, 3.7, 7.1 and 3.0 mm/y, respectively; the mean subsidence rates are about 5.2, 1.1 and 6.5 mm/y at Odessa, Sevastopol and Poti, respectively. As for Samsun station, the sea level fell at a rate of -6.9 mm/y from 1963 to 1977.

Sea level height data measured by satellite altimetry are available since early 1990s, and several studies have successfully used these data to investigate the Black Sea level change. Ginzburg et al. (2011) investigated in detail altimetry-based sea level change and wind speed along the Black Sea coastal zone, considering physical processes such as river runoff, Rim Current, etc.

They detected from along-track altimetry data that the Black Sea level rose at a rate of 13.4 ± 0.11 mm/y over 1993–2008; in the western and eastern regions this rate become as 14.2 ± 0.16 and 12.8 ± 0.12 mm/y, respectively. They pointed out that the sea level changes were closely related to annual fresh water flux (especially Danube River runoff) in this period, also the interannual variability of sea level in the southwestern Black Sea generally corresponded with the Sea of Marmara. They also compared in-situ and satellite results; the correlation coefficients between tide-gauge and altimeter measurements ranged from 0.4 to 0.7, minimum values was being obtained for tide-gauges at the western and eastern coasts, whereas maximum ones at the northern and southern coasts.

The altimeter-derived Black Sea levels and corresponding in-situ measurements have been also compared in other studies. Stanev et al. (2000) found good correlations between the data from Topex/Poseidon along-track passes and tide-gauge for 1992–1996 period: 0.76, 0.68, 0.65, and 0.51 at Tuapse, Bourgas, Varna, and Nesebar stations, respectively. From the comparison of data over 1992–1998, Goryachkin and Ivanov (2006) achieved the following correlation coefficients 0.93 for Sevastopol, 0.92 for Yalta, and 0.77 for Tuapse (Ginzburg et al. 2011).

Cazenave et al. (2002) used satellite altimetry and tide-gauge data to monitor sea level changes in the Mediterranean and Black Sea. In the study, the rate of increase in the Black Sea was determined as 27.3 ± 2.5 mm/y for a period of 6 years (1993–1998). It has been stated that this change might result from of the steric effect (mostly due to the heating of surface waters) as well as changes in regional hydrology.

Yildiz et al. (2008) compared the Black Sea level changes from satellite altimetry, tide-gauge and the Gravity Recovery and Climate Experiment (GRACE) satellite mission measurements for the common periods during the 1993–2007 period, in the Turkey's Black Sea coast. All the results showed that the annual amplitude of the change was the highest in May.

In Vigo et al. (2005), the Mediterranean was divided into 6 sub-regions including the Black Sea. By evaluating the data of satellite altimetry, sea water temperature and tide-gauge for 1993–2003 period; a sudden falling in sea level rise rate was observed in mid-1999. For the first period up to 1999, there was a high correlation between the rates of sea water temperature and sea level rise, and for the period after 1999, this correlation disappeared in the rest of the Mediterranean and decreased in the Black Sea.

Pashova and Yovev (2010) made a general evaluation about the studies on the determination of sea level changes in the Black Sea. And in order to determine absolute sea level change in the Black Sea using tide-gauge data, they pointed out that the positions of the tide-gauge along the Black Sea coast was need to monitor. They emphasized that all the Black Sea countries must evaluate satellite and terrestrial measurements collaboratively to determine the sea surface topography, compare zero points of different height systems and detect potential values (W_0) at these points.

In the Black Sea, sea level variations are determined by the ratio between atmospheric precipitation, evaporation and continental discharge, as well as by the water exchange through the straits. So the changes in these driving factors are crucial for sea level changes in the Black Sea. Yildiz et al. (2011) used the GRACE solutions to determine the mass-induced sea level changes in the Black Sea for the period 2003–2007. After removing of steric effects, the obtained results were compared with the Jason-1 altimetric observations. It has been shown that providing that the elimination of the leakage effect from GRACE results, there was a good agreement between sea level changes obtained by two different ways.

Kubryakov and Stanichnyi (2013) also pointed out that due to the cyclonic Rim Current intensification the Black Sea level was rising at 8–9 mm/y in the coastal areas that exceeded in the offshore by 1.5–2 times (4.5–6 mm/y) for the period of 1992–2005.

Feizabadi (2016) evaluated tide-gauge and satellite altimetry data at determining of the coastal Black Sea level changes using various spectral analysis methods. Thus, the advantages and drawbacks of each methods was compared analysing the monthly mean sea level observations from tide-gauge data, and grid and along-track altimetry data.

Several studies mention that low-lying deltaic plains along the Black Sea coast are highly vulnerable to the future sea level rise. Simav (2012b) evaluated overall risk status of the Turkey's coastal regions because of sea level rise with Coastal Vulnerability Index analysis, and Kızılırmak Delta has been determined as one of the most risky regions. In this context, by the year 2100 the flooding levels that might be caused by sea level rise and extreme sea level were calculated based on satellite altimeter observations, and the size of areas that could be affected was determined by mapping with a Digital Elevation Model. According to this, it was

calculated that approximately 9% of Kızılırmak Delta could be affected by flooding. Besides, it was detected a shoreline recession of 6 cm in annual average for the Kızılırmak Delta.

1.3 THESIS' OUTLINE

Indeed, this study deals with recent sea level changes in the Black Sea on a time period over which data from tide-gauges and satellite altimetry are available. During this period, in addition, the components of sea level change have been investigated, and major driving factors have been analysed. The insight of mechanisms driving the sea level change gained analysing the past changes is utilized to project sea level to the future.

In order to predict future regional sea level change accurately, it is important to reveal sea level forcing mechanisms using real observations. So, this study presents an analysis of present-day sea level changes in the Black Sea using satellite altimetry and gravity data. That is, it aims to investigate long-term total sea level change in the Black Sea by also considering the contribution of the water mass changes and steric changes.

Both tide-gauge and altimetry observations show that sea level trends in the Black Sea varies over time. However, from the beginning of available tide-gauge observations in the Black Sea that is 1870s to the first decade of the 21st century, on the average, an increase in the sea level, was generally observed, with alternating period of rise and fall.

The thesis is organized into five chapters. Chapter 2 provides a comprehensive information on the Black Sea. Chapter 3 contains an overview on sea level changes, with focusing global and regional sea level changes, and their causes, sea level measurement techniques, etc. In Chapter 4, the Black Sea level changes are analysed in details. Finally, the conclusions are drawn in Chapter 5.

CHAPTER 2

THE BLACK SEA

The Black Sea, which has different characteristics among the world seas, is a semi-enclosed sea located in southeast of the Europe. It is accepted as an isolated sea from world oceans, since it has only a restricted saltwater exchange with the Mediterranean Sea through the Turkish Straits System (the Bosporus Strait – the Sea of Marmara – the Dardanelles Strait). Besides, unlike the Mediterranean Sea (concentration basin), the Black Sea is an estuarine basin that is due to major European rivers discharge (Jaoshvili 2002, UNECE 2011). Also, another feature supported by these conditions is that the Black Sea has a specific density stratification separated by a permanent halocline (Oguz et al 2006, Özsoy and Ünlüata 1997). Because of these features, the Black Sea is a remarkable area to scientists.

The Black Sea, which is a crossroads between Europe, Asia and Africa, constitutes a convenient route to the west via the straits (Lyratzopouoou and Zarotiadis 2014). Due its geographical location, the Black Sea has been of immense strategic importance over the centuries. Moreover, the Black Sea coast has favourable natural conditions in terms of ecosystem, warm climate, fertile soils, etc. So, from antique times to present it has been a preferable life region (Grinevetsky et al. 2015).

The Black Sea, where about 17 million people inhabit its coastal regions (Vespremeanu and Golumbeanu 2018, URL-5), is surrounded by Bulgaria, Georgia, Romania, Russia, Turkey and Ukraine countries. Thus, the Black Sea is economically important to these countries, namely, it is a favourite passageway for cargo and passenger vessels. There are large ports in the shore of the Black Sea. The Black Sea coasts also host considerable tourism centres (Vespremeanu and Golumbeanu 2018). Furthermore, the Black Sea holds vast volumes of oil and gas reserves (Robinson 1997).

All these characteristics cause that the Black Sea with its coastal zone is very sensitive to climate changes and anthropogenic forcing.Morphometric characteristics and bottom topography of a sea basin determine its oceanographic characteristics including water circulation, thermohaline structure, etc. Also, depth and width of straits are essential for water exchange process in a basin. Besides, volume of water in the basin is significant for its heat content hence level changes. For regional oceanography, characteristics of wind regime are very important, as wind directly affects circulation and mixing of water, heat and water balance. The atmospheric loading effect, which is based on air pressure changes on the sea surface, causes a change between 10 and 50 cm on sea level (Seeber 1993). Indeed, all of these play an important role in sea level changes. Further information can be found in Ivanov and Belokopytov (2013). In this context, this chapter is focused on geographic, topographic, bathymetric, climatic, and oceanographic features of the Black Sea basin as well as its a brief geological history. It also presents a general overview to economic and social life in the Black Sea coastal regions in order to understand that why sea level changes can be crucial for these regions.

2.1 GEOGRAPHIC AND TOPOGRAPHIC CHARACTERISTICS OF THE BLACK SEA

The Black Sea is a basin situated between Europe, Anatolia and Caucasus, bounded by the 40.56°N - 46.33°N latitude and 27.27°E - 41.42°E longitude (Figure 2.1). The Black Sea's surface area of about 420,000 km^2 corresponds approximately one-sixth of that of the Mediterranean Sea (~ 2.5 million km^2). It has a total water volume of about 540,000 km^3, with an average water depth of about 1.2 km. Furthermore, the Black Sea with the maximum depth of about 2.2 km is one of the deepest inland seas. In this section, the size of the physical characteristics concerning the Black Sea have been provided from Allenbach et al. (2015), Bondar (2007), BSC (2008), Grinevetsky et al. (2015), Ivanov and Belokopytov (2013), Oguz et al. (2006), Todorova et al. (2018), Vespremeanu and Golumbeanu (2018), URL-3, URL-4, URL-5 and URL-6. The mentioned numerical values selected from the most recent references are also summarized in Table 2.1.

The Black Sea is one of the farthest seas among the seas of the Atlantic Ocean basin, whose only connection to this ocean is the narrow (0.76 to 3.60 km) and shallow (13 to 110 m) Bosporus Strait (Gunnerson and Özturgut 1974, URL-3) located in its southwest. In the northeast, the Black Sea is also connected with the shallow Sea of Azov (the maximum depth

of 14 m) through the Kerch Strait which has an average depth of less than 20 m (Bakan and Büyükgüngör 2000, Oguz et al. 2006, URL-3). Figure 2.1 also presents circum geographical features of the Black Sea.
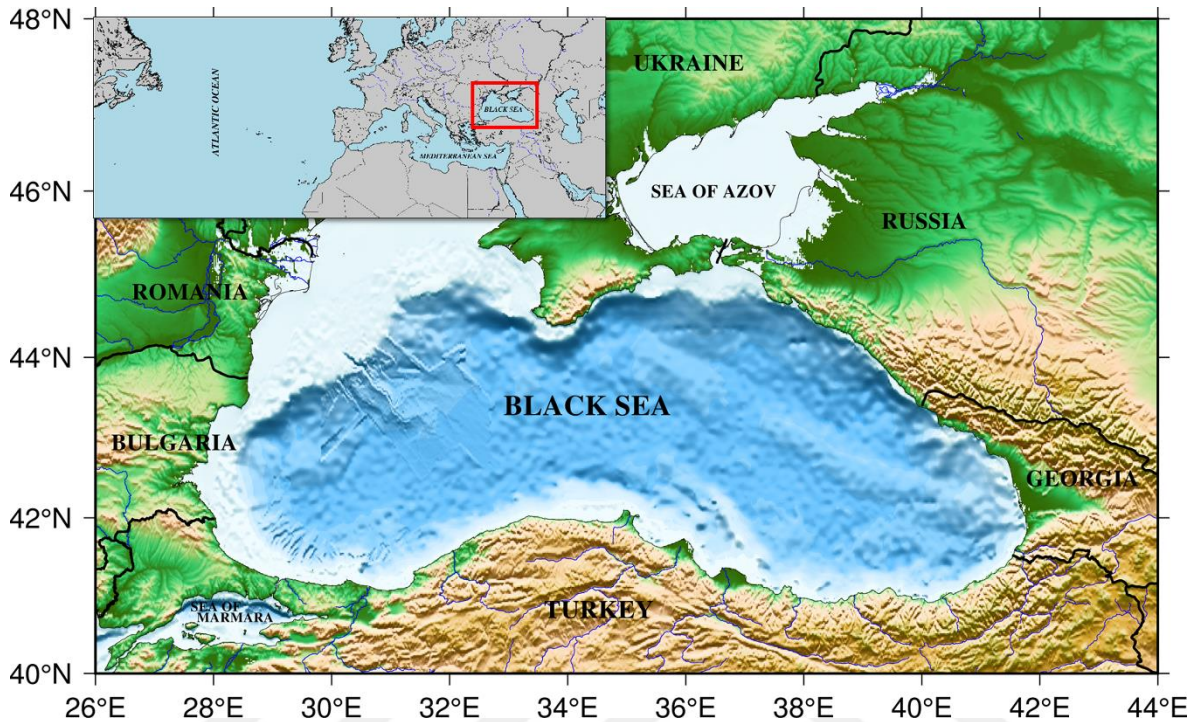
Figure 2.1 Black Sea with its location and topography. Topographic data have been provided from ETOPO1 1 Arc-Minute Global Relief Model bedrock data (Amante and Eakins 2009).

The Black Sea extends to 1,175 km in the east-west direction between the Pontic Mountains (with a maximum elevation of 3,937 m) in the south, the Crimean Mountains (1,545 m) in the north and the Caucasus Mountains (5,642 m) in the northeast (Its maximum width along the north-south is 615 km). These mountains are parallel to the coastline. Their slopes descend directly into the sea in the form of steep escarpments. The topography of the western (including the northwestern) coasts significantly differs from the other coasts. It generally shows a plain character. There is the Danube Delta lowland in the north-west and on the opposite eastern side there is the Kolkhida lowland of smaller extent (Ignatov 2008).

The total length of the Black Sea shoreline is about 4,400 km, which is mainly belongs to the coasts of Turkey on the south and Ukraine on the north. The shoreline is generally regular except for the Crimean Peninsula and the northern point of the Anatolian Peninsula. The convexity of these two landforms forms the narrowest part of the Black Sea with a width about

260 km. It splits into the entire basin as eastern and western sub-basins. The largest bays are Odessa, Karkinit and Kalamit on the northwestern coast, Samsun and Sinop on the southern coast, and Burgas on the western coast. There are no large islands in the Black Sea (the largest being Zmeyiny is only 1.5 km^2). Morphometric characteristics of the Black Sea coastline on the basis of the surrounding countries are given in Jaoshvili (2002).

Table 2.1 Physical characteristics of the Black Sea.

Water surface area	~ 420,000 km^2
Area of northwest shelf	~ 70,000 km^2
Water volume	~ 540,000 km^3
Drainage area	~ 2,400,000 km^2
Maksimum depth	~ 2,200 m
Average depth	~ 1,200 m
Total shoreline	~ 4,400 km
Sea Surface Temperature (Seasonal)	~ 2–25 °C
Salinity (Surface/Depth)	~ 18/22 PSU (‰)

The bottom topography of the Black Sea are basically defined as shelf (up to isobaths of 200 m), continental slope (from isobaths 200 to 2,000 m) and abyssal plain (over isobaths of 2,000 m) (BSC 2008, Grinevetsky et al. 2015, Özsoy and Ünlüata 1997). In this sense, the Black Sea is known as a deep basin with steep slopes and flat bottom (Vespremeanu and Golumbeanu 2018). The shelf accounts for roughly 25% of the seabed total area. There is a large shelf in the northwesterm part of the Black Sea, that it is over 200 km wide and has a depth ranging from 0 to 169 m. The continental slope splitting by underwater valleys and canyons occupies to nearly 40% of the seabed area. The Crimean, Caucasian and Anatolian coastal zones are bordered by very narrow shelves (with a depth of less than 100 m and a width of 2.2 to 15 km) and often intersected by the submarine canyons. The bottom of the basin having gradually increasing depths towards to the centre corresponds to nearly 35% of the seabed area.

According to the United Nations Environment World Conservation Monitoring Centre (UNEP-WCMC) data (URL-7), the maximum depth of the Black Sea is 2,212 m. However, the recent global relief models such as the General Bathymetric Chart of the Oceans (GEBCO)_08 grid (URL-8), and ETOPO1, based on echo-sounding and satellite observations, indicate the maximum depth of over 2,500 m (see Figure 2.1 and Figure 2.2). A detailed description of the

bottom relief of the Black Sea in terms of bottom slopes and profiles is also provided in Ivanov and Belokopytov (2013).
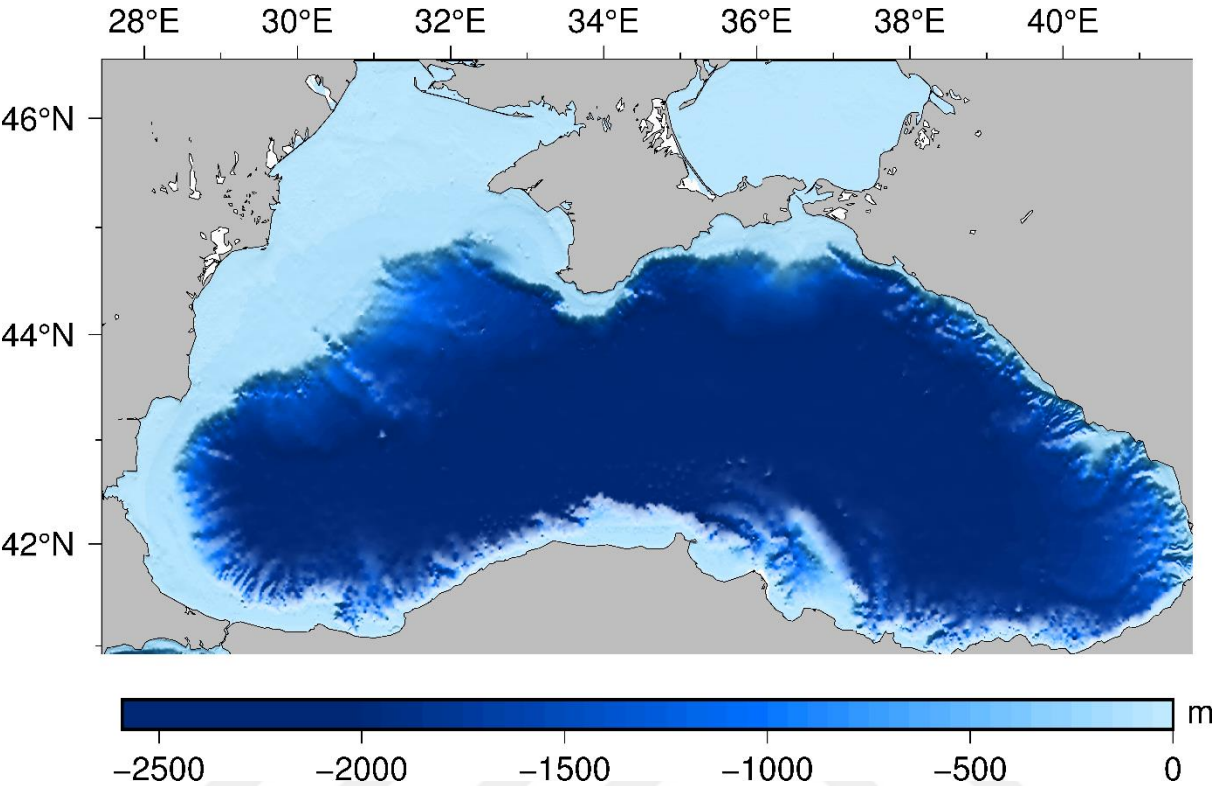
a) The Black Sea bathymetric map.
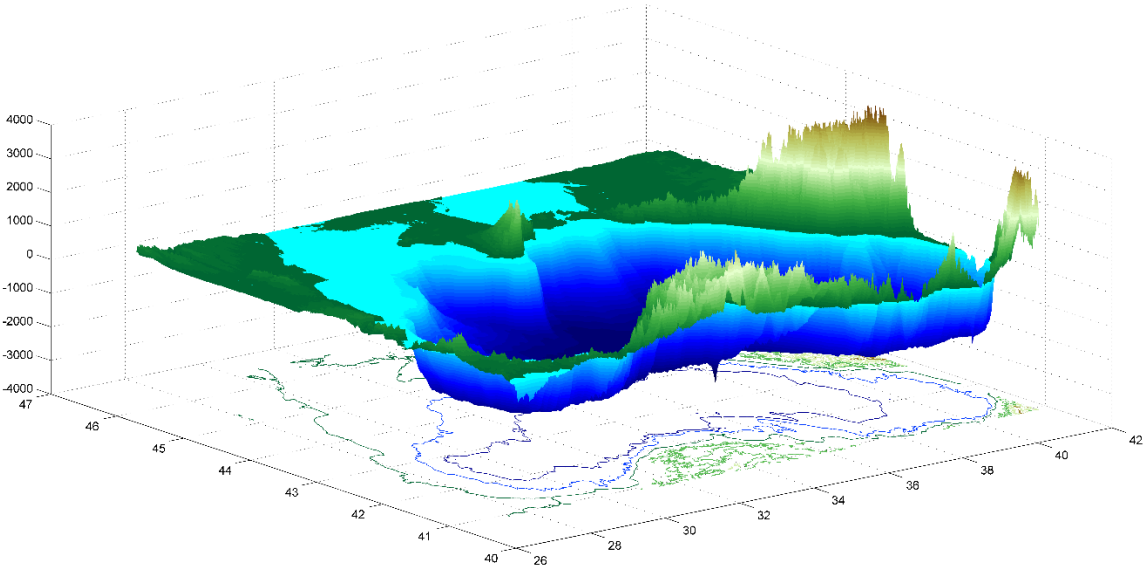
b) 3D topography of the Black Sea (contours are labelled in m).

Figure 2.2 Bathymetry of the Black Sea basin using the GEBCO_08 grid data.

The Black Sea bathymetry is generally characterized as a wide shelf (northwestern part) and a steep continental slope. The distribution of the depths is not symmetric (Figure 2.3) due to tectonic origin of the basin (Vespremeanu and Golumbeanu 2018).
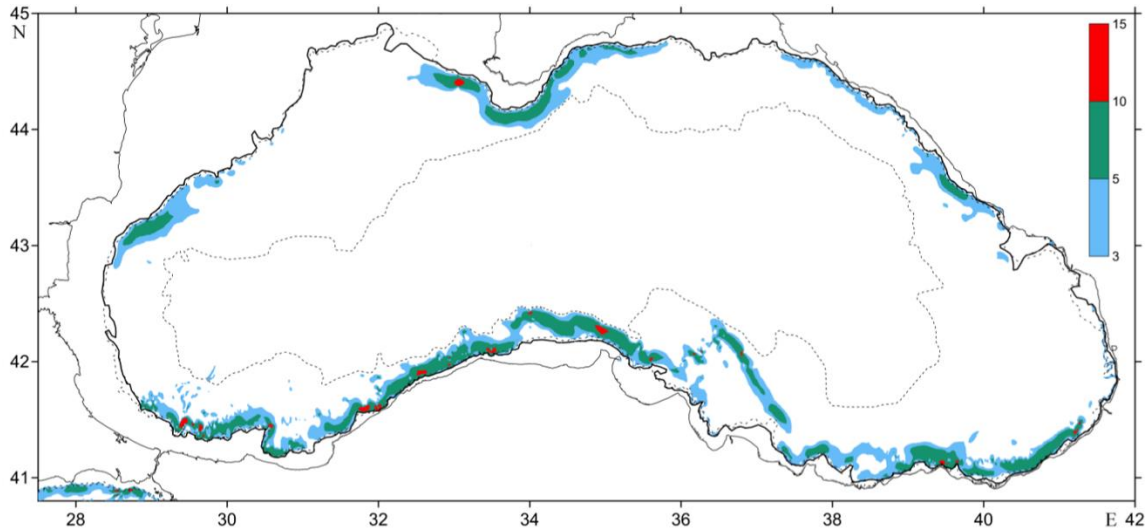
Figure 2.3 Distribution of the shelf break in the Black Sea according to the GEBCO_08 (bold black line). Solid colour means values of the bottom slope with range: 3–5°, 5–10° and 10–15°, dotted lines show isobaths of 200 m and 2,000 m (from Ivanov and Belokopytov 2013).

2.2 HISTORY OF GEOLOGICAL EVOLUTION OF THE BLACK SEA

It is generally accepted that the Black Sea have extended during the Cretaceous as a black-arc basin like all Mediterranean-type of orogens. The area has formed as a marine basin with large accumulation of sediments in the deep part of the sea. It is composed of two sub-basins with different geological history seperated by the mid-Black Sea ridge: an older western and a younger eastern basin (BSC 2008, Okay et al. 1994, Munteanu et al. 2011, Nikishin et al. 2003, Zonenshain and Le Pichon 1986). It is bordered by young mountains in the south, the east and the northeast, and by ancient platforms and tectonic basins, heavily sedimented, in the north and the west. Totaly, the Black Sea basin has developed both on the continental crust and on the oceanic crust (abyssal plain), as mentioned previously. A general overview regarding its geophysic as well as geology of the basin is presented in Vespremeanu and Golumbeanu (2018).

The Black Sea has been subject to large-scale sea level changes, and consequently strong modifications of land morphology and environmental settings all along geologic history (BSC

2008). According to a well-known hypothesis, until the end of the Last Glacial Period the Black Sea was a giant freshwater lake (Dimitrov et al. 2005, Lericolais et al. 2007, Ross and Degens 1974, Ryan 2007). With the expiration of the ice age roughly 11,000 years ago, seas rose approximately 100 m. And eventually, when the Mediterranean water level was above the Bosporus, saltwater of the Mediterranean entered the Black Sea from the Bosporus rapidly (Dimitrov et al. 2005, Ryan et al. 1997, Ryan et al. 2003). On the other hand, some studies assert that the submergence of the Black Sea was due to the slow steady rise of the sea level in the course of thousands of years rather than a catastrophic flooding (Aksu et al. 2002, Deuser 1974, Esin and Esin 2014, Preisinger and Aslanian 2003, Shmuratko 2007, URL-3). In either case, density of the water entering the Black Sea was higher due to high salt content, it did not interfere with the freshwater flowing from the top and formed the lower water layer of the Black Sea. Thus, this influx of Mediterranean water developed a density stratification in the basin. As a result, subhalocline waters of the Black Sea have been anoxic, and the life-free submarine area has formed at a depth greater than 150–200 m (URL-4, URL-6).

2.3 CLIMATIC CHARACTERISTICS OF THE BLACK SEA

The Black Sea is a part of large-scale climatic system that includes the Mediterranean and the North Atlantic. Besides, the coastal topography has a significant impact on climatic peculiarities of parts of the Black Sea. The northwestern part of the sea open to effect of the air masses from the north is characterized by steppe climate (cold winter, hot and dry summer), whereas in the southeastern part surrounded by high mountains the climate is that of moist subtropics (plenty of rainfall, hot summer and mild winter) (Grinevetsky et al. 2015, Özsoy and Ünlüata 1997, Vespremeanu and Golumbeanu 2018).

The weather over the Black Sea is generally characterized by movement of cyclones and anticyclones. In winter, either the Siberian anticyclone causing influx of cold continental air (abrupt air temperature drop and rainfall, and even bora wind) or the Mediterranean cyclone bringing about unstable weather with warm southwesterly winds and temperature fluctuations is present over the sea. As for in summer, the Azores anticyclone becomes dominant, and thus hot and dry weather is apparent with uniform thermal conditions for the entire sea area (Grinevetsky et al. 2015).

Considering averages of an entire year in the Black Sea, the high pressure field is appeared in the northern part of the sea, while the low pressure field is observed in the south. Accordingly, air temperature rises from the north to the south. The annual average temperature is round 9.9 °C in the north, whereas it is round 14.5 °C in the south. In winter the minimum air temperature in the norhern part is up to -30 °C, in the south is up to -10 °C. The region's air temperature increasing with spring reaches the highest values in July-August. The maximum values rise to 35–37 °C (Alkan vd. 2004, Grinevetsky et al. 2015, Ivanov and Belokopytov 2013).

In the Black Sea, a prevailing wind direction cannot be mentioned. However, especially in the winter, the effectiveness of the northerly winds (like bora) is seen. Wind speeds increase especially in autumn and winter periods. Weak winds (wind speed < 3 m/s) are observed in the southern and southeastern coasts, stronger winds (wind speed > 4 m/s) are more prevalent in the western and northwestern coasts. At the same time, these conditions are, likewise, acceptable for the sea's west and southeast parts. The minimum wind speed is observed in the northeastern part of the sea to the south of the Kerch Strait (Alkan vd. 2004, Ivanov and Belokopytov 2013).

Here, wind vorticity is an essential factor for the wind-driven circulation, thereby for the sea level changes. It is anticyclonic along the west coast, on the other hand it is cyclonic in the western part of the Anatolian coast. Also, in the eastern part reaching the Georgia coast it is anticyclonic, along the Caucasian coast it is cyclonic. As for the Crimean coast, during winter in the southern Crimean coast is anticyclonic vorticity, along the west coast is cyclonic; during summer cyclonic vorticity is typical for the whole Crimean coast (Ivanov and Belokopytov 2013).

The wind-induced fluctuations of the sea level are commonly seen in the Black Sea, especially for in the western and northwestern parts of the sea during autumn and winter periods. They may exceed 1 m in these parts while on the Crimean and Caucasian coasts the fluctuations are reach 30–40 cm. In addition, during autumn and winter periods sizeable waves may occur in the northwestern, northeastern and central parts of the sea. Wave height is mostly 0.5–1 m, yet in open sea it can be as high as 10 m owing to strong storms. As for the southern part of the sea, strong wave is scarce, and waves higher than 3 m are hardly ever seen in this part (Grinevetsky et al. 2015).

In the Black Sea, 70% of the annual rainfall occurs between November and March. The amount of precipitation increases from west to east. While the amount of maximum annual precipitation exceeds 2500 mm in the southeast coasts (Batumi) of the Black Sea, the minimum annual precipitation is seen in the northwest (in vicinity of mouth of the Danube River) and falls less than 400 mm (Grinevetsky et al. 2015).

Over the Black Sea, evaporation is mainly wind driven, and largest over the western part where the winds are stronger. Although the Black Sea is a basin with plenty of rainfall, as it is located in a semi-arid climate zone, the amount of evaporation is mostly higher than the amount of precipitation (Alkan vd. 2004). However, the Georgian coast and the eastern Turkey are characterized with low evaporation, as in this region in additon to the maximum precipitation, light and moderate winds are more widespread. In this connection, precipitation minus evaporation is positive in the south/southeast and negative in the north, within the basin-wide being negative (Allenbach et al. 2015).

Ice in the Black Sea is only seen as a narrow strip in the northwestern part of the sea (e.g., Gulf of Odessa). Ice period starting from mid-December generally spans more than one months, however it is longer (more than four months) in severe winters (Grinevetsky et al. 2015).

Ivanov and Belokopytov (2013) also mentioned that the radiative budget (the difference between incoming solar energy and radiated net long-wave energy) of the Black Sea is 100 Watt/m^2 on average. It reaches the maximum in June-July, while its minimum is November. From March to August, the sea receives heat; from September to February it gives off heat to the atmosphere.

2.4 OCEANOGRAPHIC AND HYDROLOGIC CHARACTERISTICS OF THE BLACK SEA

Since the Black Sea is an inland basin, its overall water budget and hydrochemical structure are totally formed by components of the hydrological balance. For example, the characteristics of near-surface waters are mostly based on the freshwater inflow. In addition to this, the restricted exchange through the shallow Bosporus Strait plays an important role on the forming: the structures of halocline and deeper layers are closely related to the inflow of Mediterranean waters through the strait (Özsoy and Ünlüata 1997).

Currently the Black Sea water level is relatively high that it is on average 30–40 cm higher than the Sea of Marmara (URL-5, URL-9), and slope of water surface along the Bosporus Strait from north to south is about 35 cm (Murray et al. 2007) (Note that according to Ginzburg et al. (2011), during 1992–2007 the value of sea level anomalies in the Sea of Marmara exceeded those in the Black Sea, so the mentioned sea level difference between two sea was less in this period). The Black Sea collects river water from large Eurasian fluvial systems as well as receiving high precipitation. Because of the location (latitude) of the Black Sea, the amount of evaporation in the basin is less than that of in the Mediterranean Sea basin, and so the Black Sea's water has a lower density. Moreover, the level balancing between the seas becomes more slowly due to the narrow and shallow straits connecting the Black Sea to the other seas. Under these circumstances, an exchange between the Black Sea and the Sea of Marmara is formed by a two-layer flow across the Bosporus Strait: 1. the upper layer leaving the Black Sea is cooler and lower-salinity surface water, and 2. the lower layer entering the Black Sea is warmer and higher-salinity deep water. The upper flow having an average thickness of 15 m moves faster than the lower flow (~ 2.5 to ~ 0.5 m/s) (Murray et al. 2007, URL-9). The volume of inflow is about 300 km^3/y, roughly half of the outflow (Ünlüata et al. 1990, Volkov and Landerer 2015). Besides, the output value reaches the maximum in summer, its minimum is observed in autumn. The input is at the highest value in autumn and in spring, in the early of summer it comes up to minimum. All of these prove that the Bosporus Strait is an active part of the hydrological process in the Black Sea.

Although the Kerch Strait is shallower, its width and length are greater than those of the Bosporus Strait. Like Bosporus, two flows through the Kerch Strait are formed based on the water density difference: the upper flow from the Sea of Azov to the Black Sea, and the opposite lower flow. The shallowness of the Kerch Strait causes that the total water exchange with the Sea of Azov is considerably smaller than with the Sea of Marmara (Ivanov and Belokopytov 2013).

Inflow of freshwater, such as river runoff, back into a seawater basin completes hydrologic cycle. As for the Black Sea, the drainage area is approximately 5.5 times greater than it surface area (Table 2.1) that almost 1/3 of the total land-water area of the Europe discharges into the Black Sea. There are nearly 1000 rivers that flow into the Black Sea, having different water volumes and basin sizes (Bondar 2007, Jaoshvili 2002, UNECE 2011). The scarcely 500 of them are more than 10 km long. The others are small rivers or seasonal short-lived

watercourses. The major rivers emptying into the Black Sea (including the Sea of Azov) are the Danube, Dnieper, Don, Rioni, Kuban, Dniester, Southern Bug, Coruh, Kizilirmak, Yesilirmak and Sakarya rivers (Figure 2.4). The Danube River alone brings along nearly more than half of the total inflow. Some runoff estimates are presented in (Table 2.2). Ivanov and Belokopytov (2013) also concluded that the total river runoff into the Black Sea is at the average is 350 km^3/y from the estimations given as 365 km^3/y in Jaoshvili (2002), and 355 km^3/y in Mikhailov and Mikhailova (2008).

In fact, taking into account to receive the northwestern shelf discharges (> 70%) from three of Europe's largest rivers (Danube, Dnieper and Dniester), the Black Sea can be accepted as an asymmetric basin. Besides that, about 13% of the total runoff enter southeastern part of the sea from the coast of Georgia, and again about 10% are provided from the south (coast of Turkey) (Grinevetsky et al. 2015, Ivanov and Belokopytov 2013). As expected, the maximum river discharges are seen during the spring period (form March to June) while the minimums are occurred in autumn (from September to November). Grinevetsky et al. (2015) stated that seasonal sea level variations in the Black Sea are mainly produced by the differences of river runoff input during the year. Also, it should be noted that the climatic and the hydrodynamic conditions of the Black Sea drainage basin are very different from the Mediterranean Sea.

Figure 2.4 The Black Sea basin (modified from URL-10).

Table 2.2 Major river discharges to the Black Sea (Sizes of all the catchment area and lengths have been provided from URL-3).

River	Area of catchment (km^2)	Length (km)	Volume of average annual runoff (km^3)			
			Murray et al. (2007)	Bondar (2007)	BSC (2008)	Grinevetsky et al. (2015)
Danube	801,463	2,850	250	196.2	190.7	200
Dnieper	504,000	2,200	51	44.2	52.6	50
Don	425,600	1,870	28	21.9	29.5	
Dniester	68,627	1,362	8	6.6	9.8	10
Kuban	57,900	870	12	9.3	13.4	
Rioni	13,390	327		8.4		
Southern Bug	63,700	806		2.8	2.6	5
Other rivers	455,510			73.7	73.7	
Total	2,390,190		349	363.1	372.3	265

2.4.1 Vertical Stratification

The Black Sea has evolved from the freshwater lake formation thousands of years ago to its present characteristics with the rise of the water level in the near geological phases. When Mediterranean-based waters filled the basin, warmer and more saline waters at the bottom, and colder and less saline waters on the surface was formed. These different water bodies are separated from each other by the density interfaces at depths of 100–150 m. This is why the Black Sea has a strongly stratified vertical structure. In the present day, the low salinity at the surface results from the freshwater inflows, whilst the higher salinity in deep waters is an imprint of the Mediterranean influence (Özsoy and Ünlüata 1997), and the only source of salt water is through the Bosporus Strait (Murray et al. 2007). Consequently, the thermohaline structure is attributed to weak vertical mixing in the entire seawater layer.

The upper 200 m of the Black Sea contains several layers with different characteristics: mixed layer, seasonal thermocline layer, Cold Intermediate Layer and permanent halocline layer (Alkan vd. 2004). Vertical temperature changes in the seasonal thermocline can reach up to 2–3 °C/m. The depth of this layer is changeable between 10–50 m. It has generally a homogeneous vertical temperature distribution.

In the Black Sea, interaction between the oxygen rich surface waters from the large river discharges, and the deep zone consisting of anoxic water is limited by a density stratification (Miladinova et al. 2017). Since the vertical distribution of water density is mainly affected by salinity, this layer is known as permanent halocline. The surface water has salinity values between 17.5 and 18.5 PSU (these values are nearly 2 times less than the salinity of the world ocean surface waters), whereas salinity at the bottom waters is around 22 PSU (Ivanov and Belokopytov 2013). High increases in salinity values are limited between the depths of 150 and 200 m in a relatively thin layer. The depth of the halocline is largely dependent on vertical movements, and decreases to 50 m in the centre of the sea.

Indeed, in the Black Sea, except for the thin surface layer where the temperature effect predominates, the salinity effect generally starts at a depth interval of 100–200 m. According to this, the permanent halocline coincides with the pycnocline. Besides, the chemocline and the oxycline, depending on similar condition, occur in the same depth intervals as the halocline (Alkan vd. 2004, Miladinova et al. 2017, Özsoy and Ünlüata 1997). Moreover, in 0–30 m, a seasonal halocline can develop from April to September, as well. During this period, the decreasing in the intensity of the general circulation, weak wind mixing, and also the redistribution of riverine water support its creation (Ivanov and Belokopytov 2013).

The Cold Intermediate Layer is defined by temperatures less than 8 °C between the seasonal thermocline and the permanent halocline (Alkan vd. 2004, Murray et al. 2001, Özsoy and Ünlüata 1997). It typically corresponds to the depths of 50–100 m, and is deeper and thicker near the margin of the sea than in the centre.

Bottom waters are maintained below around 300 m in the Black Sea. In this layer, the distributions of temperature and salinity are extremely homogeneous. The values of both parameters increase in proportion to the water depth, and the seasonal variations in their amounts do not affect the content of the bottom waters (Alkan vd. 2004). Besides, for the deep seawater, the central part of the sea is characterized by higher values of temperature as compared to peripheral area. From a depth of 1,700–1,750 m, a bottom mixed layer begins with constant temperature and salinity values, which is corresponds a bottom convection layer caused by geothermal heat flux. Consequently, the variations in the underlying deep layer are based on the lower flow through the Bosporus Strait, and geothermal heat flux from the bottom (Ivanov and Belokopytov 2013, Özsoy and Ünlüata 1997, Tuzhilkin 2008a).

For the Black Sea, the seasonal variations are significant in the sea surface having low salinity, and the pycnocline where the density gradient is greatest within the body of water.

The sea surface responds dynamically to seasonal heating and cooling. Heat and fresh water movements across the sea surface cause seasonal and interannual variations in the upper 50 m layer. The sea surface temperature increases from northwest to southeast in all the seasons, associated with the general atmospheric conditions mentioned before. In winter, with the intense cooling of the surface layer in the centre of cyclonic gyres, low water temperatures occur in the central part as well as the northwestern part of the sea. The spatial contrasts of surface water temperature are more apparent in winter; in spring and summer they are considerably smoothed (Ivanov and Belokopytov 2013). Salinity field at the sea surface is largely determined by river runoff (the northwestern shelf, the southeastern part of the sea, the central and western parts of the Anatolian coast) and precipitation (especially the southeastern part of the sea). According to this, the salinity in the basin-wide decreases in the late spring and early summer, and become minimum in July (June on the surface). The maximum salt content is observed in the end of winter (in March).

In pycnocline between depths of 50 and 200 m, the wind vorticity flux is the reason of the variations. The spatial distribution of temperature in this layer is completely formed by vertical circulation. The general pattern of vertical circulation in the Black Sea reveals in form of the ascending of water in the central part and the descent along the periphery of the sea. It indicates significant spatial differences on the vertical stratification. So, throughout the year, the temperature and the salinity is characterized by high values in the central part of the sea, and lower value on the continental slope (Ivanov and Belokopytov 2013, Özsoy and Ünlüata 1997, Tuzhilkin 2008a).

For the Black Sea, at the depths of 0–50 m, the minimum temperature in winter corresponds to the maximum values of salinity, and conversely, the minimum salinity in summer corresponds to the maximum temperature. However, in the pycnocline layer, the seasonal variations of temperature and salinity are more consistent with each other: the minimum values are observed mainly in spring (Ivanov and Belokopytov 2013).

In order to comprehend the characteristics of the Black Sea water, here it is referred to the calculations from 105,000 stations for the period of 1950–2000 provided by Ivanov and

Belokopytov (2013). According to the results, the average seawater temperature over the entire Black Sea is 8.96 °C. It is above the average temperature in the world oceans, however below that of the neighbour Mediterranean Sea. The average temperature in the upper water of 0–300 m is 8.81 °C, in the deep layer of 400–2,000 m it increases to 8.99 °C. The range of seasonal fluctuations on the sea surface can reach up to 20 °C in the northwest. However, the fluctuations reduce rapidly with depth. As for the salinity values, the average salinity is 21.96 PSU, in the layer 0–300 m 20.26 (PSU), in the layer of 400–2,000 m it increases to 22.26 PSU (For the Mediterranean Sea, the average salinity value is 34–37 PSU). As expected, the lowest salinity values of the surface water are observed near the mouths of rivers whilst the highest salinity values occurs at the location which spilling of the Sea of Marmara water. Besides those, the calculated average annual value of surface water density is $\sigma_t = 12.6$, and the maximum water density in the deep layers is $\sigma_t = 17.2$.

For a general representation, the distributions of temperature and salinity throughout the water column in the Black Sea obtained from the Conductivity, Temperature, and Depth (CTD) data are also charted in Figure 2.5. The detailed information about the data can be found in Murray et al. (1991) and Murray et al. (2007). The temperature is seasonally variable at the surface and decreases with depth. It becomes minimum at about 50 m in the Cold Intermediate Layer (Figure 2.5a). Below this layer, the temperature gradually increases all the way to the bottom. According Figure 2.5b, the salinity also increases continuously towards to the deeper. As for density, it is controlled primarily by the salinity, and increases similarly. Therefore, the density of the Black Sea water is much less than that of the world oceans (nevertheless the seawater through the Bosporus Strait has a density of $\sigma_t = 26–28$ which is close to the densest waters of the world oceans). As mentioned before, the salinity (hence density) increase rapidly until depth of ~ 200 m, whereas all three parameters increase slowly with depth in the deep water. Moreover, the characteristics of salinity, temperature and density are extremely uniform in the deep water (especially from about 1,700 m to bottom).

Here, in order to summarize the relationship between distributions of temperature and salinity in the Black Sea, a scatter diagram is used provided from Murray et al. (2001). In Figure 2.6, the data on the left represent high temperature and low salinity in the sea surface. The temperature decreases towards to the Cold Intermediate Layer, and then both parameters increase ceaselessly into the bottom.
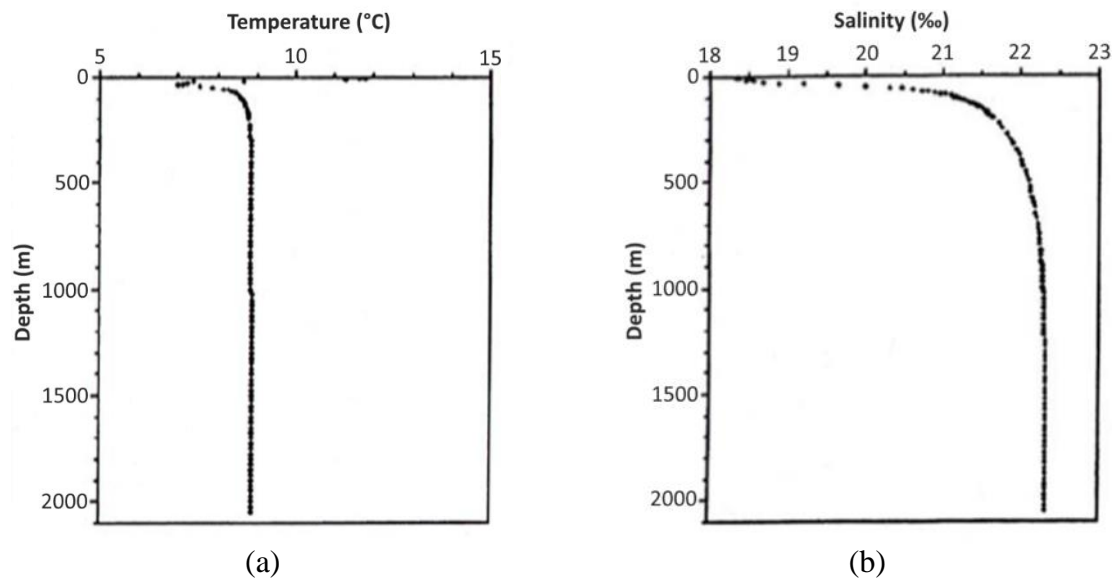
Figure 2.5 Vertical a) Temperature and b) Salinity profiles from CTD data in the Black Sea (modified from Murray et al. 2001).
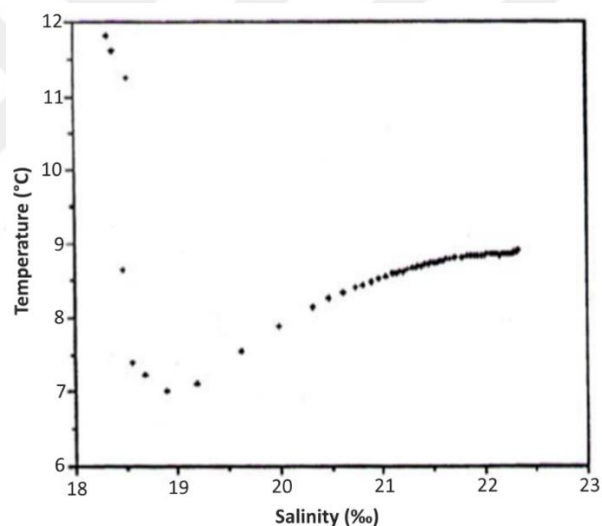
Figure 2.6 Temperature-Salinity diagram of the Black Sea water column (modified from Murray et al. 2001).

Because of the strong density stratification on the water column in the Black Sea, oxygen depletion has evolved. Oxygen is at atmospheric saturation in the upper 40 m, then decreases sharply to near zero by 60 m. Thus, the Black Sea is a classic marine anoxic basin which has an oxygenated surface layer overlying a deep water containing sulphide (Murray et al. 2007, Oguz et al. 2006, URL-6). Owing to the strong vertical stratification, the deep water is not renew with the oxygen fast enough. Murray et al. (2007) stated that there is also a suboxic zone at approximately 50–100 m depth between the oxic surface and anoxic deep layers. It is a

biogeochemical transition zone where the concentrations of both oxygen and hydrogen-sulphide are extremely low. Some fluctuations induced by climate variations can be seen in this subzone, and so its thickness can be changeable from year to year. Vespremeanu and Golumbeanu (2018) referred that about 10% of the Black Sea water volumes correspond the oxygen saturated waters, while its nearly 87% match hydrogen sulphide saturated waters.

2.4.2 General Circulation

Ocean currents have a significant effect on climate and ecosystem in and around the sea basin. Winds, water density, tides and, Coriolis Effect all drive ocean currents (McWilliams 2006). Coastal and bottom topographic features influence their location, direction, and speed (URL-11). The general character of the Black Sea circulation is predominantly cyclonic due to the prevailing cyclones above the sea, that is, water circulation in the upper layer of the sea is directed counterclockwise (Oguz et al. 1992, 1993, 1995, 1996). The cyclones create a positive wind stress curl with maximum in winter, minimum in summer over the sea. The circulation is also controlled by thermohaline fluxes, coastal topography and bathymetry in the Black Sea. For example, the Crimean Peninsula has an influence on the Black Sea circulation like that of the northern prominence of the Anatolian Peninsula. And density contrast between the intense fresh water inflow from the rivers and salt water input thorough the Bosporus Strait supports to form the cyclonic circulation in the sea. The cyclonic circulation induces the rise of the sea level toward the coast. The amplitude of sea level variation depends on season and ranges from 25 to 40 cm (Korotaev et al. 2003).

There is a distinct current system encircling the entire Black Sea and forming a large scale cyclonic gyre. This flow, which is seen in a band 40–80 km wide, is known as Rim Current (Ivanov and Belokopytov 2013, Korotaev et al. 2003, Oguz et al. 1993, Tuzhilkin 2008b). Its velocity in the upper layer can reach 40 cm/s, sometimes up to 80–100 cm/s, however it decreases towards to deeper. And it is the strongest in the winter-spring periods. Severe meanders of the Rim Current may be come across along the Anatolian coast. There are also two smaller cyclonic gyres in the western and the eastern parts of the basin (see Figure 2.7). In addition to these, anticyclonic mesoscale eddies occur in the coastal side of the Rim Current (Oguz et al. 1993, Toderascu and Rusu 2013). As for the deep circulation in the Black Sea, it is very close related to the bowl-shaped bottom topography of the basin, and its velocity is estimated around 3–4 cm/s (Tuzhilkin 2008b, URL-12).
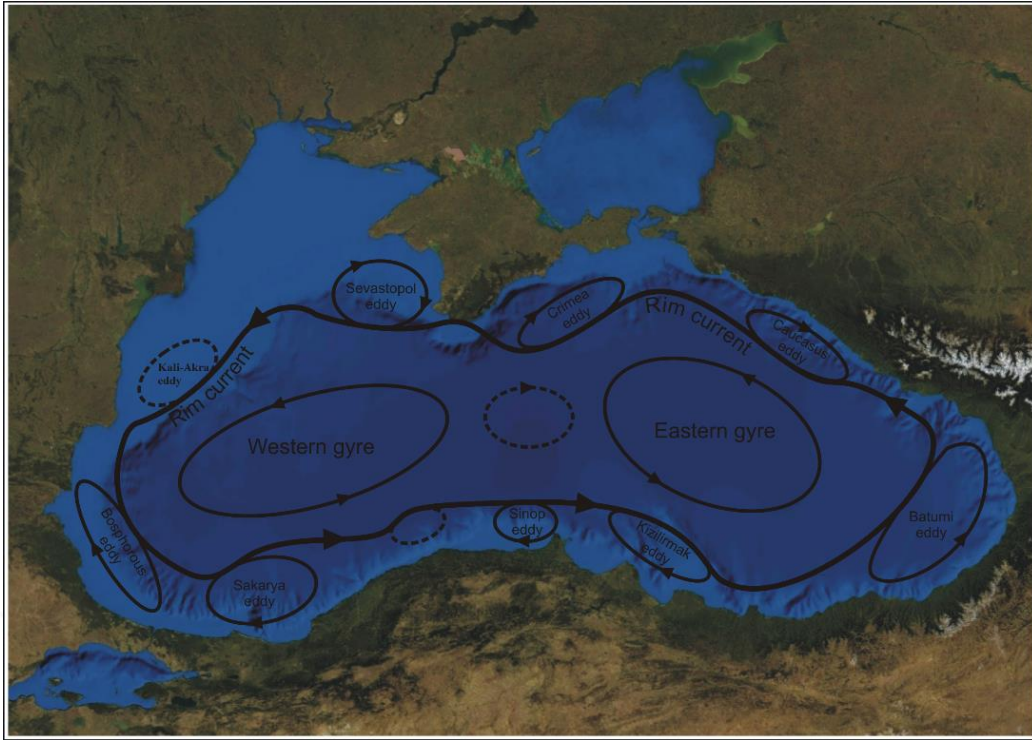
Figure 2.7 Schematic of surface circulations in the Black Sea. Solid and dashed lines represent quasi-permanent and recurrent features of the general circulation, respectively (modified from Oguz et al. 1993).

2.4.3 Water Balance

For the semi-enclosed seas having limited water exchange with oceans, like the Black Sea, water balance plays a crucial role in the formation of hydrological structure of the sea. Sea water balance equation, provided that the total volume of the basin is not changing, can be written as (Ivanov and Belokopytov 2013):

$$V_{in} - V_{out} = (R + P) - E \qquad (2.1)$$

where V_{in} is water inflow through the straits, V_{out} is water outflow through the straits, R is river runoff, P is precipitation and E is evaporation. The right side of Equation (2.1) stands for freshwater balance. If this value is greater than zero, means positive freshwater balance; or less than zero, means negative freshwater balance. Positive freshwater leads to dilution of the surface waters (i.e., dilution basin). The Black Sea is such a basin in contrast to the neighbouring Mediterranean Sea where water balance is negative (i.e., concentration basin).

Nevertheless, annual freshwater budget in the Black Sea is negative (R + P < E) between July and October, and it reaches its minimum in August; it is also positive (R + P > E) between November and June, with maximum in April or May. Due to intensive evaporation in the summer-autumn period, the negative water balance is prevailing throughout the sea. In the spring, the evaporation gets minimum with the decreasing wind speed. This condition with together higher river runoff during this period causes the maximum freshwater balance.

According to Ünlüata et al. (1990), which is one of the well accepted water budget estimates for the Black Sea, the income of water from river runoff $R = 352$ km^3/y is approximately equal to water loss through evaporation $E = 353$ km^3/y. In addition to these, the precipitation input is $P = 300$ km^3/y. Through the Bosporus Strait, while the water inflow provides for 312 km^3/y, the water outflow is estimated as 612 km^3/y. In this case, the total value of water input and output averages around 965 km^3/y. From past to present, a detailed list of other water budget estimates for the Black Sea can achieved in Ivanov and Belokopytov (2013), and Shmuratko (2007).

On the other hand, as reported in URL-6, Sorokin (2002) mentioned input and output components for the Black Sea annual water balance as follows: the freshwater inputs by rivers and precipitation are 369 km^3 and 224 km^3, respectively, and the output via evaporation is 395 km^3. The seawater inflow and outflow by Bosporus are 176 km^3 and 340 km^3, respectively. The water balance ends up to be not closed, with the residual of 34 km^3 per year. According to this, the total water budget and hence the total water volume within the basin determining the water level can change depending on the variability of the components of the annual water budget (Bondar 2007).

In the Black Sea, the largest contribution to inflow for the freshwater balance is from the river runoff (Table 2.2), especially in spring and summer. In autumn and winter, the amount of atmospheric precipitation can be seen slightly above the amount of runoff. Along the Anatolian and the Caucasus coasts which have more rainfall, the precipitation plays the leading role in water balance considering this part of the sea receives less than 25% of river runoff (Ivanov and Belokopytov 2013).

2.5 ECONOMIC AND SOCIAL SITUATION IN THE BLACK SEA REGION

The Black Sea has been hosted different civilizations throughout the ages. Thus, social, economic and political constituents have been continuously changed and developed in the Black Sea region. It always plays a critical role in the world economic system due to the diversity of its natural resources, and its geopolitical location (Grinevetsky et al. 2015).

Today, the six countries (Bulgaria, Georgia, Romania, Russia, Turkey and Ukraine) bordering the Black Sea have a total permanent population of around 17 million on their coasts. So, the Black Sea is of significant contribution to regional and global commerce of these countries via sea transport, fishery industry, wood products, tourism, and oil/gas pipelines, etc. There are important ports along the Black Sea coast, such as Constanta, Istanbul and Novorossiysk (Lyratzopouoou and Zarotiadis 2014).

The coastal zone of the Black Sea is subject to high degree urbanization. However, the population living around the Black Sea coast is unevenly distributed. Important cities along the coast are Burgas and Varna (Bulgaria), Batumi and Poti (Georgia), Constanta (Romania), Novorossiysk, Sochi and Tuapse (Russia), Istanbul, Ordu, Samsun, Trabzon and Zonguldak (Turkey), Odessa and Sevastopol (Ukraine) (URL-3). Istanbul, Odessa and Varna have also high tourism potential among the cities in the region (Vespremeanu and Golumbeanu 2018).

The Black Sea has also a strategic importance in terms of energy exports, as it is a transit route for oil and gas resources from Russia and the Caspian Sea. Moreover, there are considerable stocks of hydrogen sulphide and oil/gas available in the depth of Black Sea which support to the economic significance of the region (Robinson 1997).

On the other hand, the Black Sea – the Danube River Canal contributes significantly to the growth of the region economy (Lyratzopouoou and Zarotiadis 2014).

One of the main economic activity of the Black Sea region is agricultural production. Especially, it has an important role in global grain production (URL-13). The fertile deltaic plains along the Black Sea have been formed by the alluvial deposits of the largest rivers (Mikhailov and Mikhailova 2008). Some of the most extensive coastal deltas in the region are the Danube (Vespremeanu and Golumbeanu 2018), the Yeşilırmak and the Kızılırmak. The

Kolkheti lowland on the eastern coast is also a united extensive delta, created by several rivers. These wetlands have important biodiversity of flora and fauna as well as a vast agricultural potential.

All these values peculiar to the Black Sea require that the long-term impacts of the climate changes and the anthropogenic processes will have to carefully be assessed considering the potential consequences on the sea level changes and the coastal ecosystem.

CHAPTER 3

SEA LEVEL CHANGES

Sea level changes occur at various time scales. During geologic eras, sea level has changed drastically many times, primarily following the tectonic processes and the glacial cycles (Miller et al. 2011). In the time of the Last Glacial Maximum sea level was about 130 m lower than today, because of the large amount of water held by glaciers and ice sheets (Church et al. 2010, Clark and Mix 2002). After the major deglaciation (~ 21,000 years ago), the sea level has remained almost stable over the last 2–3 millennia (Cazenave and Remy 2011, Meyssignac and Cazenave 2012, Lambeck and Chappell 2001, Lambeck et al. 2010). However, with the beginning of the industrial age (late 18th to early 19th century), sea level rise has accelerated (Church et al. 2013, Church and White 2006, Church and White 2011, Douglas 2001, Nerem et al. 2006), triggered by abrupt changes in temperature, ice cover, precipitation, etc., rather than a part of a natural cycle. Figure 3.1 shows rates of the sea level rise on the mentioned time scales.

Indeed, natural processes like solar radiation variations, and atmosphere-ocean interactions like El Nino/Southern Oscillation (ENSO) are important drivers for sea level fluctuations from decadal to multi centennial. However, anthropogenic induced global warming has become a serious factor for sea level changes since last two centuries. Because of global warming; as the ocean warms, the waters expand, and as glaciers/ice sheets melt or shrink, fresh water mass add to the oceans, and thus sea level rises (Meyssignac and Cazenave 2012).

Sea level change is of great interest for two essential reasons (Cazenave and Nerem 2004, Nerem et al. 2006). First, changes in the rate of sea level rise are closely related to the climate changes as mentioned above. Second, sea level changes have significant socioeconomic consequences for populations living near the low-lying areas. Therefore, it is important to determine the current rate of sea level change, to determine if this rate is accelerating, and to identify the causes of the changes.

Furthermore, oceans, atmosphere and land play leading roles in global hydrologic cycle. Although the total amount of water in the Earth system is constant, the amount in any component (atmosphere, oceans, soil moisture, glaciers, ice sheets, etc.) can vary significantly over time (Chambers et al. 2004). Thus, sea level including its spatial and temporal variability (and changes) is accepted as a key parameter of the Earth system.
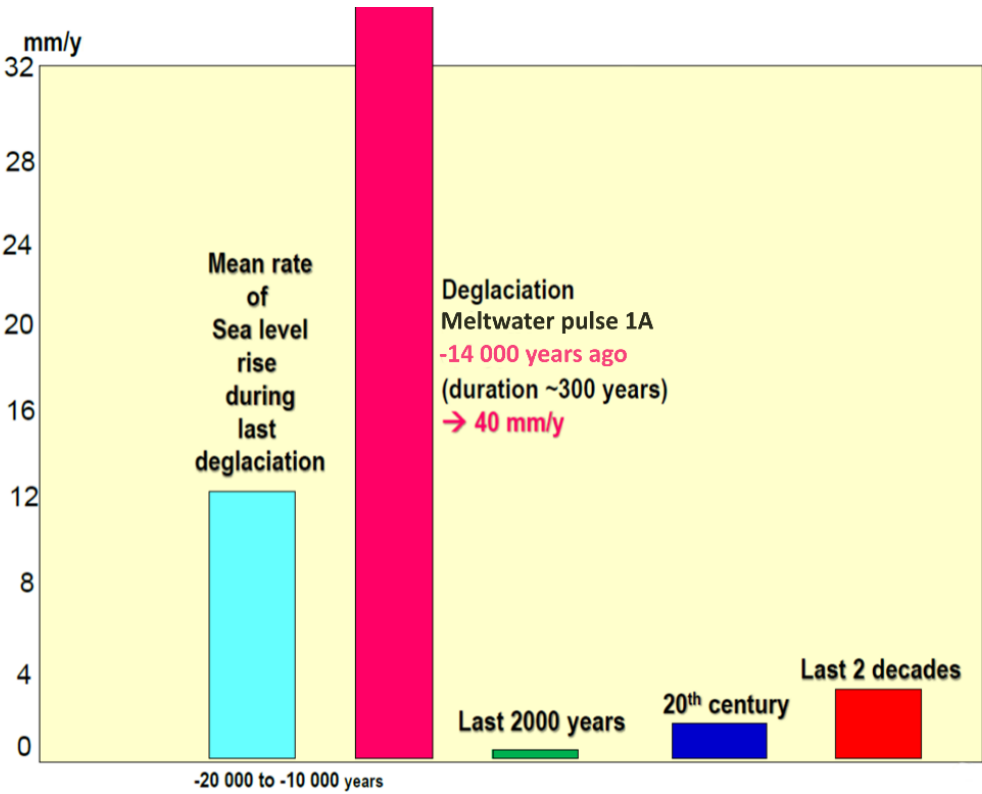
Figure 3.1 Rates of sea level rise on different time scales (from Cazenave 2014).

Since the nearly mid-18th century, the knowledge of sea level obtains from tide-gauge measurements mounted along coasts and islands (Dusto 2014). Since 1993, satellite altimetry supplies sea level observations over the entire oceanic domain (Nerem and Mitchum 2001a).

This chapter provides a general overview of sea level change. The primary factors that cause global and regional sea level changes, and sea level budget, as well as sea level observations are addressed in here. The possible consequences of sea level change are also discussed.

3.1 WHAT IS SEA LEVEL?

Sea level corresponds to the height of sea surface. When this level is referred to the Earth's centre of mass, it is defined as "absolute sea level" or "geocentric sea level" whereas when it is referred to a fixed point (e.g., benchmark), that is used as a reference, on the solid Earth, it represents "relative sea level". Thus, if considering coastal impacts of sea level change, relative sea level is the more relevant quantity, and it has been measured using tide-gauges for the past few centuries. On the other hand, since 1993, satellite altimetry has measured geocentric sea surface height with near global coverage.

The sea surface is not uniform across the Earth and not changing at the same rate globally (URL-14). If the Earth was a perfect, homogeneous and non-moving sphere, the sea level would be the same everywhere. However, since the Earth is a roughly heterogeneous oblate spheroid, and subject to gravitational influences from the Sun and the Moon, the sea level continually changes. Moreover, the variations in wind patterns, atmospheric pressure, water density, tectonic movements, etc., influence the sea level. Moreover, the Earth's changing climate causes long-term changes in the sea level (e.g., the changes due to postglacial rebound).

Global Sea Level means the average height of the Earth's oceans, and its changes are primarily attributed to changes in ocean volume due to two factors: ice melt and thermal expansion. Regional (or Local) Sea Level is a more specific term, influenced by meteorological factors, tidal range, ocean currents, rates of subsidence/uplift, etc.

Mean Sea Level (MSL) represents a temporal average for a given location, such that it is applied to remove shorter period variability. It would be assumed constant, yet in fact, it is variable as it depends on the period for which it is calculated. Accordingly, Global Mean Sea Level (GMSL) corresponds to averaged MSL spatially considering all the Earth's oceans (IPCC 2013). As more specific, MSL is the average height of sea surface relative to a fixed datum established by an average of seawater heights over a period of time. It is significant for defining the elevation of all points on the Earth. For example, the definition of the vertical datum in our country has been provided from the arithmetic average of instantaneous sea level at the Antalya tide-gauge station between 1936 and 1971 (Kılıçoğlu et al. 2007). According to the PSMSL, the MSL represents the "still water level" (without waves), which is averaged over some period (a month or a year) of time for a tide-gauge station.

As mentioned above, sea level can change, both globally and regionally. IPCC (2013) attributes these changes to three essential reasons: (1) changes in the shape of the ocean basins (on geological timescales), (2) changes in the mass of seawater, and (3) changes in ocean volume as a result of changes in the density of seawater. Sea level changes resulting from changes in water density are called "steric". That is, steric sea level change corresponds sea level change due to ocean volume change that results from temperature and salinity variations. Volume changes induced by temperature changes only are called "thermosteric" (referring to thermal expansion), while the changes induced by salinity changes are called "halosteric". If global sea level change is due to the change in the mass of seawater, it is called "barystatic" (IPCC 2013), or "eustatic" in some literatures (Cazenave and Nerem 2004, Rovere et al. 2016). It represents water mass added to or removed from the oceans as a result of water mass exchange between the oceans and other surface reservoirs (ice sheets, glaciers, land water reservoirs, and atmosphere).

The physical processes causing global and regional sea level changes are essentially different from each other, although they are related. This section presents the causes of sea level changes at global and regional scales. The understanding of primary mechanisms leading current sea level changes allows detecting spatio-temporal changes occurring in the climate system in response to natural and anthropogenic forcing, as well as to climate changes.

3.1.1 Global Sea Level Changes and Its Causes

Global sea level changes can be resulted from a variety of phenomena, but the major contributions arise from changes in ocean water temperature (thermal expansion), changes in the ice masses in mountain glaciers, Greenland and Antarctica, and changes in fresh water mass exchange with land water storages (Cazenave and Le Cozannet 2014, Cazenave and Remy 2011, Meyssignac and Cazenave 2012, Milne et al. 2009, Nerem et al. 2006). These contributions, which is also depicted in Figure 3.2, vary in response to natural climate variability and global climate change induced by anthropogenic carbon dioxide emissions.
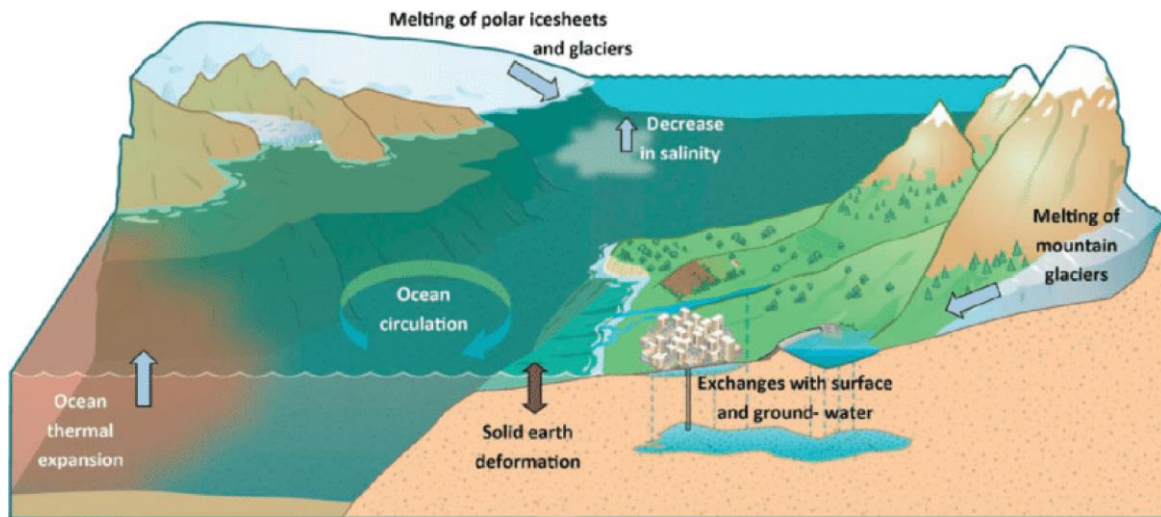
Figure 3.2 Major factors causing sea level changes (mostly rise) (from Cazenave and Le Cozannet 2014).

- Ocean water temperature changes: As ocean water warms, it expands, that is, its volume increases. On the contrary, when the water cools, it contracts and its volume decreases. Oceans are known as the largest solar energy collector on the Earth, and therefore have a central role in stabilizing the Earth's climate system (Dahlman and Lindsey 2018). However, because of increasing greenhouse gases concentrations since the last centuries, most of the excess heat (more than nearly 90% of the net energy increase) has been stored in the oceans. In this context, the increase in ocean heat content is approximately proportional to sea level rise due to thermal expansion. In situ ocean temperature data from Argo system and ships over the last 50 years prove that ocean heat content has significantly increased (Cheng et al. 2017, Levitus et al. 2012, IPCC 2013). Hence, the ocean water undergoing thermal expansion has occupied more space. This thermostatic global sea level change displays considerably interannual/decadal variability due to ongoing global warming, however its spatial distribution is not uniformly (Nerem et al. 2006). All the contributions to global sea level rise over different time intervals is seen in Table 3.1. According to Cazenave et al. (2018), the ocean warming explains about 42% of the observed sea level rise over the satellite altimetry (since 1993) and Argo time periods (since 2005). It can be noted of a significant acceleration in the rate of sea level rise due to thermal expansion during the last few decades.

- Ice volume changes: Another important contributor to sea level change is transport of water currently stored on land to the ocean, particularly from land ice masses (glaciers

35

and ice sheets). The GRACE data since 2002 have been used to detect directly ice mass changes as well as the other measurement techniques such as radar and laser altimetry, Interferometric Synthetic Aperture Radar (InSAR) (IPCC 2013, Marzeion et al. 2017). Because of ongoing global warming, the land ice masses have started to retreat worldwide over the recent few decades (Meier et al. 2007, Steffen et al. 2010). The sea level contributions of global ice mass losses are also given in Table 3.1. According to this, on average over the satellite altimetry period (1993–2015), glaciers and ice sheets have accounted for totally ~ 40% of sea level rise.

- Land water storage changes: The changes in land water storage (surface waters, wetlands, aquifers, snow packs, etc.) due to climate change (or variability) and human activities (dam building, groundwater extraction, irrigation, etc.) can affect global sea level changes (Huntington 2008, Wada et al. 2017). Climate- or anthropogenic-driven changes impact water exchange between land, ocean and atmosphere, ultimately changing sea level. For example, the increase in river runoff due to excessive pumping of groundwater can contribute to sea level rise, whereas impoundment of water in reservoirs can reduce the outflow of water to the sea. Direct observation of terrestrial reservoirs is available since 2002 through GRACE (Chen et al. 2016, Llovel et al. 2010). Also, the water change estimates based on global hydrological models are extant (Döll et al. 2016). However, Cazenave et al. (2018) asserted that owing to coarse resolution of GRACE, and inadequate modelling, both of them have significant uncertainties: for contemporary sea level changes, while the GRACE-based estimates (Reager et al. 2016) mostly indicate a negative contribution, the estimates from hydrological models (IPCC 2013) tend to positive contribution. Reager et al. (2016) found from GRACE data between 2002 and 2014 that the terrestrial water changes has slowed the rate of recent sea level rise by approximately 15%. According to IPCC (2013), the climate-related changes in land water storages do not show significant long-term trends for the recent decades, whilst the human activities have contributed to global sea level changes (see Table 3.1).

All in all, in terms of global mean, sea level budget equation is usually given as follows (Cazenave et al. 2018, Chambers et al. 2017, WCRP 2018):

$$GMSL(t) = GSSL(t) + GM_{ocean}(t) \tag{3.1}$$

where *GMSL(t)* is Global Mean Sea Level change, *GSSL(t)* is global steric sea level change, $GM_{ocean}(t)$ is change in ocean mass, and *t* is time. Accordingly, this equation is based on both ocean mass changes (i.e., due to ice melting, changes in land water storages, changes in snowpack and permafrost, and changes in atmospheric water content) and ocean volume changes (i.e., due to changes in sea water density). It means that the sum of contributions is expected to be equal the Global Mean Sea Level change within some uncertainties (Chambers et al. 2017).

Considering sea level budget, there are several studies dealing with the magnitudes of each of the contributions over different time periods and using different data sets (Cazenave et al. 2009, Chambers et al. 2017, Church and White 2011, Leuliette and Willis 2011, Nerem et al. 2018a, WCRP 2018). According to the IPCC Fifth Assessment Report (AR5) (IPCC 2013), ocean thermal expansion and glacier melting have been the dominant contributors to contemporary sea level change. While since early 1970s observations reveal that thermal expansion and glaciers explain 75% of the observed rise, the contribution of the Greenland and Antarctic ice sheets has increased since the early 1990s. Moreover, the Greenland ice sheet contribution shows a significant increase in the recent years. Overall, the total contribution of glaciers, Greenland and Antarctica is larger than that of the ocean thermal expansion during the Argo era. As for land water storage change, it has made only a small contribution. Over the past century GMSL was observed to be rising at an average rate of 1.5 ± 0.2 mm/y, increasing to 3.1 ± 0.3 mm/y during the altimetry era (Table 3.1).

Mass redistributions associated with past and ongoing land ice melt and terrestrial water storage changes induce factors causing static sea level changes (Cazenave et al. 2018, Stammer et al. 2013). The collapse of the large ice sheets during the Last Glacial Maximum, and the subsequent loading of the ocean basins resulted in deformation of the ocean floor and changes in the gravity field due to elastic response of the solid Earth. Even today, this ongoing movement of land is called Glacial Isostatic Adjustment (GIA), and it will continue in the future (Peltier 2004).

Table 3.1 Observed global sea level change with its individual contributions over different time periods (Unit: mm/y). Second and third columns have been provided IPCC (2013), while fourth and fifth columns have been adapted from Cazenave et al. (2018).

Observed contributions	1901–1990	1971–2010	1993–2015 (Altimetry era)	2005–2015 (Argo era)
Thermal expansion	–	0.8 ± 0.3	1.3 ± 0.4	1.3 ± 0.4
Glaciers	0.54 ± 0.07	0.62 ± 0.37	0.65 ± 0.10	0.74 ± 0.10
Greenland ice sheet	–	–	0.48 ± 0.10	0.76 ± 0.10
Antarctic ice sheet	–	–	0.25 ± 0.10	0.42 ± 0.10
Land water storage	-0.11 ± 0.05	0.12 ± 0.09	0.38 ± 0.12[a]	–
Observed GMSL rise	1.5 ± 0.2	2.0 ± 0.3	3.1 ± 0.3	3.5[b]

[a] Data for land water storage extend to 2010 (IPCC 2013), not 2015.

[b] Uncertain of this value has not given in Cazenave et al. (2018).

Furthermore, internal variability of the climate system (ENSO on interannual time-scale and Pacific decadal oscillation) is one of the deterministic factors of global sea level fluctuations at interannual scale. Interannual variability of GMSL is highly correlated with ENSO (IPCC 2013, Meyssignac and Cazenave 2012). Nerem et al. (2010) reported that positive and negative sea level anomalies observed during El Nino (the warm phase of ENSO) and La Nina (the cold phase of ENSO), respectively. During El Nino (especially in the tropics), associated with more rainfall over oceans and less rainfall over land an increase occurs in global sea level and temporary decline is observed in water storages on the land; and opposite variations during La Nina appears (Cazenave et al. 2012, IPCC 2013).

The altimetry-based GMSL time series is shown in Figure 3.3. It is based on the AVISO Mean Sea Level product up to 19 December 2018 (URL-2). The seasonal signal has been removed by fitting sinusoids of 6-month and 12-month periods to the data. This time series has indicated a rise of 3.34 ± 0.4 mm/y, after correcting for GIA (subtracting a -0.3 mm/y value according to Peltier 2004).
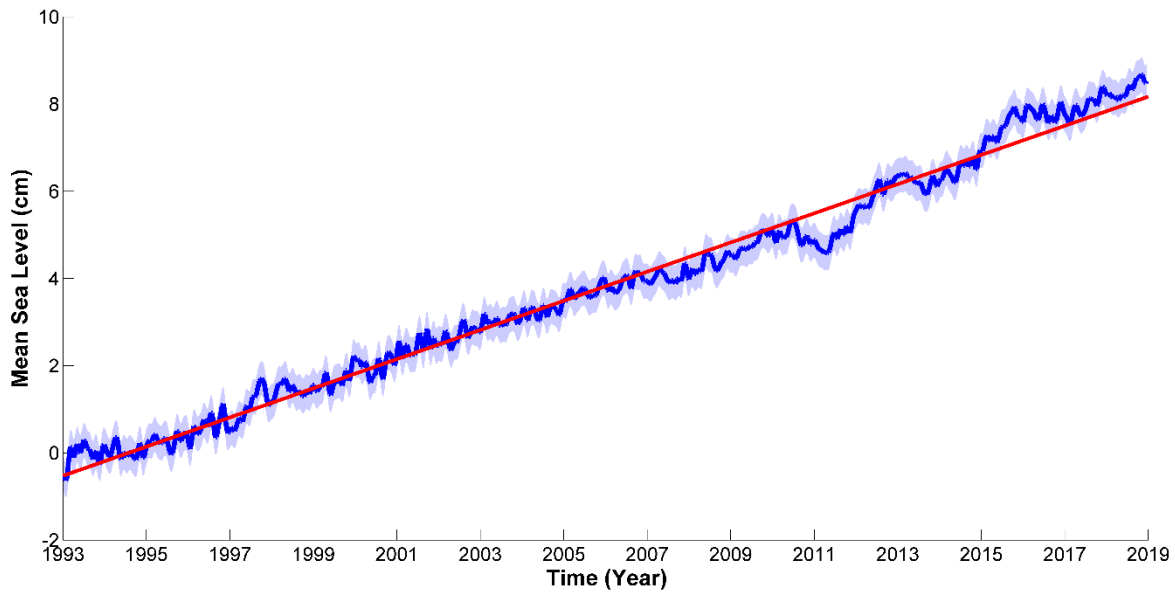
Figure 3.3 Altimetry-based GMSL time series between January 1993 and December 2018. The blue curve corresponds 2-month filtered, annual and semi-annual signals removed, GIA-corrected sea level. The red line is the best fitting slope within an uncertainty (shaded area) of ~ 0.4 mm/y at the 90% confidence level (Data from AVISO: Reference product at 10-day interval computed with the Topex/Poseidon, Jason-1, Jason-2, Jason-3 missions).

3.1.2 Regional Sea Level Changes and Its Causes

Regional (even local) sea level can manifest large deviations away from the global mean for changing periods (e.g., Miller and Douglas 2007, Palanisamy et al. 2015, Sturges and Douglas 2011). Accordingly, in addition to the global sea level change and its causes, it is essential to understand the regional variability in the rates of this change (i.e., its evolution with time and space and its drivers) in order to assess the potential impacts of the sea level rise in coastal areas (Meyssignac and Cazenave 2012). Stammer et al. (2013) stated that sea level changes at any point over the ocean are a composite of GMSL change and regional processes. General forcing for regional (or local) sea level patterns can be basically linked to (1) surface warming and cooling of the ocean, (2) exchange of freshwater with the atmosphere and land through evaporation, precipitation, and runoff, and (3) changes in the surface wind stress. The complex response of the ocean to these forcing mechanisms causes changes in ocean circulation (hence density) and mass transport. Besides, the contemporary patterns in sea level change reflect not only ongoing forcing changes but also forcing changes that occurred far in the past.

In effect, all processes causing global sea level change have a spatial and temporal variability (Milne et al. 2009). For example, ocean circulations altered with the factors such as surface wind stress, exchanges of heat and freshwater lead to changes in sea level that vary place to place (IPCC 2013). Local changes in the ocean temperature and salinity fields because of atmosphere-ocean interactions result in local sea level changes.

Large-scale deformations of the ocean basins and gravity changes associated with mass redistribution lead to sea level change in regional scale. It refers to the GIA effect in the regional variability of sea level. This effect resulted from land ice loss contributes little to the regional variability, but will become significant in the future (Cazenave et al. 2018, IPCC 2013, Meyssignac and Cazenave 2012, Milne et al. 2009, Mitrovica et al. 2009). In addition, input of freshwater to oceans, due to the land ice melting, influences the density structure of the ocean (hence ocean circulation).

The response of ocean floor to all kinds of loading can change sea level at regional scale, even so very low on average (Moucha et al. 2008). Atmospheric loading is particularly significant for the regional changes (Wunsch and Stammer 1997). On timescales longer than a few days, the ocean adjusts nearly isostatically to changes in atmospheric pressure (inverse barometer effect), such that for each 1 mbar increase in local sea level pressure (compared with the global ocean average) the ocean is depressed by approximately 10 mm (Stammer et al. 2013). The regional sea level variability related to this effect is higher in the equatorial regions than at high latitudes. Eventually, all tectonic processes cause local fluctuations in sea level (IPCC 2013). Indeed, especially in coastal areas, in addition to the global mean plus regional components, vertical motions of the land lead to relative sea level changes (Stammer et al. 2013, Wöppelmann and Marcos 2016).

Moreover, the atmospheric circulations can create locally small dynamics variations in sea level (Stammer et al. 2013). Besides, in the coastal areas, small-scale processes occurring at the land-sea interface (fresh water input from rivers in estuaries, wind-driven ocean circulation and wave height changes, etc.) may be added to the larger-scale sea level changes.

In this context, Cazenave et al. (2018) form the regional sea level budget as follows:

$$RSL(t) = RSSL(t) + RM_{ocean}(t) + static\ terms + atmospheric\ circulations \qquad (3.2)$$

where *RSL(t)* is Regional Sea Level change, *RSSL(t)* is regional change in steric sea level, *GM$_{ocean}$(t)* is regional change in ocean mass, and *t* is time. As mentioned before, the static terms correspond to the changes due to GIA and other solid deformations as well as gravity field changes.

The global coverage of satellite altimetry measurements enables to map the regional variability of the rates of sea level change. Figure 3.4, which is provided from AVISO (URL-2), shows the recent altimetry-based spatial trend patterns in sea level between September 1992 and September 2018.

During the altimetry era, the dominant contribution to observed regional sea level changes comes from the steric effects (Cazenave et al. 2018, Cazenave and Le Cozannet 2014, IPCC 2013, Stammer et al. 2013). In this sense, Meyssignac and Cazenave (2012) mentioned that the thermosteric component is the most important contributor, however, the halosteric effect is also significant for some areas like the Atlantic Ocean and Arctic region. On the other hand, because of coastal currents the steric effects in coastal zones may be considerably different from those in open oceans.

Besides, Meyssignac et al. (2012) confirmed that the sea level regional (or local) variability observed by altimetry is closely related to natural modes of the climate system such as ENSO, North Atlantic Oscillation (NAO), and Pacific decadal oscillation. Because, the altimetry-based patterns are not long-lasting, such that the thermosteric origin of the regional variability varies in time and space, depending on the internal variability of climate system (Fu 2014).
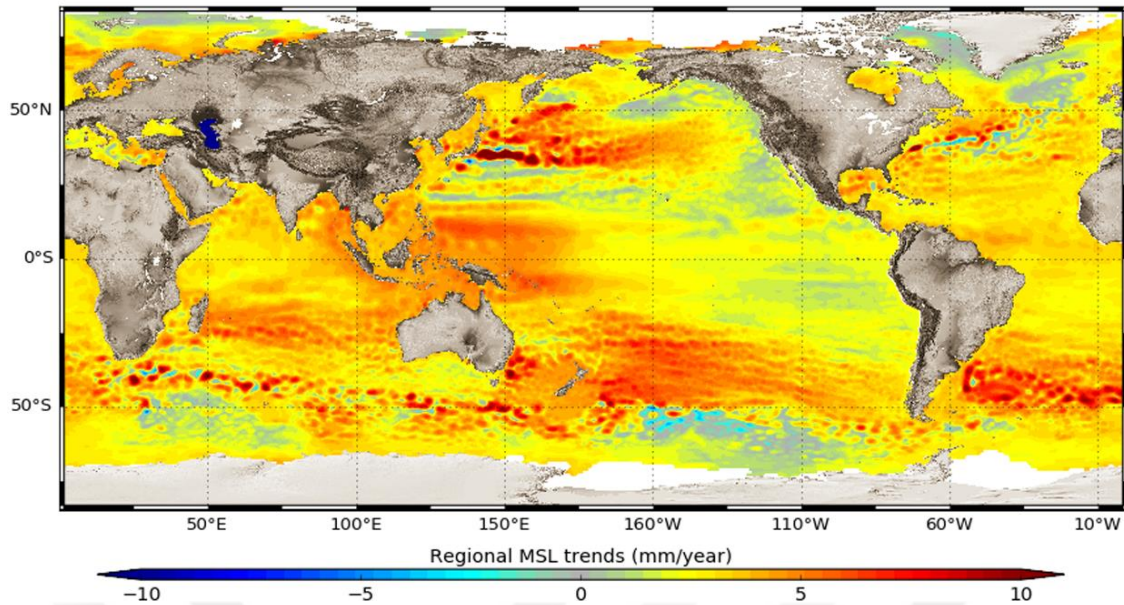
Figure 3.4 Regional patterns of observed sea level from September 1992 to September 2018. This map generated by using gridded, multi-mission altimetry data has been supplied from URL-2.

As known, ocean waters regularly and periodically rise and fall due to tides. Gravitational attraction of celestial bodies (Sun and Moon) causes tides at the time scales extending a few hours to multiple years. The moon has major influence on the Earth's tides. Most coastal areas generally, but not always, experience two low tides and two high tides every lunar day (or 24 hours and 50 minutes) (URL-11). In addition to this, once every 28 days, the moon reaches a perigee, its closest point of approach to the Earth. This is the point at which the gravitational pull of the moon is strongest. During this period, a slight increase becomes in the average range of tides. Moreover, the maximum range of lunar influences on the tides occurs over cycles of about 18.6 years, referred to nodal tide. During this cycle, the moon induces a harmonic fluctuation with small amplitude on sea surface. It is at a maximum at the poles whereas it is negligibly small at latitudes between 35°N and 35°S (Pugh 1996). Solar tides are about half as large as lunar tides, and are expressed as a variation of lunar tidal patterns, not as a separate set of tides. The solar tide has an additive effect on the lunar tide (URL-11). The magnitude of tides can be strongly influenced by the shape of the shoreline. Furthermore, the shape of bays and estuaries, geographic location and weather patterns all can affect local tidal intensity. Tides are generally measured by tide-gauges along the coasts. Besides, global ocean tides and overlay effects of ocean tides on shore (ocean loading) can be modelled (Le Provost 2001). For example, since tides are well known periodic signals, they can be calculated by harmonic analysis (Mayer-Gürr et al. 2012).

3.2 MEASURING SEA LEVEL CHANGE

Oceans are an important part of climate system. In addition, the height systems in many countries are determined basing on mean sea level. So, measuring of sea level and the amount of its change has been an objective for scientists a long time. Short-term sea level fluctuations (e.g., tides), and extreme events (such as storm surges and tsunami) require considering of sea level changes (or variations) for coastal planning, safe navigation and transport, protection of coastal ecosystem, etc. On the other hand, slower changes in sea level are also significant. Because, the known past sea levels were lower or higher from that of the present-day, and it is crucial to understand how sea level might change in the future.

Generally, sea level measurements are carried out for several purposes as follows:

- Monitoring of sea level change and its impacts,
- Defining of vertical datum and geoid determination,
- Detecting of vertical land motion,
- Interpreting of sea surface slope for ocean circulation and eddy estimates,
- Generating tide predictions for port operations and fishermen,
- Providing of safe navigation and transport,
- Projecting and building of coastal structures,
- Estimation and early warning of storm surges, tsunamis, and other factors leading to short-term coastal inundation.

Indeed, sea level changes occur on different time and spatial scales. Different observing systems are used to measure the various components of existing change. For example, changes of atmospheric components (air temperature, winds, precipitation, air pressure, etc.), or knowledge of temperature and salinity of sea water, or mass loss from ice sheets and glaciers, or water storage changes on land and in atmosphere require input from a large number of disciplines. Besides, sea level can be directly recorded from instrumental measurements or be determined through satellite observations. In this sense, there are two main techniques of measuring sea level change: the contemporary sea level information are provided tide-gauges and satellite altimetry. All these techniques determine sea level with respect to different reference frames.

Historical sea level can be determined from geological evidence indirectly (e.g., sedimentary records, diatom analysis, pollen analysis, carbon dating, etc.) (Lambeck et al. 2010, Mitchum et al. 2010, Murray-Wallace and Woodroffe 2014, Rashid 2014). It is generally referred to "paleo indicators" (URL-15). They are mostly natural (e.g., raised beaches, wave cut notches, fossil shells, etc.), but sometimes man-made. Their age or height information can give useful results on sea level histories.

3.2.1 Tide-Gauge Measurements

Prior to the early 1990s, the direct measurements of tide-gauges installed at the coasts had been provided the primary information for sea level changes (Nerem et al. 2006). Indeed, the first tide-gauges, as the names implied, were used to provide information on ocean tides (Tamisiea et al. 2014). Whereas some tide-gauge records (Amsterdam, Stockholm, Liverpool, Brest and Swinoujscie in Europe, Sidney and Freemantle in Australia) extend back 100 years or more, most of the records are less than 50 years in length (Cipollini et al. 2017, Meyssignac and Cazenave 2012, Mitchum et al. 2010). Today, tide-gauge observations are used to estimate sea level changes (and variability) as well as predict tides, quantify the size of tsunamis and storm surges (Cipollini et al. 2017). Besides, tide-gauge records can be utilized for calibration of altimeter measurements (Mitchum 1998, 2000, Nerem and Mitchum 2001b).

First tide-gauge systems were simply graduated markings inscribed on rocks, walls or levelling rods in ports, to enable sea level observations as visually. The first mechanical (analogue) tide-gauge systems (called stilling well tide-gauge) equipped with clocks and chart recorders, and detecting high frequency wave motion emerged in the 1830s. Today, modern tide-gauges (Figure 3.5) are known as acoustic gauge based on the acoustic transmission in sounding tubes or open air of a sound wave, radar gauge using the travel time of a radar pulse, and pressure gauge converting hydrostatic pressure measurement into vertical distance (i.e., sea level) after correction for water density and gravity (Aarup et al. 2006, Sezen 2006, Simav 2007, URL-16).

Tide-gauges records have mostly data gaps, and are not homogeneous in terms of data quality and length as well as their geographical distributions (Cipollini et al. 2017, Nerem and Mitchum 2001b). Tide-gauges enable to measure of the slow variations of sea level relative to the adjacent land. In this sense, their records also include motions of land to which tide-gauges are attached. In active tectonic and volcanic regions, or in areas subject to strong land subsidence

due to natural causes (e.g., sediment loading in river deltas) or human activities (ground water and oil/gas extraction), or in the rising land areas due to the GIA, tide-gauge records are directly affected by the corresponding land motions. In order to determine absolute sea level change (especially local or regional), the land motions need to be removed (Meyssignac and Cazenave 2012, Woodworth and Player 2003). The measurement of such vertical land movement rates is available from Global Navigation Satellite System (GNSS) (episodic or continuous), Doppler Orbitography and Radiopositioning Integrated by Satellite (DORIS), absolute gravity, and precise levelling.

Furthermore, there is no common datum for individual tide-gauge records, and this leads a problem of assessing records together (Cipollini et al. 2017).

The above-mentioned limitations pose a major challenge for computing long-term global averaged sea level from tide-gauges. However, a number of studies based on various approaches -from direct averaging of tide-gauge time series, to Empirical Orthogonal Functions (EOF)s also utilizing altimetry time series- (Meyssignac and Cazenave 2012, Mitchum et al. 2010) manifest tide-gauge-based estimates of GMSL. For example, over a continuous spatial domain, the studies depending on only tide-gauge data (Dangendorf et al. 2017, Jevrejeva et al. 2014), or the reconstruction studies combining temporal and spatial information from tide-gauge and altimetry data, respectively (i.e., using EOF analysis) (Church and White 2006, 2011), or the studies combining tide-gauge data with ocean models (Meyssignac et al. 2011) enable to determine the long-term evolution of global sea level changes. According to Cazenave et al. (2018), the estimates obtained from such the studies vary from 1.2 to 1.9 mm/y. These estimates can be affected by number and distribution of the selected tide-gauge stations. Moreover, Douglas (2001) suggested that in order to minimize the impact of low-frequency variability from each tide-gauge, the records longer than 50 years should be used for long-term sea level trend estimates.

As for regional or local sea level estimates from tide-gauge data, many studies can be mentioned dealing with generally coastal sea level changes and comparing it with the estimates obtained from altimetry (e.g., Cazenave et al. 2002, Feng et al. 2013, Fenoglio-Marc 2002, Fenoglio-Marc et al. 2012, Marcos and Tsimplis 2008, Tsimplis and Spencer 1997, Simav vd. 2008, Yıldız ve Deniz 2006, Yıldız vd. 2003). In such studies, the consistency of two data sets at regional scale are typically examined.

Considering the sparse sampling from tide-gauges; the need for global, regional or national sea level monitoring networks and data centres has been getting more important. Global Sea Level Observing System (GLOSS) (URL-17), European Global Ocean Observing System (EuroGOOS) (URL-18), and the Permanent Service for Mean Sea Level (PSMSL) (URL-19) serve as data centres, providing association of high-quality sea level observations from local stations. Moreover, in order to monitor real-time data from national and regional networks, a global station monitoring service (URL-20) supported by the United Nations Educational, Scientific and Cultural Organization - Intergovernmental Oceanographic Commission (UNESCO-IOC) has been also formed. Besides, University of Hawaii Sea Level Center (UHSLC) (URL-21) maintains an international tide-gauge network for sea level and tsunami observations.

In effect, the primary resource for several studies dealing with global or regional sea level change from tide-gauge data is mostly provided from the PSMSL. Since 1933, tide-gauge data have been collected and distributed by the PSMSL, hosted by the United Kingdom National Oceanography Centre (NOC) (Holgate et al. 2012, Woodworth and Player 2003). Today, the PSMSL supplies monthly and annual means of sea level records from over 65,000 stations free of charge (URL-19). Figure 3.6 shows locations of tide-gauge stations in the PSMSL database. It is also responsible for an archive of delayed-mode sea level data from the GLOSS network. Moreover, in order to analyse time series of sea level measurements at each station efficiently, the PSMSL has formed a common datum called as "Revised Local Reference (RLR)". The RLR datum at each tide-gauge station is defined to be approximately 7000 mm below mean sea level. Most of the distributed data have been adjusted to this common reference level.

In Turkey, sea level observations are currently conducted at 20 tide-gauge stations (Figure 3.7) within the Turkish National Sea Level Monitoring System (TUDES) network operated by the GDM (Akyol vd. 2012, URL-16). The TUDES is a part of the GLOSS designed a global core network, and so implements the GLOSS requirements (Aarup et al. 2006). At present, most of the TUDES stations are acoustic-type tide-gauges (Sezen 2006). Figure 3.5a and b show the Antalya tide-gauge station with acoustic (old-form) and radar (modernized-form) gauges, respectively (URL-16). As seen in Figure 3.5a, ancillary meteorological parameters (air temperature, air pressure, humidity and wind) as well as sea level are also observed at each TUDES station. The modernized tide-gauge stations in the TUDES have been also equipped with a GNSS receiver (Figure 3.5b). Data quality controls and analysis, database management

and data distribution activities are carried out at the data centre in Ankara (Simav vd. 2011). The TUDES sea level data at the Turkish national height datum (Turkish National Vertical Control Network-1999 – TUDKA-99) are provided with subscription and fee to users (URL-16). Nevertheless, accessing sea level data at the local datum is freely available to users as 30 seconds (measurement interval), 10 minutes, 15 minutes and hourly averaged data.

a) Digital and automatic acoustic-type tide-gauge (1998–2019) (left), the TUDES data transmission system (top-right), the integrated measurement systems for meteorological parameters (bottom-right).
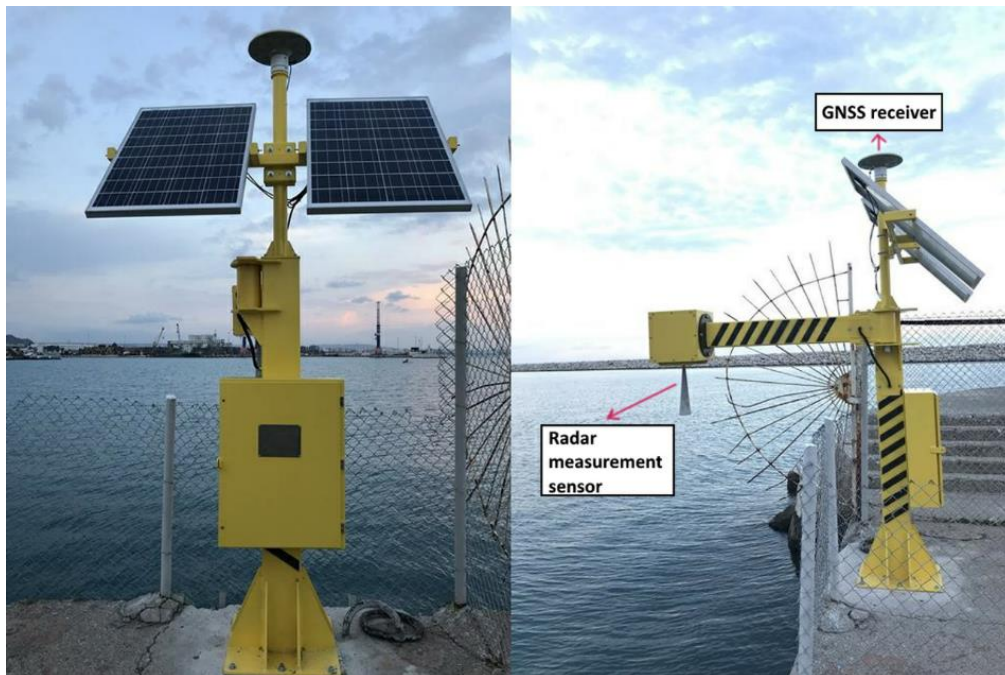
b) Tide-gauge with radar sensor, also integrated GNSS receiver (since February 2019).

Figure 3.5 Tide-gauge station in Antalya (modified from URL-16).
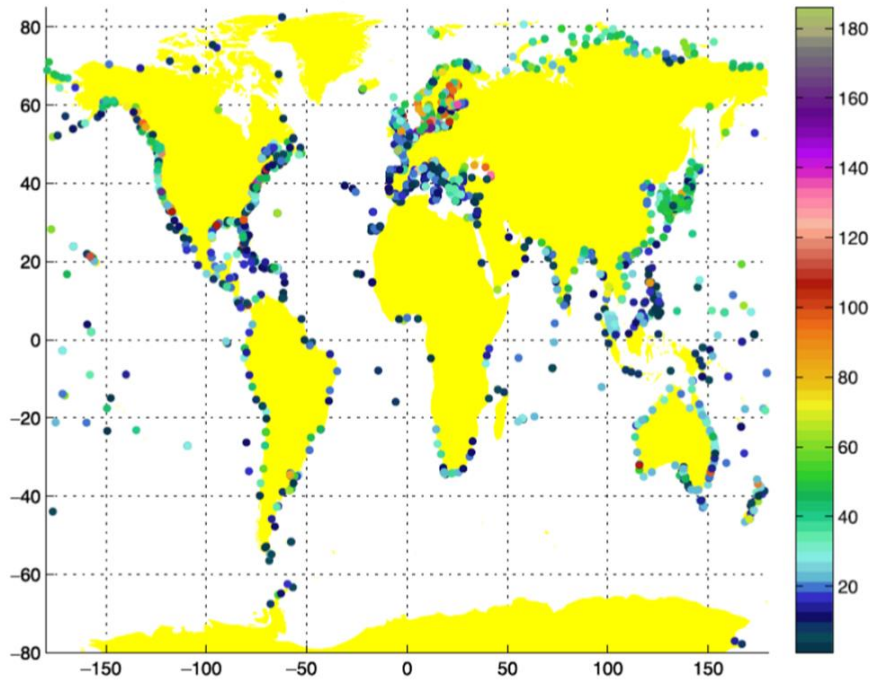
Figure 3.6 Permanent Service for Mean Sea Level (PSMSL) tide-gauge locations. The legend refers to the number of available annual records in each station (from Cipollini et al. 2017).
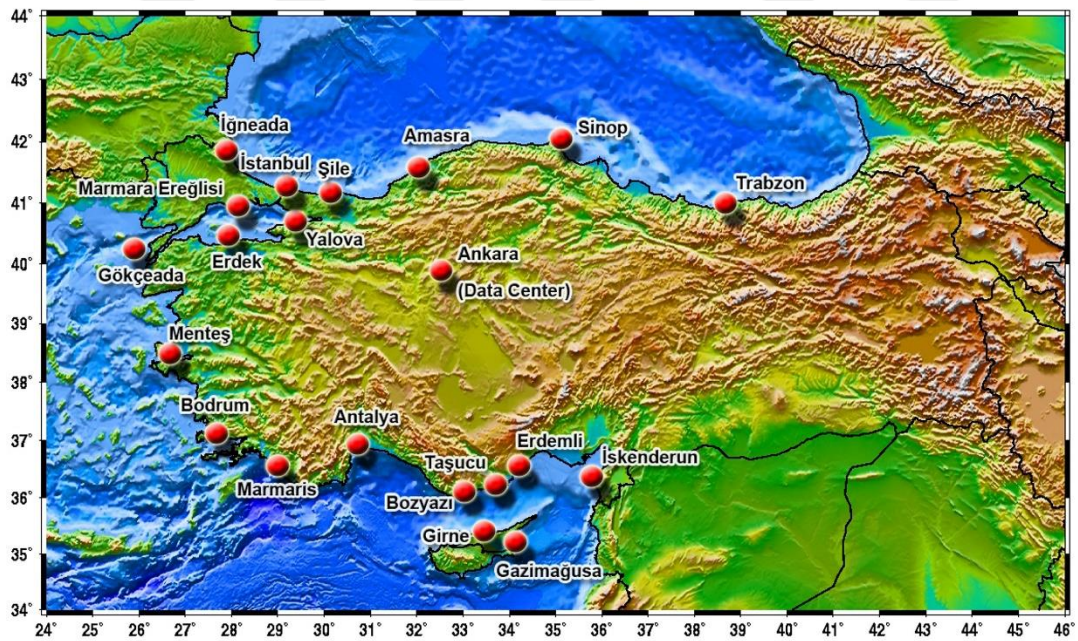
Figure 3.7 Turkish National Sea Level Monitoring System (TUDES) network (from URL-16).

48

Furthermore, the combination of the tide-gauge and altimetry data is used to estimate vertical land motions (e.g., Fenoglio-Marc et al. 2004, Garcia et al. 2012, Nerem and Mitchum 2002, Yildiz et al. 2013).

3.2.2 Satellite Altimetry Measurements

Since the early 1990s, sea level changes (and variations) have been derived from satellite altimetry observations. Essentially, satellite altimetry technique is a remote sensing technique used in several fields (oceanography, geodesy, glaciology, geophysics, hydrology, atmospheric science, etc.) of Earth sciences (Fu and Cazenave 2001, Stammer and Cazenave 2018). It allows high-precision and high-resolution measurements of sea surface topography with global coverage and a revisit time of a few days (10 to 35 days) (Cazenave et al. 2018). Moreover, these measurements are not affected by clouds, night or even vegetation (Rosmorduc et al. 2018).

Indeed, satellite altimetry technique was developed in the 1960s (URL-2), however, the first experiments was deployed on Skylab space station in 1973 (Rosmorduc et al. 2018, Seeber 2003). The Topex/Poseidon (T/P) satellite, launched in 1992 (ended in 2006), enabled to high-precision (approximately decimetre precision) sea surface height measurements (Fu et al. 1994). With the data of its successors – Jason-1 (2001–2013), Jason-2 (2008–present) and Jason-3 (2016–present) –, the precision has reached ~ 1 cm level (Cazenave et al. 2018, Meyssignac and Cazenave 2012, WCRP 2018). Recent data of these altimetry satellites allow a long-term record of sea level globally and regionally, from 1993 to present (Ablain et al. 2017). Additionally, data of complementary satellite missions – European Remote Sensing (ERS)-1&2 (1991–2011), Geosat Follow-On (GFO) (1998–2008), Environmental Satellite (EnviSat) (2002–2012), CryoSat-2 (2010-present), HaiYang (HY)-2A (2011–present), HY-2B (2018–present), Satellite with ARgos and ALtika (SARAL)/AltiKa (2013–present), Sentinel-3A (2016–present), Sentinel-3B (2018–present), Chinese-French Oceanic SATellite (CFOSAT) (2018–present) – serve to improve spatial resolution and coverage of high-latitude ocean areas (Legeais et al. 2018, WCRP 2018). The detailed information all these satellite altimetry missions are given in Escudier et al. (2018), Rosmorduc et al. (2018), Seeber (2003) and URL-2. It should be noted that a GMSL estimate obtained by averaging the individual measurements (assuming 1 cm accuracy) from a satellite mission over an orbital cycle results

in an uncertainty of 4–5 mm (Cazenave et al. 2018, Escudier et al. 2018, Meyssignac and Cazenave 2012).

Altimeter is basically an instrument for measuring height (Braun and Shum 2004, URL-2). Satellite altimeters are nadir-pointing active microwave instruments, whose principal aim is to measure as accurately as possible the two-way travel time of short pulses reflected from the Earth's surface. That is, satellite altimetry is a range altimeter based on "distance = velocity x travel time" relation for a signal. The altimeter emits a radar signal at very high frequency (over 1,700 pulses per second) towards to sea surface, and this signal partly reflects back to the altimeter's antenna. Determination of the round-trip travel time of the signal propagating with velocity of light provides distance (i.e., range) from the satellite's centre of mass to the instantaneous sea surface (For oceanographic applications, the accuracy on the derived range must be of the order of centimetres). And by combining this altimeter measurement with precise satellite location data, sea surface heights, which are referenced to the same frame, are obtained (Rosmorduc et al. 2018, URL-2, URL-22). Figure 3.8 demonstrates the altimetry's basic principle.
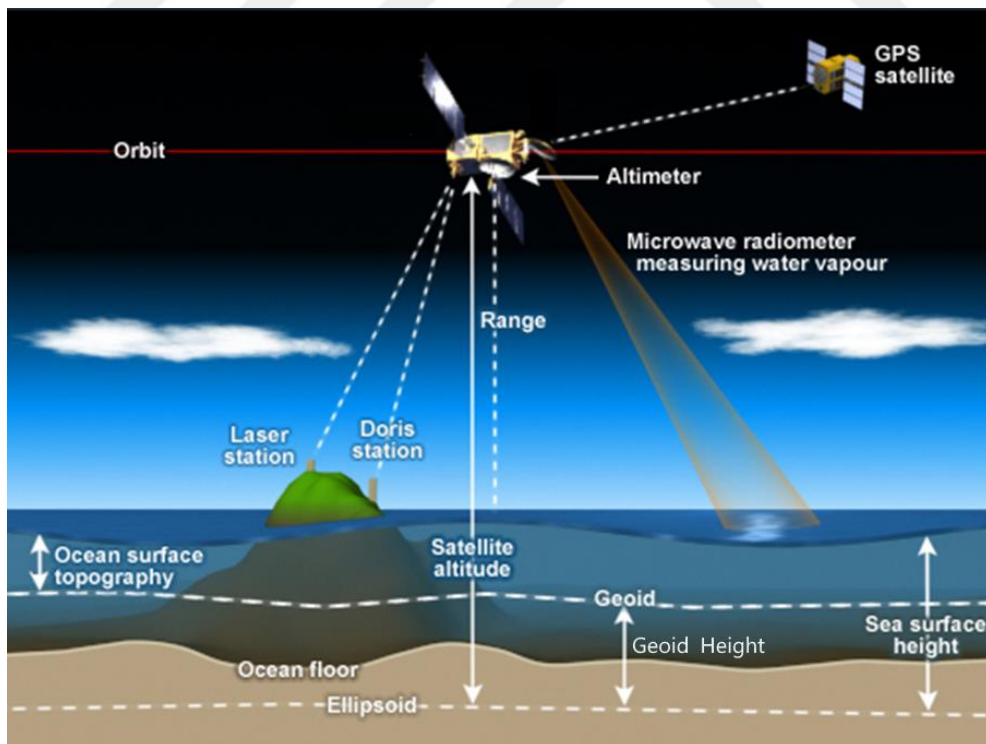
Figure 3.8 Basic principle of satellite altimetry (modified from URL-23).

Here, the satellite's position with respect to an arbitrary reference surface (i.e., reference ellipsoid) is determined using the satellite's orbital parameters (from a laser retro-reflector array, and the tracking systems such as DORIS, and Precise Range And Range-Rate Equipment – PRARE) and precise positioning systems like Global Positioning System (GPS). A radiometer on the board also measures the total water vapour content along the signal path (see Figure 3.8). It is used to correct the altimeter measurements (Seeber 2003, URL-2). Moreover, these microwave passive radiometers provide to extract information on wind speed, rain rate, cloud liquid water, and sea surface temperature.

According to mentioned above, satellite altimetry data are that they are not simply the product of an instrument, but provided by a measurement system combining of several different observations. How altimeter range measurements are collected and how they are converted to sea level measurements are given in Nerem and Mitchum (2001a) and Vergos (2002). This technique takes measurements only at the nadir (i.e., just under below the satellite), with a rather narrow (antenna beam widths ~ 1 degree) footprint (sea surface area which is illuminated by the radar antenna), and is averaging everything in that footprint. That is, the obtained distance actually corresponds a mean height of the sea surface that is covered by the radar footprint. The altimeter footprint is actually determined by the duration of the emitted pulse (hence pulse-limited altimeter) (URL-24). Radius of the footprint also depends on satellite height, signal propagation speed, wave width and sea state, and varies between 1 km (at the calm sea) and 10 km (at the rough sea) (Simav 2007). Up-to-date detailed descriptions of the satellite altimetry system and measurements, as well as the applied corrections, are provided in Escudier et al. (2018). Altimeter calibration required for attaining an accurate sea level record can also be found in Nerem and Mitchum (2001a).

Comprehending of the geometry of altimeter observations allows understanding the definitions related to sea level. Figure 3.9 shows the heights and reference surfaces which are useful for different applications, they can be derived from altimeter observations.
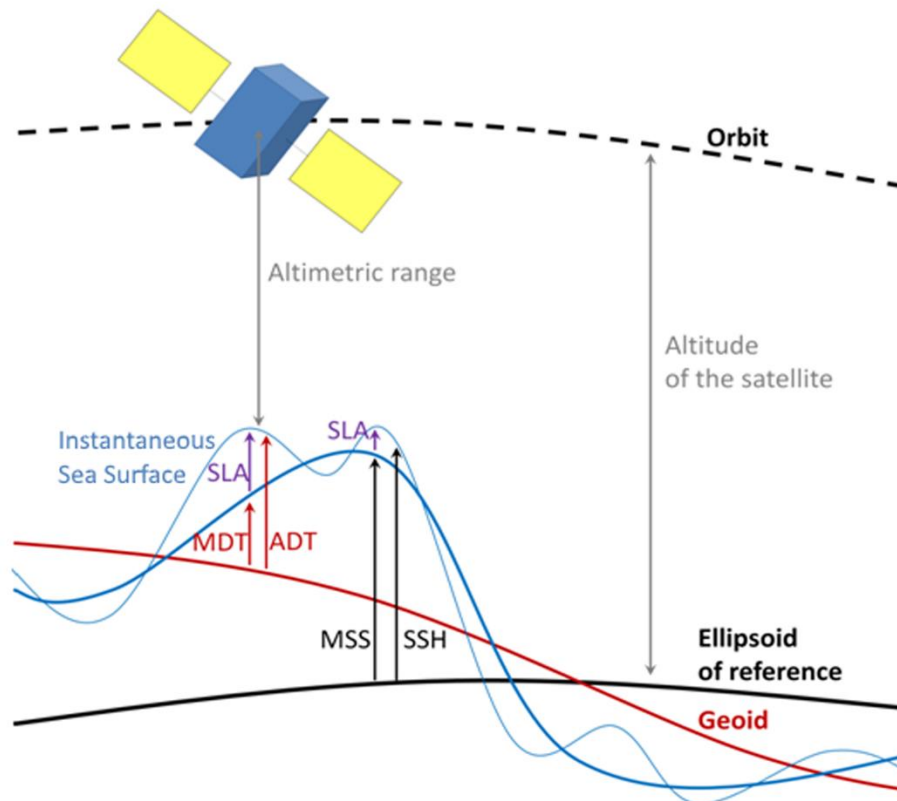
Figure 3.9 Different heights and reference surfaces related to sea level. SSH: Sea Surface Height, MSS: Mean Sea Surface, SLA: Sea Level Anomaly, ADT: Absolute Dynamic Topography, MDT: Mean Dynamic Topography (modified from URL-25).

As seen in Figure 3.9, the Sea Surface Height (SSH) is the difference between the satellite's altitude relative to the reference ellipsoid, and the altimetric range. That is, it equals to the height from the reference ellipsoid to the instantaneous sea surface:

$$SSH = Satellite\ Altitude - Altimetric\ Range \qquad (3.3)$$

Here, the definition relative to the reference ellipsoid provides an accurate and homogeneous quantity for sea surface height. Because the sea depth (sea surface height relative to ocean floor) is not known accurately everywhere (URL-2). In altimetry, for Topex/Poseidon, Jason-1 and Jason-2 satellite missions the T/P ellipsoid (equatorial radius (a) = 6378136.3 m, flattening (f) = 1/298.257), and for ERS-1, ERS-2, EnviSat satellite missions the WGS84 ellipsoid (a = 6378137.0 m, f = 1/298.257223563) typically used (Rosmorduc et al. 2018).

The geoid is a physical model of the Earth that mirrors the shape of the sea surface in the absence of the effects of waves, winds, currents, tides and other perturbations (like the loading

of atmospheric pressure) (URL-22). It is a very irregular, undulating surface reflecting the Earth's gravity field. The dynamic topography (or Absolute Dynamic Topography – ADT, or Ocean/Sea Surface Topography – OST), of the order of 1–2 m, is the difference between this unperturbed surface and the actual sea surface. The dynamic topography (i.e., the dynamical part of ocean signal), which is corresponding ocean circulations, comprises a permanent stationary component (permanent circulation linked to Earth's rotation, permanent winds, etc.) and a highly variable component (due to wind, eddies, seasonal variations, etc.) (Rosmorduc et al. 2018). It is expected that in order to obtain the dynamic topography the geoid height is subtracted from the SSH derived by the altimetry. However, available resolution of geoid is not sufficient for estimating the ADT directly (Fu 2014). Therefore, in practice, in order to reveal to small wavelengths of the dynamical ocean signal, a Mean Sea Surface (MSS) field is used (PUM 2019, Rosmorduc et al. 2018, URL-25). This surface represents permanent component of the SSH, and is computed from the altimetry, averaging data over several years. It essentially shows the mean shape of the sea surface during a defined reference period. The MMS, given as a grid with spacing, is not to be confused with the MSL, which is a measure of the sea level variations over time. Sea Level Anomaly (SLA) reflects displacement of the sea surface relative to a mean profile (i.e., the MSS) of the SSH. That is, the SLA corresponding the variable part of the ocean signal is sea surface height with respect to the MSS. It is obtained by subtracting the MSS from the SSH (Equation (3.4a)). A Mean Dynamic Topography (MDT) field corresponding the Mean Sea Surface above the geoid can then be used to retrieve the ADT (Equation (3.4c)) (URL-25). It is clear that this field represents permanent stationary component of the ADT. This mean circulation is not produced directly from altimetry data. If the geoid is determined precisely, by subtracting the MSS the MDT can be computed (Equation (3.4b)) (Rosmorduc et al. 2018).

Consequently, the relations between the quantities derived from the altimeter measurements can be defined as follows:

$$SLA = SSH - MSS \tag{3.4a}$$
$$MDT = MSS - Geoid\ Height \tag{3.4b}$$
$$ADT = SLA + MDT \tag{3.4c}$$

$$SSH = Altitude - Range - Corrections = Geoid\ Height + ADT$$
$$= MSS + SLA = Geoid\ Height + MDT + SLA \tag{3.5}$$

In Equation (3.5), "Corrections" term represents the external values, which are related to the effects of various physical phenomena. In order to obtain more accurate SSH measurements, it should be taken into account disturbance suffered by the radar signal. The related corrections are defined as follows (Nerem ve Mitchum 2001a, Rosmorduc et al. 2018, URL-2):

- *Propagation corrections:* The radar return signal is subjected to a path delay when it passes through the Earth's atmosphere. Eventually, the ionospheric correction due to the atmosphere's electron content, the wet tropospheric correction due to cloud liquid water and water vapour in the atmosphere, and the dry tropospheric correction due to dry gases in the atmosphere are required.

- *Geophysical corrections:* The corrections (Ocean, solid Earth, and pole tides) for the variations associated with the attraction of the Sun and Moon should be taken into account. In addition, the corrections for height variations (loading effect) due to changes in tide-induced forces acting on the Earth's surface are considered.

- *Ocean surface correction:* The correction for the sea state (different reflectivity of wave crests and troughs), which directly affects the radar signal, (electromagnetic bias) are calculated from empirical models. Bias uncertainty is currently the biggest factor in altimeter error budgets.

- *Atmospheric corrections:* As mentioned before, the response of the sea surface to changes in atmospheric pressure (atmospheric loading) has a large effect on sea level changes. Thus, it should be taken account of the Inverse Barometer (IB) correction (low frequency). Besides, the atmospheric dynamics correction is used for the ocean's response to atmosphere's high frequency dynamics.

- *Instrumental corrections (Rosmorduc et al. 2018):* The corrections (Ultra-stable oscillator correction; Correction for variations in the satellite's centre of gravity; Correction tables derived from altimeter simulations for instrument and algorithm effects; Correction for effects due to filters used to eliminate certain frequencies in the return radar signal) are determined by depending on the satellites' characteristics.

The calculated and applied corrections typically vary from one satellite mission to the next (URL-2). For further information on their orders of magnitudes and how they are calculated, refer to Escudier et al. (2018) and Rosmorduc et al. (2018).

In fact, satellite altimetry basically determine the distance from the satellite to a target surface (sea, ice, river, and land) by measuring the satellite-to-surface travel time of a radar or laser pulse. Radar altimetry, which operates on most altimetry mission, works over water and ice, while laser altimetry works on water, ice and land (Braun and Shum 2004). For example, main measurement instrument of the Ice, Cloud, and land Elevation Satellite (ICESat) (2003–2009) & (ICESat-2) (2018–present) missions is a laser altimeter system.

The magnitude and shape (waveform) of the reflected signal also contain a lot of information about the characteristics of the surface which caused the reflection. Here, sea state is basic: a calm sea reflects the signal properly, whereas a rough sea scatters and deforms it. In case of a rough sea surface, the return signal to altimeter is weaker (Rosmorduc et al. 2018):

- Significant wave height: It is calculated from the slope of the reflected radar signal (Abdalla 2015).
- Backscatter coefficient (sigma nought): It is a measure of the reflective strength of the target surface.
- Wind speed: It can be calculated from the mathematical relationship with the backscatter coefficient and the significant wave height using empirical models. The amplitude of return radar signal is significant to detect wind speed (Abdalla 2015).

In this sense, satellite-altimeter measurements also provide useful by-products for studying waves, winds, rain, etc. In comparison with in-situ measurements, the satellite altimetry allows measuring the shape of sea surface globally and frequently. Such measurements have a wide range of applications to Earth sciences (sea level change studies, determination of ocean variability, monitoring of general ocean circulations, coastal applications, detecting of ice topography, ice classification, bathymetry, geoid determination, marine geophysics, modelling of tsunami propagation and dissipation, forecast of ocean dynamics such as eddies and tides, hydrology, climatology studies, etc.) (Fu and Cazenave 2001, Rosmorduc et al. 2018, URL-2):

- **Geodesy:** As mentioned before, the altimeter measurements make it possible to compute the Mean Sea Surface (Rosmorduc et al. 2018) which is a particular time-averaged formation of the continuously fluctuating boundary between the oceans and the atmosphere (Tapley and Kim 2001). The MSS is shaped by permanent ocean currents, however predominantly, by the gravity field (see Equation (3.4)). Figure 3.10 shows an example of recent Mean Sea Surface provided from the AVISO. The gravity field depends on distribution and density of materials on the ocean floor.
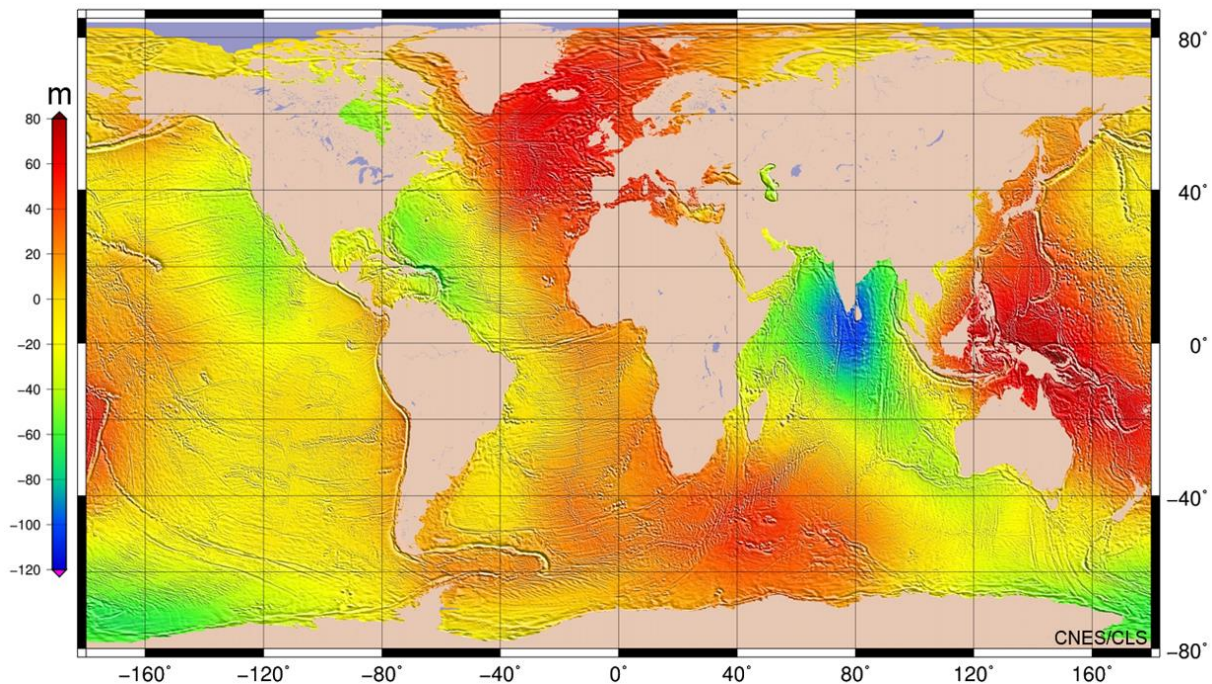
Figure 3.10 CNES CLS 2015 Global Mean Sea Surface, computed from 20-year altimetry data. It is available on regular grid of 1 minute. Further information and data can be find in URL-2.

In ocean's surface, very small variations in the Earth's gravitational (which is the component of gravity) field cause large 'bumps' in places where gravity is high and pulling more water closer, or 'valleys' where gravity is low (Figure 3.11b and c) (Rosmorduc et al. 2018, URL-8, URL-26). For example the extra gravitational attraction of a massive mountain on the ocean floor attracts water towards it causing a local bump in the ocean surface. This bump cannot be seen with the naked eye because the slope of the ocean surface is very low. That is why that the tilt in the direction of gravity, called a 'deflection of the vertical', is equal to the slope of the sea surface, and is measured in microradians. One microradian of deflection appears as a 1 mm change in sea surface height per 1 km of horizontal distance (URL-8). Nevertheless, this is measurable from

space. In this context, satellite altimetry provides measurements of sea surface topography which is an integral of the ocean interior.

The geoid defines an equipotential surface of the Earth's gravity field that is closely associated with the location of the Mean Sea Surface (Rosmorduc et al. 2018). This equipotential surface deviates with extreme values of approximately 83 m and -106 m from the reference ellipsoid which is the smooth, mathematical model of the Earth's figure. The geoid is not directly observable: its height above the reference ellipsoid can be calculated from a model of the Earth's gravity field. The geoid determination is traditionally carried out on land and at sea areas using gravity anomaly and altimetry data. Determination of the geoid at mesoscale and shorter wavelengths has come from altimetry (Smith 2010).

Accordingly, a marine geoid, which is the hydrostatic equilibrium shape that sea level would take in the absence of tides, currents and winds (Smith 2010), refers distance above the reference ellipsoid. At sea, the altimetry data give the dominant geoid information (Li and Sideris 1997, Vergos 2002). This is so, altimeter measurements have a vital importance for geodesy, and provide a nearly direct measurement of the main estimation quantity of geodesy, i.e., geoid heights. Since the altimetric observations (i.e., SSHs) correspond to the separation of the sea surface from the reference ellipsoid, and are very close to geoid heights. Thus, the deviations of the geoid above the ellipsoid can be derived from these measurements using appropriate procedures. Marine gravity field modelling and marine geoid determination using satellite altimetry data were analysed in detail by Vergos (2002).
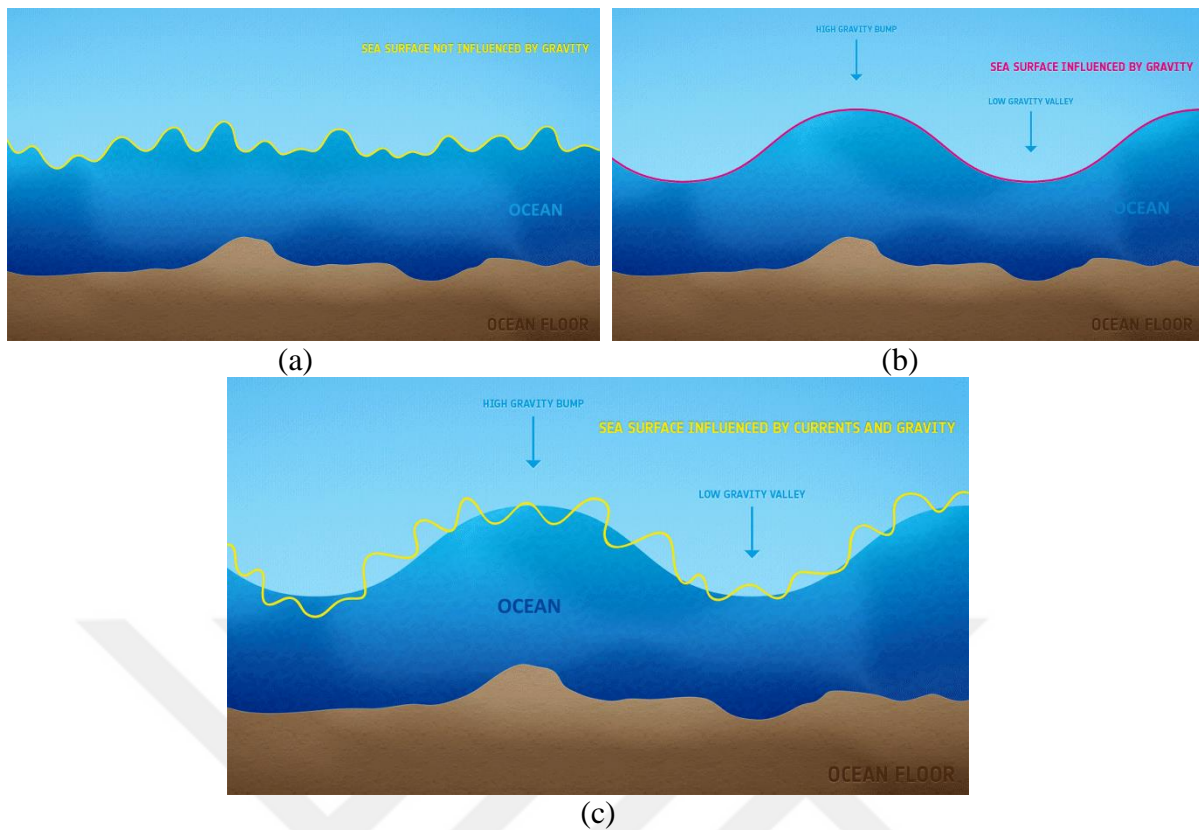
Figure 3.11 Sea surface slopes induced by a) only ocean currents, b) only gravity variations, c) both ocean currents and gravity (modified from URL-26).

- **Bathymetry:** Bathymetry is the measurement of the ocean depths. An Earth-orbiting radar in space cannot see the sea bottom, but it can measure Sea Surface Height variations induced by sea floor topography. That is, although it is not possible to map the floor topography of the ocean basins directly from space, the dense satellite-altimeter measurements can be used in combination with sparse measurements of sea floor depth to construct a uniform resolution map of the sea floor topography. As stated above, the data obtained from the satellite-altimeter measurements mostly reflect the gravity field variations of ocean basin. As a result, gravity anomaly variations are highly correlated with sea floor topography and thus, enable to recover topography information (Rosmorduc et al. 2018, Sandwell and Smith 2001, Vergos 2002, URL-8). Nevertheless, it should be noted that the correlation is stronger over rough topography in deeper ocean where sediment cover is thinner, while it is weaker on continental margins and abyssal plains (URL-8).

- **Oceanography:** Satellite altimetry provides a powerful tool for determining sea level change on both the global (see Section 3.1.1) and regional (see Section 3.1.2) scales. At the present time, thanks to the global coverage of satellite altimetry, estimates of the rise in sea level have improved in accuracy. Even with 15-year sea level time series, it is possible to observe trends (Rosmorduc et al. 2018).

  Satellite altimetry also enables to monitor marine currents and ocean circulations. The ocean surface is constantly moving because of the Sun. Since the Earth's axis of rotation is tilted, the Sun's heat is not felt equally everywhere. Natural circulation of heat between the atmosphere and oceans, driven by currents and winds, smooths out any imbalances (URL-22). For example, the ocean currents are moving bodies of water, and hence altering ocean surface topography by a few tens of cm to more than one m. As described above, such a case causes the difference called ADT between the geoid and the actual sea surface. The main application of the ADT is for the determination of large-scale ocean circulations (like Gulf Stream). This is used to calculate the speed and direction of ocean currents. Thus, it provides information to study weather, climate, and other dynamic ocean phenomena. As mentioned before, in the absence of any motions, the ocean surface would be conformed to the geoid. In order to see ocean currents alone, the shape from gravity needs to be removed (Figure 3.11a). It means that the geoid should be determined independently with sufficient accuracy, for example from satellite gravimetry. The detailed information about how to obtain the dynamical topography with sufficient resolution can be found in Fu (2014) and Vergos (2002).

  Moreover, ocean eddies playing an important role in ocean circulation and heat transport as well as in the ocean's biogeochemical cycles can be monitored using merged altimetry data (Rosmorduc et al. 2018).

  Satellite altimetry also provides measurements of Sea Surface Heights in the open ocean accurate to 2-3 cm, and as such, the observations allow improving tide prediction models. These tide models are used to remove tidal effects from altimetry data (Le Provost 2001).

- **Glaciology:** If both of the Greenland and Antarctica ice sheets were to melt, the sea level would rise by about 80 m (URL-2). Satellite altimetry enables to observe the dynamics of ice sheets and sea ices. Altimeter measurements can be used to determine topography of mountain glaciers (Foresta et al. 2016) as well as mass changes of the Antarctica and Greenland ice sheets (McMillan et al. 2015). Altimetry is the only tool measuring the thickness of sea ice (like that of covering the Arctic Ocean) which is

seawater that has frozen, and typically floating (Laxon et al. 2013). In addition, altimeters allow observing snow accumulation rate and snow drift caused by wind, by providing backscatter coefficient and waveform which are indicator of surface roughness, and snow pack characteristics such as stratification and ice grain size (Rosmorduc et al. 2018).

- **Climate studies:** Ocean is a vital component of the climate system (Bigg et al. 2003). It is constantly on the move, and exchanges heat and other climate quantities with the atmosphere. Therefore, the ocean's influence upon the atmosphere is regarded as a decisive factor of climate forecasting (URL-2). On the other hand, the oceans are being disproportionately impacted by the climate changes. Satellite altimetry provides data for the forecasting models of ocean-atmosphere coupled events such as El Nino, NAO or other decadal oscillations. It means that these recurring atmospheric phenomena over the years in close step with the ocean can be well documented via the satellite data. Actually, better knowledge of ocean circulation allows understanding and predicting climate more accurately (McWilliams 2006). This is why that sea surface temperature and sea level anomalies in the intertropical Pacific affect climate worldwide. In the tropical Pacific, there are a strong interaction between ocean and atmosphere (especially for trade winds) circulations (Rosmorduc et al. 2018). Some years, heat transfers between ocean and atmosphere are considerable and lead to devastating precipitations and storms when reaching South America. For example, this case can be appeared as positive sea level anomalies. In this sense, satellite altimetry missions have monitored the ocean-climate changes in the Pacific Ocean, such as warm El Nino (1992, 1994, 1997, 2002, 2004, 2006 and 2009) and cold La Nina episodes (1995, 1996, 1998, 1999 and 2007). The El Nino and La Nina patterns versus normal pattern are explained in URL-2.

  As for Atlantic, NAO index, which is driven by ocean interaction with pressure differences between a high-pressure system over the Azores and a low-pressure system over Iceland, has a direct impact on the climate of Europe. Wave heights in winter are very sensitive to pressure variations over the North Atlantic. Fluctuations in the NAO cause changes in sea level. Such that, the ocean responses to shifts in the prevailing winds, which drive the currents, waves, sea surface temperature, etc., and thus SSH varies. These all variations are observed by altimetry satellites (Rosmorduc et al. 2018). Altimetry is also helping seasonal climate forecasts by providing information on the ocean dynamics (URL-2).

- **Atmospheric studies:** As previously explained, altimetry data can be used to compute wave height and wind velocity (Abdalla 2015). In this context, satellite altimetry can provide near real-time (within 3 to 48 hours) data to improve weather forecasting models (Rosmorduc et al. 2018). Long-term data statistics belonging to these quantities enables to very useful information for offshore industries or navigation. In addition, wave periods can be derived from altimeter measurements. Moreover, sea level anomaly, which is one of determiners of the warm currents, thus makes it possible to determine the hurricanes from their energy source. Also, using the dual-frequency altimeters, rain rate over the entire ocean can be found out. Furthermore, carbon dioxide absorption increases with sea surface roughness, thus altimetry data can be used for detecting air-sea gas transfer rates. For more detailed information on using of satellite altimetry data for the atmosphere studies, see Rosmorduc et al. (2018).
- **Hydrology:** The levels of lakes and rivers can be monitored by satellite altimetry (Jiang et al. 2017). The level information is significant especially for regional climate changes.

Here, it is also noteworthy that Synthetic Aperture Radar (SAR) altimetry has been used for nearly 10 years in many applications such as monitoring of inland waters, detecting of the variations in the thickness of ice sheets, etc., (Rosmorduc et al. 2018). The observations from SAR altimetry present reduced measurement noise, improved performance in coastal regions and improved spectral information content for sea level anomaly at the ocean mesoscale (Gommenginger et al. 2013). This is why that the greater pulse-to-pulse averaging leads to better precision in range, and a much smaller along-track footprint enables to the ability to resolve shorter-scale ocean features, and improves performance near land. Besides, because of Delay-Doppler processing, SAR mode provides an improved along-track resolution with respect to conventional low resolution (pulse-limited altimeter) mode (e.g. ~ 300 m compared to few km), and hence a reduced land contamination. CryoSat-2 is the first satellite offering SAR mode, and is being followed by the Sentinel-3 satellites.

Depending on the orbit characteristics, each satellite is flying in different patterns. Projected onto the Earth's surface, the flight lines are called tracks (Braun and Shum 2004). The significant orbital parameters for satellite altimetry missions are altitude (to obtain SSH), inclination (for the covering area) and period (for temporal resolution) (URL-2). In this context, a combination of several satellites enables high-precision altimetry. URL-2 demonstrates that at least two altimetry satellites are required to map the ocean and monitor its movements

precisely, particularly at mesoscale. If a satellite has a longer orbital cycle, it enables a higher spatial resolution. For example, merging of four altimetry satellites data, the resolution of Sea Surface Height measurements is greatly enhanced. At least three satellites are needed to observe eddies.

Altimetry products (e.g., GMSL, along-track and/or gridded SLA time series at 10-day or monthly intervals, wind and wave data) have been available in the French Archiving, Validation and Interpretation of Satellite Oceanographic Data (AVISO) (URL-2), Copernicus Marine Environment Monitoring Service (CMEMS) (URL-27), Radar Altimeter Database System (RADS) (URL-28), and Open Altimeter Database (OpenADB) (URL-29) through different means such as File Transfer Protocol (FTP). Besides, many research groups provide recent GMSL information by processing data from the various altimetry missions: National Aeronautics and Space Administration (NASA) (URL-30), National Oceanic and Atmospheric Administration (NOAA) (URL-23), European Space Agency (ESA) Climate Change Initiative (CCI) Programme (URL-31), University of Colorado (URL-32), and Commonwealth Scientific and Industrial Research Organisation (CSIRO) (URL-33).

For example, the Data Unification and Altimeter Combination System (DUACS) is one of processing system used to produce altimetry sea level products (URL-25). Here, along-track (L3) and gridded (L4) sea level products are processed over different regions and in Near Real Time (NRT) and Delayed Time (DT) conditions (PUM 2019). These products were previously distributed by the AVISO, while they are now produced and distributed as part of the CMEMS.

3.2.2.1 Coastal Altimetry

In fact, satellite altimetry is designed for open ocean. Nevertheless, there are a requirement for the altimeter-derived measurements of sea level, wind speed and significant wave height in the coastal zone, where human populations, and hence commercial and social activities are more concentrated, but having larger variations in water levels. Exploitation of altimetry data along the coast is significant for coastal erosion, flood risk assessment, extreme weather forecasting, high-resolution bathymetry, ocean-estuary interactions, maintaining coastal structures, etc. However, while satellite altimeters perform very well over the open ocean, a number of problems arise in the vicinity of land, related to inaccurate geophysical corrections and artifacts in the reflected signals linked to the presence of land within the footprint (i.e., contamination

of the waveforms) (Figure 3.12) (Gommenginger et al. 2011, Vignudelli et al. 2006). And standard altimetry data are normally flagged as "bad" or "not reliable" in official products for these such areas; even so, the altimeter-derived measurements can be recovered. Coastal altimetry, which is defined as a branch of altimetry, is applied over such ocean area close to land where standard processing is problematic (Vignudelli et al. 2011). In this context, the coastal altimetry is a set of techniques for retrieving altimetry information close to the shore by retracking and/so providing improved corrections (Roblou et al. 2011, URL-34).
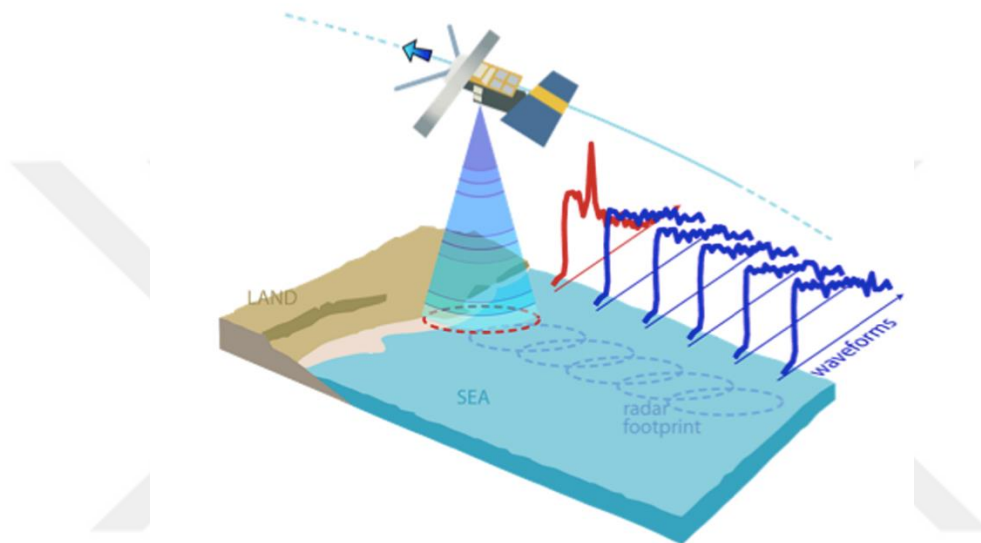
Figure 3.12 Corruption of altimeter waveforms near the shore (from URL-34).

In coastal systems, shorter spatial and temporal scales lead a complex ocean dynamics, and the temporal and spatial sampling of current altimeter missions is not mostly fine enough to capture such variability (Roblou et al. 2011). For example, tides are much more complex near the shores than in the open sea, and require a highly precise knowledge of the coastal geography to be accurately computed. In addition, rapid (i.e., with high frequency) variations must be taken into account in these areas (for the tides and atmospheric pressure). Wet tropospheric corrections are also less precise, or even missing, near the coasts (URL-2). Actually, this case is explained as follows (Vignudelli 2016):

- Up to shore (0–10 km): The altimetric echoes are affected by land and specular reflections. Improved tides, wet tropospheric corrections and waveform retracking are needed.

- Coastal strip (0–30 km): Radiometer-derived wet tropospheric correction is affected by land vicinity. Improved tide, high frequency atmospheric effects and wet tropospheric corrections are applied.

- On the shelf (0–100 km): Main problem is the correction of tides and high frequency atmospheric effects: A good tidal and atmospheric models are needed.

The quality of coastal altimetry depends on improving of understanding of the ocean at short scales, and attaining the extra resolution. Today's altimetry missions such as CryoSat-2, AltiKa and Sentinel-3 satellites already have been enabling to better nadir-viewing to improve both quantity and quality of coastal altimetry data. It is foreseen that the NASA's future mission Surface Water and Ocean Topography (SWOT) satellite (launching date is 2021) will provide a wide-swath (Vignudelli 2016).

Furthermore, as mentioned before, since SAR altimetry provides a finer spatial resolution along the track, it leads less contamination close to land. Moreover, it exploits coherent processing of groups of transmitted pulses, and thus enables to the most efficient use of the power reflected from the surface. SAR altimetry can also detect small signals in noisy coastal environment. Therefore, this technique is very well suited for coastal altimetry (Abulaitijiang et al. 2015, Idzanovic et al. 2018).

Moreover, many space agencies have been supporting the coastal altimetry with several projects from past to present; such as Prototype Innovant de Systeme de Traitement pour les Applications Cotieres et l'Hydrologie (PISTACH) (2007–present) (Mercier et al. 2009) funded by the French National Centre for Space Studies (Centre National d'Etudes Spatiales - CNES), and the ESA development of COASTal ALTimetry (COASTALT) (URL-35) (2008–2011) followed by eSurge (2011–2015) (URL-34). The PISTACH products are provided by the AVISO (URL-2). Besides, there are a few experimental datasets depending on various reprocessed satellite data: Center for Topographic studies on the Ocean and Hydrosphere (CTOH) coastal products (URL-36), Adaptive Leading Edge Subwaveform (ALES) retracker products (URL-29), and Prototype for Expertise on AltiKa for Coastal, Hydrology and Ice (PEACHI) coastal altimetric datasets (Valladeau et al. 2015, for data: URL-2).

3.2.3 Measuring Components of Sea Level Change

Both globally and regionally, change (and variation) in the sea level can result from change (and variation) in mass of the water column, or change (called steric) (and variation) in density caused by temperature and salinity fluctuations. Steric sea level forms with the density variations in the water columns, as the temperature increases or the salinity decreases it rises or when the reversal occurs it falls. However, since the density-induced fluctuations do not cause changes in the ocean bottom pressure, they do not cause any change in the gravitational field of the Earth. On the other hand, the mass-induced sea level variations arise from either its redistribution by movement of ocean mass or adding/subtracting water mass to/from the water columns. And it causes the ocean bottom pressure to change thereby the Earth's gravitational field (hence the Earth's gravity field) (Simav 2012a).

Satellite altimetry observes total sea level change, that is, altimeter sea level measurements include the signal caused by steric effect, and non-steric barotropic and mass variations (Chambers et al. 2004, Garcia-Garcia et al. 2010). The steric changes can be estimated from depth profiles of temperature and salinity, oceanographic in-situ measurements, and/or Ocean General Circulation Models (OGCM)s which often assimilate the mentioned measurements. The mass-induced changes, which having a gravitational signature, can be estimated from time-variable gravity measurements, such as those available from the satellite mission of the Gravity Recovery and Climate Experiment (GRACE) launched in 2002.

3.2.3.1 Measuring Steric-Induced Change

Temperature and salinity are key factors that determines the density of ocean water and thus forms the convection and re-emergence of water masses (URL-27). The saltier the water, the higher its density. When water warms, it expands and becomes less dense. According to this, cold water is denser and sinks to the bottom of the ocean while warm water remains on the surface. The thermohaline (thermo = temperature, haline = salinity) circulation crosses all the oceans in surface and at depth, driven by temperature and salinity, and affects rainfall patterns, wind patterns, hurricanes and monsoons. It directs large scale movement of waters in the ocean basins. Winds drive surface circulation, and surface circulation carries the warm upper waters poleward from the equator. The cooling and sinking of waters in the polar regions drive deep

circulation. The cold water from the poles back to the tropics. It is known as "global ocean conveyor belt" (URL-37, URL-38). Eventually, the steric-induced changes occur in sea level.

Sea Surface Temperature (SST) is the temperature of the water near the ocean surface; the temperature of seawater is fixed at the sea surface by heat exchange with the atmosphere. Meteorological phenomena such as El Nino, and tropical hurricanes/cyclones are the direct consequences of specific temperature variations at the sea surface. The SST varies between -1.8 °C (temperature at which sea water freezes), and 30 °C in the vicinity of the equator (URL-27). Since water is transparent, the Sun's heat penetrates beneath the surface and is transferred to deeper levels by mixing. Most of solar energy is absorbed within a few meters of the ocean surface, directly heating the surface water. Due to the high specific heat of water, diurnal and seasonal temperature variations are relatively small compared to the variations on land; oceanic temperature variations are on the order of a few degrees, except in very shallow water. Shorter wavelengths penetrate deeper than longer wavelengths. A turbulent mixing by winds and waves establishes a mixed surface layer that can be as thick as 200–300 m, and even more at mid-latitudes in the open ocean in winter or less than 10 m in coastal waters in summer. Between about 200–1000 m depth, the temperature declines rapidly throughout much of the ocean. This region is known as "permanent thermocline", beneath which, from about 1000 m to the ocean floor, there is virtually no seasonal variation and the temperatures are around 2 °C (Paytan 2006).

Sea Surface Salinity (SSS) has also a significant role at estimating the influence of oceans on climate, like the SST. The salinity of surface water depends primarily the balance between evaporation and precipitation. Accordingly, the highest salinities are found in the sub-tropical regions where evaporation is extensive but rainfall is minimal. The influence of surface fluctuations in salinity because of changes in evaporation and precipitation is generally small below 1,000 m, where the salinities are mostly between about 34.5 and 35 PSU at all latitudes (Paytan 2006). Zones where the salinity decreases with depth are typically found at low and mid latitudes, between the mixed surface layer and the deep ocean. These zones are called as "haloclines".

The temperature and salinity of sea water can be measured by satellites and/or in-situ techniques. The satellite-based instruments which are capable of observing the SST are listed as follows (URL-27):

- *Infrared radiometers:* The Advanced Very High-Resolution Radiometer (AVHRR) on board the Meteorological Operational (Metop) satellites (2006–present), the Advanced Along Track Scanning Radiometer (AATSR) on the EnviSat, the Sea and Land Surface Temperature Radiometer (SLSTR) on Sentinel-3 satellites, the Visible Infrared Imaging Radiometer Suite (VIIRS) on the Suomi National Polar-orbiting Operational Environmental Satellite System (NPOESS) Preparatory Project (NPP) mission (2011–present), etc.

- *Microwave radiometers:* The Special Sensor Microwave Imager (SSM/I) aboard the Defense Meteorological Satellite Program (DMSP) missions (1962–present), the Advanced Microwave Scanning Radiometer for EOS (AMSR-E) on the Aqua satellite, the EnviSat Micro-Wave Radiometer (MWR), Topex/Poseidon Microwave Radiometer (TMR), the enhanced Jason-1 Microwave Radiometer (JMR), the Advanced Microwave Radiometer (AMR, AMR-2) on Jason-2 satellite, MicroWave Radiometer (MWI) on HY-2 satellites, etc.

- *Spectroradiometer:* The Moderate Resolution Imaging Spectroradiometer (MODIS) on the Aqua satellite (2002–present).

The ESA's Soil Moisture and Ocean Salinity (SMOS) (2009–present), the NASA's Aquarius (2011–2015) and Soil Moisture Active/Passive (SMAP) (2015–present) satellite missions also contain an L-band microwave radiometer which is able to measure SSS (Dinnat 2019), for example the *2D Microwave Imaging Radiometer with Aperture Synthesis (MIRAS)* on board the SMOS.

In-situ observing systems can provide temperature and salinity from surface to bottom. For this, various platforms and instruments can be used: Research and other vessels, fixed platforms, submersibles or towed vehicles, floats and drifters, etc. For example, the temperature and salinity of the subsurface oceans can be measured from research ships using several data collection instruments. At past, temperature sensors that ships lowered into the ocean with copper wire were mostly used. The wire was transferring data from the sensor to the ship for recording until the wire broke and the sensor drifted away. Although research vessels provide high-accurate parameters from sea surface to the floor, note that these data are with intermittent spatial coverage. So a large-scale distributions of temperature and salinity have generally limited with the sparseness. In order to measure physical properties of the sea water, vehicles are required that can be lowered into the water (to the bottom, if required) to record and take

sea water samples for later analysis in the lab. Typical instruments include (URL-27, URL-37, URL-39, URL-40):

- *Submerged drifters (Argo profiling floats):* Argo is a global array of ~ 3,800 free-drifting profiling floats, spaced about every 3° of latitude and longitude, moving up and down in the water column from the sea surface to 2,000 m every 10 days, and making up to 1,000 measurements of temperature, salinity, and depth during every ascent to the sea surface (Roemmich and Owens 2000, URL-41). They upload the data via satellites. The first Argo floats were deployed in late 1999. Since the early 2000s, the Argo data are made freely available by a collaborative international program which is a part of the Global Ocean Observing System (GOOS) (URL-41, URL-42). Figure 3.13 explains Argo system.

- *Surface drifters:* These drifters are primarily deployed in the context of meteorological data collection programmes. Surface metrological data is collected with sensors on top of the float and a temperature and occasionally a salinity sensor below the float. Surface drifters have a float at sea surface and can therefore transmit data via satellite (Figure 3.14a). They are generally fitted with a sea anchor or holey sock. The NOAA's Global Drifter Program includes satellite-tracked surface drifting buoy observations of currents, sea surface temperature, atmospheric pressure, winds and salinity (URL-43).
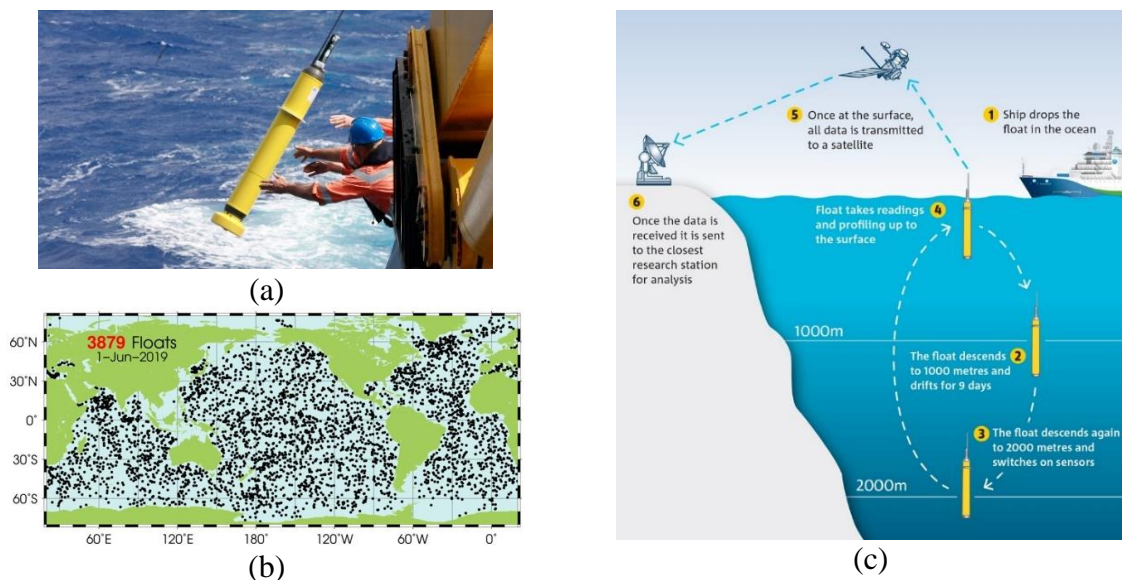
Figure 3.13 Argo system a) Launch of an Argo profiling float (from URL-15), b) Recent locations of the active Argo floats (from URL-41), c) Argo float cycle process (from URL-15).

- *Conductivity, Temperature, and Depth (CTD) profilers:* It is a commonly used tool for determining essential physical properties of sea water. With the CTDs, water sampling is often carried out at specific depths to inform about the physical properties of the water column are at that particular place and time. A CTD operation, depending on water depth, requires 30 minutes to 2 hours.

- *Rosette Sampler:* The CTDs are attached to a much larger metal frame called a rosette (Figure 3.14b), which may hold water-sampling bottles that are used to collect water at different depths. When it is brought back on deck, samples can be tapped from the bottles, and taken to the lab for processing (Figure 3.14c).

- *eXpendable BathyThermograph (XBT):* An XBT is a small probe that is dropped from a ship (Figure 3.14d) and measures the temperature as it falls through the water. Small wires transmit the temperature data back to the ship for be recording. Data can be obtained from the surface down to 450–750 m below sea surface. Since the probe falls through the water at a known rate, the depth of the probe can be inferred from the time of launch, and then a temperature profile as a function of depth can be plotted. For example, the NOAA Atlantic Oceanographic and Meteorological Laboratory (AOML) XBT Network consists of transects across all ocean basins where XBT are used to collect temperature observations of the upper 1 km of the ocean (URL-43).

- *Moorings:* Moorings are used wherever measurements are required at one location over an extended time period. They consist of steel wire or synthetic rope which holds the sensors plus associated buoys made of glass or foam to provide sufficient buoyancy to keep the mooring upright (Figure 3.14f). The moorings record data internally. The buoyancy element can be located at the surface, or subsurface buoy systems can be used. The mooring instruments can capture a time series of the temperature, salinity, etc., nevertheless the limited spatial coverage is compensated by deploying a number of moorings (referred to as an array). Within Tropical Ocean Global Atmosphere (TOGA) program (Anderson 1995), it can be seen a large number of moorings along the equator in the Pacific Ocean.
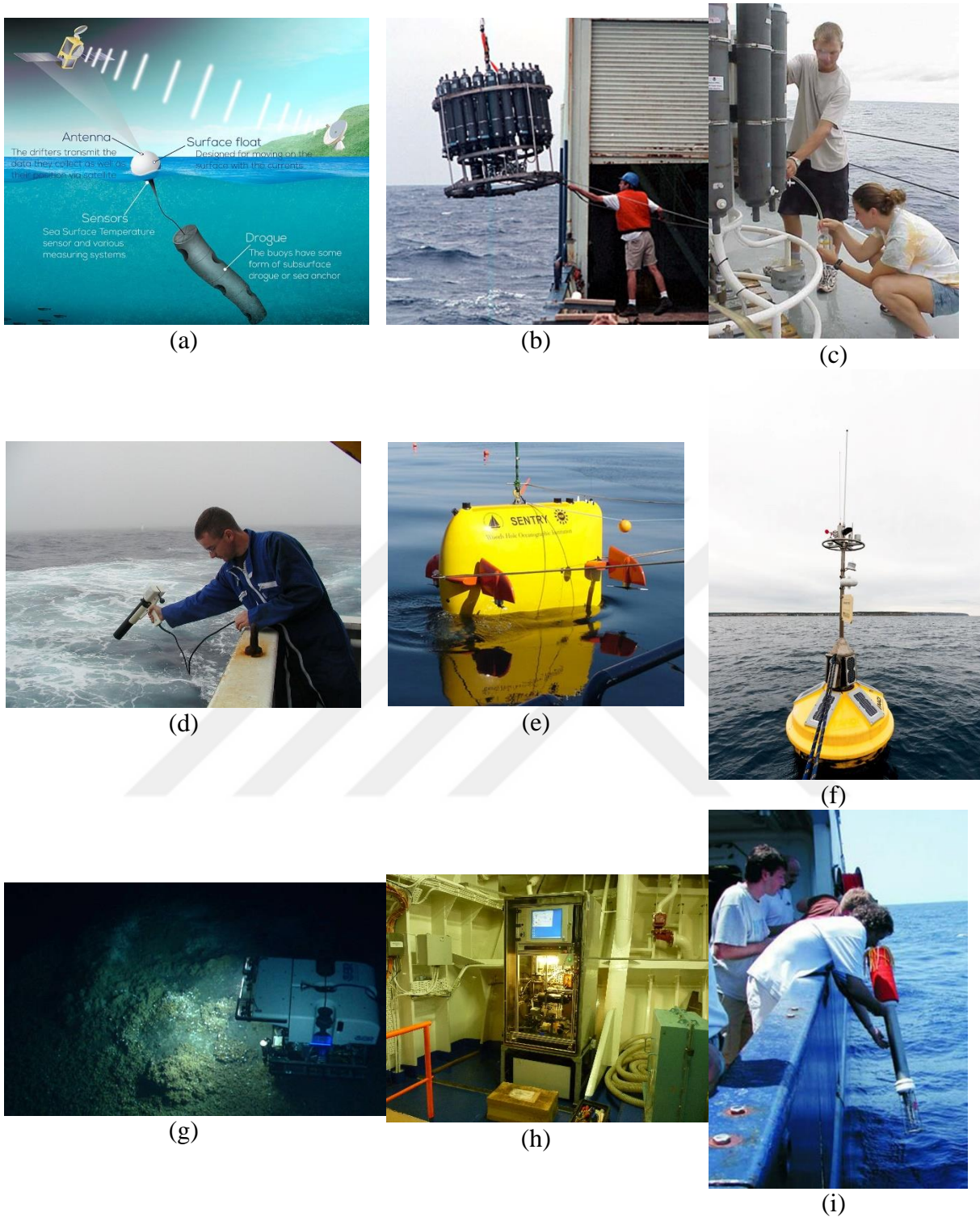
Figure 3.14 In-situ observing systems a) Drifter illustration (from URL-43), b) A CTD Rosette which is being lowered into the water (from URL-39), c) Samples are being tapped from the Rosette bottles (from URL-39), d) A XBT which is being launched from a vessel (from URL-27), e) An AUV which is designed to dive as deep as 6,000 m (from URL-37), f) A moored buoy (from URL-27), g) A ROV on the ocean floor (from URL-37), h) A ferry box on board (from URL-27), i) Deployment of a microstructure profiler (from URL-40).

- *Gliders and Autonomous Underwater Vehicles (AUV)s:* These instruments combine sensors that have been in use for many years in moored systems with a mobile platform. While the floats are carried by ocean currents without any external control, the AUVs and gliders can independently move through the oceans. The AUVs are driven by a conventional propeller and are characterized by their high speed (Figure 14e). The AUVs are considered autonomous because they have no physical connection to their operator, who may be on shore or aboard a ship. They are self-guiding and self-powered vehicles. Fully autonomous operations carry power on board (for example lithium-ion batteries). Power provides propellers or thrusters to move an AUV through the water: it is also necessary to operate sensors on board the AUVs. More information on AUVs, can be find in URL-37. As for gliders, they have no propellers and can only move at relatively slow speed through the oceans. They can be steered from shore via satellite. The gliders can provide physical data from surface to 1,000 m below the surface, whereas some AUVs are designed to operate up to 6,000 m depth.

- *Remotely Operated Underwater Vehicles (ROV)s:* ROVs are highly maneuverable underwater robots operated by someone in the ship. A group of cables send electrical signals back and forth between the operator in the ship and the vehicle. Most ROVs are equipped with a camera to record and send images to the ship (Figure 14g). In order to measure water clarity, water temperature, water density, etc., additional equipment is commonly added like the AUVs. For more information on ROVs, can be seen in URL-37.

- *Ferry boxes:* Ferry boxes, which are used to measure hydrographic properties of the sea water, are found on board ferries, regional ships, small boats, or shores (Figure 14h). It allows a fast survey of temperature, salinity, water depth, oxygen, etc., (URL-44).

- *Microstructure profile:* The microstructure profiler is an instrument designed to measure velocity shear and temperature variability on vertical scales of less than a mm and simultaneously record other physical parameters of the ocean (URL-40). The profiler is constructed to descent to depths as far as 2,000 m with a free falling at a specific velocity (Figure 14i). In order to obtain data on micro scales, the probe operates with a very high sampling rate and is equipped with a fast temperature sensor (micro thermistor), as well as the standard CTD sensors with a lower sampling rate to measure sea water temperature.

Both at global and regional scales, the physical parameters of seas are observed using different in-situ techniques by many institutes and agencies, that some of them are organised in various networks that are coordinated within global, the European or international programmes. The processed data are distributed by national data centres or operational agencies (URL-27) such as the Joint IOC-World Meteorological Organization Technical Commission for Oceanography and Marine Meteorology in situ Observations Programme Support Centre (JCOMMOPS) (URL-45), OceanSITES (URL-46), IOC International Oceanographic Data and Information Exchange (IODE) (URL-47), European Contribution to the Argo Program (Euro-Argo RI) (URL-48), EuroGOOS (URL-18) as well as the NOAA (URL-49). Furthermore, satellite-based data are freely provided by the Copernicus (URL-27), NOAA (URL-49, URL-50), NASA (URL-51), etc.

In addition to the satellite and in-situ observations, the Ocean General Circulation Models provide the information on the physical and biogeochemical processes in the sea. These numerical models enable to predict the properties of oceans as well as the ocean circulations (URL-49). Because, the oceanic general circulation includes the associated pressure, density, temperature, and salinity fields, plus all other elements involved in establishing the dynamical balances for these fields (McWilliams 2006). Therefore, the parameters such as SST or SSS can be estimated by modelling external (winds, evaporation/precipitation, river runoffs, etc.) and internal (horizontal transport, vertical mixing, etc.) influences (URL-27). The ocean models are calibrated by comparing the quantities produced by the model with that measured by different sensors.

The density characteristics of seawater can be defined at the sea surface, as the temperature and salinity of seawater are affected by the processes occurring at the air-sea interface. As above mentioned, the temperatures of seawater vary widely between -1 and 30 °C, whereas the salinity range is small (35 ± 2 PSU). The North Atlantic contains the warmest and saltiest water of the major oceans, the Southern Ocean (the region around Antarctica) is the coldest, and the North Pacific has the lowest average salinity (Paytan 2006). Since the temperature and salinity are the main factors controlling density, the density exhibits a similar behaviour with the salinity towards the ocean floor. The ocean is typically divided into three horizontal depth zones based on density: the mixed layer, pycnocline, and deep layer (URL-38). Wind-driven surface currents are restricted mostly to the ocean's uppermost layer, thus this surface layer having typically thickness 100 m or less is called as the mixed layer. The pycnocline, situated between

the mixed layer and the deep layer, is where water density increases rapidly with depth due to changes in temperature and/or salinity. Sure enough, this layer is also considered as both thermocline and halocline. Typically, the pycnocline extends to a depth of 500 to 1,000 m (However, its width can change at seasonal scale). The dark, cold deep layer below the pycnocline accounts for most of the ocean's mass. Within the deep layer, the density increases gradually with depth. Note that, at high latitudes the mixed layer and pycnocline is improbable.

In general, the density of seawater is not measured directly, it is formulated as a function of temperature, salinity and pressure. The average density (ρ) of seawater is approximately 1.025 g/cm^3. The significant part of this number is generally in and beyond the third decimal. Thus, the convention is to report density as the function (Paytan 2006):

$$\sigma_{S,T,P} = (\rho_{S,T,P} - 1) \times 1000 \tag{3.6}$$

where S, T, P refer to salinity, temperature and pressure (not precipitation), respectively. Thus, a density of $\rho_{S,T,P} = 1.02544$ g/cm^3 becomes $\sigma_{S,T,P} = 25.44$ (Recall that, the density unit of seawater is generally called as only σ_t). The relationship between pressure and density is determined by observing the effect of pressure on the density of seawater at 0 °C and 35 PSU. A one-metre column of seawater produces a pressure of about one decibar, and the pressure increases with depth (i.e., at the sea surface $P = 0$ decibar, at the depth of 1,000 m $P = 1,000$ decibars).

3.2.3.2 Measuring Mass-Induced Change

Interactions between the different components of climate system involve mass variations in land water storages (rivers, lakes, ground water, snow cover, polar ice sheets and mountain glaciers), as well as the mass redistribution within and between ocean and atmosphere. The observations of water and ice mass redistribution in the Earth system at various time scales are critical for understanding the driving factors of observed sea change. Not too far in the past, the mass components of sea level change could only be inferred from the ocean models that do not include water mass flux between the ocean and land, or from a limited number of ocean bottom pressure gauges (Chambers 2006).

Satellite gravimetry measures spatial and temporal change in the gravity field caused by mass variations from space. In this context, the launch of the Gravity Recovery and Climate Experiment (GRACE) on 17 March 2002 has revolutionized understanding of mass transport in the Earth system (URL-52). The GRACE mission ended on 12 October 2017, due to battery failure, nevertheless it operated in an extended mission phase which was ten years longer than the nominal mission lifetime. Now, GRACE Follow-On (GRACE-FO), which launched 22 May 2018, is a successor to the GRACE mission (URL-52). The primary purpose of the GRACE satellite missions, a collaboration between the NASA and the German Aerospace Centre (Deutsche Zentrum für Luft- und Raumfahrt - DLR), is to determine variations in the Earth's gravity field at monthly intervals and at a spatial resolution of several hundred km. By measuring gravity, the GRACE missions show how mass is distributed around the Earth and how it varies over time. Theoretically, the dominant source of time variable gravity is movement of water mass. The GRACE data is an important tool for studying Earth's ocean and climate. Tapley et al. (2019) describe the contributions of GRACE to the climate science with details. Many studies also shows that GRACE data can be used to determine non-steric mean sea level changes (also variations) at both global (Chambers et al. 2004, Chambers 2006, Chen et al. 2018) and regional (Garcia-Garcia et al. 2010, Feng et al. 2013, Simav 2012a) scales. In these studies, generally, by combining current data (satellite altimetry and GRACE, or satellite altimetry and steric) are compared against other sea level observations. Moreover, several studies such as Cazenave et al. (2009), Chambers et al. (2017), Leuliette and Miller (2009) deal with an assessment of the global sea level budget with the measurements from satellite altimetry, GRACE and Argo.

The GRACE missions consist of two identical spacecraft that fly about 220 km apart in a near-polar orbit with an average altitude of about 450 km (Figure 3.15) (URL-52). These missions map the Earth's gravity field by measuring of the distance between the two satellites, which varies due to individual gravitational attractions on the satellites as they pass over the Earth's surface. This measurement is carried with a microwave tracking system accurately. The other equipment on board includes GPS receivers for precise satellite positioning, star cameras for attitude determination, and accelerometers for the removal of non-gravitational forces.

The GRACE twin satellites provide global coverage of the Earth's gravity field every 30 days. After a month, the collected measurements allow an estimate of a global spherical harmonic model of the Earth's gravity field, which is then used to estimate mass changes on the Earth's

surface (Tapley et al. 2019). The GRACE data are processed by the GRACE Science Data System which is between the NASA Jet Propulsion Laboratory (JPL), University of Texas Center for Space Research (CSR) and German Research Centre for Geosciences (GeoforschungsZentrum Potsdam - GFZ). Thus, the level-1B data (calibrated instrument data) are generated, and then the level-2 datasets provided in the form of truncated sets of harmonic coefficients at the monthly intervals (or shorter) are released. These datasets are known as GRACE time-variable gravity field models (or solutions) (Avsar and Ustun 2012).
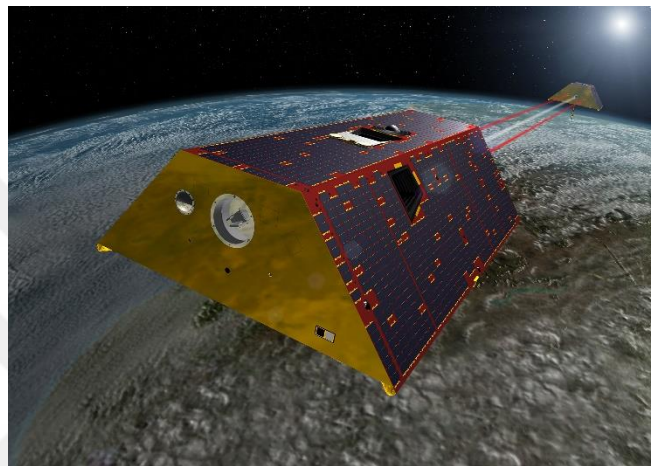
Figure 3.15 Illustration of GRACE Follow-On satellite mission (from URL-52).

On the other hand, the surface mass changes are obtained by subtraction of a mean-field from the GRACE measurements (URL-52). This mean-field mean can be thought of as a spatially-varying-but-constant-in-time reference field. That is, it is referenced to a time-period. After the mean field is subtracted, the remaining signals reflect mass gains (positive change), and mass losses (negative change).

Most of the temporal gravity changes are related to movement of water. This is because water (and also gas) are much more mobile than rock. Ocean surface and/or deep ocean currents, the variations in runoff and ground water storage, ice sheet and glacier changes, and total water cycle are all processes that can move water. How much the mass has changed due to the movement of water averaged over a month is typically expressed as Equivalent Water Thickness (EWT) (URL-52). The vertical extent of the mass changes is measured in centimetres of EWT. It is much smaller than the horizontal scales of the changes, which are measured in kilometres. In this sense, the GRACE data are monthly mass grids corresponding changes in

the EWTs relative to a time-mean baseline. These grids, land and ocean grids, are processed with different filters to remove the noise. Data are based on two different GRACE outputs: Spherical harmonic coefficients and mass concentration blocks (mascons). For information about the monthly mass grids and the related data are found in URL-52. Using these ocean mass grids, monthly estimates of the Earth's gravity field from the GRACE missions can be used to construct a time series of ocean mass changes.

3.3 POTENTIAL IMPACTS OF SEA LEVEL CHANGE

As mentioned in Section 3.1.1, global sea level is rising, and there is evidence that the rate is accelerating. Increasing atmospheric concentrations of greenhouse gases, primarily from human contributions, are warming the atmosphere and oceans. The higher temperatures raise sea level by expanding ocean water, melting glaciers, and possibly increasing the rate at which ice sheets discharge water into the oceans. Today, nearly 10% of the world population is living in coastal areas less than 10 m above sea level (Cazenave and Le Cozannet 2014, Nicholls and Cazenave 2010). Therefore, rising sea level and its possible consequences pose an increasing threat to coastal cities, residential communities, infrastructure, wetlands, ecosystems, and beaches (Nicholls 2010). Furthermore, modelling of future climate change under different radiative forcing scenarios points out that sea level will continue to rise during the next centuries (IPCC 2013). Rising Mean Sea Level and potentially more intense storms will exacerbate possible consequences, and more frequent extreme sea level events will occur.

Sea level rise has adverse effects on the natural system. The main impacts have been typically treated by Leatherman (2001) and Nicholls (2010) as follows:

- Inundation, flood, submergence and storm damage: These effects can be formed as flooding from the sea (surge) or rivers.
- Wetland loss.
- Erosion of soft coastal morphology.
- Saltwater intrusion into aquifers and surface waters.
- Rising water tables without drainage.

Here, the immediate effects are submergence and flooding of coastal land, as well as saltwater intrusion into surface waters. Over time, longer-term effects including wetland loss and change

in response to higher water tables and increasing salinity, erosion of beaches and soft cliffs, and saltwater intrusion into groundwater also appear.

These effects frequently interact with climate and non-climatic factors, and these factors generally aggravate them. For example, sediment supply and shoreline morphology are crucial factors for coastal changes due to sea level rise. Or for example, different wind and wave patterns appearing with changing climate trigger the extreme sea level events (Figure 3.16a and b).

As described before, at regional and local scales along the coast, vertical movements of the land surface can also contribute significantly to sea level change. Thus, along with climate-induced sea level change, relative (e.g., from geological processes such as subsidence) sea level change is also significant in terms of coastal impacts (Nicholls and Cazenave 2010). The relative sea level falls where land uplifts, for example during the Last Glacial Maximum. In contrast, relative sea level is rising more rapidly than climate-induced trends on subsiding coasts. In many regions, human activities (e.g., groundwater withdrawal) are exacerbating subsidence on susceptible coasts. For example, Nicholls and Cazenave (2010) referred to the subsidence of coasts by up to 5 m in Tokyo, 3 m in Shanghai, and 2 m in Bangkok over the 20th century. And they accentuated that as the sea level rise accelerates in response to global warming, the impacts will become more apparent, especially in certain coastal zones with dense populations, low elevations, appreciable rates of subsidence, and/or inadequate adaptive capacity.

The world's coastline is about a million km in length and consists of a wide variety of landforms, from cliffs to coastal plains (Leatherman 2001). Rising sea levels potentially impact all coastal areas to varying degrees, however sandy beaches, coastal wetlands, deltaic areas, and small islands are the most affected.

Sea level observations show that the rate of rise displays strong regional variations (Section 3.1.2). And sea level rise is especially a major threat to low-lying coastal areas (Wong et al. 2014). For example, Nicholls (2010) remarked that the considerable populations in the countries such as Belgium, Canada, China, Germany, Italy, Japan, the Netherlands, Poland, Thailand, the UK, and the USA already live below normal high tides. Besides, according to Nicholls (2010) that the most vulnerable regions to sea level rise are the small island regions of the Caribbean, Indian Ocean, and Pacific Ocean. However, absolute increases in the frequency of flooding are largest in the southern Mediterranean (largely in the Nile Delta), West and East

Africa, South and Southeast Asia. This is so, when taking account of population exposure, sensitivity, and adaptive capacity, these regions appear to be most vulnerable due to storm-induced flooding combined with sea level rise. Furthermore, Nicholls (2004) asserted that roughly 800 million people by the 2080s due to rising population including coastward migration may be vulnerable to flooding by extreme sea levels.
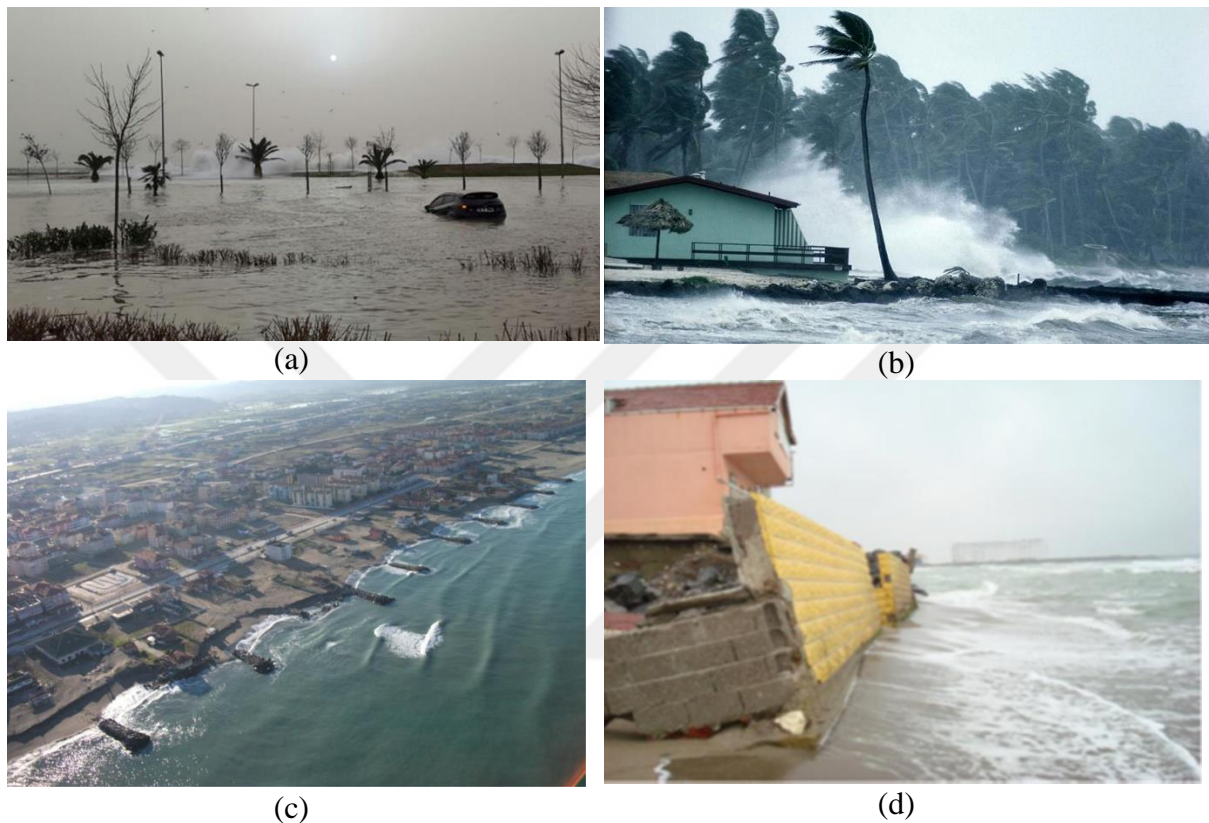
Figure 3.16 Examples of the impacts of present sea level rise a) Pendik-Kadıköy (Istanbul, Turkey) coastal road which was underwater due to the waves raised by the strong southwest wind in February 2015 (from URL-53), b) Hurricane Harvey, Texas, USA (from URL-53), c) Coastal erosion in Karasu (Sakarya) region on northwest coast of Turkey (from Görmüş et al. 2014), and d) A damaged beach house because of the erosion on the shore of Karasu (from Görmüş et al. 2014).

Sea level determines shoreline position, and there is a causal relationship among some factors: sea level, sediment supply, wave energy, and shoreline position (Leatherman 2001). Rising sea level increases coastal erosion unless this area is offset abundant sediment supply. In this sense, the erosion is the most apparent problem of rising sea level (Cazenave and Le Cozannet 2014). Sea level rise generally leads to erosion and causes the shoreline to retreat landwards (shoreline recession) especially on sandy coasts (Figure 3.16c and d). Its reasons were explained in Leatherman (2001). It is estimated that nearly 70% of the world's beaches are currently

experiencing erosion, and erosion of the large magnitude may have significant impacts on coastal ecosystems, infrastructure, land tenure and beaches. The amount of such erosion caused by sea level rise can be approximated by a beach profiling technique such as the Bruun Rule (Bruun 1962) which says that shoreline recession happens at a rate in the order of 100 times the amount of sea level rise, or by more new approaches (such as Armenio et al. 2018, Cooper and Pilkey 2004). In addition to numerical calculations; satellite images, aerial photographs and GNSS technique, terrestrial Light Detection and Ranging (LiDAR), Terrestrial Laser Scanning (TLS), etc., are used to measure coastal profile change (Ali et al. 2010, Görmüş et al. 2014, Le Cozannet et al. 2013, Maktav et al. 2002).

The coastal wetlands (seasonal and permanent coastal marshes or freshwater reservoirs, etc.) and deltaic areas (formed where terrigenous sediment accumulated to the coast by rivers) have both ecological and economic value, also exist in breakable balance with sea level, and thus are vulnerable to even small increases of sea level (Nicholls 2004, Simav 2012b). Because of comprising extensive low-lying and plain land, the deltaic coasts are particularly vulnerable to any diminishment of sediment supply because of dams and/or any acceleration in the rate of sea level rise. Along these areas, rising sea level (even some tides) often causes direct inundation or submergence of the upland. Consequently; higher water tables, boggy soils, and saltwater intrusion can severely impair these fertile areas (Leatherman 2001).

Sea level projections show that the impacts of a 1 m rise could be significant, and adaptation costs substantial (Nicholls 2010). Leatherman (2001) indicated that the assessments of economic impacts manifest that the cost for a 1 m rise is high for even the developed nations. Nicholls (2010) also focuses on the adaptation and mitigation of sea level rise. The mitigation requires a global-scale activity, whereas the adaptation can be carried out via local and/or national activities. The mitigation should aim to reduce greenhouse gas emission, and hence by minimizing climate change, slow the global sea level rise via a sustainable climate policy. As for adaptation, it means to reduce the impacts of sea level rise via a collective coastal management policy. For this, the coastal management mechanisms should be strengthened by considering existing impacts and potential climate change.

CHAPTER 4

SEA LEVEL CHANGES IN THE BLACK SEA

The Black Sea is a deep sea, although it is one of the farthest seas among the seas of the Atlantic Ocean basin. And it has rather limited water exchange with the neighbouring seas. According to Volkov and Landerer (2015), in the Black Sea, the seasonal sea level budget shows similar contributions of fresh water fluxes (precipitation, evaporation, and river discharge) and the outflow (through to the straits) (see Section 2.4.3), while the impact of the net surface heat flux is smaller although not negligible. The non-seasonal sea level budget is dominated by precipitation and evaporation over the sea itself, but external processes such as river discharge and changes in the outflow can also cause some large-scale sea level anomalies. Sea level is also strongly coupled to terrestrial water storage over the Black Sea drainage basin, which is modulated by the NAO (Aksoy 2017, Woolf and Tsimplis 2002). Consequently, the forcing of sea level in the Black Sea is dominated by the basin's freshwater budget and the water exchange through the Bosporus Strait as well as depth-integrated changes in the seawater density.

Sea level measurements are mainly based on two techniques: 1. Tide-gauge stations, 2. Satellite altimetry. At the tide-gauge stations, the height difference between instantaneous sea level and a geodesic point on land (tide-gauge benchmark) is measured. As described in Section 3.1, the position of sea level relative to an earth-centred datum is absolute sea level, and the time-dependent change of this level is called absolute sea level change. However, it is known that the land consistently moves in vertical direction (subsidence or uplift) due to various reasons (tectonic, etc.). Accordingly, the movement of the sea level relative to the land on which tide-gauge station is located, is relative sea level change. In other words, relative sea level is measured at a tide-gauge station. Absolute sea level changes are determined by satellite altimetry technique (see Section 3.2.2). Long-term sea level data are required to determine sea level changes with high accuracy. At least 50 year-records are needed to separate secular, decadal and interannual variations, and obtain more accurate trend estimations of sea level change (Douglas 2001, Fenoglio-Marc and Tel 2010).

In this section of the study; seasonal and long-term sea level changes in the Black Sea have been investigated by using data from satellite altimetry and tide-gauge stations. This section presents an evaluation of present-day sea level change in the Black Sea.

4.1 DATA ANALYSIS

Data analysis requires collection of data and process of them using various statistical methods and numerical models. In this study, in order to analysis sea level data from tide-gauge, satellite altimetry, satellite gravimetry, etc., over the Black Sea, firstly these data have been provided from the related agencies, and the outlier detection has been performed using 3σ-rule. Then, monthly averaged time series of the sea level observations have been obtained to provide concurrent analysis. For sea level time series analysis, harmonic analysis method has been preferred. All the analysis in this study have been carried out using MATLAB software.

4.1.1 Outlier Detection and Interpolation of Data

Outlier detection is a primary step in the data analysis. An outlier is an observation that appears to deviate clearly from other observations. Sea level observations are sometimes contaminated by outliers. In this case, if possible, outliers should be excluded from the related data set. The methods for outlier detection were given in Ben-Gal (2005) and Lehmann (2013).

A simple and in practice widespread method for outlier detection is known as 3σ-rule (Lehmann 2013). An observation is considered as an outlier if its least squares residual exceeds three times its standard deviation. In this study, the 3σ-rule is used to find outliers in the sea level measurements.

Some sea level time series (especially tide-gauge and GRACE) contain the missing values. The linear interpolation has become sufficient to estimate the data gaps of sea level observations. Linear interpolation provides to estimate a new value by connecting two nearest known values with a straight line. Accordingly, here, the data with more than 4 consecutive missing months in one year have not been used. Other missing data have been interpolated linearly.

4.1.2 Harmonic Analysis

Harmonic analysis describes periodically recurrent phenomena. It provides to analyse sinusoidally varying with time. The mathematical expression for a periodic function are not generally unknown. However, these functions can be expressed as the sum of a number of sine and cosine terms, and the determination of the coefficients of these terms is defined harmonic analysis. For further information on harmonic analysis, it can be find in Feizabadi (2016) and Pugh (1996).

Sea level changes have a periodic character. In this context, sea level time series exhibit a strong seasonality as well as a linear trend as mentioned in Cazenave et al. (2001). The seasonal variation of sea level time series can be determined by harmonic analysis. As for the long-term trend of sea level time series, it can be estimated by a simple linear regression. So, a model including seasonal components (annual and semi-annual harmonics) and linear trend has been used in this study (Feng et al. 2013):

$$M(t) = M(t_0) + v(t - t_0) + \sum_{k=1}^{2} A_k \cos(\omega_k(t - t_0) + \varphi_k) + \varepsilon(t) \tag{4.1}$$

where $M(t)$: sea level time series, t: time, t_0: beginning time (for example for altimetry: 1 January 1993), $M(t_0)$: mean sea level at t_0, v: the rate of sea level change (linear trend), $k = 1$ annual signal, $k = 2$ semi-annual signal, A: amplitude, ω: angular frequency, φ: phase, $\varepsilon(t)$: unmodelled residual term. Here, in order to estimate trend, phase and amplitude, the least squares method has been employed (Pugh 1996).

4.2 RELATIVE SEA LEVEL CHANGE IN THE BLACK SEA

4.2.1 Tide-Gauge Records along the Black Sea Coast

The results obtained with the satellite altimetry for sea level changes belong to after 1993. However, the existence of long-term data in many tide-gauge stations is still one of the most important reasons for using these stations in sea level measurements. Nevertheless, there are some problems in tide-gauge stations along the Black Sea coast, such as poor spatial distribution. Each station has a different data length. Moreover, most of the records suffer from

data gaps and/or short data period. Note that the numbers of obtainable tide-gauge station data are limited. In this study, data of 13 tide-gauge stations on the Black Sea coast (including 1 station in the Bosporus) have been used, which have different time intervals. 7 tide-gauge stations (Poti, Batumi, Sevastopol, Tuapse, Varna, Bourgas, and Constantza) located at along the Black Sea coast have been chosen from the Permanent Service for Mean Sea Level (PSMSL) and other 6 tide-gauge (Amasra, Igneada, Istanbul, Trabzon, Sinop, and Sile) are from the Turkish Sea Level Monitoring System (TUDES). Figure 4.1 shows the locations of all the stations in this study. An overview of the tide-gauges is given in Table 4.1.
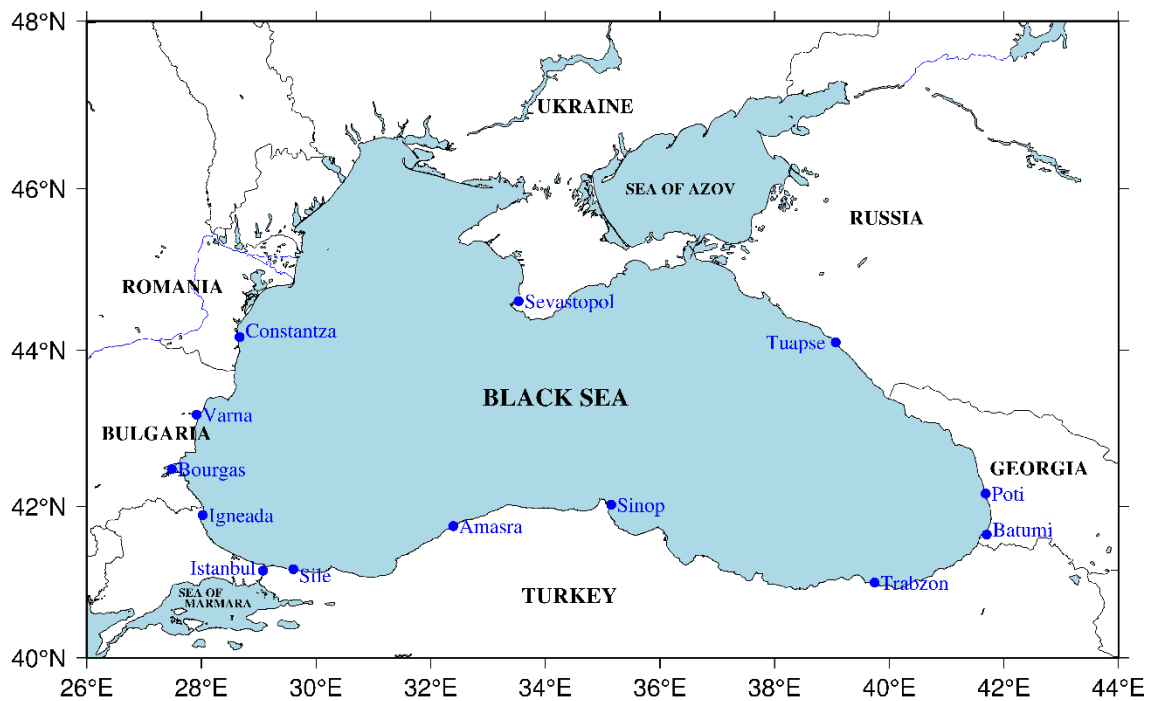
Figure 4.1 Tide-gauge locations along the Black Sea coast used in the study.

The Revised Local Reference (RLR) data from the PSMSL are the monthly averaged time series, spanning from 65 to 140 years in the period of 1874–2013. As for the TUDES data, the data have been provided at 15-minute intervals in the TUDKA-99 datum. In the study, the monthly averaged time series of the TUDES data have been derived at each station. The record with the longest time period among these stations extends to mid-2001 at Amasra (see Table 4.1). Figure 4.2 (from a to m) shows the records of relative sea level change at 13 tide-gauge along the Black Sea coast.

Table 4.1 General information on all the tide-gauges in this study.

Tide-gauge station (Country)	Location		Time-span	Date of first data
	Latitude	Longitude		
Poti (Georgia)	42 10 N	41 41 E	1874–2013	January 1874
Batumi (Georgia)	41 38 N	41 42 E	1882–2013	January 1882
Sevastopol (Ukraine)	44 37 N	33 32 E	1910–1994	January 1910
Tuapse (Russia)	44 06 N	39 04 E	1917–2011	January 1917
Varna (Bulgaria)	43 11 N	27 55 E	1929–1996	January 1929
Bourgas (Bulgaria)	42 29 N	27 29 E	1929–1996	January 1929
Constantza (Romania)	44 10 N	28 40 E	1933–1997	January 1933
[*]Amasra (Turkey)	41 45 N	32 24 E	2001–2014	13 June 2001
[*]Igneada (Turkey)	41 53 N	28 01 E	2002–2014	29 June 2002
[*]Trabzon (Turkey)	41 00 N	39 44 E	2002–2014	14 July 2002
[*]Sinop (Turkey)	42 01 N	35 09 E	2005–2014	18 June 2005
[*]Sile (Turkey)	41 11 N	29 37 E	2008–2014	16 July 2008
[*]Istanbul (Turkey)	41 09 N	29 04 E	2011–2014	27 June 2011

[*]TUDES stations
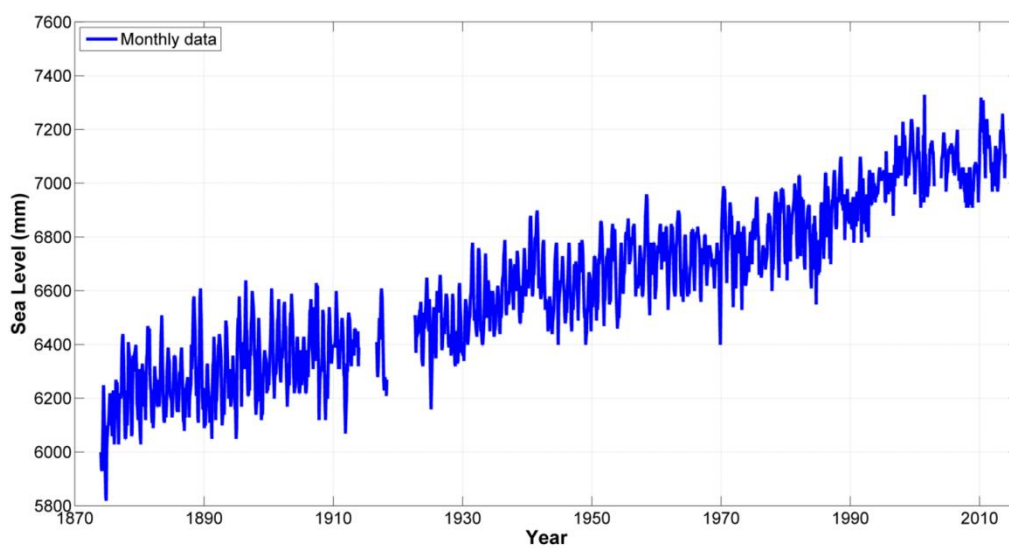
a) Poti tide-gauge station.

Figure 4.2 Monthly Mean Sea Level changes along the Black Sea coast.
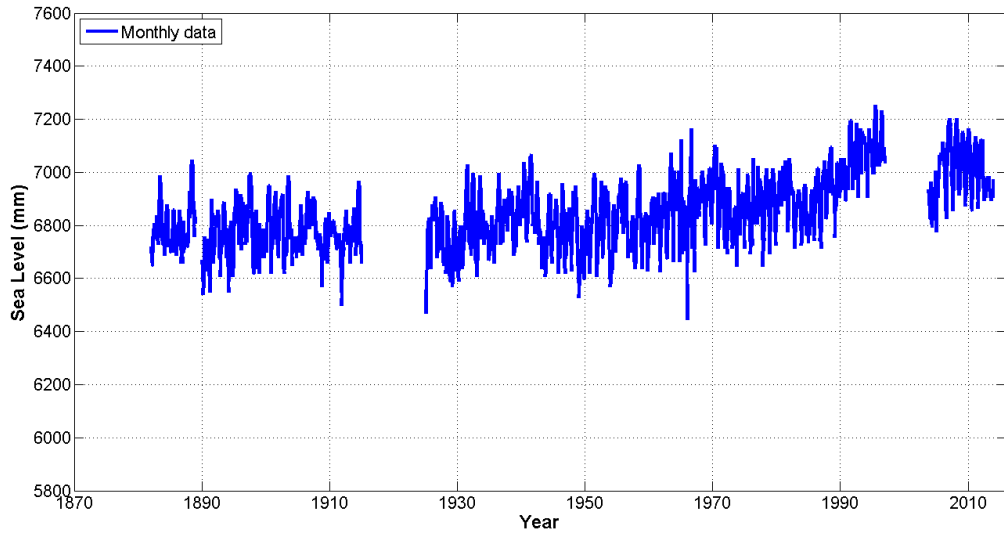
b) Batumi tide-gauge station.
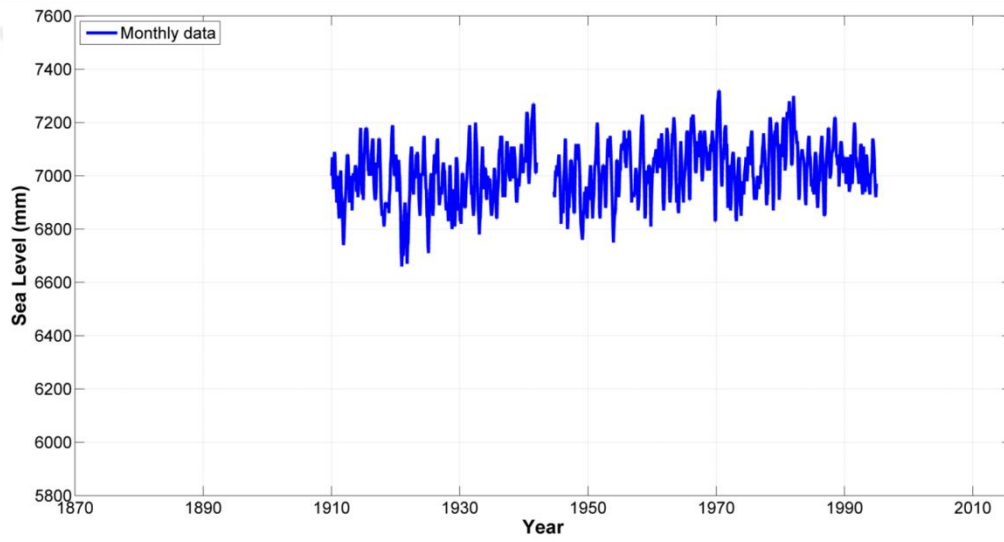
c) Sevastopol tide-gauge station.
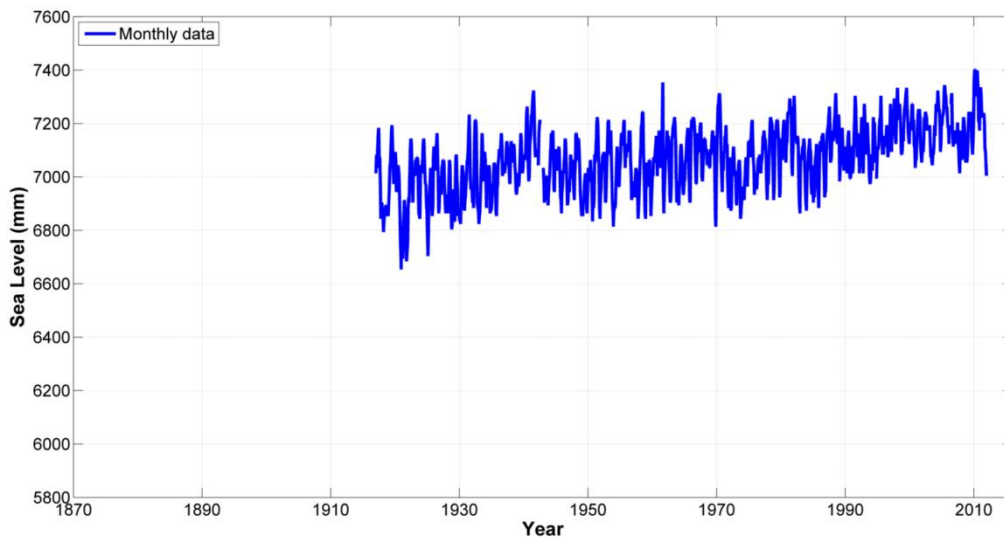
d) Tuapse tide-gauge station.

Figure 4.2 (continued).
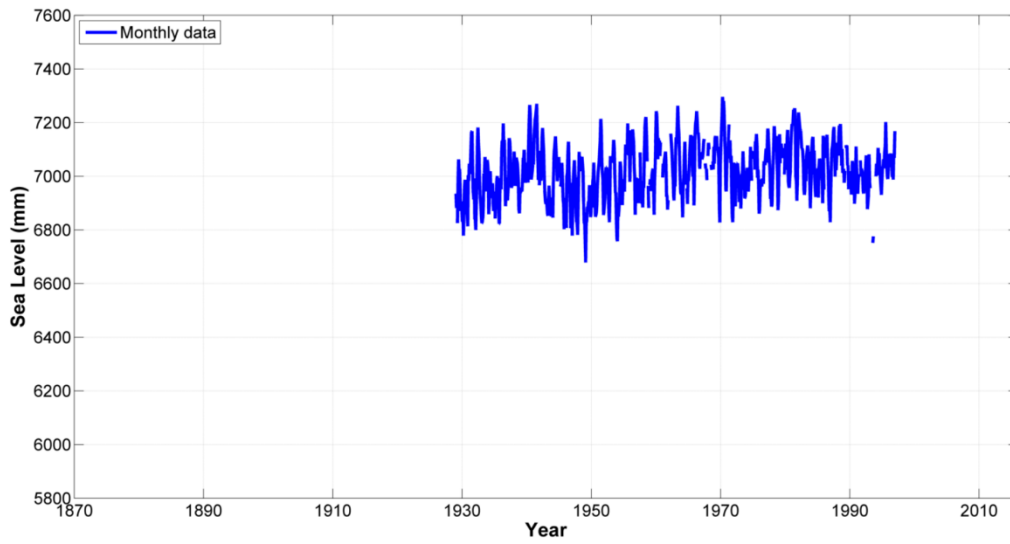
e) Varna tide-gauge station.
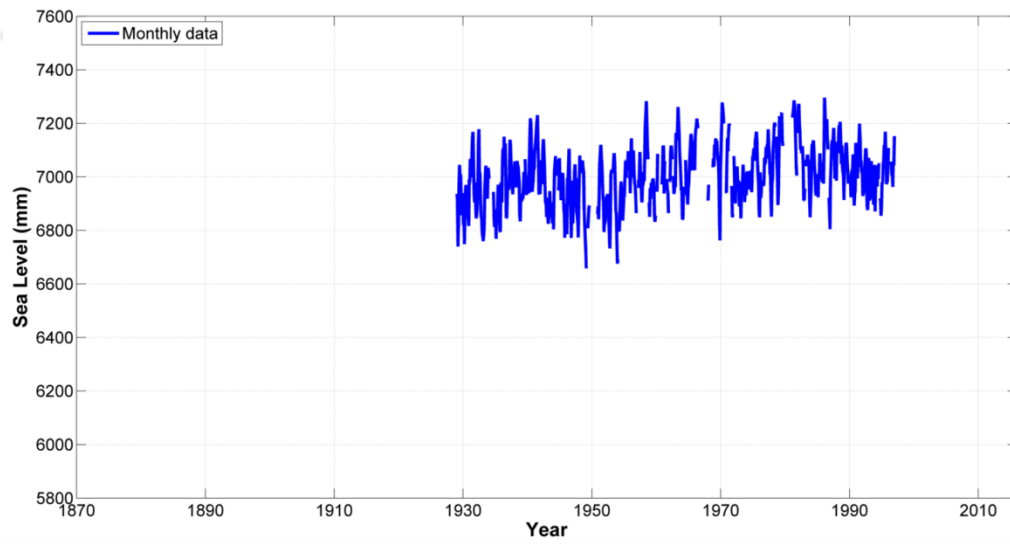
f) Bourgas tide-gauge station.
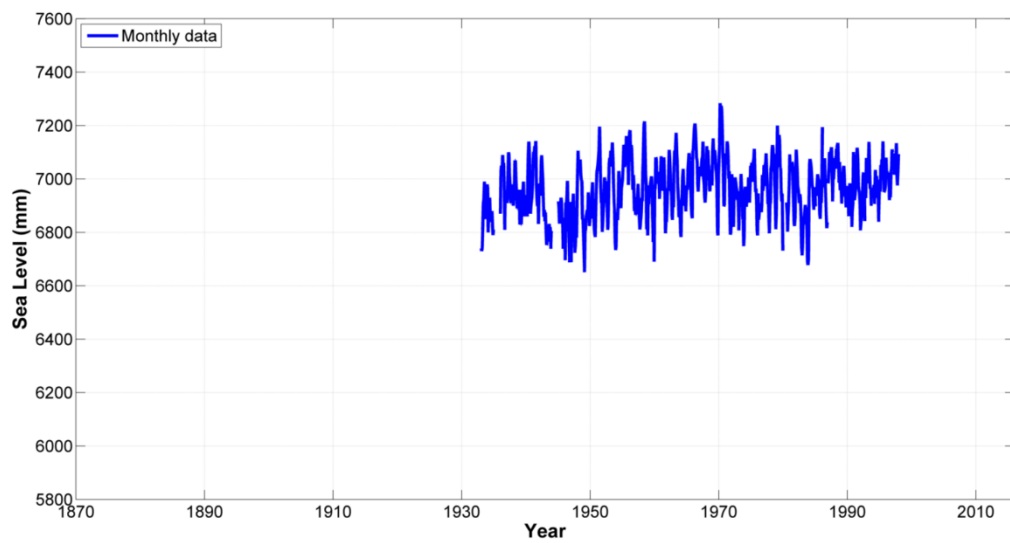
g) Constantza tide-gauge station.

Figure 4.2 (continued).
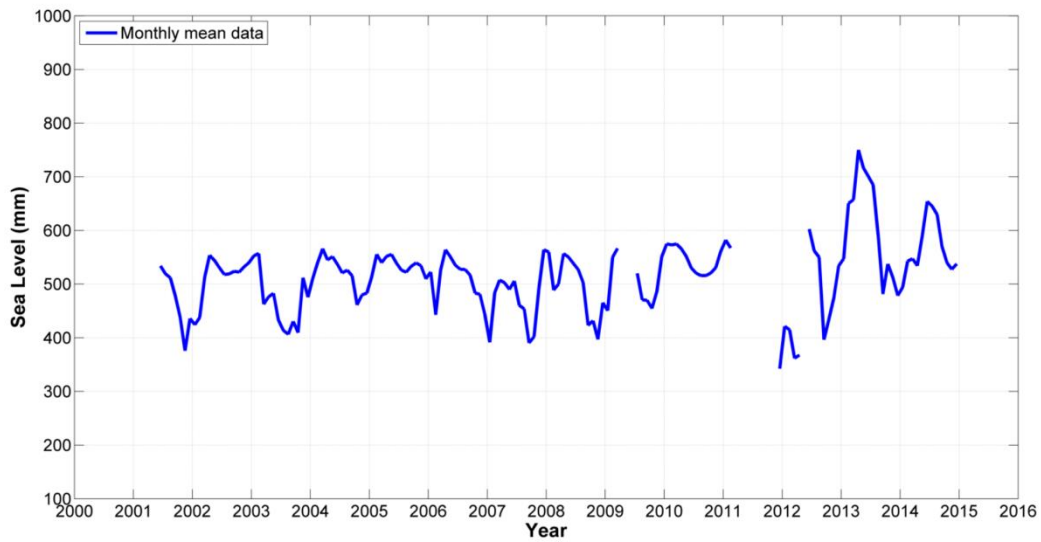
h) Amasra tide-gauge station.
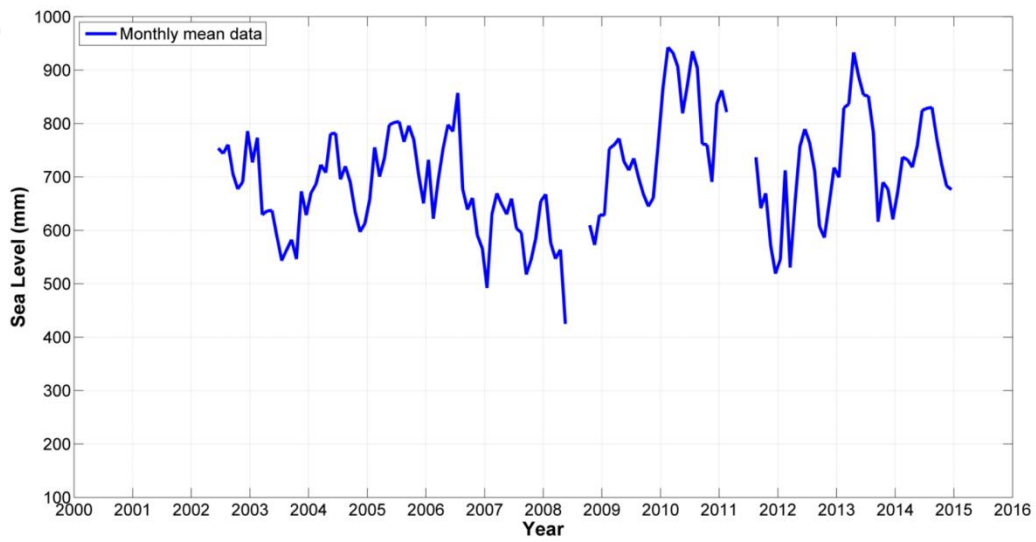
i) Igneada tide-gauge station.
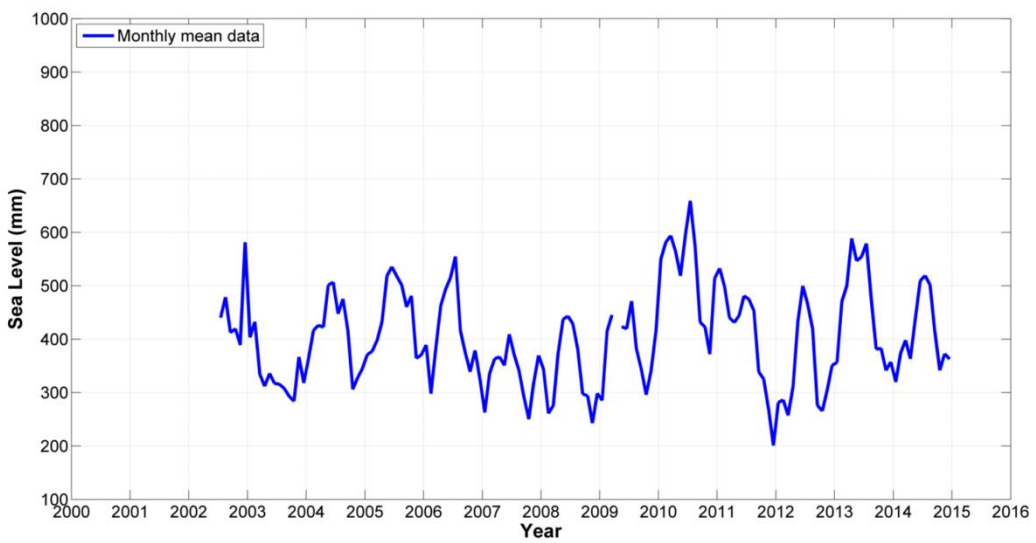
j) Trabzon tide-gauge station.

Figure 4.2 (continued).

88
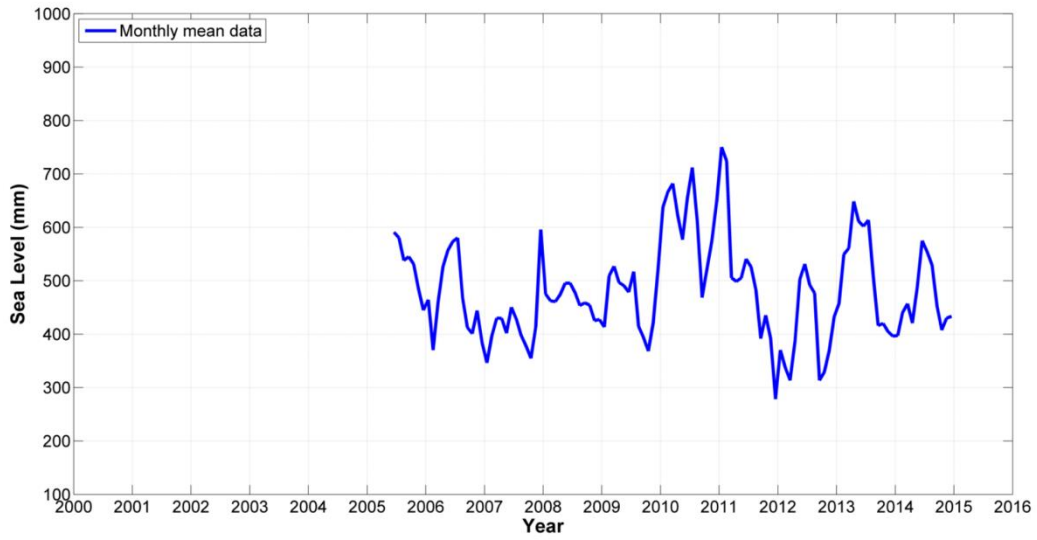
k) Sinop tide-gauge station.
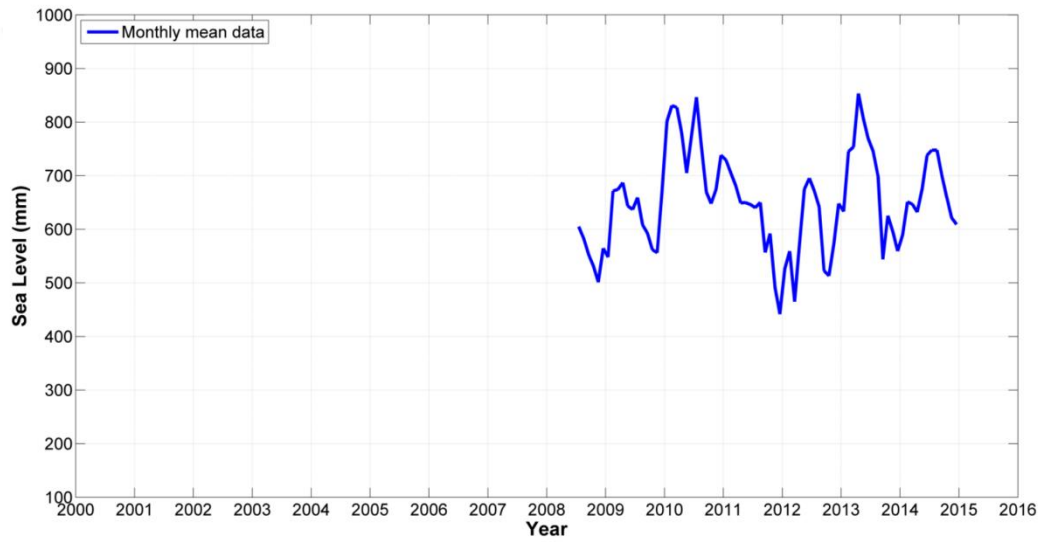
l) Sile tide-gauge station.
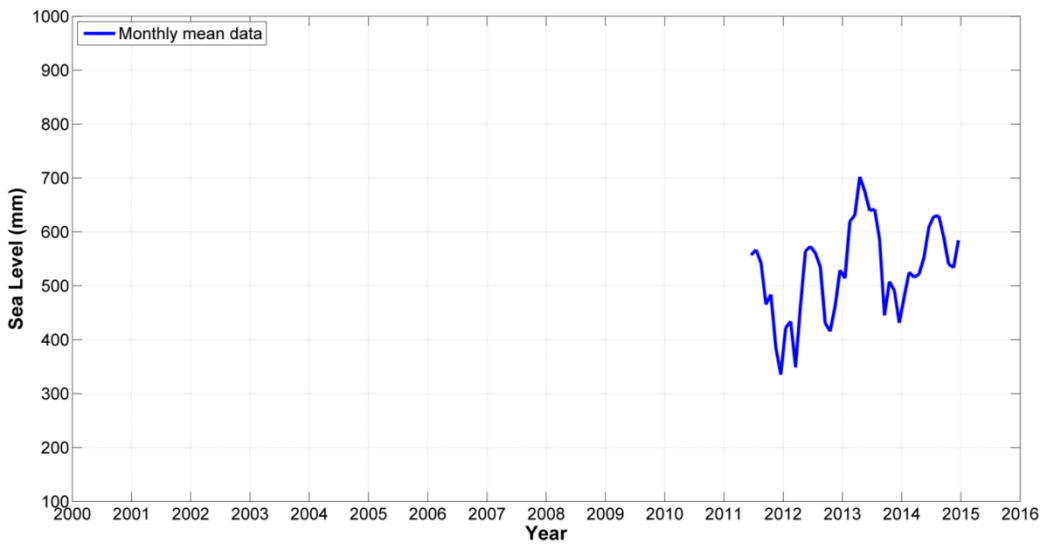
m) Istanbul tide-gauge station.

Figure 4.2 (continued).

4.2.2 Analysis of Tide-Gauge Data

As stated before, the least 50-year of data is needed for long-term sea level change studies. However, sea level measurements from the TUDES network along the Black Sea coast are not long-term (< 20 years) while the tide-gauge time series provided from the PSMSL have an enough period for long-term trend estimation. In addition, some time series contain the missing observations. For example, although the Batumi station has a sea level record of 21-year, nearly 32% of its records are invalid.

Although the data of some tide-gauge stations are short-term, the time series of sea level change for all the stations have indicated a trend and seasonal fluctuations. Therefore, Equation (4.1) was used in the analysis of the relative sea level time series from the tide-gauge stations along the Black Sea coast. In the evaluation, the data gaps that result from due to reasons such as equipment failure, power failure, etc., in the stations, have been excluded. However, the data with less than 4 consecutive missing months have been used through linearly interpolating. According to this, the linear variation with time and seasonal components of observed sea level in the tide-gauge stations are given in Table 4.2. As an example, the trend and harmonic model of the Amasra tide-gauge data are represented in Figure 4.3.
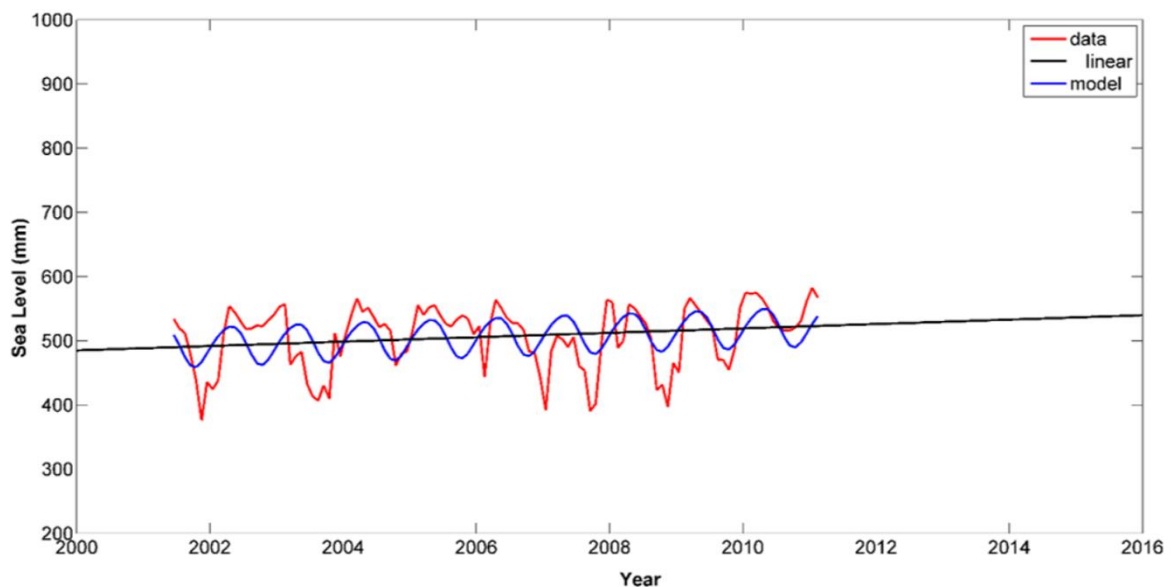
Figure 4.3 Trend and harmonic model of ~ 10-year sea level time series at Amasra tide-gauge station.

For purposes of this analysis, the trend and seasonal components of each tide-gauge station have been derived for the varying record lengths along the Black Sea coast. The results in Table 4.2 show that rate of the relative sea level varies from coast to coast. Consequently, nearly all the tide-gauge stations (except for Bourgas) indicated the rising sea levels. In addition, the Sinop station showed no significant sea level change. The non-significant results may be related to the short records, since trend estimations are sensitive to the record length. Moreover, all the results are based on local sea level measurements, that is, these measurements also contain some geophysical (i.e., non-oceanographic) signals as tide-gauges measure sea level relatively to the ground. For example, at the Poti station a highly sea level trend of 7.01 ± 0.12 mm/y were calculated. This relative sea level rise may be resulted from the subsidence at the Poti coast as described in Bondar (1989) (Ginzburg et al. 2011). On the other hand, the distribution of the data gaps in Bourgas sea level time series did not allowed a reliable trend estimate for this station, despite the interpolation.

Accordingly Table 4.2, the semi-annual amplitudes of the relative sea changes are about 2–3 times smaller than the annual amplitudes. Seasonal (annual and semi-annual) sea level change signals have generally reached their maximum values in May-June. However, the maximum annual amplitude of sea level change at Amasra occurs in April with nearly one month earlier than those of the other stations.

Table 4.2 Trend and annual and semi-annual components of relative sea level changes at the tide-gauge stations along the Black Sea coast (The longest data periods of the tide-gauges were used for the analysis).

Tide-gauge	Time-span	Trend (mm/y)	Annual		Semi-annual	
			Amplitude (mm)	Phase (º)	Amplitude (mm)	Phase (º)
Poti	August 1922 – December 2002	7.01 ± 0.12	77.42 ± 4.05	157.76 ± 0.05	35.86 ± 4.05	26.52 ± 0.11
Batumi	January 1925 – December 1996	3.52 ± 0.15	78.93 ± 4.43	158.48 ± 0.06	35.19 ± 4.43	22.01 ± 0.13
Sevastopol	September 1944 – December 1994	1.56 ± 0.22	79.41 ± 4.58	139.65 ± 0.06	30.07 ± 4.59	16.25 ± 0.15
Tuapse	January 1943 – December 2011	2.92 ± 0.14	70.42 ± 3.85	142.41 ± 0.06	37.00 ± 3.85	29.78 ± 0.10
Varna	January 1926 – November 1961	1.53 ± 0.48	69.54 ± 6.42	152.73 ± 0.09	27.38 ± 6.41	344.06 ± 0.23
Bourgas	February 1981 – January 1996	-7.52 ± 1.33	67.23 ± 8.13	141.78 ± 0.12	20.84 ± 8.12	19.83 ± 0.39
Constantza	January 1945 – December 1979	3.02 ± 0.46	78.14 ± 6.55	127.94 ± 0.08	15.74 ± 6.55	26.34 ± 0.42
Amasra	June 2001 – February 2011	3.43 ± 1.42	30.69 ± 5.71	104.70 ± 0.18	3.47 ± 5.66	340.66 ± 1.63
Igneada	June 2002 – December 2014	6.94 ± 2.18	49.16 ± 11.17	130.14 ± 0.23	16.01 ± 11.22	50.66 ± 0.70
Trabzon	July 2002 – December 2014	2.33 ± 1.75	62.77 ± 8.93	153.45 ± 0.14	27.09 ± 8.93	17.09 ± 0.33
Sinop	June 2005 – December 2014	0.43 ± 2.88	49.04 ± 11.26	135.82 ± 0.23	29.53 ± 11.28	12.06 ± 0.38
Sile	July 2008 – December 2014	5.03 ± 4.84	62.92 ± 12.84	128.86 ± 0.20	22.90 ± 12.84	49.11 ± 0.56
Istanbul	June 2011 – December 2014	36.77 ± 9.07	71.34 ± 13.14	159.70 ± 0.19	18.43 ± 13.28	16.29 ± 0.72

4.3 ABSOLUTE SEA LEVEL CHANGE IN THE BLACK SEA

4.3.1 Satellite Altimetry Observations in the Black Sea

Since 1993, satellite altimetry has provided accurate measurements of Sea Surface Height with near-global coverage. These measurements have also improved understanding of how sea levels are changing regionally. In this sense, in this study, satellite altimetry data have been used to investigate the mean sea level change throughout the Black Sea.

As expressed in Section 3.2.2, the altimetry data are released as along-track and gridded products of the DUACS. The grid data enable to more acceptable sampling achieved by pooling measurements in a given range of latitudes and longitudes in comparison to the along-track data (Woolf and Tsimplis 2002). Accordingly, the altimetry dataset preferred in this study is Daily Sea Surface Heights (SSH)s from 1993-01-01 to 2017-05-15 for the Black Sea, provided from the Copernicus Marine Environment Monitoring Service. These data in delayed-time are gridded (1/8° by 1/8°) Sea Level Anomalies computed with respect to a twenty-year 2012 mean. These SLAs have been estimated by Optimal Interpolation, merging the measurement from the different altimeter missions: Jason-3, Sentinel-3A, HY-2A, Saral/AltiKa, Cryosat-2, Jason-2, Jason-1, T/P, ENVISAT, GFO, ERS1/2. Necessary geophysical (solid earth, ocean and pole tides, ocean tide loading effect, sea state bias, and inverse barometer response of the ocean) and atmospheric (ionosphere, and dry/wet troposphere effects) corrections have been applied to the data set by the data centre (PUM 2019, URL-25). Further information on the data can be found the CMEMS (URL-27).

There are 3249 altimetric grid points in the Black Sea when excluding the Sea of Azov (Figure 4.4a). For the evaluation, at each grid point monthly averages have been computed from the daily altimetry data, and then by averaging spatially the monthly Mean Sea Level changes over the entire Black Sea were obtained. Figure 4.4b shows time evolution of the Black Sea level for the monthly averages from January 1993 to May 2017.

a) 3249 altimetric grid points with 1/8° x 1/8° interval.

b) Monthly sea level time series from January 1993 to May 2017 (Seasonal signals retained).
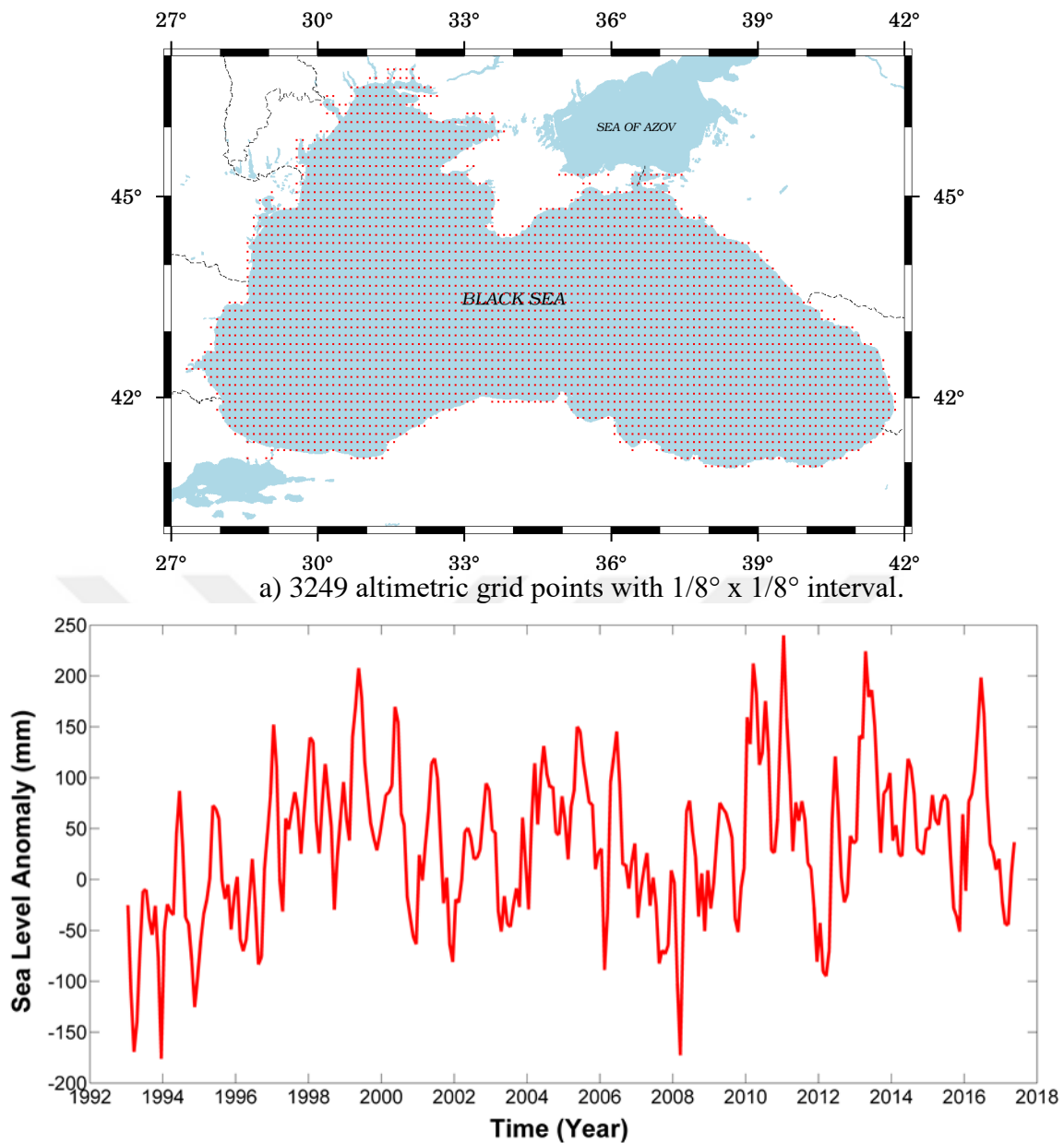
Figure 4.4 Altimetric grid points, and over these grid points basin-averaged Sea Level Anomalies in the Black Sea.

4.3.2 Seasonal Cycle of Sea Level Variations

Seasonal variation is one of the important components of sea level time series. Meteorological (air pressure changes, winds, precipitation, evaporation, etc.), oceanographic (ocean currents, etc.) and hydrological (underground and surface water flows) processes are driving factors forming the seasonal sea level variations.

In the study, satellite altimetry data were used to analysis the components (phase and amplitude) of the seasonal sea level variation in the Black Sea and their spatial distributions. For the analysis, the monthly anomalies obtained by means of arithmetic average of daily data at 3249 grid point covering the Black Sea were used. Then, averages of monthly anomalies (average for all the January months, average for all the February months, etc.) for the altimetry period of 24-year were calculated at each grid point as follows (Tsimplis and Spencer 1997):

$$MA_i = \frac{1}{N} \sum Y_{ik} \tag{4.2}$$

where MA_i: average monthly anomalies, $i = 1,\ldots,12$ (months), $k = 1,\ldots,N$ (years), N: number of years. The average monthly anomalies are shown for each grid point in Figure 4.5. According to the figure, the maximum sea level in the Black Sea occurs in May-June, while the minimum sea level is observed in autumn (September-October-November).
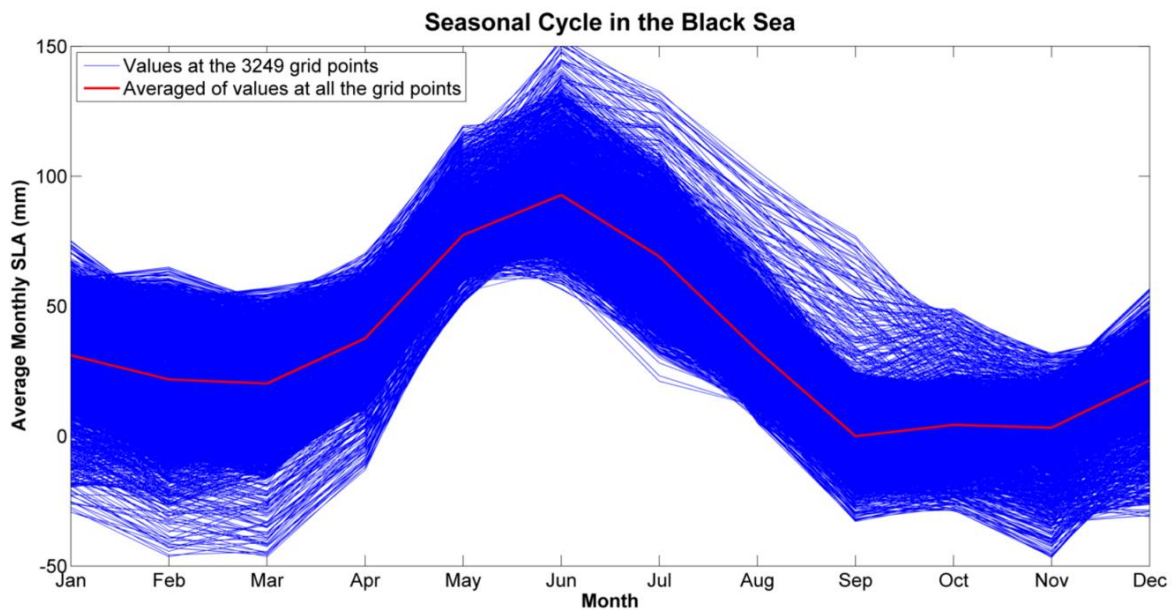
Figure 4.5 Seasonal cycle in the Black Sea.

On the other hand, the phases and amplitudes of the seasonal (annual and semi-annual) sea level cycle were determined by harmonic analysis of the calculated averages of the monthly sea level anomalies. Here, by taking the averages of the monthly anomalies as the observations in the harmonic analysis model, the seasonal components were estimated by the least squares method:

$$MA_i = A_{S_a}\left(cos\frac{2\pi}{12}t_i - \varphi_{S_a}\right) + A_{S_{sa}}\left(cos\frac{2\pi}{6}t_i - \varphi_{S_{sa}}\right) \qquad t_i = i - 0.5 \qquad (4.3)$$

Here, S_a and S_{sa} represent annual and semi-annual components of the seasonal cycle, respectively. Accordingly, the phases and amplitudes of the seasonal variation in the Black Sea were obtained over all the grid points, and averaged. The results are presented in Table 4.3. Accordingly, the average annual phase value confirmed that the seasonal sea level variations in the Black Sea reach the maximum annual amplitude in May-June. In the Black Sea, the largest contribution for the freshwater balance is from the river runoff, especially in spring and summer. And annual freshwater budget is positive (River + Precipitation > Evaporation) between November and June, with maximum in April or May. These conditions support the results of this study. When considering the spatial distributions of the related components, the greatest values were observed in the southeast part of the sea (Figure 4.6). In this part, the annual amplitude of the seasonal cycle was found to be approximately 9 cm. The difference between the maximum and minimum values of the annual phase over the entire Black Sea is approximately 4 months. In general, the annual phases vary in the deep and shallow regions. According to this, it can be stated that the annual cycle of the seasonal sea level variation reaches its maximum value in shallow regions approximately 4 months ago. The determined spatial distributions of seasonal components are closely related to the basin dynamics driving the distribution of the water mass of the Black Sea.

Table 4.3 Amplitudes and phases of the annual (*a*) and semi-annual (*sa*) cycles of SLA in the Black Sea.

	Maximum	Minimum	Mean
A_{S_a} (mm)	90.3 ± 18.1	17.2 ± 11.6	37.4 ± 0.2
$A_{S_{sa}}$ (mm)	32.2 ± 19.2	16.4 ± 13.9	23.4 ± 0.1
φ_{S_a} (°)	218.1 ± 0.5 (7.3rd month)	87.8 ± 0.5 (2.9th month)	145.9 ± 0.5 (4.9th month)
$\varphi_{S_{sa}}$ (°)	359.9 ± 0.9 (12th month)	-359.9 ± 0.8 (0.01st month)	338.7 ± 0.6 (11.3rd month)

a) Annual amplitude.

b) Annual phase.
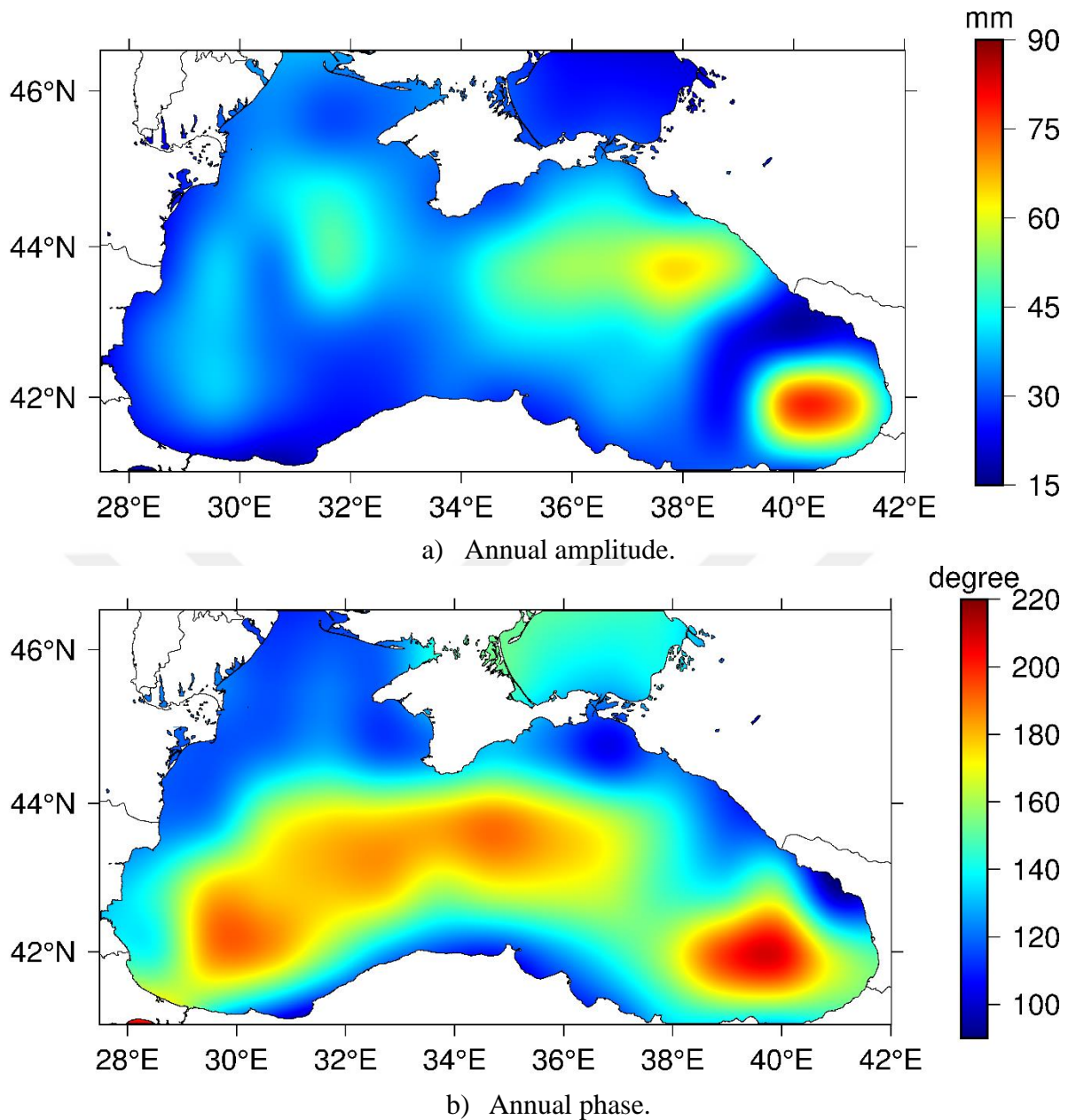
Figure 4.6 Spatial distribution of annual components of seasonal cycle.

4.3.3 Analysis of Long-Term Trend and Seasonal Variation from Satellite Altimetry Data

As stated before, to examine the long-term and seasonal sea level variability of the basin average in the Black Sea, a linear trend, and seasonal components (annual plus semi-annual) through a least-squares fit of Equation (4.1) have been estimated.

Here, in order to examine the inter-annual variability of the sea level time series, the seasonal components have removed from the monthly values (Figure 4.7a). The results show that the

Black Sea level has risen at a rate of about 2.5 ± 0.5 mm/y between January 1993 and May 2017. On the other hand, the latest period for the available tide-gauge data in the Black Sea for this study is until to December 2014. Besides, the other dominant periodic behaviours (after removing seasonal cycles) in the altimetry time series have been determined using the Cycles Analysis & Timeseries Software (CATS) - v1.0 (CATS 2010). Figure 4.7b demonstrates the dominant cycles over the Black Sea level time series from January 1993 to May 2017. As seen in the figure, the period of January 1993 – December 2014 indicates a more apparent trend for this sea level time series. An average trend of 3.2 ± 0.6 mm/y over the Black Sea has been also determined for the period 1993–2014. The satellite altimetry observations from 1993 to 2014 yield the standard deviation of 7.5 cm for sea level anomalies in the Black Sea. In 2010 mean sea level anomaly was about 20 cm above the 1993 average. And this was the highest annual average in the satellite record from 1993 to present, and the record high sea level anomalies occurred in March 2010, January 2011 and April 2013. Moreover, satellite altimetry data show there have been some strong fluctuations of sea level in the Black Sea; the difference between mean sea level anomalies from December 2009 to January 2010 reached about 15 cm.

Figure 4.8 shows the spatial distribution of the Black Sea level trends over 1993–2014. As seen from the figure; the trend values were positive in whole basin, however they were not spatially uneven. Accordingly, over all the Black Sea basin, the rates of sea level change for the period 1993–2014 varied from 0.2 to 5.0 mm/y. The rate of sea level rise in coastal and shelf areas was greater than in the centre of the basin. Especially the southeastern region showed a larger rate of rise than the other parts in the Black Sea. Kubryakov et al. (2017) asserted that the observed spatial differences in the sea level rise were related to the basin dynamics, which redistributed water mass within the basin. It was attributed that the observed long-term intensification of the cyclonic wind curl strengthened divergence in the centre of the basin, which caused a rise of the sea level along the coast and over the northwestern shelf, and a fall of sea level in the interior of the basin. In addition, the changes in distribution and intensity of mesoscale eddies led to the local extremes in sea level trends. In particular, an extension of the Batumi anticyclone resulted in an excess sea level rise in the southeastern part of the basin over 1993–2014.
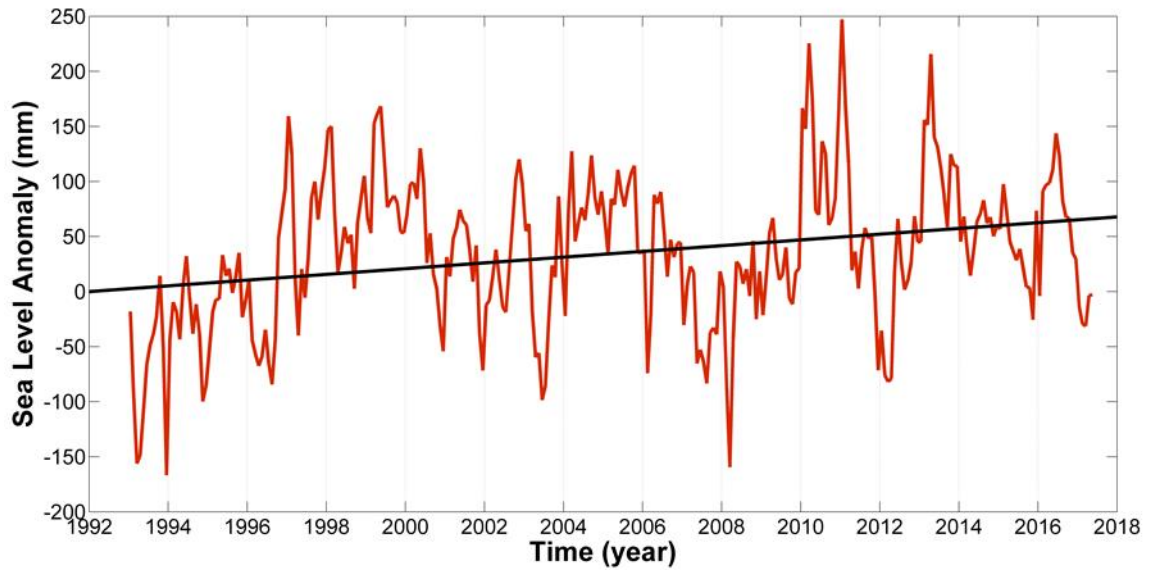
a) Non-seasonal sea level time series with its linear fitting.
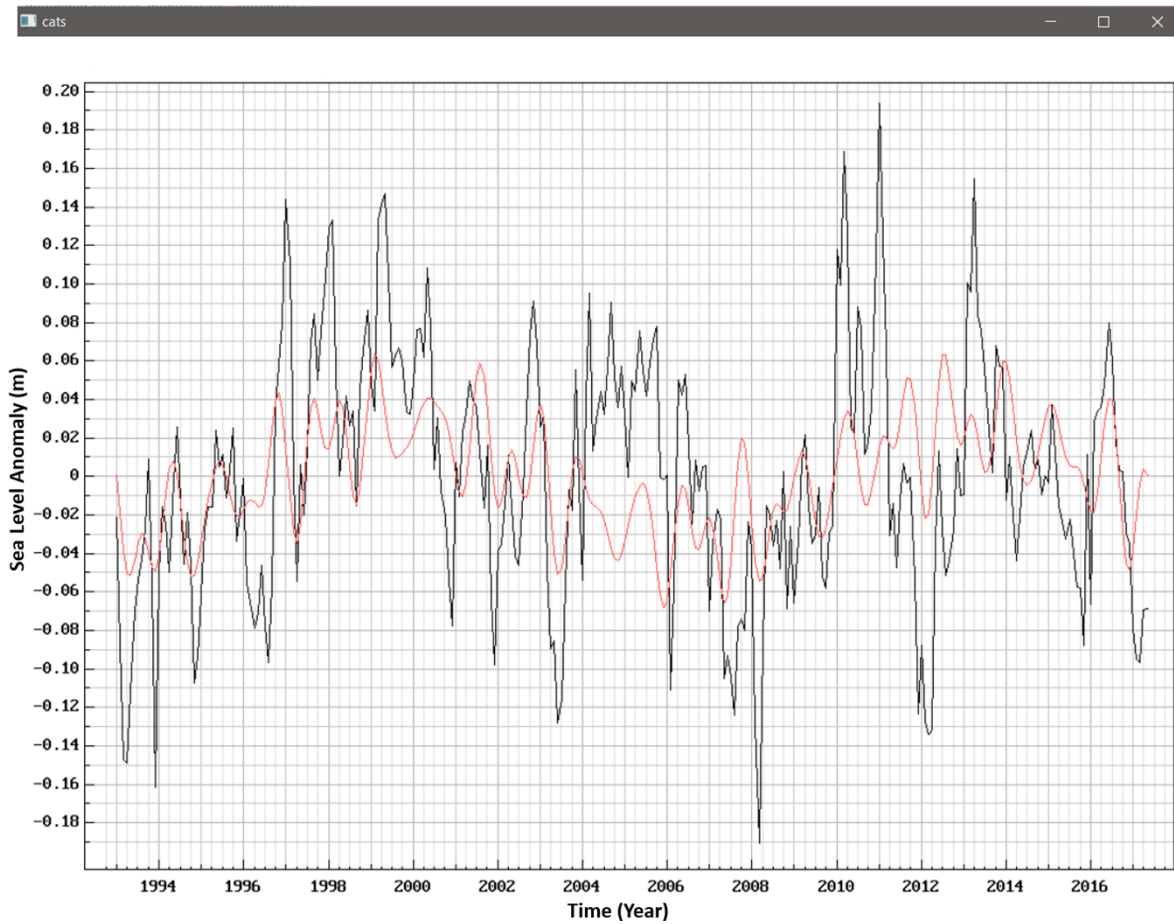
b) Dominant cycles (red) over the detrended and non-seasonal sea level time series (black).

Figure 4.7 Monthly sea level time series in the Black Sea over 1993–2017 from the satellite altimetry data.
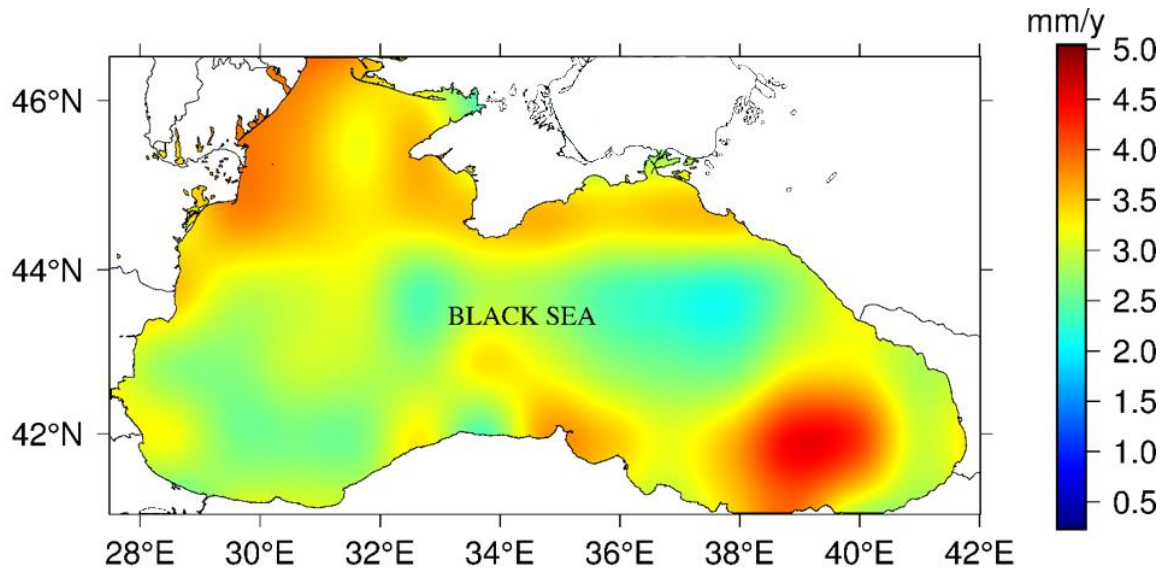
Figure 4.8 Spatial distribution of sea level trend over the Black Sea from the multi-mission satellite altimetry data between January 1993 and December 2014.

As for seasonal components of the Black Sea level variations, the average annual and semi-annual amplitudes are about 38.02 ± 6.01 mm and 23.74 ± 6.01 mm, respectively, from the satellite altimetry. And the average annual and semi-annual phases are $147.38 \pm 0.17°$ ($\sim 4.9^{th}$ month) and $338.04 \pm 0.26°$ ($\sim 11.3^{rd}$ month), respectively. Accordingly, the annual cycles of sea level variations measured by the altimetry reaches the maximum value in about May as mentioned in Section 4.3.2.

4.4 MASS-INDUCED AND STERIC SEA LEVEL CHANGES IN THE BLACK SEA

According to the dynamics of sea level outlined before, several factors may be expected to play a role in the Black Sea level change, including thermal expansion, changes in the air-sea freshwater flux to the basin, variations in river runoff, etc. As noted before, the general consensus is that at seasonal time scales, the forcing of sea level in the Black Sea is dominated by freshwater balance. At longer time scales, up to decadal, variability in the hydrological data also exhibits a significant correlation with the variations in sea level (Stanev and Peneva 2002). At multidecadal timescales, for Tsimplis et al. (2004) indicated that the precipitation minus evaporation variations were the primary cause for the observed sea level rise for the period 1949 to 2003.

Observations of sea level in the Black Sea showed a continuous multidecadal increase of about 2 mm/y between 1960 and the early 1990s, a period during which the neighbouring Mediterranean Sea experienced sea level fall (Tsimplis and Baker 2000). Between the early 1990s and 1998, sea level rises in both the basins were observed with accelerated values, in the Black Sea of the order of 27 mm/y (Cazenave et al. 2002). During the same period the Sea Surface Temperature in the Black Sea rose, thus leading Cazenave et al. (2002), Simav vd. (2008), and Vigo et al. (2005) to conclude that this increase in the sea level was steric in nature.

As explained in Section 3.2.3, total change in sea level at seasonal and longer time scales is the sum of steric and mass (non-steric) induced changes. Satellite altimetry observes total sea level change. Nevertheless, it is possible to estimate mass changes using satellite gravity data, and steric changes through in-situ and/or satellite measurements. This section presents recent sea level changes in the Black Sea depending on satellite gravity and in-situ/satellite oceanographic measurements. But before, the Sea Surface Temperature changes in the Black Sea are analysed.

4.4.1 Sea Surface Temperature Change in the Black Sea

Sea Surface Temperature is a crucial indicator determining physical and biological characterizes of oceans (see Section 3.2.3). The temperature within the relatively thin upper layer (about 10 m in summer and 80 m in winter) of the Black Sea resulting from its very high density stratification is known to respond very rapidly to the atmospheric forcing (Ginzburg et al. 2004, Nardelli et al. 2010, Staneva et al. 1995). In addition, the heat changes due to water transports through currents, river discharges, straits, precipitations, upwelling and downwelling influence SST variability in the Black Sea. Tsimplis et al. (2004) also investigated the correlation coefficients between the NAO and, temperature and salinity for the Black Sea layers. They found that the highest value was for the upper layer temperature of -0.57. Thus, the Black Sea SST is subject to significant seasonal and interannual variability. Furthermore, the local changes in SST may result from regional peculiarities of the precipitation, oil film and accumulated different matter contents at the water surface (Ginzburg et al. 2004).

This study has used the Optimum Interpolation 1/4 degree daily Sea Surface Temperature (OISST) anomaly data (Reynolds et al. 2007) from the NOAA in order to analyse Sea Surface Temperature variability in the Black Sea. This dataset is the high-resolution blended anomaly data corresponding to the daily OISST minus a 30-year mean, during the period from September

1981 to November 2015. It is an analysis constructed by combining observations from the AVHRR infrared satellite sensors interpolated with the sensors on ships and buoys. This analysis includes a bias adjustment of remote sensors and in-situ observations, enabling to compensate for platform differences and sensor biases.

Since these SST data have a global coverage, the Black Sea data including 877 grid points excluding the land have been cut out from all the data. The monthly averages for the related period have been calculated using the daily data at all the grid points in the Black Sea basin. Figure 4.9 shows time evolution of the basin-averaged SST anomalies in the Black Sea for the period 1981–2015.

(a)

(b)
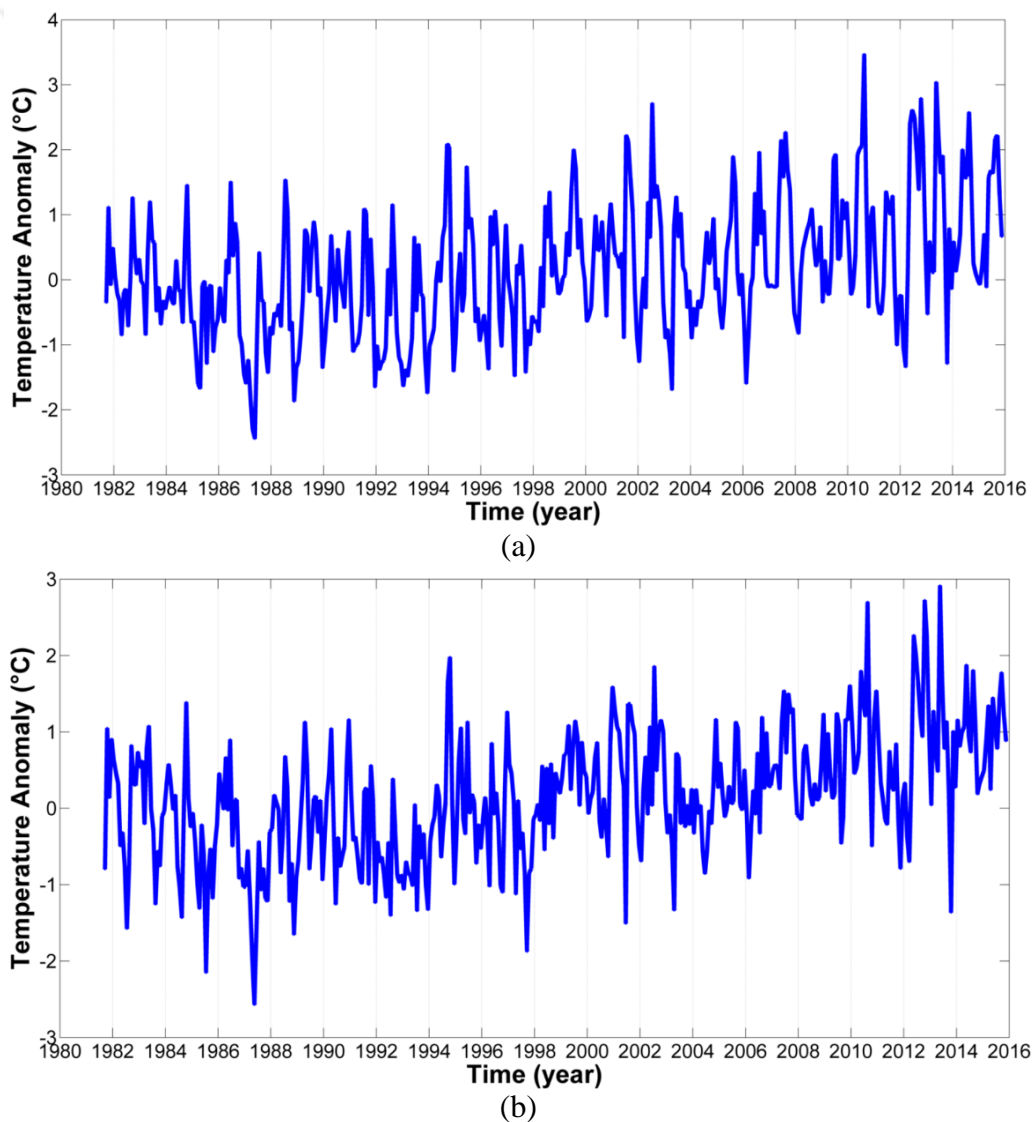
Figure 4.9 SST time series in the Black Sea from September 1985 to November 2015
a) Seasonal signals retained, b) Seasonal signals removed.

The linear regression indicates that the SST anomalies in the Black Sea showed a general increasing trend of 0.04 ± 0.005 °C/y during the 1981–2015 period. As can be seen in Figure 4.9, a drop in the anomaly values was observed during 1980s, and then the SST anomalies demonstrated an unequivocal rise acceleration since 1994. Here, in order to show up interannual variability of the Black Sea SST, it was focused on the residual mean SST after removing the seasonal signal (Figure 4.9b). Accordingly, the record high SST anomalies occurred in August 2010, October 2012 and May 2013. In 2012, mean SST anomaly was about 1.2 °C above the 1982 average. And this was the highest annual average in the SST data from 1982 to 2014. After 1994, the SST exhibited a continuous rising trend in summer months (from May to August), while there were more natural fluctuations in the winter period. Nevertheless, since 1994, warmer surface waters, as compared to previous winters, were observed in the Black Sea.

Here, the monthly Sea Surface Temperature time series over the period 1981–2015 are also subjected to the harmonic analysis (by Equation (4.1)) to determine components of seasonal variations. In order to fit the SST time series for each grid point, the least squares method has been used. The spatial distribution of SST trends over the Black Sea is seen in Figure 4.10. The map shows that SST has been rising almost everywhere across the Black Sea since 1981. The maximum trend values were observed through the Kerch Strait. For the SST changes in the Black Sea, the mean annual amplitude is ~ 0.8 °C and the mean annual phase is ~ 221° (7.4th month); and the mean semi-annual amplitude is ~ 0.2 °C and the mean semi-annual phase is ~ 128° (4.3rd month). According to this, the maximum annual amplitude of SST changes occurs in August.

Seasonal cycle of the SST in the Black Sea have been also investigated using Equation (4.2). The results confirm from the 33-year data that the maximum SST occurs in August, whereas its minimum occurs in January-March.
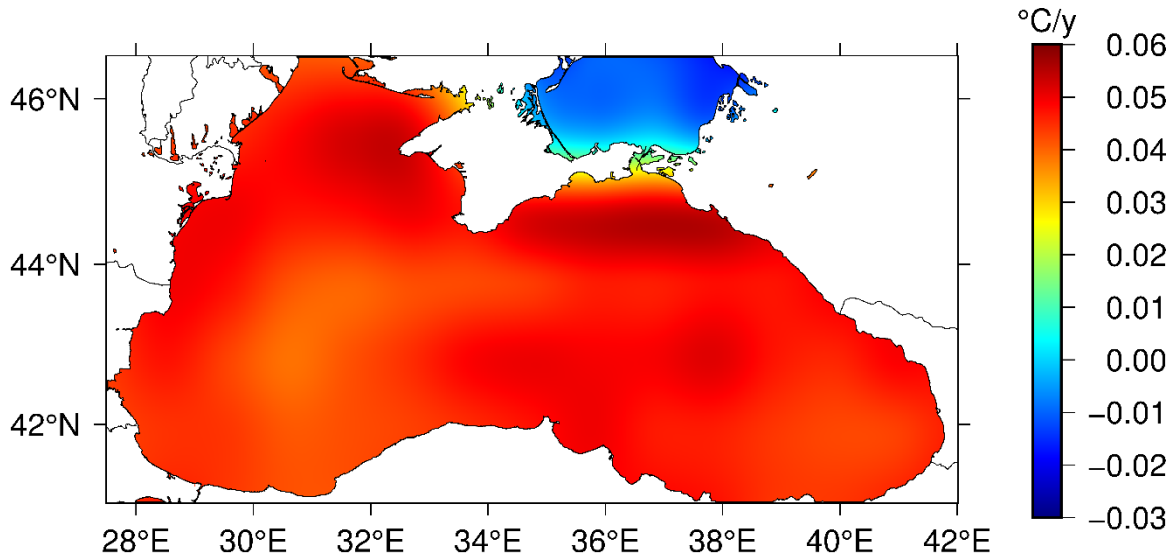
Figure 4.10 Spatial distribution of the Black Sea SST trend over September 1981 – November 2015.

4.4.1.1 Relationship between Sea Surface Temperature and Sea Level Changes

The cause-effect relationship between the observed trends in Sea Surface Temperature and sea level over the Black Sea has been analysed in the study. Here, interpolation of sea level trend values has been implemented at all the grid points of 1/4° for comparison to the corresponding SST trend values. Figure 4.11 shows spatial distributions of the interpolated Sea Level Anomaly trend values along with those of the SST anomalies between January 1993 and November 2015. According to figure, a positive trend tendency at basin scale for both parameters is seen. Since SST changes contain shorter spatial wavelengths, the SST trend maps appears smoother everywhere than the sea level trend map (Cazenave et al. 2002).

On the other hand, Figure 4.12 presents non-seasonal sea level and SST anomalies time series over the Black Sea from January 1993 to December 2014. In the Black Sea level, a change from rising to falling was observed in 1999 while a change from falling to rising was observed in 2008. As it is seen in Figure 4.12, the overall curve of sea level anomaly dramatically shows an abrupt change in its slope that took place in mid-1999 and early-2008. Therefore, in this study, the whole period (January 1993 – December 2014) has been divided into three parts to analyze the relationship between sea level and SST anomalies changes in the Black Sea: Period I: January 1993 – June 1999 (6.5 years), Period II: July 1999 – March 2008 (~ 9 years) and Period III: April 2008 – December 2014 (~ 7 years). A similar division had been performed by Vigo et al. (2005).

a) for Sea Surface Temperature Anomalies

b) for Sea Level Anomalies
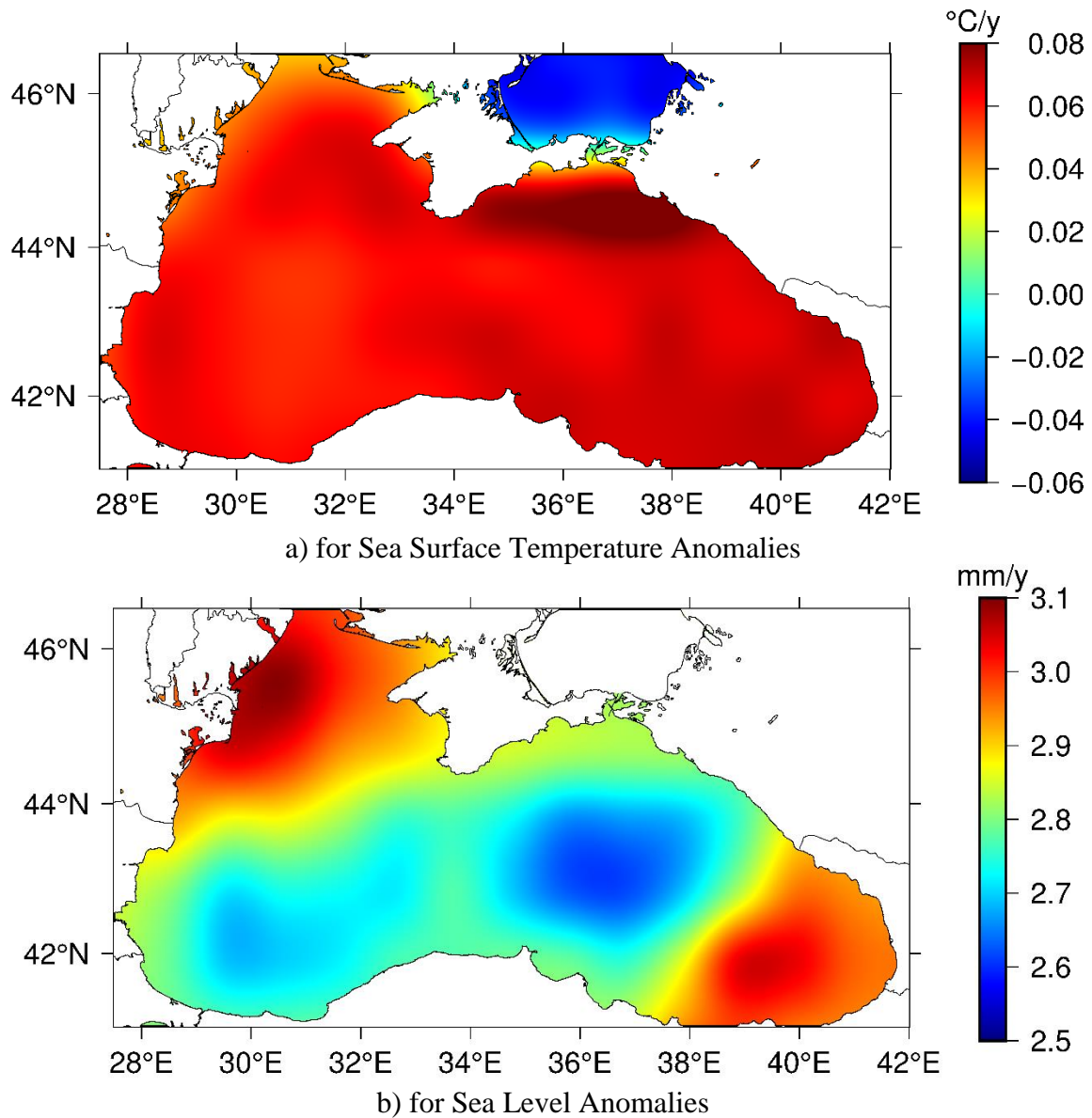
Figure 4.11 Spatial distributions of SST and SLA trends in the Black Sea over 1993–2015.

Upon splitting the SST time series similarly, the behavior of the curve is similar to that of sea level for the Periods I and III. However, in the Period II while the SSTs increase slightly, a decreasing sea level trend is seen. The rates of changes of sea level and SST anomalies, and the correlations of their spatial distributions for Periods I, II and III are given in Table 4.4, separately. The results showed a good correlation between sea level and SST anomalies trends for Periods I and III; however this correlation was greatly disappeared for Period II. According to this, prior to mid-1999 and following early-2008 steric effect was seen as an important factor in interannual variability of the Black Sea level.
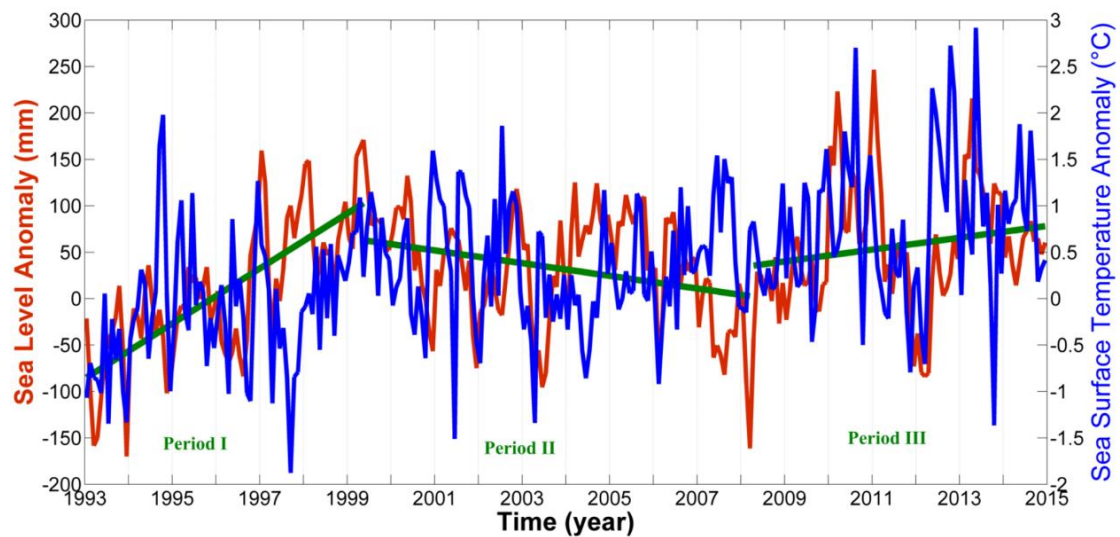
Figure 4.12 Non-seasonal SST (blue curve) and sea level (red curve) time series in the Black Sea, which are splitted into three periods.

Table 4.4 Linear trends of sea level and SST time series in the Black Sea, and correlation coefficients between their spatial distributions over the Periods I, II and III.

Period	SLA trend (mm/y)	SST trend (°C/y)	Correlation
I (January 1993 – June 1999)	29.9 ± 3.1	0.106 ± 0.04	0.67
II (July 1999 – March 2008)	-6.4 ± 2.2	0.002 ± 0.02	-0.21
III (April 2008 – December 2014)	6.4 ± 3.8	0.067 ± 0.04	0.50

4.4.2 Steric Changes in the Black Sea

Steric sea level changes reflect volumetric expansion of the seawater due to density changes at shallow and deep. In the study, as steric data, global steric sea level (thermosteric, halosteric, and total) anomaly fields were used from the NOAA National Centers for Environmental Information (NCEI) (URL-49). These data are 3-month sea level anomalies (Levitus et al. 2012). They provide steric (thermosteric and halosteric) components of sea level change of the 0–700 m layer. Their time periods are 2005–present for total steric and halosteric sea levels, 1955–present for thermosteric sea level. Here, the Black Sea data have been cut out from all the ocean steric data. Figure 4.13 demonstrates the total steric sea level variations as well as the individual contributions of thermal and haline expansion. In addition, the 3-month SLA changes (altimetry-derived) from

January 1993 to December 2014 were calculated, and added to Figure 4.13. In order to remove datum differences, transformations were performed between the altimetry-derived sea level and all the steric sea levels via the calculated translation parameters.

Mean sea level rise due to thermal expansion is approximately proportional to the increase in ocean heat content (IPCC 2013). The 3-month heat content of the 0–700 m layer of the Black Sea can be seen in Figure 4.14. The data have been provided from Levitus et al. (2012). According to figure, thermal expansion contribution to sea level change shows an acceleration after 2004.
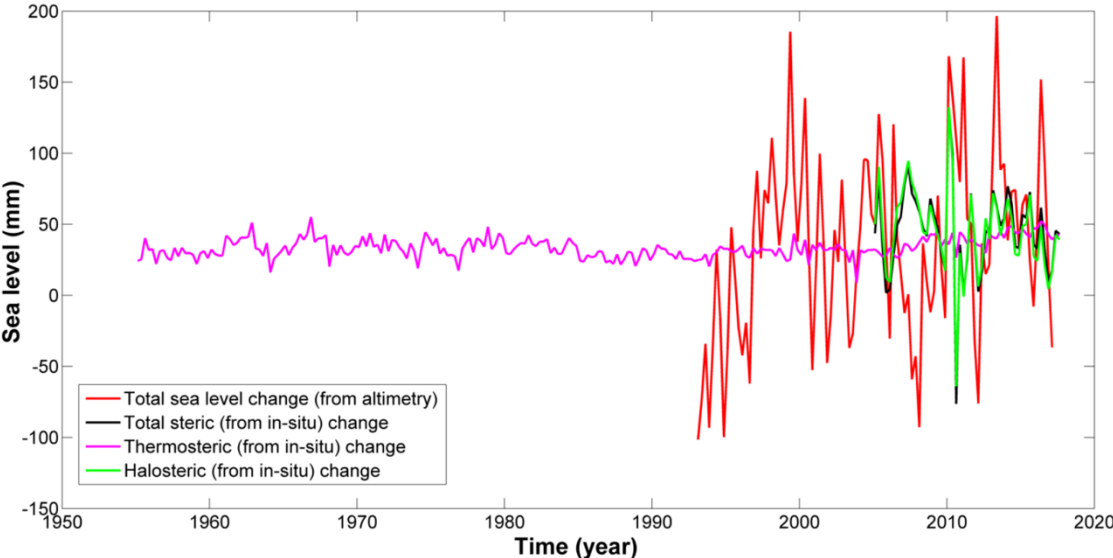
Figure 4.13 Total and steric sea level changes in the Black Sea for 3-month time evolutions.
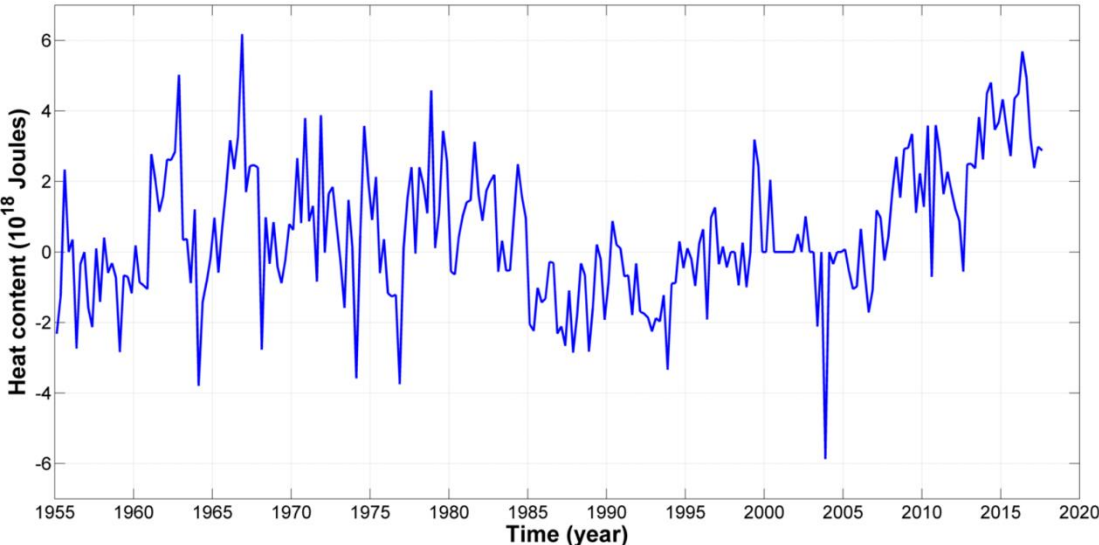
Figure 4.14 3-month heat content of the Black Sea from 1955 to present.

4.4.3 Water Mass Change in the Black Sea from GRACE Satellite Mission

In many studies (Ginzburg et al. 2013, Kubryakov et al. 2017, Stanev et al. 2000, Volkov and Landerer 2015, Yildiz et al. 2011), changes in the water budget (balance) of the Black Sea have been considered as the main reason for the basin-averaged sea level changes. As referred before, water mass-induced sea level changes can be estimated from its time-variable gravity signals. In the study, to estimate water mass variations in the Black Sea, GRACE RL05 Mascon solutions from the CSR were preferred (Save et al. 2016). These GRACE products from April 2002 to June 2017 are monthly mass grids corresponding changes in equivalent water thickness relative to a time-mean baseline. Mass Concentration blocks (mascons) are essentially another form of gravity field basis functions (including spherical harmonics) to which GRACE's inter-satellite ranging observations are fit. Each mascon has a specific known geophysical location. These data are represented on a 0.5° lon-lat grid, but they represent the equal-area geodesic grid of size 1°x1° at the equator. Mascon solutions typically do not need to be destriped or smoothed unlike spherical harmonic coefficients. Moreover, they allow a better separation of land and ocean areas. Nevertheless, here, in order to minimize leakage along the coastline, an ocean mask were applied. The data also have a GIA correction. For further information on the data, and the used mask, see URL-54.

For this study, the Black Sea data have been cut out from the global dataset. The basin-averaged time series of equivalent water thickness have been obtained from the 133 grid points covering the Black Sea. For the analysis, the 20 missing solutions (months) in the GRACE data between April 2002 and June 2017 have been interpolated linearly. Then, the mass-induced contribution to sea level change in the Black Sea was analysed using Equation (4.1). Accordingly, the result shows a rate of the non-seasonal seawater mass change of about 2.3 ± 1.0 mm/y over the last 15 years. Figure 4.15 shows a map of mass change trends over 2002–2017. Here, note that the missing solutions have not been considered at calculation of trend of each grid point.

In addition, Figure 4.16 depicts the monthly time series of the Black Sea level from April 2002 to May 2017 from satellite altimetry (Sea Level Anomalies) and satellite gravity (Equivalent Water Thickness). Here, the altimetry-derived sea level has been interpolated at all the grid points of 0.5° associated with the mascon grid interval. For this period, while the sea level rise from satellite altimetry was about 2.0 ± 1.1 mm/y, the GRACE observations indicated sea water mass change at a rate of 2.3 ± 1.1 mm/y.
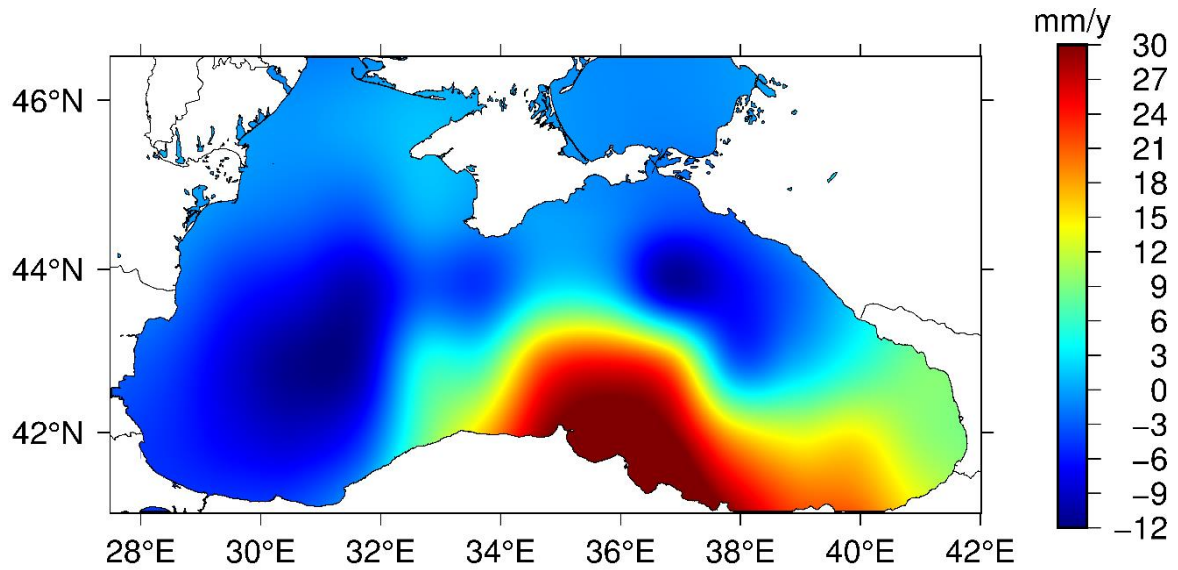
Figure 4.15 Spatial distribution of rates of the seawater mass change in the Black Sea from the GRACE data over 2002–2017.
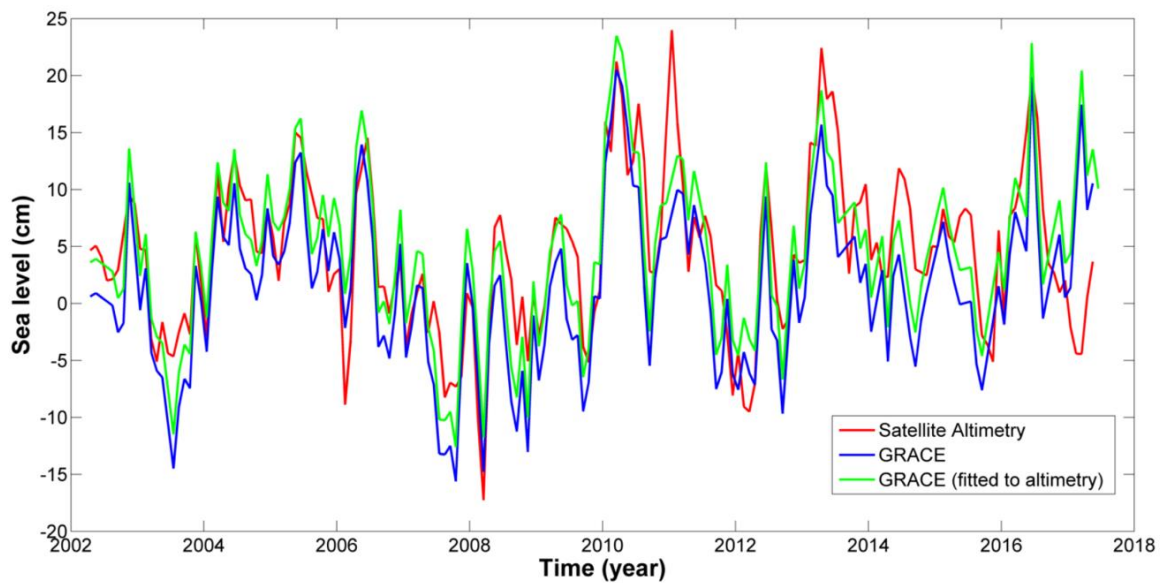
Figure 4.16 Monthly sea level time series of the Black Sea from satellite altimetry and satellite gravity over 2002–2017 (Seasonal signals retained). Blue curve shows GRACE-derived EWTs, whereas green curve is achieved by translating these EWTs with respect to the altimetry-derived sea level**.**

According to Figure 4.16, both the observations (altimetry and GRACE) exhibit similar fluctuations especially in some time periods. For example, the mass-induced sea level changes may be major factor for the increase of sea level in the Black Sea in the early 2010s.

Moreover, 3-month GRACE data have been obtained from monthly solutions. Eventually, 3-month time evolution of sea level in the Black Sea are charted in Figure 4.17. In spite of different uncertainties and systematic errors from altimetry, gravimetry and in-situ measurements; the 3-month time evolution of sea level in the Black Sea shows that the observed sea level change and total of observed contributions almost exhibit similar fluctuations.
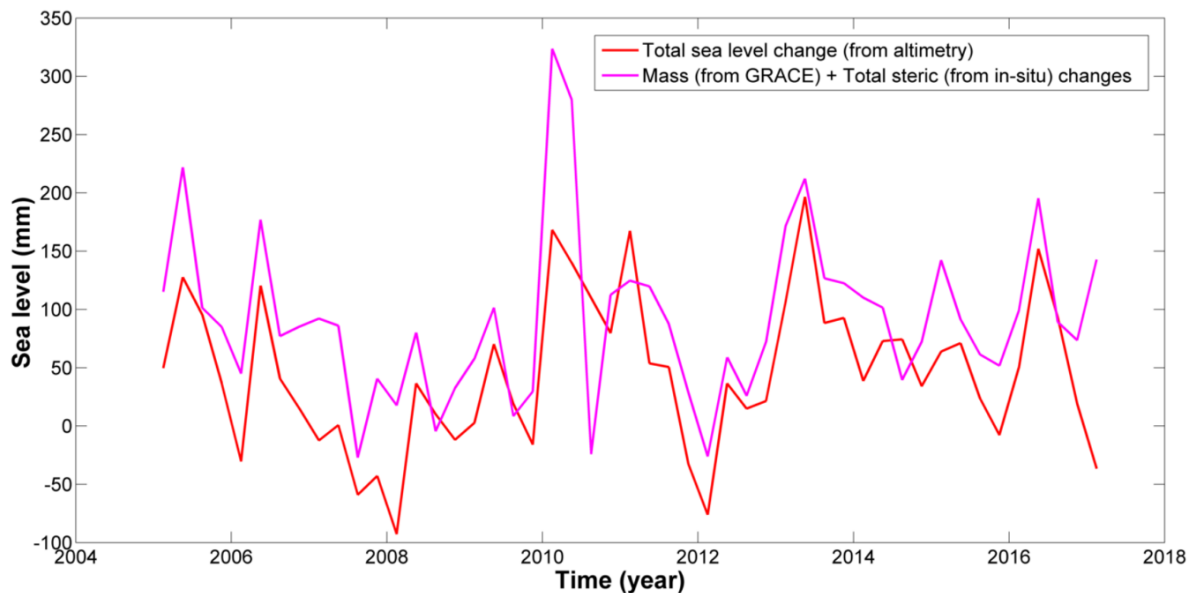
Figure 4.17 Black Sea level changes from satellite altimetry data, and mass plus steric data for 2005–2017.

4.5 COASTAL SEA LEVEL CHANGES IN THE BLACK SEA

Sea level changes are not spatially uniform. Moreover, the rates of sea level change vary at coasts, from global, regional and even local means. Over shorter intervals the coastal sea level changes faster and over longer intervals slowly than the global mean (Church and White 2011, Fenoglio-Marc and Tel 2010). In the Black Sea, although the geographical distribution of the rate of Black Sea level rise was mostly uniform, it was detected bigger than the mean in the southeastern coastal part (see Figure 4.8). Besides, Kubryakov and Stanichnyi (2013) stated that cyclonic Rim Current causes a higher sea level rise at the coastal parts of the Black Sea. On the other hand, sea level rises pose a serious threat especially for the unprotected coastal zones. Therefore, monitoring and detecting of coastal level changes are important.

The study focuses on sea level changes along the Black Sea coast in this section. For this purpose, the linear trends of sea level time series at the 8 tide-gauge stations used in this study

(except for Istanbul, Sevastopol, Varna, Bourgas, and Constantza) were estimated from both tide-gauge and satellite altimetry data. In addition, the seasonal variations were analysed. The consistency of the results derived from both the observations were investigated and interpreted.

4.5.1 Assessment of Satellite Altimetry Data along the Black Sea Coast

As discussed in Section 3.2.2, satellite altimeter measurements are exposed to a number of problems in the vicinity of coast. So, the improved (coastal) altimetry data can be used in the coastal areas. However, for the inland seas such as the Black Sea, such dataset is not still common. In the study, the gridded daily Sea Level Anomalies maps with spacing of 1/8° x 1/8° provided from the AVISO have been used. The dataset, which is a product of combined data from several altimetry missions, spans the period from January 1993 to December 2014. Here, it should be noted that the Copernicus Marine and Environment Monitoring Service is taking over the processing and distribution of the altimetry products from May 2015. More details can be found at the AVISO and CMEMS web sites.

As stated previous Section, there are 3249 altimetric grid points in the Black Sea. In order to compare with tide-gauge results, the altimetry measurements at the closest points to the tide-gauge sites were selected (Figure 4.18). According to grid interval, the altimetric points were chosen with less than 10 km to the tide-gauges (Table 4.5). Furthermore, in order to compare the trends at the same location, it was interpolated from the trends obtained at the altimetric grid points in the defined neighbouring area with a diameter of 0.125° using a weighted average interpolation algorithm at each tide-gauge site. Considering the time-spans of the tide-gauge records, the altimeter monthly sea level time series were used.
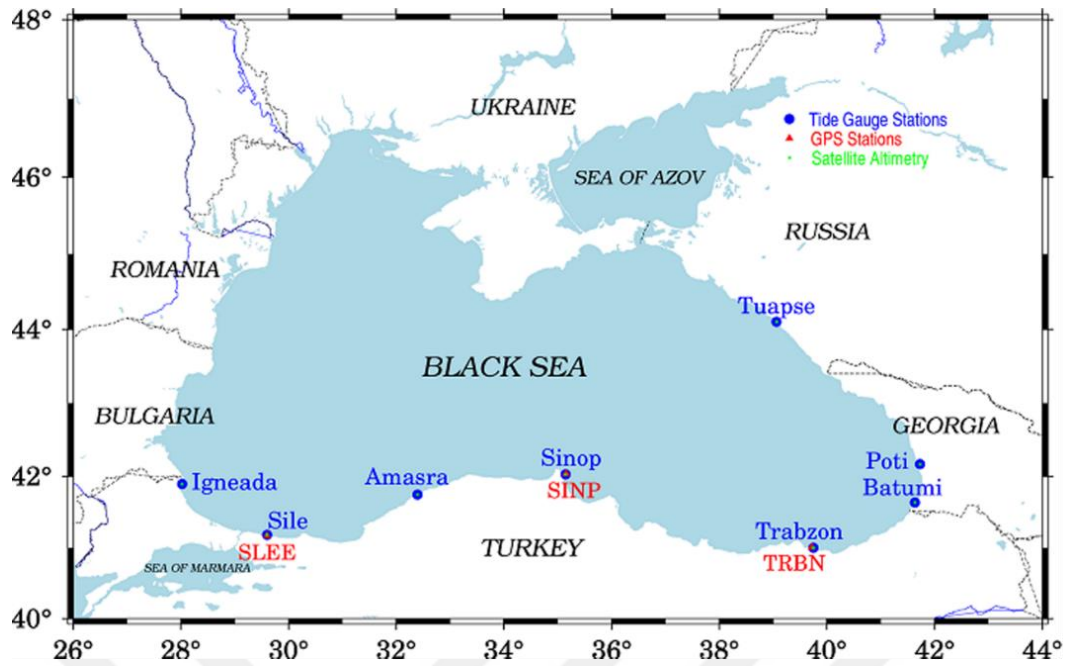
Figure 4.18 Data locations in the study: Tide-gauge stations (blue), GPS stations (red), and altimeter grid points (green).

4.5.1.1 Comparison with the Results from Tide-Gauges

To compare with the satellite altimeter measurements, the only data after 1993 from the long-term tide-gauge records have been used in this Section. Some tide-gauge time series include missing observations; therefore, the data gaps in these time series were eliminated. For example, at the Batumi station only 10-year record was useful for present study. In addition, because of some problems in tide-gauges, such as less data and short overlapping period, it has been concentrated on the analysis of sea level change at only 8 tide-gauge locations along the eastern and southern coasts of the Black Sea (Figure 4.18).

As an example, the sea level time series at the Trabzon tide-gauge location are depicted in Figure 4.19. As seen in the figure, the time series from altimeter and tide-gauge measurements show almost similar behaviour in the sea level change.
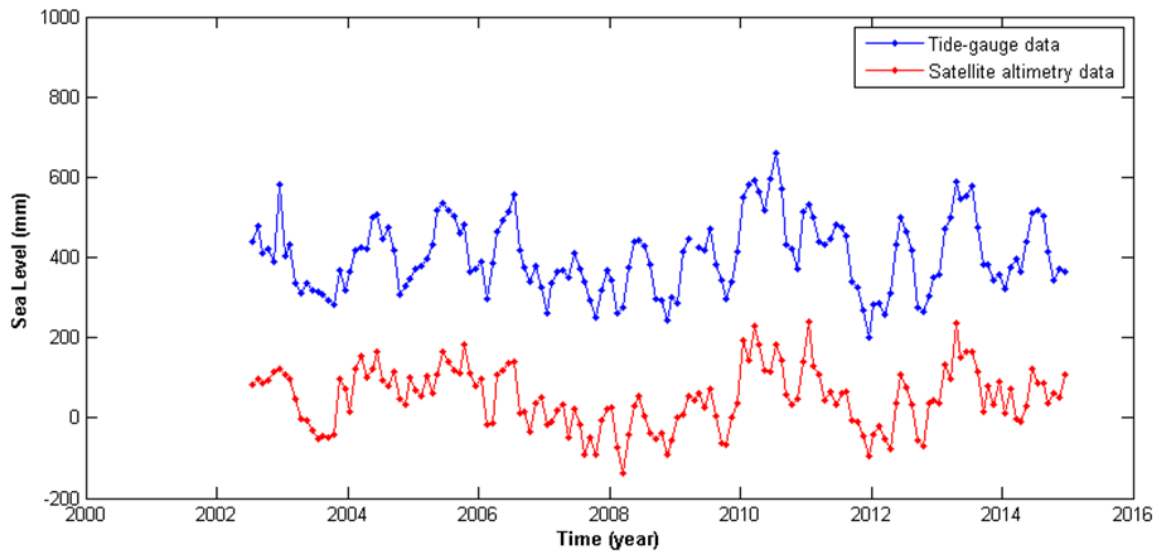
Figure 4.19 Sea level time series at the Trabzon tide-gauge location from satellite altimetry (red line) and tide-gauge (blue line) observations.

For the monthly time series of both the sea level measurements at 8 tide-gauge locations, the trend and seasonal components have been estimated by calculating Equation (4.1) with the least squares method.

The linear trends are shown in Table 4.5 and Figure 4.20 for each station. The results for the stations with long-term records such as Poti and Tuapse have a good agreement. At some stations like Amasra, the linear rates of both observation data are not statistically significant with a correlation coefficient of -0.08 between both the time series. It may result from the short time-span or the data gaps. As referred previously (Douglas 2001), sea level trends of tide-gauges records which are shorter than about 50 years are corrupted by interdecadal sea level variation. Church and White (2011) also stated that tide-gauge records have considerable interannual and annual variability.

In order to compare the trends estimated from satellite altimetry data at exact location of the tide-gauge site, also a neighbouring area with a diameter of 0.125° around each tide-gauge site was defined. Thus, to derive the trend at the tide-gauge site from altimetry data, it was utilized from the altimetric grid points in this area. The trend values were computed using a weighted average interpolation algorithm at each tide-gauge site. Here, the weighting is based on the inverse of the square of the distance between the tide-gauge site and the neighbour altimetric points. Here, the weighting and the area boundary were chosen empirically. However,

113

interpolated trend values were not very different from the trends obtained at the closest altimetric grid points. So, these values were not included in the study.

Table 4.5 Trends of sea level change from satellite altimetry and tide-gauge data at same observation period.

Tide-Gauge station	Distance (km)	Time-span	Trend (mm/y)	
			Satellite Altimetry	Tide-Gauge
Poti	2.4	Jan. 1993 – Dec. 2013	3.45 ± 0.78	4.13 ± 0.78
Tuapse	4.2	Jan. 1993 – Dec. 2011	3.42 ± 0.86	4.30 ± 0.88
Batumi	6.2	Sep. 2003 – Dec. 2013	1.38 ± 2.29	3.47 ± 2.56
Amasra	7.9	June 2001 – Dec. 2012	0.95 ± 1.72	0.07 ± 1.45
Igneada	7.9	July 2002 – Dec. 2014	2.19 ± 1.66	6.74 ± 2.08
Trabzon	8.6	July 2002 – Dec. 2014	-0.38 ± 1.65	2.33 ± 1.76
Sinop	6.0	June 2005 – Dec. 2014	7.05 ± 2.48	0.43 ± 2.88
Sile	5.5	July 2008 – Dec. 2014	3.61 ± 4.57	5.03 ± 4.84
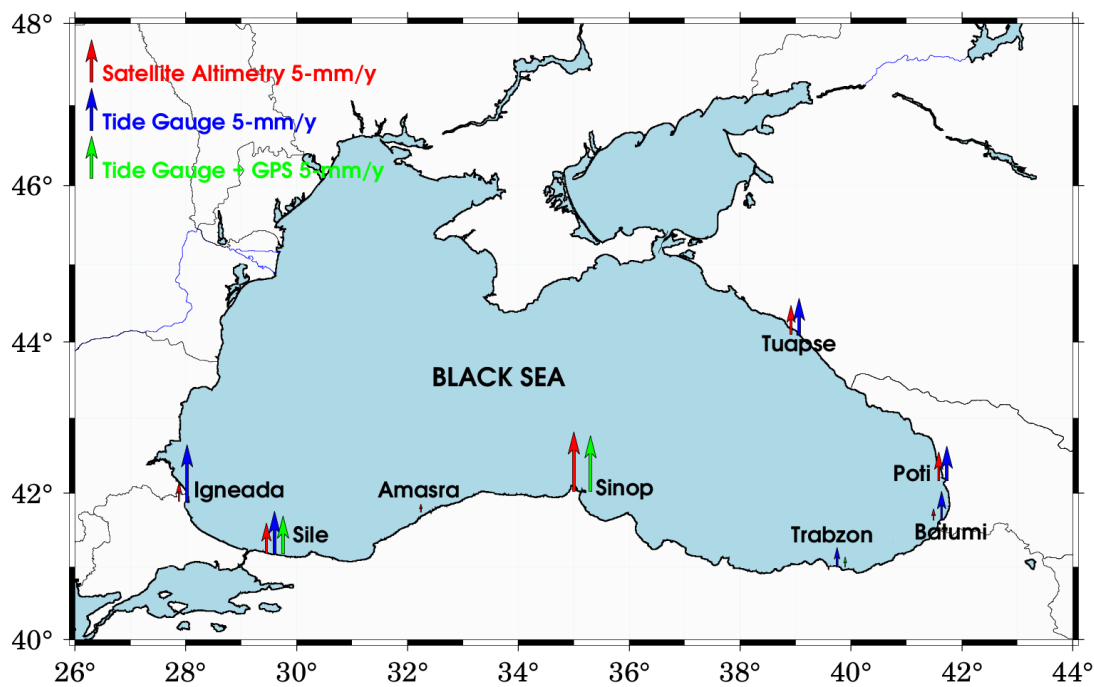
Figure 4.20 Trends along the Black Sea coast.

Seasonal components of the sea level change along the Black Sea coast are given in Table 4.6. Accordingly, the results are generally in good agreement with each other. The average annual amplitude of sea level variations is about 35.44 mm from the satellite altimetry, and 55.72 mm from the tide-gauges. The annual cycle of sea level change measured by the altimetry reaches

114

the maximum value almost a month later than that of sea level change obtained from the tide-gauge. The correlation coefficients between seasonal components of two time series are 0.45 and 0.48 for the annual amplitude and the annual phase, respectively.

Since tide-gauge measurements are made with respect to a local fixed reference level on land, the tide-gauge data reflect the relative sea level change (Section 3.2.1). If there is a vertical land motion at that tide-gauge location, the tide-gauge record is a combination of local sea level change and vertical land motion at the location. Therefore, in order to obtain absolute coastal sea level change, the vertical land motion should be added via levelling and/or GNSS observations.

Table 4.6 Seasonal components of satellite altimetry and tide-gauge time series.

Tide-gauge station	Satellite Altimetry				Tide-Gauge			
	Annual		Semi-annual		Annual		Semi-annual	
	Amplitude (mm)	Phase (°)	Amplitude (mm)	Phase (°)	Amplitude (mm)	Phase (°)	Amplitude (mm)	Phase (°)
Poti	30.70±6.68	-33.83±0.17	23.65±6.68	-44.67±0.28	45.97±6.86	-44.65±0.15	17.22±6.87	-76.77±0.40
Tuapse	42.76±6.71	3.47±0.01	19.50±6.70	-64.21±0.34	55.75±6.85	-31.93±0.09	26.80±6.83	-78.81±0.25
Batumi	43.52±9.62	22.74±0.12	26.24±9.62	80.35±0.37	90.08±10.87	-46.46±0.12	14.37±10.75	71.98±0.75
Amasra	24.59±8.15	-44.89±0.33	20.44±8.11	76.50±0.40	27.40±6.78	-43.90±0.24	9.30±6.57	69.17±0.72
Igneada	23.16±8.59	-37.91±0.32	11.54±8.50	62.00±0.74	52.11±10.89	-66.09±0.27	22.54±10.88	16.59±0.49
Trabzon	22.46±8.44	-16.91±0.16	22.46±8.43	-57.83±0.38	62.65±8.99	-48.58±0.15	27.27±9.01	-77.18±0.33
Sinop	33.41±9.73	-36.02±0.24	26.50±9.68	72.16±0.37	49.04±11.26	-60.82±0.28	29.52±11.27	47.94±0.38
Sile	62.92±12.84	-23.86±0.12	22.90±12.84	70.87±0.56	62.74±12.66	-51.00±0.20	22.84±12.66	48.96±0.55

Generally, continuously operating GNSS stations co-located with tide-gauge stations, or episodic GNSS and precise levelling measurements (like at the TUDES network) are used to monitor the vertical land motions at the tide-gauge sites. Moreover, a number of studies have utilized nearby GNSS stations from national or international networks (e.g., Bouin and Wöppelmann 2010) or DORIS observations (Ray et al. 2010) to observe vertical land motions. In this study, to estimate absolute sea level changes from the tide-gauges, 3 GPS stations (TRBN, SINP, and SLEE), which are nearly co-located tide-gauge stations, from the Turkish National Permanent Real Time Kinematic Network (TUSAGA-Active) (URL-55) have been used. The GPS data were spanning from 1 January 2010 to 31 December 2014. Using the IERS (International Earth Rotation Service) solid Earth tide and pole tide model, and a 10° elevation cut-off angle, the vertical coordinates of GPS stations were obtained using the GAMIT/GLOBK scientific software package (Herring et al. 2015).

As mentioned above, for this study, the vertical land motions at 3 tide-gauge sites along the southern Black Sea coast were estimated from nearby GPS stations (using Equation (4.1)), and added to the results obtained from the tide-gauge data. For the Trabzon, Sinop and Sile tide-gauge locations, the trends of sea level change from tide-gauge + GPS are presented in Table 4.7 along with those computed from the satellite altimetry. The results derived from the satellite altimetry, tide-gauge, and tide-gauge + GPS are also shown in Figure 4.20. It is clearly seen that the results of satellite altimetry and tide-gauge + GPS have a better agreement.

Table 4.7 Sea level trends from satellite altimetry, and tide-gauge + GPS time series at 3 tide-gauge locations along the Black Sea coast.

Tide-Gauge station	GPS station	Distance	Trend (mm/y)	
			Satellite Altimetry	Tide-Gauge + GPS
Trabzon	TRBN	2.8	-0.38 $\pm$ 1.65	1.21 $\pm$ 1.78
Sinop	SINP	0.8	7.05 $\pm$ 2.48	6.63 $\pm$ 3.81
Sile	SLEE	1.2	3.61 $\pm$ 4.57	4.44 $\pm$ 4.85
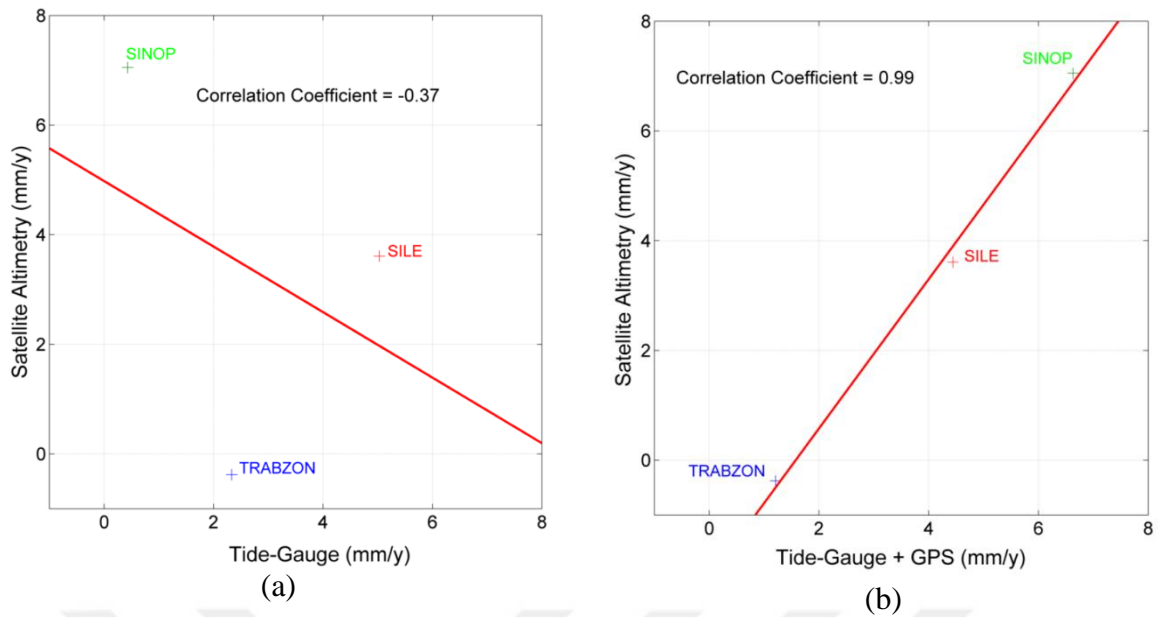
Figure 4.21 Correlations for the Trabzon, Sinop and Sile tide-gauge locations between trends of a) satellite altimetry and tide-gauge time series, b) satellite altimetry and tide-gauge + GPS time series.

Their relationships are further analysed (see Figure 4.21). The correlation between satellite altimetry and tide-gauge + GPS has much improved. Figure 4.22 shows the differences between the trends obtained from the satellite altimetry, the tide-gauge and tide-gauge + GPS. When including GPS vertical motion, the tide-gauges' results are much closer to the satellite altimetry results for all of the 3 stations. Especially for the Sinop station, the trend difference between satellite altimetry and tide-gauge + GPS is much smaller than that difference between satellite altimetry and tide-gauge. These results reveal that the vertical land motion varying at tide-gauge stations should be taken into account to get the absolute sea level change when using tide-gauges data.
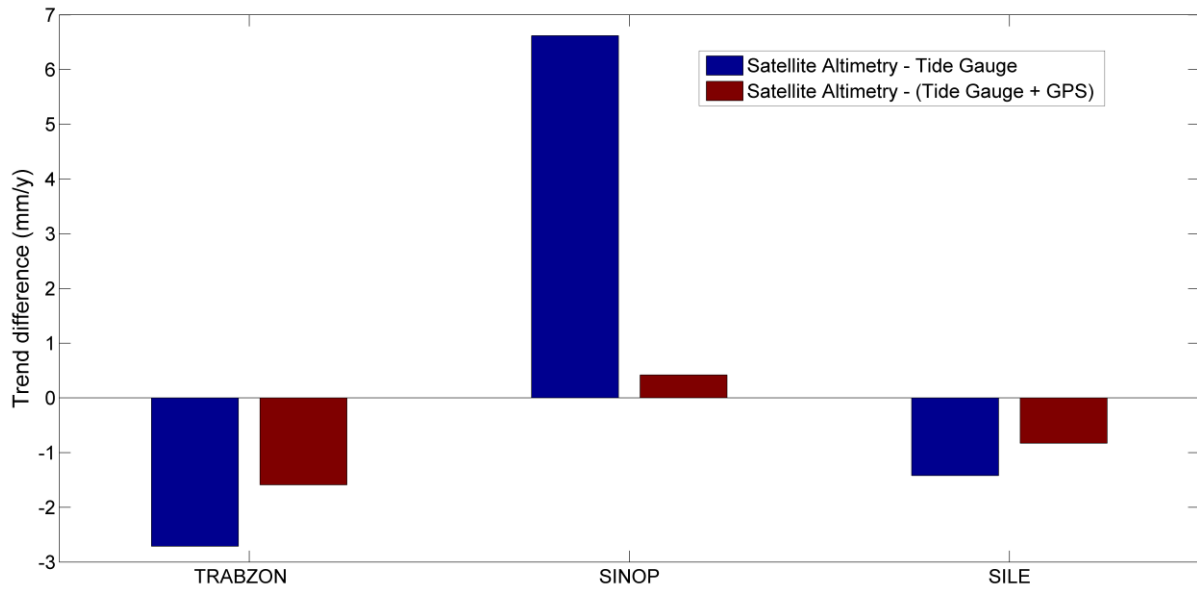
Figure 4.22 Comparison of the trend differences from satellite altimetry, tide-gauge, and tide-gauge + GPS at the Trabzon, Sinop and Sile locations.

4.5.2 Estimation of Vertical Land Motion along the Black Sea Coast

Different spatial and temporal sampling, measurement noise, modelling errors and corrections applied to the data, etc., induce a negligible difference between the sea level changes obtained from tide-gauge and satellite altimetry measurements (Fenoglio-Marc and Tel 2010). However, more importantly, tide-gauges measure Sea Surface Height relative to a benchmark on the land whereas altimetry provides absolute Sea Surface Height with respect to a geocentric reference frame. Therefore, as highlighted in the previously, tide-gauge records also contain geophysical signals related to land motion. Accordingly, the essential difference between altimeter and tide-gauge observations is geocentric vertical land motion at the tide-gauge location. That is to say, the combination of these two sea level measurements enables to assess vertical displacement at the tide-gauge location independently of the well-known geodetic techniques such as GNSS.

A number of studies based on the approach of subtracting tide-gauge data relative to the coast from geocentric altimetry data for estimating vertical land motion have been carried out over the past 20 years (such as Cazenave et al. 1999, Garcia et al. 2007, 2012, Nerem and Mitchum, 2002). Recently, various approaches (Kuo et al. 2004, Ray et al. 2010, Wöppelmann and Marcos, 2012, 2016) adapted from the aforesaid approach have been appeared, aiming to improve vertical motion estimates.

Such studies have been less along the Black Sea coast due to the deficiency of available set of long-term tide-gauge records in the region. For example; for the 1993–2001 period, Garcia et al. (2007) reported a land uplift rate of 3.5 ± 2.7 mm/y and 6.2 ± 1.7 mm/y at the Poti and Tuapse tide-gauge locations, respectively and, a land subsidence rate of -12.3 ± 7.4 mm/y and -25.5 ± 6.1 mm/y at the Bourgas and Varna tide-gauge locations, respectively, from $1° \times 1°$ gridded altimetry data (from Topex/Poseidon and ERS1/2 satellites), and tide-gauge data. Kubryakov and Stanichnyi (2013), also, analysing the differences between sea level time series for the period of 1993–2005, from along-track data of Topex/Poseidon and Jason-1 satellites, and tide-gauge stations along the Ukraine's Black Sea coast, demonstrated that coasts of the Eastern Crimea and Odessa subsided with the rate of -8.8 ± 1.7 mm and -5.1 ± 3.6 mm per year, respectively.

This section presents an assessing of vertical land movements at the 13 tide-gauge sites along the Black Sea coast from the difference between altimetry and tide-gauge observations, by also considering measurements from the nearby GPS stations.

A brief overview of the geological evaluation of the Black Sea has been already given in Section 2.2. Tectonic situation of the Black Sea region are also decisive in investigating the vertical land motions (Sosson et al. 2010). The Black Sea is surrounded by the Eurasian plate in the north, and the African and the Arabian plates in the south (Figure 4.23). The ongoing interactions between these plates, and so the westward motion of the Anatolian block are noteworthy in terms of tectonics of the Black Sea basin.
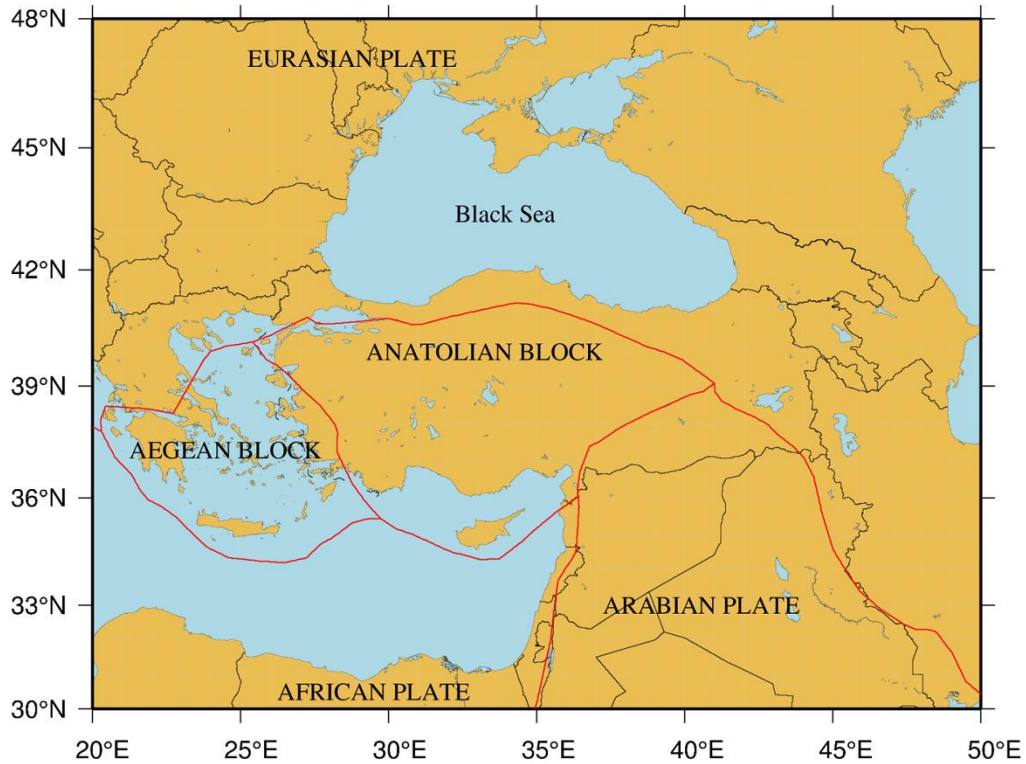
Figure 4.23 Plate boundaries in the circum Black Sea according to Bird (2003).

According to Tari et al. (2000), a compressional tectonic regime is active in the eastern of the region and there is a north-south shorting at the southeast coast, whereas the southwest parts do not show an apparent seismic activity to resolve whether compressional or extensional regime is active. Some geophysical researches also show an average subsidence in the Black Sea basin by about 1 mm/y (Bondar 2009), which exceeded in the Crimean coast (-2 mm/y), Odessa (-5 mm/y) and Poti (-6 mm/y), aforementioned. Besides, a considerable crust subsidence was reported at Varna and Bourgas in Goryachkin and Ivanov (2006) (Bondar 2009). Pashova (2002) also addressed strong irregular local subsidence in the harbour areas Varna and Bourgas. Furthermore, at some specific locations along the Black Sea coast, anthropogenic effects might be dominant for vertical movements, for example related to groundwater pumping, oil/gas extraction or land settlement (Garcia et al. 2012, Pashova and Yovev 2010).

On the other hand, note that according to the GIA models, the post glacial rebound effect is minimal in the Black Sea region. The present-day rates of land movement because of the ongoing post-glacial rebound are mapped in Figure 4.24, according to the ICE-6G_C (VM5a) model from Peltier et al. (2015).
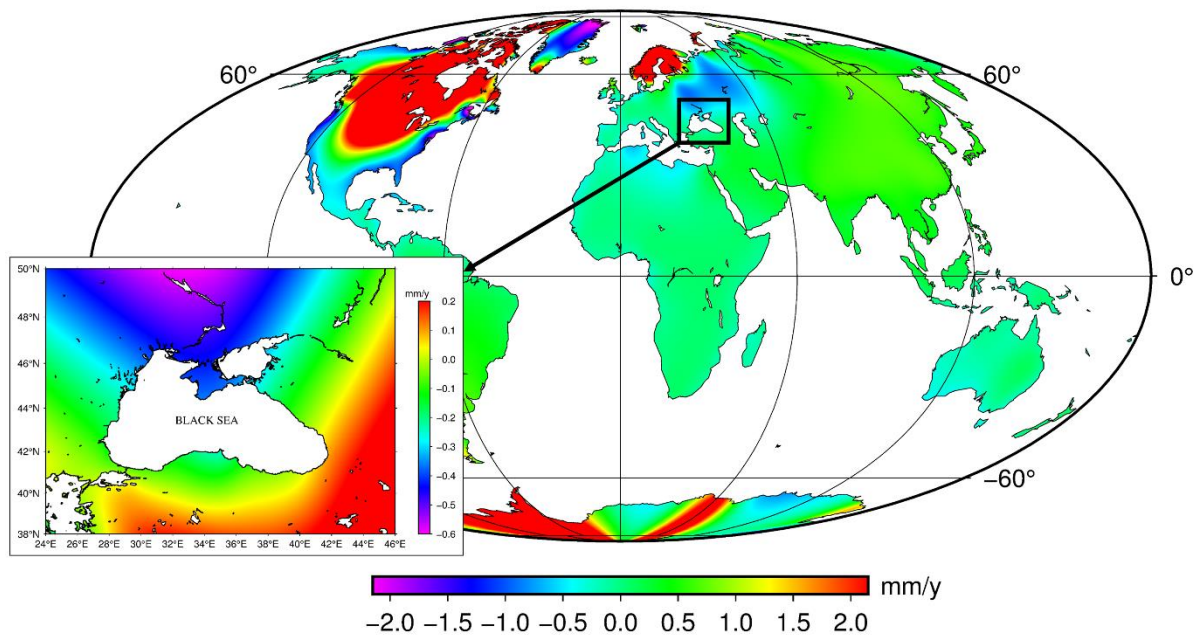
Figure 4.24 Predicted present-day rate of vertical motion of the solid Earth due to GIA according to the ICE-6G_C (VM5a) model from Peltier et al. (2015) (Area surrounding the Black Sea is zoomed-in).

4.5.2.1 Sea Level Differences from Satellite Altimetry and Tide-Gauges

As stated above, in this study, the vertical land motion was investigated using the differences between satellite altimetry and tide-gauge monthly sea level time series at each tide-gauge location along the Black Sea coast. Hereby, the contribution of changes in ground level to coastal sea level changes in the Black Sea has been examined.

This study followed the same idea presented in Garcia et al. (2007), however utilized more tide-gauge data, and the time period was extended up to 21 years for some stations like Poti. Prior to the computations of the difference time series, the seasonal signals have been removed from the original time series as their presence can distort trend estimates of the short time series as pointed out in Garcia et al. (2007), and Wöppelmann and Marcos (2012).

As remarked in Douglas (2001), since low-frequency sea level signals can affect the accuracy of long-term vertical land motion estimates (Wöppelmann and Marcos 2012) or not allow to estimate a stable trend in land movement. On the other hand, the long-time interval (>= 50-year) is available only for a few tide-gauges used in this study. In view of the effective number of available stations along the Black Sea coast, the tide-gauge stations having the incomplete

records have not been ignored for this study. Figure 4.25 shows the tide-gauge stations used in this study, and also the data gaps in the tide-gauge time series given in Table 4.8.
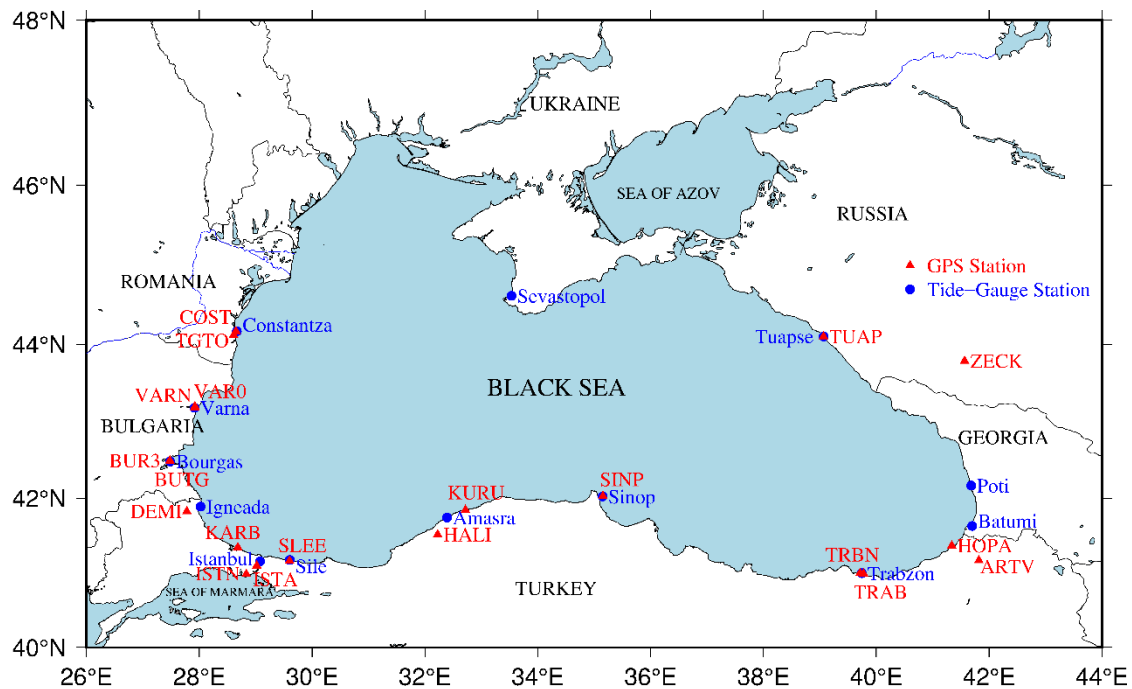
Figure 4.25 Data locations in the study.

As satellite altimetry data, the gridded altimetry data that is used in the previous section have been preferred. Here, note that, Yildiz et al. (2013) used along track, gridded and coastal altimetry products to estimate vertical land motion along the southwestern of Turkey, and compared their results by considering the distance to the tide-gauges, the correlation and the RMS of the differences between satellite altimetry and tide-gauge time series. The results indicated that the gridded altimetry data provide the best agreement with tide-gauge data due to their smoother variability both in space and time than the along-track data. Moreover, Yildiz et al. (2013) asserted that the making use of the coastal altimetry data did not improve the vertical land motion estimates importantly.

For this study, the altimetry observations at the closest points to the tide-gauge sites have been used as applied in the previous section. Each point can be as far as roughly 9.8 km to the corresponding tide gauge. The distances between the tide gauges and the altimetric points are given in Table 4.8.

Wöppelmann and Marcos (2012) also pointed out that the overlapping period of both data type is of major importance for a reliable estimate of vertical land motion rate. In order to investigate vertical land motion at the tide-gauge locations, they employed tide-gauge data which were contemporary to altimetry data for at least 8 years by testing the different overlapping periods' stabilities, whereas Cazenave et al. (1999) used about 5-year common data period. Wöppelmann and Marcos (2012) asserted that the short overlapping periods cause larger rate uncertainties. In this study, the available tide-gauge data beginning from January 1993 have been used associated with the corresponding to altimetry data (see Table 4.8). Thus, short overlapping periods are assessable for some tide-gauges (Sevastopol: ~ 2 years, Varna: ~ 4 years, Bourgas : ~ 4 years and Constanza: ~ 4 years). Also, the data from the Istanbul station have been provided since only June 2011. In fact, the estimated vertical land motion rates in such studies are limited by the short-term (interannual and decadal) variability of observed sea level signal. This is why that the short tide-gauge records with not sufficiently long altimetry time series are mostly obtainable for vertical land motion analysis. Nevertheless, many studies (such as Cazenave et al. 1999, Garcia et al. 2007, Nerem and Mitchum 2002) demonstrated that the combination of available tide-gauge and altimetry data can provide worthwhile results for vertical land motion estimation.

In order to estimate vertical land motion at the tide-gauge locations along the Black Sea coast, the approach implemented in the study is based on the classical approach using the difference time series for altimetry minus tide gauge. Here, a similar notation in Garcia et al. (2007) has been followed, that is, TG(t) and SA(t) denote the sea level time series of tide-gauge records, and satellite altimetry measurements at the closest available point to tide-gauge site, respectively. As previously noted, when forming the difference between SA(t) and TG(t) for a common observation period, apart from the deviations caused by measurement noise, data gaps because of power outages, instrumental drifts or calibration errors, the only existing would be geocentric vertical land motion at the tide-gauge site. In here, for comparison of two sea level time series, the distance (see Table 4.8) between the location of tide-gauge and corresponding point of the altimetric grid has been ignored (Garcia et al. 2007, Yildiz et al. 2013).

The trend estimates of vertical land motion are strongly affected by the seasonal signals. Therefore, the original time series of altimetry and tide-gauges should be isolated from such signals. Here, the seasonal signals have been removed from both time series by simple subtraction of the estimates obtained by least squared fitting of seasonal sinusoids with annual and semi-annual periods as

defined in Garcia et al. (2007) and Wöppelmann and Marcos (2012). And the non-seasonal differences between SA(t) and TG(t) have been computed for each tide-gauge.

In order to qualify the estimates, the correlation between altimetry and tide-gauge sea level time series, and the Root Mean Square (RMS) of non-seasonal differences were also taken into consideration in the study. Figure 4.26a and b depict correlation between the non-seasonal sea level time series, and histogram of their differences, respectively by considering all altimetry and tide-gauge observations used in this study. Furthermore, the correlation between both non-seasonal time series, and the RMS of difference time series are also given in Table 4.8 separately for each tide-gauge location. It is clear from Table 4.8 and Figure 4.26a that despite of several possible error sources mentioned above, the tide-gauge and altimetry data are in good agreement except for Batumi. The RMS value of differences is 14.7 cm and the correlation coefficient is -0.27 between SA(t) and TG(t) at the Batumi station. It is very likely that this case is related to nearly 7-year gaps in the records of the Batumi station. Figure 4.26a shows a correlation of 0.59 (a moderate linear relationship) for all the data. Accordingly, the data are somewhat scattered in a wider band; however the correlation coefficient is 0.76 (a strong linear relationship) without the Batumi data. Although the tide-gauge data of Tuapse show the best agreement with the altimetry data among all the tide-gauges, the TUDES network's tide-gauges exhibit better statistics than the PSMSL tide-gauges in terms of the correlation coefficient. According to Figure 4.26b, the differences have an approximately normal distribution with a mean of 33 mm, and most of them fall in range of -25 to 100 mm. It is worth mentioning again that the discrepancies of SA(t) and TG(t) may result from the instrumental error factors (measurement noise, power outages, drifts, etc.), the data processing methodology (different corrections applied for altimetry and tide-gauge data, interpolation for deriving altimetric grids, etc.), and the different spatial and temporal sampling from both techniques. Nevertheless, the influence of differences due to such factors on vertical land motion estimates is in any case small in magnitude (Garcia et al. 2007).
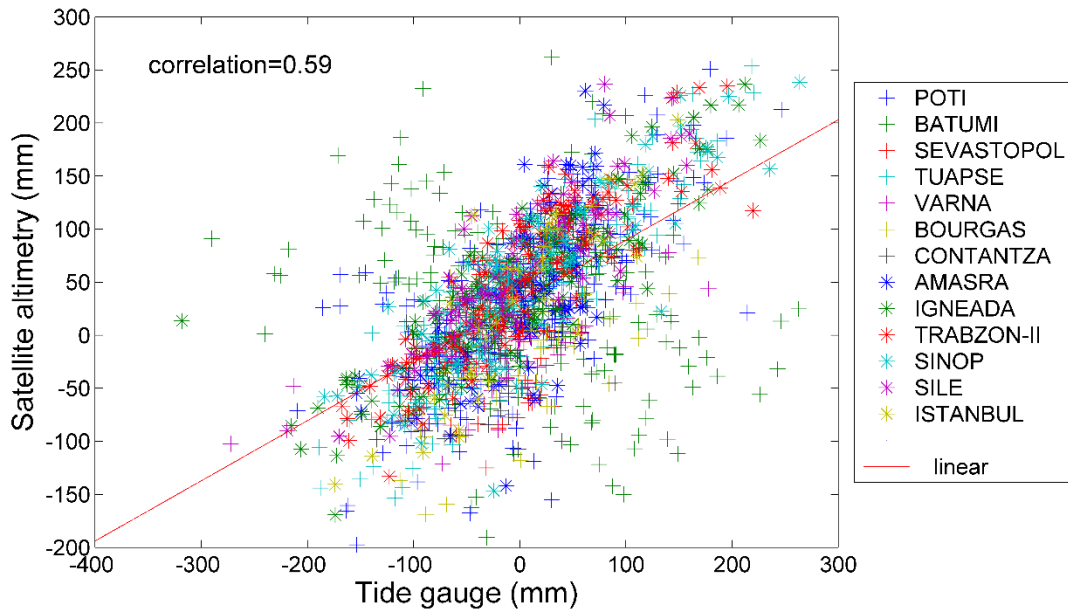
a) Scatter plots of satellite altimetry and tide-gauge data.
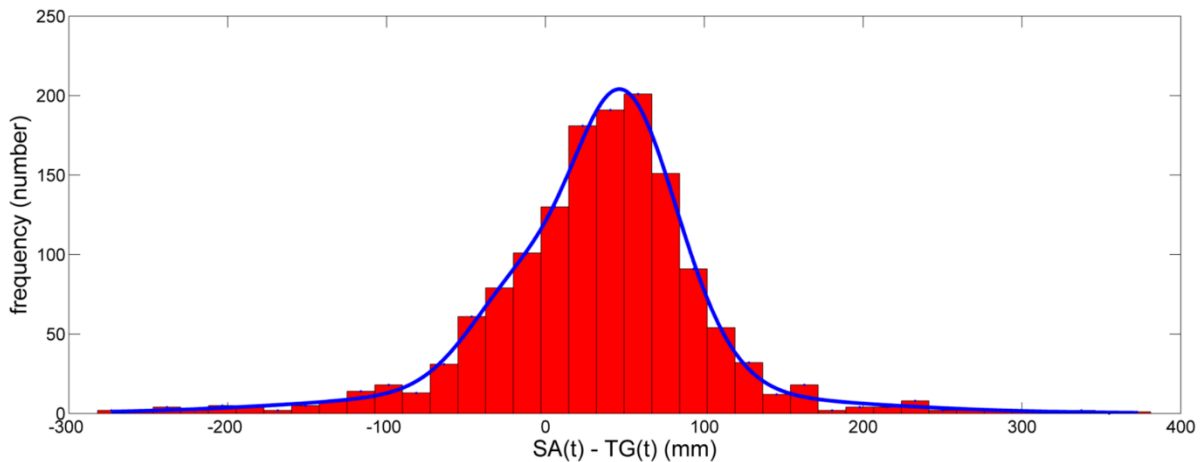
b) Histogram of differences between satellite altimetry and tide-gauge data.

Figure 4.26 For non-seasonal SA(t) and TG(t) at 13 tide-gauge stations along the Black Sea coast.

As can be seen from Table 4.8, the common period of tide-gauge and altimetry data is very short for Sevastopol. Thus, this station was discarded from the analysis despite its agreement with high correlation. Eventually, a linear regression has been applied to derive the rates of change of non-seasonal differences, and their standard errors at all the tide-gauge locations. Consequently, the linear trend computed for each tide-gauge is given in Table 4.9. Here, the positive trend represents land uplift while the negative trend represents land subsidence (Cazenave et al. 1999, Garcia et al. 2007).

Table 4.8 An evaluation of tide-gauge and satellite altimetry data on the basis of tide-gauge stations along the Black Sea coast over the common time-span.

Tide-gauge station	Common time-span	Gaps (%)	Distance (km)	Correlation	RMS (cm)
Poti	1993–2013	5.2	2.4	0.69	7.0
Batumi	1993–2013	31.8	6.2	-0.27	14.7
Sevastopol	1993–1994	0	6.8	0.70	5.7
Tuapse	1993–2011	1.3	4.2	0.89	4.8
Varna	1993–1996	16.7	2.4	0.66	6.0
Bourgas	1993–1996	10.4	7.2	0.66	6.0
Constantza	1993–1997	8.3	3.3	0.71	4.5
Amasra	2001–2012	9.4	7.9	0.70	6.1
Igneada	2002–2014	5.3	7.9	0.86	6.6
Trabzon	2002–2014	0.7	8.6	0.88	6.2
Sinop	2005–2014	0	6.0	0.82	6.8
Sile	2008–2014	0	5.5	0.88	7.2
Istanbul	2011–2014	0	3.3	0.88	5.0

4.5.2.2 Analysis of Vertical Velocities of GPS Stations Nearby Tide-Gauge Stations

The estimated vertical land motion rates at the tide-gauge locations have been also compared with vertical velocities of the continuous GNSS or the campaign GPS stations that are neighbouring to these tide-gauge stations (All the stations, hereinafter referred to as GPS stations as in previous section). The GPS stations in this study were chosen by considering their proximity to the tide-gauges.

For comparison, the measurements from total 20 GPS stations which are co-located at or close to a tide-gauge station along the Black Sea coast have been used (Figure 4.25, Table 4.9). The vertical displacement time series of 4 stations (TUAP, VARN, BUR3 and TGTO) in the region have been obtained from the Nevada Geodetic Laboratory (NGL) (URL-56). 7 stations (ARTV, KURU, TRBN, SINP, SLEE, ISTN and KARB) from the TUSAGA-Active, 3 stations (ZECK, TRAB and ISTA) from the International GNSS Service (IGS) Network (URL-57) and also 1 station (COST) from the EUREF Permanent Network (EPN) (URL-58) data have been processed using the GAMIT/GLOBK software. Data belong to continuous GNSS stations around the Black Sea, which were processed in this study, vary from 2000 to 2017 (see Table 4.9). In addition to these continuous GNSS stations, the GPS campaign measurements from 1991 to 1998 around the Black Sea, which were provided from the collaborated study between

Istanbul Technical University (ITU), Massachusetts Institute of Technology (MIT) and Joint Institute of Physics of the Earth (Tari et al. 2000) were used: HOPA, VAR0, BUTG, HALI and DEMI. However, the data belong to early 90s could not be included in the processing due to lack of precise orbit information.

In the GAMIT phase of evaluations while applying loose constraints to estimate coordinates and atmospheric parameters, the global permanent sites (15 stations from the IGS) have been used to establish the link between regional and global networks. The final product of IGS as precise orbit, tidal and non-tidal atmospheric pressure loading with the Earth's center of mass frame (Tregoning and van Dam 2005) have been preferred in the GAMIT software. Zenith delay unknowns have been computed based on the Saastamoinen troposphere model with Vienna mapping function (Boehm et al. 2006). The second- and third-order of the ionospheric effects were neglected in the processing. For ocean loading, FES2004 model has been used which is asserted to be most accurate in the Black Sea region (Gurbuz and Jin 2016).

4.5.2.3 Comparison of Vertical Land Motion Estimates

Generally, TG(t) and SA(t) show similar temporal behaviours in sea level fluctuations for tide-gauge locations along the Black Sea coast (as seen in Figure 4.19). However, when examining long-term behaviour of the sea level signal, some discrepancies have revealed. These discrepancies are mostly related to vertical land motions at the tide-gauge sites. As the examples of the comparison, in Figure 4.27a and b, the original time series for both observations (at the top), the remaining time series after removal of the seasonal signal (in the middle), and the difference time series with their regression lines (at the bottom) are shown for the Tuapse and Sinop stations, respectively.

Table 4.9 Linear trends of the vertical land motions at the tide-gauge locations along the Black Sea coast from the altimetry minus tide-gauge, and the GPS time series.

Tide-gauge station	GPS station	Time-span		Distance (km)	Vertical land motion (mm/y)		GIA (mm/y)
		TG(t)	GPS(t)		SA(t) - TG(t)	GPS(t)	
Poti	ZECK	1993–2013	1997–2013	186.7	-0.7 ± 0.6	-1.6 ± 0.5	0.02
Batumi	HOPA	1993–2013	1994–1998	41.9	11.2 ± 1.4	14.6 ± 5.5	0.04
	ARTV		2010–2014	51.9		-0.8 ± 0.1	
Tuapse	TUAP	1993–2011	2015–2017	0.05	-1.0 ± 0.4	-1.7 ± 0.5	-0.15
Varna	VAR0	1993–1996	1996–1998	0.7	-30.7 ± 7.5	-16.8 ± 8.3	-0.14
	VARN		2005–2017	2.1		-1.1 ± 0.1	
Bourgas	BUTG	1993–1996	1996–1998	0.08	-11.5 ± 6.9	-6.5 ± 2.4	-0.08
	BUR3		2009–2014	1.5		4.2 ± 0.2	
Constantza	COST	1993–1997	2010–2014	0.9	7.3 ± 4.2	6.9 ± 1.8	-0.18
	TGTO		2009–2010	7.1		2.3 ± 0.03	
Amasra	HALI	2001–2012	1994–1998	28.6	0.5 ± 1.4	5.2 ± 1.8	-0.15
	KURU		2010–2014	29.2		-5.3 ± 0.9	
Igneada	DEMI	2002–2014	1992–1998	21.4	-4.8 ± 1.0	-6.3 ± 0.5	-0.11
Trabzon	TRBN	2002–2014	2009–2014	2.8	-2.7 ± 0.8	-1.9 ± 0.3	-0.05
	TRAB		1999–2007	2.8		-0.3 ± 0.01	
Sinop	SINP	2005–2014	2010–2014	0.8	6.6 ± 1.5	6.2 ± 2.5	-0.26
Sile	SLEE	2008–2014	2009–2014	1.2	-1.3 ± 2.3	-3.0 ± 0.6	-0.11
Istanbul	ISTN	2011–2014	2011–2014	27.6	16.1 ± 5.8	25.7 ± 3.6	–
	KARB		2009–2011	38.7		-0.8 ± 0.2	
	ISTA		2011–2014	7.7		4.2 ± 0.1	

The results in Table 4.9 show land subsidence motions at Poti, Tuapse, Varna and Bourgas from the PSMSL tide-gauges, and Igneada and Trabzon from the TUDES tide-gauges. On the other hand, land uplift motions have been seen at Batumi and Constantza from the PSMSL tide-gauges, and Sinop and Istanbul from the TUDES tide-gauges. Also, the trends of vertical land motions at Amasra and Sile indicate the values statistically indistinguishable from zero within 1 standard deviation. It means to determine no significant motions for both the sites from altimetry minus tide-gauge. At the tide-gauge stations (Varna, Bourgas, Constantza and Istanbul), which have overlapping time-span with the altimetry period less than 5 years, the standard errors of vertical land motion rates are larger. Note again that the tide-gauge record in Batumi contains 32% data gaps. This lack mainly distorts the trend estimation of vertical land motion at this site. All the trend estimates of vertical land motion along the Black Sea coast are also illustrated in Figure 4.28 for sensing their spatial distributions.

For the 1993–2001 period, the similar results have been found in Garcia et al. (2007). They used 0.125° x 0.125° gridded satellite altimetry data, and determined vertical motions as follows: 2.98 ± 2.53 mm/y at Poti, and 4.05± 1.20 mm/y at Tuapse. However, the results for longer data period indicated a land subsidence rate at the Poti station as in Bondar (2009).

Besides, the estimates of vertical land motion along the Black Sea coast have been compared with the GPS-derived vertical displacement rates. As mentioned above, this comparison has included the time series, denoted by GPS(t), from 15 continuous GNSS stations and 5 GPS campaign stations in the Black Sea region. As an example, the GNSS monthly vertical position time series for the SINP station is also seen in Figure 4.27b.

The distances between tide-gauge and nearby GPS stations are given in Table 4.9. Accordingly, 8 tide-gauges stations in the study are located in less than 10 km from a GPS stations in the study (can be regarded as co-located). In general, the time-span of GPS(t) does not exactly coincide with the overlapping duration between SA(t) and TG(t) (see Table 4.9). This fact can be lead some discrepancies between both the trend estimates for vertical land motion (Garcia et al. 2012).
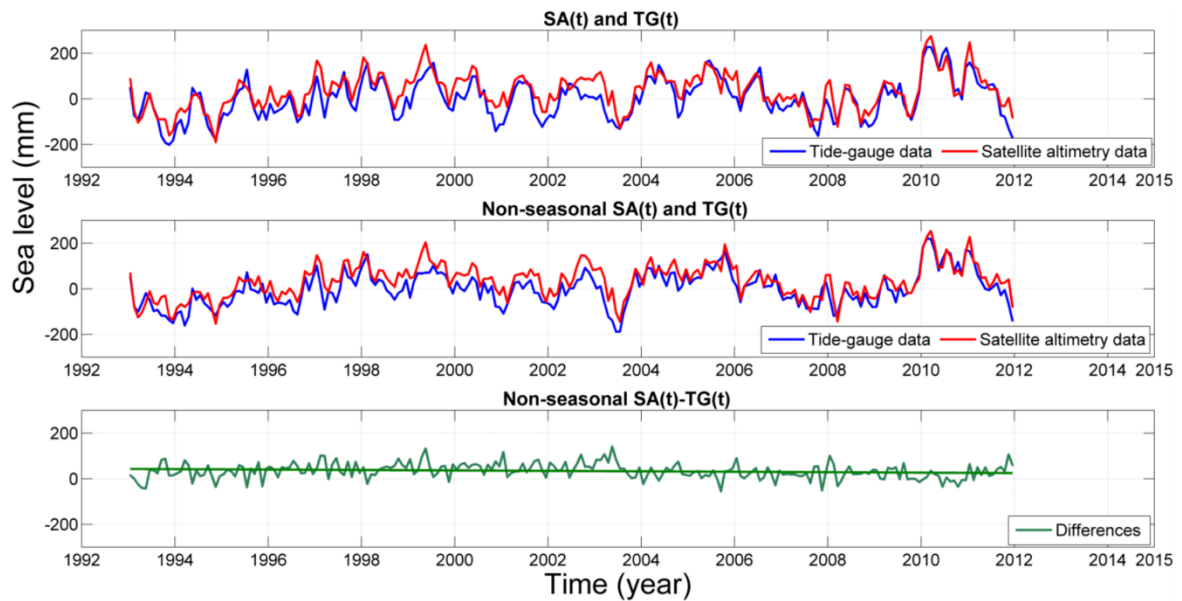
a) Tuapse tide-gauge location.
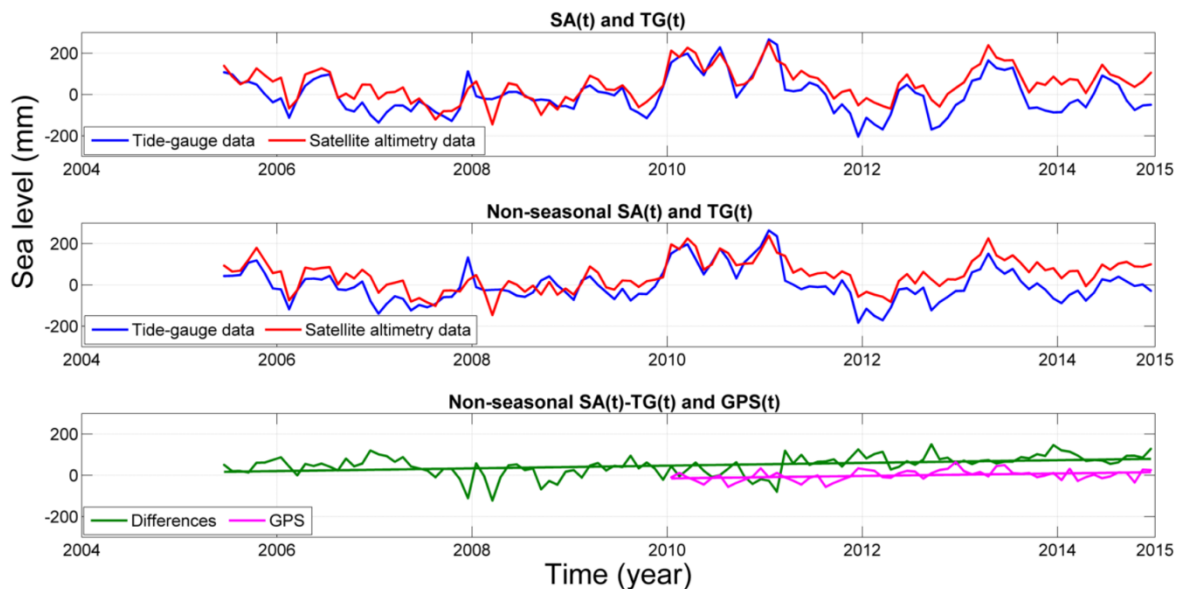
b) Sinop tide-gauge location.

Figure 4.27 Original time series (top), non-seasonal time series (middle), and non-seasonal difference time series and fit with linear regression (bottom) at Tuapse and Sinop tide-gauges (The vertical displacement time series at SINP TUSAGA-Active station and its linear fit are also seen at the bottom figure).

On the other hand, the distance between both the stations (GPS and tide-gauge), the various geophysical corrections applied to GPS, tide-gauge and altimetry data, the short time-spans of these datasets, etc. no doubt influence estimates. Nevertheless, the altimetry minus tide-gauge derived estimates have been in good agreement with the rates from the GPS measurements especially at Tuapse, Constantza, Igneada, Trabzon and Sinop tide-gauge locations (see Table 4.9 and Figure 4.28). The estimates for Poti and Batumi stations, despite of their longer distance

131

than 50 km from a GPS station, are consistent with the GPS-derived vertical velocities. At most of tide-gauge sites, both the estimates indicate a land motion in same direction. However, unlike the trend of SA(t)-TG(t), the trend of GPS(t) shows a significant subsidence motion at Sile. At this tide-gauge location, the larger uncertainty of the estimate from altimetry minus tide-gauge can be caused by the higher RMS value of differences between altimetry and tide-gauge data (see Table 4.8). Figure 4.29 demonstrates the difference of both rates at the co-located tide-gauge sites. It should be noted that most results of this study also agree with those inferred from the geological research.
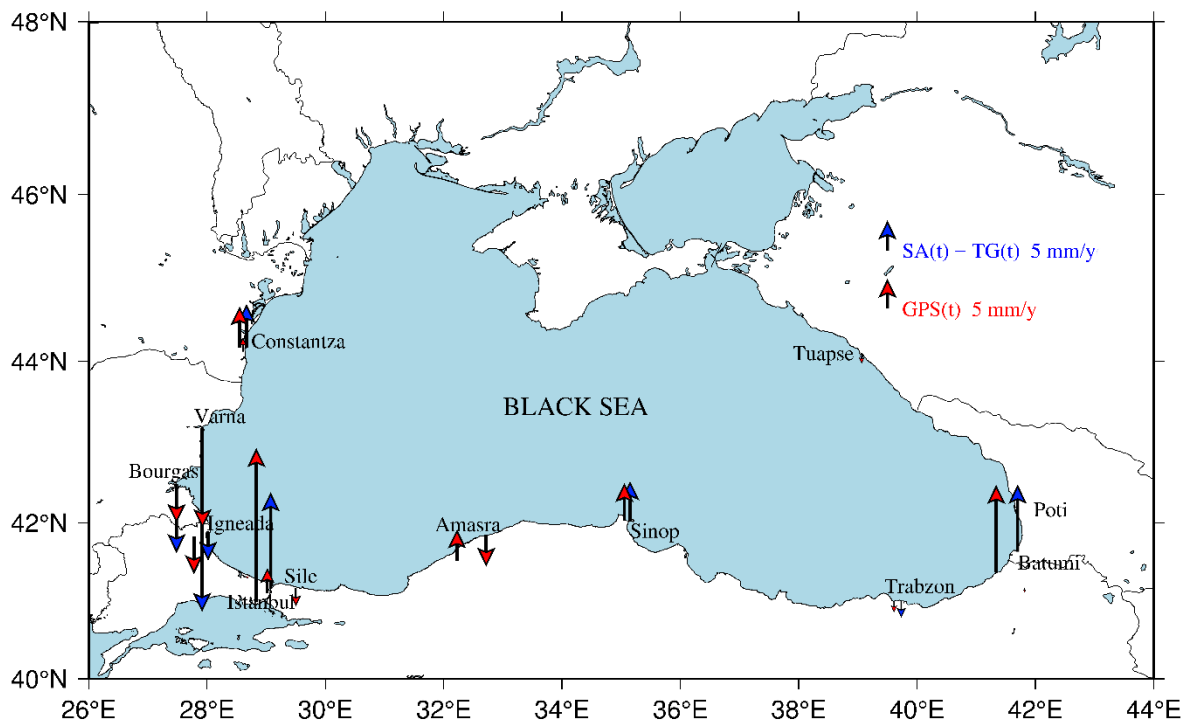
Figure 4.28 Vertical land motion at tide-gauge locations along the Black Sea coast derived from altimetry minus tide-gauge, and the corresponding GPS time series.

In addition, this study includes GIA-related land motion in the Black Sea region. In order to clarify whether it contributes to the determined motion at each tide-gauge site significantly, the ICE-6G_C (VM5a) model (Peltier et al. 2015) has been used in the study. According to this model, the vertical motion due to GIA is relatively small (see the last column in Table 4.9 and Figure 4.24) in the circum Black Sea. So, GIA effect in the region can be negligible. Nevertheless, it is noteworthy that at the Tuapse site, the GIA effect was in charge of around 15% of the estimated vertical land motion.
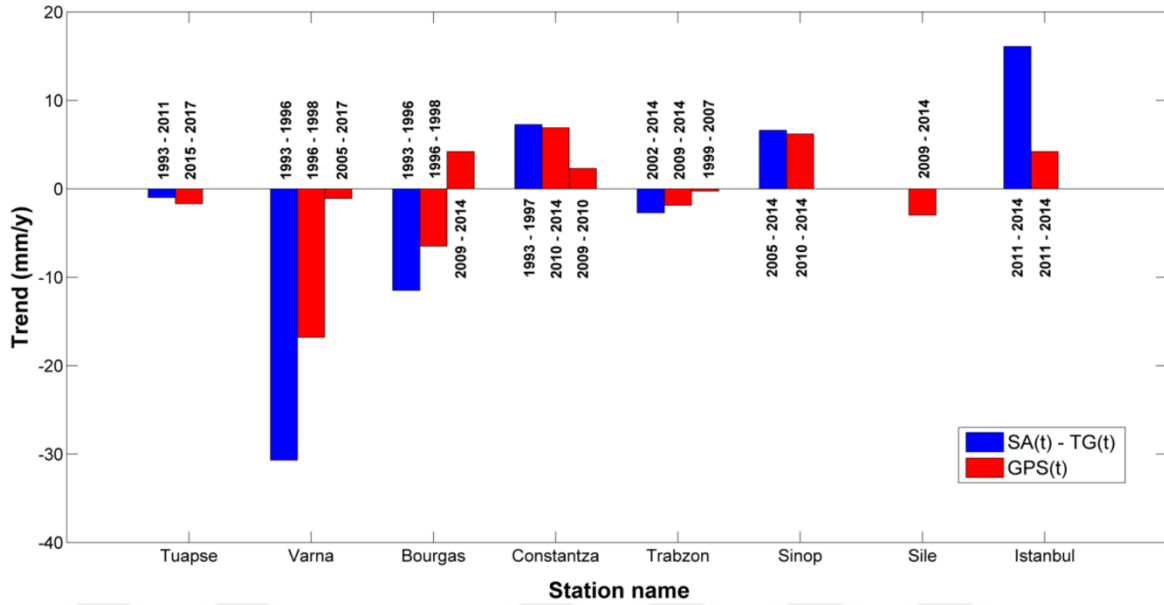
Figure 4.29 Trend estimates from SA(t)-TG(t) and GPS(t) at the tide-gauge stations which are nearly co-located (distance < 10 km) with the GPS stations (According to SA(t)-TG(t), the Sile station shows no significant vertical land motion).

CHAPTER 5

CONCLUSIONS AND RECOMMENDATIONS

Sea level is a dynamical parameter related to climate change. Scientific researches reveal that GMSL rise will accelerate during the 21st century in response to ocean thermal expansion and glaciers/ice sheet melting, and sea level change will have a strong regional pattern.

In the Black Sea, having a limited interaction with the Atlantic Ocean, there are strong temporal mass variations owing to its wide drainage area covering a large part of Europe and Asia. The Black Sea level change is closely related to its hydrological balance. Recent studies based on altimetry and tide-gauge data have revealed the Black Sea level has risen. In this context, accurately determining the sea level change in the Black Sea and understanding the main driving forces of observed change are critical for determining its long-term variability and prevent its negative impacts.

Figure 5.1 focuses on the spatial distributions of low-lying areas in the circum Black Sea. Since coastal slope is the main indicator of coastal vulnerability, these areas are highly vulnerable to sea level rise. According to the figure, in all the countries along the Black Sea coast, there are many hazardous areas. In order to estimate vulnerable of these areas to sea level rise, the general characteristic of the regions should examined in terms of soil type, land use, population, income, etc.
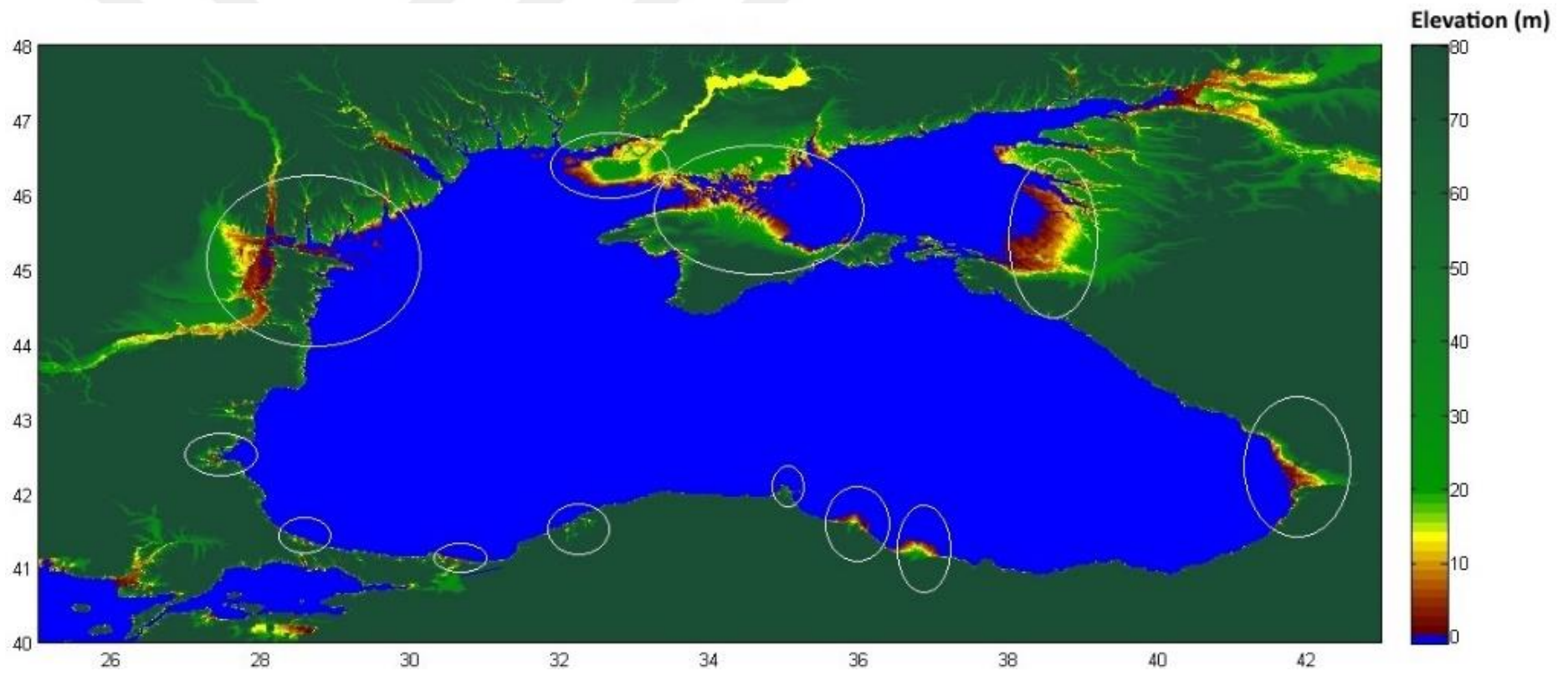
Figure 5.1 Low sloping areas along the Black Sea shore.

In this study, a comprehensive analysis of sea level changes in the Black Sea has been carried out using satellite and in-situ data. For this aim,

- The present-day sea level changes in the Black Sea were investigated using multi-mission gridded satellite altimetry data covering ~ 24.5 years from January 1993 to May 2017. The mean rate of sea level rise has been detected as 2.5 ± 0.5 mm/y over the entire Black Sea. On the other hand, if considering the dominant cycles, until December 2014, the Black Sea level has risen at a rate of about 3.2 ± 0.6 mm/y. When the geographical distribution of sea level trends was investigated, the maximum rate (~ 5 mm/y) was observed in the part which is between of 38º–40º northern latitudes and 41º–42º eastern longitudes of the Black Sea. Although there are no low-lying areas in this part, it should be considered. Besides, during this period, it was seen that inter-annual variability of the non-seasonal sea level change was quite strong.

- Analysis of satellite altimetry data indicated the maximum sea level in the Black Sea occurs in May-June, while the minimum sea level is observed during the autumn period, associated with its hydrological balance.

- Coastal sea level changes were analysed from 13 tide-gauge stations along the Black Sea coast. However, most tide-gauge data are not up to date and there are no data for each country in the Black Sea coast. Nevertheless, using the available data relative sea level changes along the Black Sea were assessed, and generally seen a rise in the relative sea level. The results showed that at some tide-gauge locations, there were significant vertical movements. For example, at the Poti tide-gauge station, a relative sea level rise implying a significant subsidence was observed.

- The sea level change along the Black Sea coast were also investigated from joint satellite altimetry, tide-gauge and GPS observations. At the tide-gauge stations with long-term records such as Poti (~ 21 years) and Tuapse (~ 19 years), the results obtained from the satellite altimetry and tide-gauge observations showed a remarkably good agreement. Some big differences were existed between satellite altimetry and tide-gauge at other stations. However, for the nearly co-located GPS and tide-gauge stations (at Trabzon, Sinop and Sile locations), after determining vertical motion from the GPS measurements, correlation coefficient between the trends were greatly improved from 0.37 to 0.99.

- In this study, vertical land motions estimates along the Black Sea coast from satellite altimetry minus tide-gauge generally exhibit a good agreement with the GPS-derived estimates. Besides, most of the results show a general consistent with the present geodynamics in the Black Sea coastal region. Accordingly, of 12 tide-gauge stations along the Black Sea coast (except for Sevastopol), 10 (Poti, Batumi, Tuapse, Varna, Bourgas, Constantza, Igneada, Trabzon, Sinop and Istanbul) indicate significant vertical land motion, whereas no significant trends have been found in the other 2 tide-gauges (Amasra and Sile) from altimetry minus tide-gauge. While the results showed land subsidence motions at Poti, Tuapse, Varna, Bourgas, Trabzon and Igneada locations, land uplift motions were seen at Batumi, Constantza, Istanbul and Sinop locations during the observation periods. At Sile tide-gauge location, for the nearly same period, a land subsidence movement was determined at SLEE from GPS observations.

- Long-term variability of SST in the Black Sea were investigated from the combining observations (satellite and in-situ). The result shows a rising trend of 0.04 ± 0.005 °C/y from September 1981 to November 2015. Moreover, sea surface warming coinciding sea level changes from satellite altimetry data was also analysed during the period 1993–2014. This period was examined as three parts. Accordingly, prior to mid-1999 and following early-2008 steric effect was an important factor in interannual variability of the Black Sea level, whereas it became less important as a forcing factor from mid-1999 to early-2008.

- The annual cycle of the SST changes in the Black Sea reaches the maximum value in August.

- Present-day sea level change in the Black Sea were also estimated from satellite gravity measurements. Mass contribution to the sea level change for the period 2002–2017 has been detected as 2.3 ± 1.0 mm/y from the GRACE mascon solutions.

- 3-month total steric data as well as halosteric and thermosteric data of the water column in the Black Sea were also considered in this study. Along with mass-induced contributions, thermal and haline contributions exhibited a good agreement total sea level changes from satellite altimetry for the Black Sea.

From 1993 to present, although the Black Sea level has been rising at a mean rate of ~ 2.5 mm/y, a slowdown of this rate has been recorded over the last about 3 years. Nevertheless, in order to confirm this supposition, the dominant cycles in the Black sea level time series should be examined spectrally. Thus, the recent rate of sea level rise can be estimated more accurately.

As known, sea level rise causes devastating effects on coastal habitats. Coastal erosion and saltwater intrusion are major threats for the Black Sea coasts. So, tracking sea level changes in the Black Sea is important in terms of coastal risk assessment and coastal planning. Figure 5.2 depicts the coastal areas in the Black Sea under the water, if sea level rises 1 m.

Furthermore, according the Bruun Rule, the shoreline recession happens at a rate in the order of 100 times the amount of sea level rise. This equates to around 50 m landward erosion for a sea level rise of 0.5 m. In this case, the observed rise rates along the Black Sea coast may be significant for coastal erosion threat. It is already known that an important part of the most critical coastal erosion areas in the Europe is in the Black Sea coastline. At present, coastal erosion is a major challenge especially for alluvial areas. On the other hand, in particular some coastal zones such as those of Bulgaria and Romania have far less protection. The results of this study show that accurately modelling of sea level changes depending on time and location in the Black Sea, that is known as a semi-closed sea, is crucial for risk assessments related to sea level rise, analysis of coastal change and planning of coastal area use. Local, regional and national patterns of potential consequences of sea level rise should be assessed, and coastal vulnerabilities should be identified in this region. The implications of sea level rise should be considered for population location, economic, infrastructure, and construction planning. This issue should be regarded as higher priority in coastal management. The related governments and local authorities should design long-term policy for coastal planning. The necessary precautions for reducing effects of sea level rise should be implemented for all coastal areas.

The determination of the vertical land motion along the Black Sea coast from altimetry minus tide-gauge, investigated in this study, will contribute to interpret the Black Sea's geophysical mechanism from a different viewpoint. It is worth mentioning that the approach applied in this study could lead to improvements in the assessment of vertical land motion along the Black Sea coast by verifying GPS, etc. The results of this study confirm that in order to monitor vertical land movements along the coasts, even though not directly observing this, the combination of altimetry and tide-gauge measurements can provide a valuable information. Here, the relative contribution of local land movement to the Black Sea level change has been revealed. Thus, this study will also enable to detect climate-related regional sea level change in the Black Sea. It is suggested that a regional network portal of tide-gauge stations having a suitable spatial distribution with co-located continuous GNSS stations along the Black Sea coast should be established for this purpose, which will also contribute to investigate absolute sea level changes.
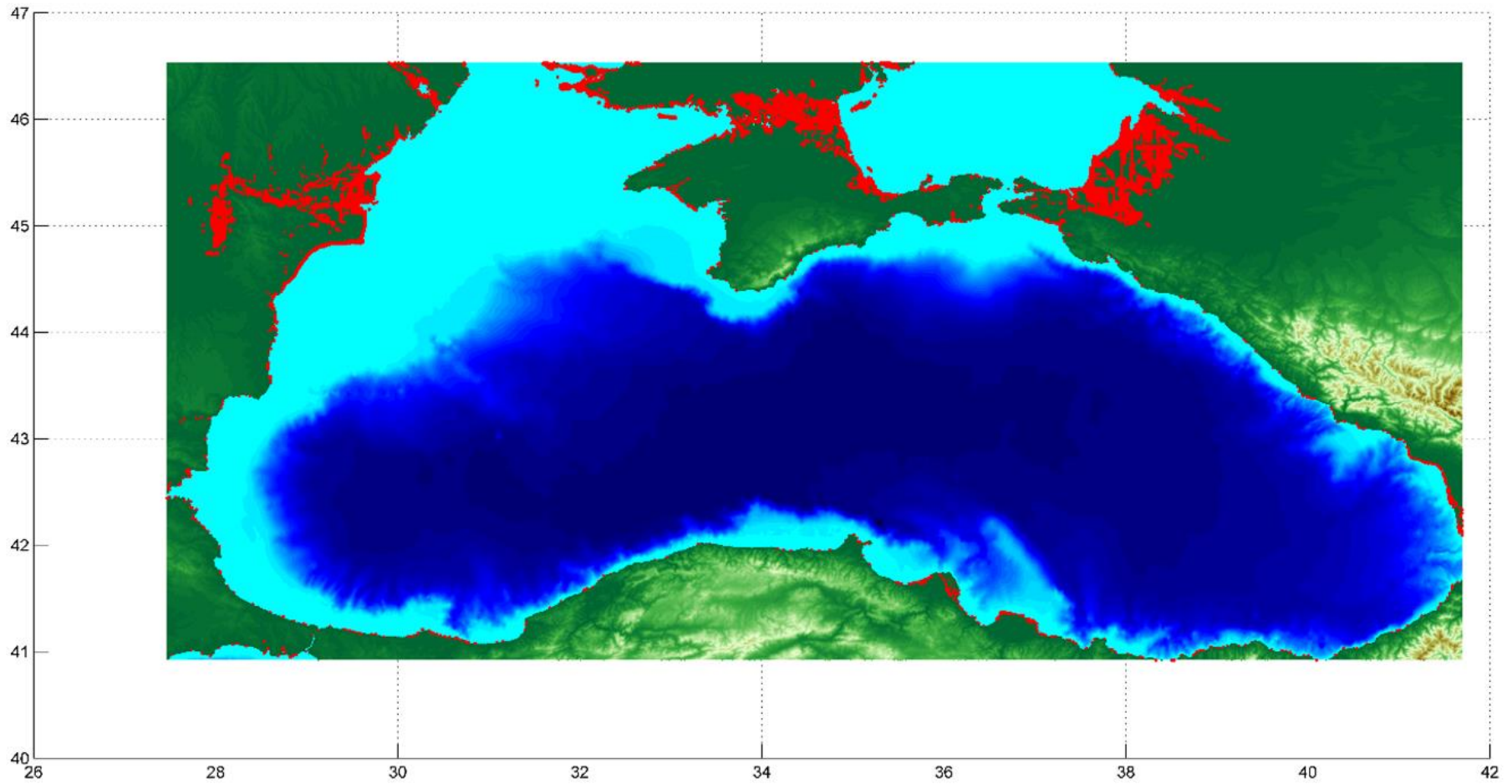
Figure 5.2 Coastal areas under the water, if sea level rises 1 m.

REFERENCES

Aarup T, Merrifield M, Perez B, Vassie I and Woodworth P (Eds.) (2006) *Manual on Sea-level Measurements and Interpretation, Volume IV: An update to 2006*. IOC Manuals and Guides No.14, JCOMM Technical Report No.31; WMO/TD. No. 1339, Paris, 78 pp.

Abdalla S (2015) Active Techniques for Wind and Wave Observations: Radar Altimeter, *Seminar on Use of Satellite Observations in Numerical Weather Prediction*, 08–12 September 2014, Shinfield Park, Reading, United Kingdom.

Ablain M, Legeais J F, Prandi P, Marcos M, Fenoglio-Marc L, Dieng H B, Benveniste J and Cazenave A (2017) Satellite Altimetry-Based Sea Level at Global and Regional Scales. *Surveys in Geophysics*, 38 (1): 7–31.

Abulaitijiang A, Andersen O B and Stenseng L (2015) Coastal Sea Level from Inland CryoSat-2 Interferometric SAR Altimetry. *Geophysical Research Letters*, 42 (6): 1841–1847.

Aksoy A O (2017) Investigation of Sea Level Trends and the Effect of the North Atlantic Oscillation (NAO) on the Black Sea and the Eastern Mediterranean Sea. *Theoretical and Applied Climatology*, 129 (1–2), 129–137.

Aksu A E, Hiscott R N, Yaşar D, Işler F I and Marsh S (2002) Seismic Stratigraphy of Late Quaternary Deposits from the Southwestern Black Sea Shelf: Evidence for Non-Catastrophic Variation in Sea-Level during the Last ~10000 Years. *Marine Geology*, 190: 61–94.

Akyol S, Simav M, Sezen E, Kurt A İ, Türkezer A ve Kurt M (2012) Türkiye Ulusal Deniz Seviyesi İzleme Sistemi (TUDES), *Türkiye Ulusal Jeodezi Komisyonu (TUJK) 2012, Türkiye Yükseklik Sisteminin Modernizasyonu Çalıştayı*, 28–30 Mart 2012, Zonguldak, Türkiye.

Ali I, Braun A and Sideris M G (2010) Monitoring Coastal Erosion Using Satellite Altimetry, GPS, and Terrestrial Laser Scanning on Galveston Island, Texas, *ESA 4th Coastal Altimetry Workshop 2010*, 14–15 October 2010, Porto, Portugal.

Alkan A, Zengin B, Yıldırım C ve Serdar S (2004) *Trabzon Açıklarında Deniz Suyunun Bazı Fiziksel ve Kimyasal Özelliklerinin İncelenmesi*. Proje Sonuç Raporları Serisi, No: 2004-1, Su Ürünleri Merkez Araştırma Enstitüsü Müdürlüğü, Sakarya Matbaacılık, Trabzon, 102 s.

Allenbach K, Garonna I, Herold C, Monioudi I, Giuliani G, Lehmann A and Velegrakis A F (2015) Black Sea Beaches Vulnerability to Sea Level Rise. *Environmental Science & Policy*, 46, 95–109.

Alpar B, Dogan E, Yuce H and Altıok H (2000) Sea Level Changes along the Turkish Coasts of the Black Sea, the Aegean Sea and the Eastern Mediterranean. *Mediterranean Marine Science*, 1(1): 141–156.

Amante C and Eakins B W (2009) *ETOPO1 Arc-Minute Global Relief Model: Procedures, Data Sources and Analysis*. NOAA Technical Memorandum NESDIS NGDC-24, Boulder, Colorado, 19 pp.

Anderson D L T (1995) The Tropical Ocean Global Atmosphere Programme. *Contemporary Physics*, 36: 245–265.

Armenio E, De Serio F, Mossa M and Petrillo A F (2018) Coastline Evolution Based on Statistical Analysis and Modelling, *Natural Hazards and Earth System Sciences*, in review.

Avsar N B and Ustun A (2012) Analysis of Regional Time-Variable Gravity Using GRACE's 10-Day Solutions, *FIG Working Week 2012*, 06–10 May 2012, Rome, Italy.

Bakan G and Büyükgüngör H (2000) The Black Sea. *Marine Pollution Bulletin*, 41 (1–6): 24–43.

Ben-Gal I (2005) Outlier Detection. *Data Mining and Knowledge Discovery Handbook*, Maimon O and Rokach L (Eds.), Springer, Boston, MA, 131–146.

Bigg G R, Jickells T D, Liss P and Osborn T J (2003) The Role of the Oceans in Climate. *International Journal of Climatology*, 23 (10): 1127–1159.

Bird P (2003) An Updated Digital Model of Plate Boundaries. *Geochemistry, Geophysics, Geosystems*. 4 (3): 1027.

Boehm J, Werl B and Schuh H (2006) Troposphere Mapping Functions for GPS and Very Long Baseline Interferometry from European Center for Medium-Range Weather Forecasts Operational Analysis Data. *Journal of Geophysical Research: Solid Earth*, 111: B02406.

Boguslavsky S G., Kubryakov A I and Ivashchenko I K (1998) Variations of the Black Sea Level, *Physical Oceanography*, 9 (3): 199–208.

Bondar C (2007) The Black Sea Level Variations and the River-Sea Interactions. *Geo-Eco-Marina*, 13: 43–50.

Bondar C (2009) Book Review (Part I) "Black Sea level: past, present and future". *Geo-Eco-Marina (Sedimentary Processes and Deposits within River-Sea Systems)*, 15: 175–179.

Bouin M N and Wöppelmann G (2010) Land Motion Estimates from GPS at Tide-Gauges: A Geophysical Evaluation. *Geophysical Journal International*, 180 (3): 193–209.

Brown S, Nicholls R J, Vafeidis A, Hinkel J and Watkiss P (2011) *The Impacts and Economic Costs of Sea-Level Rise on Coastal Zones in the EU and the Costs and Benefits of Adaptation, Summary of Results from the EC RTD ClimateCost Project*. Watkiss P (Ed.), The Climate Cost Project, Final Report, Volume 1: Europe, ISBN: 978-91-86125-35-6, Stockholm Environment Institute, Sweden, 44 pp.

Bruun P (1962) Sea-Level Rise as a Cause of Shore Erosion. *Journal of the Waterways and Harbors Division*, 88 (1): 117–132.

BSC (2008) *State of the Environment of the Black Sea (2001–2006/7)*. Oguz T (Ed.), Publications of the Commission on the Protection of the Black Sea Against Pollution (BSC) 2008-3, Istanbul, Turkey, 448 pp.

CATS (2010) *CATS Cycles Analysis and Timeseries Software*, Version 1.0, Ray Tomes and Radiance Trust, 30 pp.

Cazenave A (2014) Sea Level Changes Recent Past, Present, Future, *EGU General Assembly 2014 GIFT Workshop*, 27–30 April 2014, Vienna, Austria.

Cazenave A, Bonnefond P, Mercier F, Dominh K and Toumazou V (2002) Sea Level Variations in the Mediterranean Sea and Black Sea from Satellite Altimetry and Tide-gauges, *Global and Planetary Change*, 34: 59–86.

Cazenave A, Cabanes C, Dominh K and Mangiarotti S (2001) Recent Sea Level Changes in the Mediterranean Sea Revealed by TOPEX/POSEIDON Satellite Altimetry. *Geophysical Research Letters*, 28 (8): 1607e10.

Cazenave A and Cozannet G L (2014) Sea Level Rise and Its Coastal Impacts. *Earth's Future*, 2 (2): 15–34.

Cazenave A, Dominh K, Guinehut S, Berthier E, Llovel W, Ramillien G, Ablain M and Larnicol G (2009) Sea Level Budget over 2003–2008: A Revaluation from GRACE Space Gravimetry, Satellite Altimetry and Argo. *Global and Planetary Change*, 65: 83–88.

Cazenave A, Dominh K, Ponchaut F, Soudarin L, Cretaux J F and Le Provost C (1999) Sea Level Changes from TOPEX-Poseidon Altimetry and Tide Gauges, and Vertical Crustal Motions from DORIS. *Geophysical Research Letters*, 26: 2077–2080.

Cazenave A, Henry O, Munier S, Delcroix T, Gordon A L, Meyssignac B, Llovel W, Palanisamy H and Becker M (2012) Estimating ENSO Influence on the Global Mean Sea Level, 1993–2010. *Marine Geodesy*, 35 (sup1): 82–97.

Cazenave A and Nerem R S (2004) Present-Day Sea-Level Change: Observations and Causes, *Reviews of Geophysics*, 42, RG3001.

Cazenave A, Palanisamy H and Ablain M (2018) Contemporary Sea Level Changes from Satellite Altimetry: What have We Learned? What are the New Challenges?. *Advances in Space Research*, 62 (7): 1639–1653.

Cazenave A and Remy F (2011) Sea Level and Climate: Measurements and Causes of Changes. *Wiley Interdisciplinary Reviews: Climate Change*, 2 (5): 647–662.

Chambers D P (2006) Observing Seasonal Steric Sea Level Variations with GRACE and Satellite Altimetry, *Journal of Geophysical Research: Oceans*, 111, C03010.

Chambers D P, Cazenave A, Champollion N, Dieng H, Llovel W, Forsberg R, Schuckmann K v and Wada Y (2017) Evaluation of the Global Mean Sea Level Budget Between 1993 and 2014. *Surveys in Geophysics*, 38 (1): 309–327.

Chambers D P, Wahr J and Nerem R S (2004) Preliminary Observations of Global Ocean Mass Variations with GRACE, *Geophysical Research Letters*, 31, L13310.

Chen J, Famigliett J S, Scanlon B R and Rodell M (2016) Groundwater Storage Changes: Present Status from GRACE Observations. *Surveys in Geophysics*, 37: 397–417.

Chen J, Tapley B, Save H, Tamisiea M E, Bettadpur S and Ries J (2018) Quantification of Ocean Mass Change Using Gravity Recovery and Climate Experiment, Satellite Altimeter, and Argo Floats Observations. *Journal of Geophysical Research: Solid Earth*, 123 (11): 10,212–10,225.

Cheng L, Trenberth K E, Fasullo J, Boyer T, Abraham J and Zhu J (2017) Improved Estimates of Ocean Heat Content from 1960 to 2015. *Science Advances*, 3 (3), e1601545.

Church J A, Aarup T, Woodworth P, Wilson W S, Nicholls R J, Rayner R, Lambeck K, Mitchum G T, Steffen K, Cazenave A, Blewitt G, Mitrovica J X and Lowe J A (2010) Sea-Level Rise and Variability: Synthesis and Outlook for the Future. *Understanding Sea-Level Rise and Variability*, Church J A, Woodworth P, Aarup T and Wilson W S (Eds.), ISBN: 9781444334517, Wiley-Blackwell Publishing, London, UK, 402–419.

Church J A, Clark P U, Cazenave A, Gregory J M, Jevrejeva S, Levermann A, Merrifield M A, Milne G A, Nerem R S, Nunn P D, Payne A J, Pfeffer W T, Stammer D and Unnikrishnan A S (2013) Sea Level Change. *Climate Change 2013: The Physical Science Basis. Contribution of Working Group I to the Fifth Assessment Report of the Intergovernmental Panel on Climate Change*, Stocker T F, Qin D, Plattner G -K, Tignor M, Allen S K, Boschung J, Nauels A, Xia Y, Bex V and Midgley P M (Eds.), Cambridge University Press, Cambridge, United Kingdom and New York, NY, USA, 1137–1216.

Church J A and White N J (2006) A 20th Century Acceleration in Global Sea-Level Rise. *Geophysical Research Letters*, 33: L01602.

Church, J A and White N J (2011) Sea-Level Rise from the Late 19th to the Early 21st Century. *Surveys in Geophysics*, 32 (4–5): 585–602.

Cipollini P, Calafat F M, Jevrejeva S, Melet A and Prandi P (2017) Monitoring Sea Level in the Coastal Zone with Satellite Altimetry and Tide-gauges. *Integrative Study of the Mean Sea Level and Its Components*, Cazenave A, Champollion N, Paul F and Benveniste J (Eds.), Space Sciences Series of ISSI, Volume 58, Springer, Cham, 35–59.

Clark P U and Mix A C (2002) Ice Sheets and Sea Level of the Last Glacial Maximum. *Quaternary Science Reviews*, 21 (1–3): 1–7.

Cooper J A G and Pilkey O H (2004) Sea-Level Rise and Shoreline Retreat: Time to Abandon the Bruun Rule. *Global and Planetary Change*, 43 (3–4): 157–171.

Creel L (2003) Ripple Effects: Population and Coastal Regions. Address: https://www.prb.org/rippleeffectspopulationandcoastalregions/

Dahlman L and Lindsey R (2018) Climate Change: Ocean Heat Content. *NOAA Climate.gov*. Address: https://www.climate.gov/news-features/understanding-climate/climate-change-ocean-heat-content

Dangendorf S, Marcos M, Wöpelmann G, Conrad C P, Frederikse T and Riva R (2017) Reassessment of 20th Century Global Mean Sea Level Rise. *Proceedings of the National Academy of Sciences of the United States of America*, 114 (23): 5946–5951.

Deuser W G (1974) Evolution of Anoxic Conditions in the Black Sea during the Holocene. *The Black Sea Geology – Geology, Chemistry and Biology*, Degens E T and Ross D A (Eds.), Volume 20, ISBN electronic: 978-162-98-1215-1, American Association of Petroleum Geologists, 133–136.

Dimitrov D P, Dimitrov P S, Solakov D P and Peychev V D (2005) The Newest Geological History of the Black Sea and Problem About the Flood, *IGCP 521 "Black Sea-Mediterranean Corridor during last 30 ky: Sea level change and human adaptation", First Plenary Meeting*, 8–15 October 2005, Istanbul, Turkey, 37–38.

Dinnat E P, Le Vine D M, Boutin J, Meissner T and Lagerloef G (2019) Remote Sensing of Sea Surface Salinity: Comparison of Satellite and In Situ Observations and Impacts of Retrieval Parameters. *Remote Sensing*, 11 (7): 750.

Douglas B C (2001) Sea Level Change in the Era of the Recording Tide-gauge. *Sea Level Rise, History and Consequences*, Douglas B C, Kearney M S and Leatherman S P (Eds.), 1st edition, Volume 75, Academic Press, USA, 37–64.

Douglas B C, Kearney M S and Leatherman S P (Eds.) (2001) *Sea Level Rise History and Consequences*. 1st edition, Volume 75, ISBN: 0-12-221345-9, Academic Press., USA, 232 pp.

Döll P, Douville H, Güntner A, Müller Schmied H and Wada Y (2016) Modelling Freshwater Resources at the Global Scale: Challenges and Prospects. *Surveys in Geophysics*, 37: 195–221.

Dusto A (2014) Reading between the tides: 200 years of measuring global sea level. *NOAA Climate.gov*. Address: https://www.climate.gov/news-features/climate tech/reading-between-tides-200-yearsmeasuring-global-sea-level

Escudier P, Couhert A, Mercier F, Mallet A, Thibaut P, Tran N, Amarouche L, Picard B, Carrere L, Dibarboure G, Ablain M, Richard J, Steunou N, Dubois P, Rio M-H and Dorandeu J (2018) Satellite Radar Altimetry: Principle, Accuracy, and Precision. *Satellite Altimetry over Oceans and Land Surfaces*, Stammer D and Cazenave A (Eds.), ISBN: 978-1-4987-4345-7, CRC Press, Boca Raton, 1–62.

Esin N V and Esin N I (2014) Mathematical Modelling of the Black Sea Level Change for the Last 20000 Years. *Quaternary International*, 345: 32–47.

Feizabadi M (2016) An Investigation of Coastal Sea Level Changes of Blacksea Using Tide-Gauge and Satellite Altimetry Data. *Master Thesis*, Istanbul Technical University, Graduate School of Natural and Applied Sciences, Department of Geomatics, Istanbul, 155 pp.

Feng G, Jin S and Zhang T (2013) Coastal Sea Level Changes in Europe from GPS, Tide-gauge, Satellite Altimetry and GRACE, 1993–2011. *Advances in Space Research*, 51 (6): 1019–1028.

Fenoglio-Marc L (2002) Long-Term Sea Level Change in the Mediterranean Sea from Multi-Satellite Altimetry and Tide-gauges. *Physics and Chemistry of the Earth*, 27 (32–34): 1419–1431.

Fenoglio-Marc L, Braitenberg C and Tunini L (2012) Sea Level Variability and Trends in the Adriatic Sea in 1993–2008 from Tide-gauges and Satellite Altimetry. *Physics and Chemistry of the Earth*, 40–41: 47–58.

Fenoglio-Marc, L, Dietz C and Groten E (2004) Vertical Land Motion in the Mediterranean Sea from Altimetry and Tide-gauge Stations. *Marine Geodesy*, 27 (3–4): 683–701.

Fenoglio-Marc L and Tel E (2010) Coastal and Global Sea Level. *Journal of Geodynamics*, 49 (3), 151–160.

Foresta L, Gourmelen N, Palsson F, Nienow P, Björnsson H and Shepherd A (2016) Surface Elevation Change and Mass Balance of Icelandic Ice Caps Derived from Swath Mode CryoSat-2 Altimetry. *Geophysical Research Letters*, 43: 12138–12145.

Fu L -L (2014) Ocean Surface Topography. *Encyclopedia of Remote Sensing*, Njoku E G (Ed.), ISBN: 978-0-387-36698-2, Springer Science + Business Media, New York, 455–461.

Fu L -L and Cazenave A (Eds.) (2001) *Satellite Altimetry and Earth Sciences: A Handbook of Techniques and Applications*. International Geophysics Series, Volume 69, Academic Press, San Diego, 463 pp.

Fu L -L, Christensen E J, Yamarone C A, Lefebvre M, Menard Y, Dorrer M and Escudier P (1994) TOPEX/POSEIDON Mission Overview. *Journal of Geophysical Research: Oceans*, 99 (C12): 24369–24381.

Garcia D, Vigo I, Chao B F and Martinez M C (2007) Vertical Crustal Motion along the Mediterranean and Black Sea Coast Derived from Ocean Altimetry and Tide Gauge Data. *Pure and Applied Geophysics*, 164 (4): 851–863.

Garcia F, Vigo M I, Garcia-Garcia D and Sanchez-Reales J M (2012) Combination of Multisatellite Altimetry and Tide-gauge Data for Determining Vertical Crustal Movements along Northern Mediterranean Coast. *Pure and Applied Geophysics*, 169 (8), 1411–1423.

Garcia-Garcia D, Chao B F and Boy J P (2010) Steric and Mass-Induced Sea Level Variations in the Mediterranean Sea, Revisited. *Journal of Geophysical Research: Oceans*, 115, C12016.

Ginzburg A I, Kostianoy A G and Sheremet N A (2004) Seasonal and Interannual Variability of the Black Sea Surface Temperature as Revealed from Satellite Data (1982–2000). *Journal of Marine Systems*, 52: 33–50.

Ginzburg A I, Kostianoy A G, Sheremet N A and Lebedev S A (2011) Satellite Altimetry Applications in the Black Sea. *Coastal Altimetry*, Vignudelli S, Kostianoy A G, Cipollini P and Benveniste J (Eds.), ISBN: 978-3-642-12795-3, Springer, Berlin, Heidelberg, 367–387.

Ginzburg A I, Lebedev S A, Kostianoy A G and Sheremet N A (2013) Interannual Variability of the Black Sea Level Basing on the Radar Altimetry. *The 20 years of Progress in Radar Altimetry*, 24–29 September 2012, Venice, Italy, Ouwehand L (Ed.), ESA SP-710, February 2013.

Gommenginger C, Martin-Puig C, Amarouche L and Raney R K (2013) *Review of State of Knowledge for SAR Altimetry over Ocean*. EUSETMAT REFERENCE: EUM/RSP/REP/14/749304, 21 November 2013, Version 2.2, National Oceanography Centre, Southampton, 57 pp.

Gommenginger C, Thibaut P, Fenoglio-Marc L, Quartly G, Deng X, Gomez-Enri J, Challenor P and Gao Y (2011) Retracking Altimeter Waveforms near the Coasts. *Coastal Altimetry*, Vignudelli S, Kostianoy A G, Cipollini P and Benveniste J (Eds.), ISBN: 978-3-642-12795-3, Springer, Berlin, Heidelberg, 61–101.

Görmüş K S, Kutoğlu Ş H, Şeker D Z, Özölçer İ H, Oruç M and Aksoy B (2014) Temporal Analysis of Coastal Erosion in Turkey: A Case Study Karasu Coastal Region. *Journal of Coastal Conservation*, 18 (4): 399–414.

REFERENCES (continued)

Grinevetsky S R, Zonn I S, Zhiltsov S S, Kosarev A N and Kostianoy A G (2015) *The Black Sea Encyclopedia*. ISBN: 978-3-642-55226-7, Springer Berlin Heidelberg, 889 pp.

Gunnerson C G and Özturgut E (1974) The Bosporus. *The Black Sea Geology – Geology, Chemistry and Biology*, Degens E T and Ross D A (Eds.), Volume 20, ISBN electronic: 978-162-98-1215-1, American Association of Petroleum Geologists, 99–114.

Gurbuz G and Jin S G (2016) Evaluation of Ocean Tide Loading Effects on GPS-Estimated Precipitable Water Vapor in Turkey. *Geodesy and Geodynamics*, 7: 32–38.

Hay C, Morrow E, Kopp R E and Mitrovica J X (2015) Probabilistic Reanalysis of Twentieth-Century Sea-Level Rise. *Nature*, 517 (7535): 481–484.

Herring T, King R W, Floyd M A and McClusky S C (2015) *Introduction to GAMIT/GLOBK*, Massachusetts Institute of Technology, 50 pp.

Holgate S J, Matthews A, Woodworth P L, Rickards L J, Tamisiea M E, Bradshaw E and Pugh J (2012) New Data Systems and Products at the Permanent Service for Mean Sea Level. *Journal of Coastal Research*, 29 (3): 493–504.

Huntington T G (2008) Can We Dismiss the Effect of Changes in Land-Based Water Storage on Sea-Level Rise?. *Hydrological Processes*, 22: 717–723.

Idzanovic M, Ophaug V and Andersen O B (2018) Coastal Sea Level from CryoSat-2 SARIn Altimetry in Norway. *Advances in Space Research*, 62 (6), 1344–1357.

Ignatov E I (2008) Coastal and Bottom Topography. *The Black Sea Environment. The Handbook of Environmental Chemistry*, Kostianoy A and Kosarev A (Eds.), Vol. 5, Part Q, Springer-Verlag, Berlin Heidelberg, 47–62.

IPCC (2013) Stocker T F, Qin D, Plattner G -K, Tignor M, Allen S K, Boschung J, Nauels A, Xia Y, Bex V and Midgley P M (Eds.) *Climate Change 2013. The Physical Science Basis. Contribution of Working Group I to the Fifth Assessment Report of the Intergovernmental Panel on Climate Change.* ISBN: 978-1-107-05799-1 hardback, Cambridge University Press, Cambridge, United Kingdom and New York, NY, USA, 1535 pp.

IPCC (2014) Field C B, Barros V R, Dokken D J, Mach K J, Mastrandrea M D, Bilir T E, Chatterjee M, Ebi K L, Estrada Y O, Genova R C, Girma B, Kissel E S, Levy A N, MacCracken S, Mastrandrea P R, and White L L (Eds.) *Climate Change 2014. Impacts, Adaptation, and Vulnerability. Part A: Global and Sectoral Aspects. Contribution of Working Group II to the Fifth Assessment Report of the Intergovernmental Panel on Climate Change.* ISBN: 978-1-107-05807-1 hardback, Cambridge University Press, Cambridge, United Kingdom and New York, NY, USA, 1132 pp.

REFERENCES (continued)

Ivanov V A and Belokopytov V N (2013) *Oceanography of the Black Sea*. ISBN 978-966-022-6165-5, National Academy of Sciences of Ukraine Marine Hydrophysical Institute, Sevastopol, Ukraine, 210 pp.

Jaoshvili S (2002) The rivers of the Black Sea. *European Environmental Agency Technical Report, No: 71*, Khomerki I, Gigineishvili G and Kordzadze A (Eds.), 58 pp. https://www.eea.europa.eu/publications/technical_report_2002_71

Jevrejeva S, Moore J C, Grinsted A, Matthews A P and Spada G (2014) Trends and Acceleration in Global and Regional Sea Levels since 1807. *Global and Planetary Change*, 113: 11–22.

Jiang L, Schneider R, Andersen O and Bauer-Gottwein P (2017) CryoSat-2 Altimetry Applications over Rivers and Lakes. *Water*, 9 (3): 211.

Karaca M and Nicholls R J (2008) Potential Implications of Accelerated Sea-Level Rise for Turkey. *Journal of Coastal Research*, 24: 288–298.

Kılıçoğlu A, Fırat O, Demir C and Aktug B (2007) Definition of Local Geoidal Potential and Datum Height Difference of Turkish National Vertical Control Network (TUDKA99), *IUGG XXIV General Assembly Earth, Our Changing Planet*, 2–13 July 2007, Perugia, Italy.

Korotaev G, Oguz T, Nikiforov A and Koblinsky C (2003) Seasonal, Interannual, and Mesoscale Variability of the Black Sea Upper Layer Circulation Derived from Altimeter Data. *Journal of Geophysical Research*, 108 (C4): 3122.

Kubryakov A I, Korotaev G K, Dorofeev V L, Ratner Y B, Palazov A, Valchev N, Matescu R and Oguz T (2012) Black Sea Coastal Forecasting System. *Ocean Science*, 8 (2): 183–196.

Kubryakov A A and Stanichnyi S V (2013) The Black Sea Level Trends from Tide-gauges and Satellite Altimetry. *Russian Meteorology and Hydrology*, 38 (5): 329–333.

Kubryakov A A, Stanichny S V and Volkov D L (2017) Quantifying the Impact of Basin Dynamics on the Regional Sea Level Rise in the Black Sea, *Ocean Science*, 13: 443–452.

Kuo C, Shum C, Braun A and Mitrovica J X (2004) Vertical Crustal Motion Determined by Satellite Altimetry and Tide Gauges Data in Fennoscandia. *Geophysical Research Letters*, 31: L01608.

Lambeck K and Chappell J (2001) Sea Level Change through the Last Glacial Cycle. *Science*, 292 (5517): 679–686.

Lambeck K, Woodroffe C D, Antonioli F, Anzidei M, Gehrels W R, Laborel J and Wright A J (2010) Paleoenviromental Records, Geophysical Modelling, and Reconstruction of Sea-Level Trends and Variability on Centennial and Longer Timescales. *Understanding Sea-Level Rise and Variability*, Church J A, Woodworth P, Aarup T and Wilson W S (Eds.), ISBN: 9781444334517, Wiley-Blackwell Publishing, London, UK, 61–121.

Laxon S W, Giles K A, Ridout A L, Wingham D J, Willatt R, Cullen R, Kwok R, Schweiger A, Zhang J, Haas C, Hendricks S, Krishfield R, Kurtz N, Farrell S and Davidson M (2013) CryoSat-2 Estimates of Arctic Sea Ice Thickness and Volume. *Geophysical Research Letters*, 40 (4): 732–737.

Leatherman S P (2001) Social and Economic Costs of Sea Level Rise. *Sea Level Rise History and Consequences*, Douglas B C, Kearney M S and Leatherman S P, Academic Press, Orlando, Florida, 181–223.

Le Cozannet G, Garcin M, Petitjean L, Cazenave A, Becker M, Meyssignac B, Walker P, Devilliers C, Le Brun O, Lecacheux S, Baills A, Bulteau T, Yates M and Wöppelmann G (2013) Exploring the Relation Between Sea Level Rise and Shoreline Erosion Using Sea Level Reconstructions: An Example in French Polynesia. *Journal of Coastal Research*, 65: 2137–2142.

Legeais J F, Ablain M, Zawadzki L, Zuo H, Johannessen J A, Scharffenberg M G, Fenoglio-Marc L, Fernandes M J, Andersen O B, Rudenko S, Cipollini P, Quartly G D, Passaro M, Cazenave A and Benveniste J (2018) An Improved and Homogeneous Altimeter Sea Level Record from the ESA Climate Change Initiative. *Earth System Science Data*, 10: 281–301.

Lehmann R (2013) 3σ-Rule for Outlier Detection from the Viewpoint of Geodetic Adjustment. *Journal of Surveying Engineering*, 139 (4): 157–165.

Le Provost C (2001) Ocean Tides. *Satellite Altimetry and Earth Science: A Handbook of Techniques and Applications*, Fu L –L and Cazenave A (Eds.), International Geophysics Series, Volume 69, Academic Press, San Diego, 267–303.

Lericolais G, Popescu I, Guichard F, Popescu S M and Manolakakis L (2007) Water-level fluctuations in the Black Sea since the Last Glacial Maximum. *The Black Sea Flood Question: Changes in Coastline, Climate, and Human Settlement*, Yanko-Hombach V, Gilbert A S, Panin N and Dolukhanov P M (Eds.), ISBN: 978-1-4020-5302-3, Springer, The Netherlands, e-book, 437–452.

Leuliette E W and Miller L (2009) Closing the Sea Level Rise Budget with Altimetry, Argo, and GRACE. *Geophysical Research Letters*, 36, L04608.

Leuliette E W and Willis J K (2011) Balancing the sea level budget. *Oceanography*, 24 (2): 122–129.

REFERENCES (continued)

Levitus S, Antonov J I, Boyer T P, Baranova O K, Garcia H E, Locarnini R A, Mishonov A V, Reagan J R, Seidov D, Yarosh E S and Zweng M M (2012) World Ocean Heat Content and Thermosteric Sea Level Change (0–2000 m), 1955–2010. *Geophysical Research Letters*, 39, L10603.

Li J and Sideris M G (1997) Marine Gravity and Geoid Determination by Optimal Combination of Satellite Altimetry and Shipborne Gravimetry Data. *Journal of Geodesy*, 71: 209–216.

Llovel W, Becker M, Cazenave A, Cretaux J-F and Ramillien G (2010) Contribution of Land Water Storage Change to Global Mean Sea Level from GRACE and Satellite Altimetry. *Comptes Rendus Geoscience*, 342: 179–188.

Lyratzopouoou D and Zarotiadis G (2014) Black Sea: Old Trade Routes and Current Perspectives of Socioeconomic Co-Operation. *Procedia Economics and Finance*, 9: 74–82.

Maktav D, Sunar Erbek F and Kabdasli S (2002) Monitoring Coastal Erosion at the Black Sea Coasts in Turkey Using Satellite Data: A Case Study at the Lake Terkos, North West Istanbul. *International Journal of Remote Sensing*, 23 (19): 4115–4124.

Marcos M and Tsimplis M N (2008) Coastal Sea Level Trends in Southern Europe. *Geophysical Journal International*, 175: 70–82.

Marzeion B, Champollion N, Haeberli W, Langley K, Leclercq P and Paul F (2017) Observation Based Estimates of Global Glacier Mass Change and its Contribution to Sea-Level Change. *Surveys in Geophysics*, 38: 105–130.

Mayer-Gürr T, Savcenko R, Bosch W, Daras I, Flechtner F and Dahle C (2012) Ocean Tides from Satellite Altimetry and GRACE. *Journal of Geodynamics*, 59: 28–38.

McMillan M, Shepherd A, Sundal A, Briggs K, Muir A, Ridout A, Hogg A and Wingham D (2015) Increased Ice Losses from Antarctica Detected by CryoSat-2. *Geophysical Research Letters*, 41 (11): 3899–3905.

McWilliams J C (2006) *Oceanic Circulation*. UCLA Department of Atmospheric and Oceanic Sciences, Los Angeles, CA, USA, 330 pp.

Meier M F, Dyurgerov M B, Rick U K, O'Neel S, Pfeffer W T, Anderson R S, Anderson S P and Glazovsky A F (2007) Glaciers Dominate Eustatic Sea-Level Rise in the 21st Century. *Science*, 317 (5841): 1064–1067.

Mercier F, Picot N, Thibaut P, Cazenave A, Seyler F, Kosuth P, and Bronner E (2009) CNES/PISTACH Project: An Innovative Approach to Get Better Measurements over Inland Water Bodies from Satellite Altimetry. Early results. *EGU General Assembly Conference Abstracts*, 11: 11674.

REFERENCES (continued)

Meyssignac B, Becker M, Llovel W and Cazenave A (2011) An Assessment of Two-Dimensional Past Sea Level Reconstructions over 1950–2009 Based on Tide-Gauge Data and Different Input Sea Level Grids. *Surveys in Geophysics*, 33: 945–972.

Meyssignac B and Cazenave A (2012) Sea Level: A Review of Present-Day and Recent-Past Changes and Variability. *Journal of Geodynamics*, 58: 96–109.

Meyssignac B, y Melia D S, Becker M, Llovel W and Cazenave A (2012) Tropical Pacific Spatial Trend Patterns in Observed Sea Level: Internal Variability and/or Anthropogenic Signature?. *Climate of the Past*, 8: 787–802.

Miladinova S, Stips A, Garcia-Gorriz E and Macias Moy D (2017) Black Sea Thermohaline Properties: Long-Term Trends and Variations. *Journal of Geophysical Research: Oceans*, 122 (7): 5624–5644.

Mikhailov V N and Mikhailova M V (2008) River Mouths. *The Black Sea Environment. The Handbook of Environmental Chemistry*, Kostianoy A and Kosarev A (Eds.), Vol. 5, Part Q, Springer-Verlag, Berlin Heidelberg, 91–133.

Miller L and Douglas B C (2007) Gyre-Scale Atmospheric Pressure Variations and Their Relation to 19th and 20th Century Sea Level Rise. *Geophysical Research Letters*, 34: L16602.

Miller K, Mountain G S, Wright J D and Browning J V (2011) A 180 Million Year Record of Sea Level and Ice Volume Variations from Continental Margin Deep Sea Isotopic Records. *Oceanography*, 24 (2): 40–53.

Milne G A, Gehrels W R, Hughes C W and Tamisiea M E (2009) Identifying the Causes of Sea-Level Change. *Nature Geoscience*, 2 (7): 471.

Mitchum G T (1998) Monitoring the Stability of Satellite Altimeters with Tide-gauges. *Journal of Atmospheric and Oceanic Technology*, 15 (3): 721–730.

Mitchum G T (2000) An Improved Calibration of Satellite Altimetric Heights using Tide-gauge Sea Levels with Adjustment for Land Motion. *Marine Geodesy*, 23 (3): 145–166.

Mitchum G T, Nerem R S, Merrifield M A and Gehrels W R (2010) Modern Sea-Level-Change Estimates. *Understanding Sea-Level Rise and Variability*, Church J A, Woodworth P, Aarup T and Wilson W S (Eds.), ISBN: 9781444334517, Wiley-Blackwell Publishing, London, UK, 122–142.

Mitrovica J X, Gomez N and Clark P U (2009) The Sea-Level Fingerprint of West Antarctic Collapse. *Science*, 323: 753.

Munteanu I, Matenco L, Dinu C and Cloetingh S (2011) Kinematics of Back-Arc Inversion of the Western Black Sea Basin. *Tectonics*, 30: TC5004.

<div align="center">

REFERENCES (continued)

</div>

Murray J W, Top Z and Ozsoy E (1991) Hydrographic Properties and Ventilation of the Black Sea. *Deep-Sea Research*, 38: 663–689.

Murray J W, Stewart K, Kassakian S, Krynytzky M and DiJulio D (2007) Oxic, Suboxic, and Anoxic Conditions in the Black Sea. *The Black Sea Flood Question: Changes in Coastline, Climate and Human Settlement*, Yanko-Hombach V, Gilbert A S, Panin N and Dolukhanov P M (Eds.), ISBN: 978-1-4020-5302-3, Springer, The Netherlands, e-book, 1–21.

Murray-Wallace C V and Woodroffe C D (2014) *Quaternary Sea-Level Changes: A Global Perspective*. 1st edition, ISBN: 978-0-521-82083-7, Cambridge University Press, New York, 504 pp.

Nardelli B B, Colella S, Santoleri R, Guarracino M and Kholod A (2010) A Re-Analysis of Black Sea Surface Temperature. *Journal of Marine Systems*, 79: 50–64.

Nerem R S, Ablain M, Cazenave A, Church J and Leuliette E (2018a) A 25-Year Long Satellite Altimetry-Based Global Mean Sea Level Record: Closure of the Sea Level Budget and Missing Components. *Satellite Altimetry over Oceans and Land Surfaces*, Stammer D and Cazenave A (Eds.), ISBN: 978-1-4987-4345-7, CRC Press, Boca Raton, 187–204.

Nerem R S, Beckley B D, Fasullo J T, Hamlington B D, Masters D and Mitchum G T (2018b) Climate-Change–Driven Accelerated Sea-Level Rise Detected in the Altimeter Era. *Proceedings of the National Academy of Sciences of the United States of America*, 115 (9), 2022–2025.

Nerem R S, Chambers D P, Choe C and Mitchum G T (2010) Estimating Mean Sea Level Change from the TOPEX and Jason Altimeter Missions. *Marine Geodesy*, 33 (sup1): 435–446.

Nerem R S, Leuliette E and Cazenave A (2006) Present-Day Sea-Level Change: A Review. *Comptes Rendus Geoscience*, 338 (14–15): 1077–1083.

Nerem R S and Mitchum G T (2001a) Observation of Sea Level Change from Satellite Altimetry. *Sea Level Rise History and Consequences*, Douglas B C, Kearney M S and Leatherman S P, Academic Press, Orlando, Florida, 121–163.

Nerem R S and Mitchum G T (2001b) Sea Level Change. *Satellite Altimetry and Earth Sciences: A Handbook of Techniques and Applications*, Fu L -L and Cazenave A (Eds.), International Geophysics Series, Volume 69, Academic Press, San Diego, 329–349.

Nerem R S and Mitchum G T (2002) Estimates of Vertical Crustal Motion Derived from Differences of TOPEX/Poseidon and Tide-gauge Sea-Level Measurements. *Geophysical Research Letters*, 29 (19): 40–1–40–4.

Nicholls R J (2004) Coastal Flooding and Wetland Loss in the 21st Century: Changes under the SRES Climate and Socio-Economic Scenarios. *Global Environmental Change*, 14 (1): 69–86.

Nicholls R J (2010) Impacts of and Responses to Sea Level Rise. *Understanding Sea-Level Rise and Variability*, Church J A, Woodworth P, Aarup T and Wilson W S (Eds.), ISBN: 9781444334517, Wiley-Blackwell Publishing, London, UK, 17–51.

Nicholls R J and Cazenave A (2010) Sea-Level Rise and Its Impact on Coastal Zones. *Science*, 328: 1517–1520.

Nikishin A M, Korotaev M V, Ershov A V and Brunet M F (2003) The Black Sea Basin: Tectonic History and Neogene-Quaternary Rapid Subsidence Modelling. *Sedimentary Geology*, 156 (1–4): 149–168.

Oguz T, La Violette P E and Unluata U (1992) The Upper Layer Circulation of the Black Sea: Its Variability as Inferred from Hydrographic and Satellite Observations. *Journal of Geophysical Research: Oceans*, 97 (C8): 12569–12584.

Oguz T, Latun V S, Latif M A, Vladimirov V V, Sur H I, Markov A A, Özsoy E, Kotovshchikov B B, Eremeev V V and Ünlüata Ü (1993) Circulation in the Surface and Intermediate Layers of the Black Sea. *Deep-Sea Research*, 40 (8): 1597–1612.

Oguz T, Malanotte-Rizzoli P and Aubrey D (1995) Wind and Thermohaline Circulation of the Black Sea Driven by Yearly Mean Climatological Forcing. *Journal of Geophysical Research: Oceans*, 100 (C4): 6845–6863.

Oguz T and Malanotte-Rizzoli P (1996) Seasonal Variability of Wind and Thermohaline Driven Circulation in The Black Sea: Modeling Studies. *Journal of Geophysical Research: Oceans*, 101 (C7): 16551–16569.

Oguz T, Tugrul S, Kideys A E, Ediger V and Kubilay N (2006) Physical and Biogeochemical Characteristics of the Black Sea. *The Sea*, Robinson A R and Brink K H (Eds.), Volume 14, ISBN: 0-674-01527-4, Harward University Press Cambridge, MA, 1333–1371.

Okay A I, Celal Sengor A M and Görür N (1994) Kinematic History of the Opening of the Black Sea And Its Effect on The Surrounding Regions. *Geology*, 22(3): 267–270.

Özsoy E and Ünlüata Ü (1997) Oceanography of the Black Sea: A Review of Some Recent Results. *Earth-Science Reviews*, 42: 231–272.

Palanisamy H, Cazenave A, Delcroix T and Meyssignac B (2015) Spatial Trend Patterns in Pacific Ocean Sea Level during the Altimetry Era: The Contribution of Thermocline Depth Change and Internal Climate Variability. *Ocean Dynamics*, 65 (3): 341–356.

Pashova L (2002) Investigation of Sea-Level Variations at Two Tide Gauges in Bulgaria. *Vistas for Geodesy in the New Millennium*, Jozsef A and Schwarz K P (Eds.), IAG Symposia, Volume 125, Springer, Berlin, 475–480.

REFERENCES (continued)

Pashova L and Yovev I (2010) Geodetic Studies of the Influence of Climate Change on the Black Sea Level Trend. *Journal of Environmental Protection and Ecology*, 11 (2): 791–801.

Paytan A (2006) *Marine Chemistry, Lecture 3: Temperature, Salinity, Density and Ocean Circulation*. Stanford University, Ocean Biogeochemistry Lab, Stanford, CA, USA, 17 pp.

Peltier W R (2004) Global Glacial Isostasy and the Surface of the Ice-Age Earth: The ICE-5G (VM2) Model and GRACE. *Annual Review of Earth and Planetary Science*, 32: 111–149.

Peltier W R, Argus D F and Drummond R (2015) Space Geodesy Constrains Ice-Age Terminal Deglaciation: The Global ICE-6G_C (VM5a) Model. *Journal of Geophysical Research: Solid Earth*, 120: 450–487.

Preisinger A and Aslanian S (2003) The Black Sea during the Last 20000 Years: Sea Level, Salinity, Climate, *2003 Seattle Annual Meeting (Geological Society of America 2003 Annual Meeting)*, 2–5 November 2003, Seattle, Washington, USA, p. 461.

Pugh D T (1996) *Tides, Surges and Mean Sea-Level*. Reprinted with corrections, John Wiley & Sons Ltd., Chichester, UK, 486 pp.

PUM (2019) *Product User Manual For Sea Level SLA Products*, Copernicus Marine Environment Monitoring Service, REF: CMEMS-SL-PUM-008-032-062, 21.01.2019, Issue: 1.0, 40 pp.

Rashid T (2014) Sea Level Research: Methods and Techniques. *Holocene Sea-Level Scenarios in Bangladesh*, ISBN: 978-981-4560-99-3, Springer, Singapore, 11–33.

Ray R, Beckley B and Lemoine F (2010) Vertical Crustal Motion Derived from Satellite Altimetry and Tide-gauges, and Comparisons with DORIS Measurements. *Advances in Space Research*, 45 (12): 1510–1522.

Reager J T, Gardner A S, Famiglietti J S, Wiese D N, Eicker A and M –H Lo (2016) A Decade of Sea Level Rise Slowed by Climate-Driven Hydrology. *Science*, 351 (6274): 699–703.

Reynolds R, Smith T, Liu C, Chelton D, Casey K and Schlax M (2007) Daily High-Resolution Blended Analysis for Sea Surface Temperature. *Journal of Climate*, 20 (22): 5473–5496.

Robinson A G (Ed.) (1997) *Regional and Petroleum Geology of the Black Sea and Surrounding Region*. AAPG Memoir 68, ISBN electronic: 9781629810782, The American Association of Petroleum Geologists, Tulsa, Oklahoma, USA, 385 pp.

Roblou L, Lamouroux J, Bouffard J, Lyard F, Le Henaff M, Lombard A, Marsaleix P, De Mey P and Birol F (2011) Post-Processing Altimeter Data towards Coastal Applications and Integration into Coastal Models. *Coastal Altimetry*, Vignudelli S, Kostianoy A G, Cipollini P and Benveniste J (Eds.), ISBN: 978-3-642-12795-3, Springer Berlin Heidelberg, 217–246.

Roemmich D and Owens W B (2000) The ARGO Project: Global Ocean Observations for Understanding and Prediction of Climate Variability. *Oceanography*, 13 (2): 45–50.

Rosmorduc V, Benveniste J, Bronner E, Dinardo S, Lauret O, Maheu C, Milagro M, Picot N, Ambrozio A, Escola R, Garcia-Mondejar A, Schrama E, Restano M and Terra-Homem M (2018) Radar Altimetry Tutorial, Issue 3a, Benveniste J and Picot N (Eds.), http://www.altimetry.info

Ross D A and Degens E T (1974) Recent Sediments of the Black Sea. *The Black Sea Geology – Geology, Chemistry and Biology*, Degens E T and Ross D A (Eds.), Volume 20, ISBN electronic: 978-162-98-1215-1, American Association of Petroleum Geologists, 183–199.

Rovere A, Stocchi P and Vacchi M (2016) Eustatic and Relative Sea Level Changes. *Current Climate Change Reports*, 2 (4): 221–231.

Ryan W B F (2007) Status of the Black Sea Hypothesis. *The Black Sea Flood Question: Changes in Coastline, Climate and Human Settlement*, Yanko-Hombach V, Gilbert A S, Panin N and Dolukhanov P M (Eds.), ISBN: 978-1-4020-5302-3, Springer, The Netherlands, e-book, 63–88.

Ryan W B F, Major C O, Lericolais G and Goldstein S L (2003) Catastrophic Flooding of the Black Sea. *Annual Review of* Earth *and Planetary Sciences*, 31: 525–554.

Ryan W B F, Pitman III W C, Major C O, Shimkus K, Moskalenko V, Jones G A, Dimitrov P, Gorür N, Sakinç M and Yüce H (1997) An Abrupt Drowning of the Black Sea Shelf. *Marine Geology*, 138: 119–126.

Sandwell D T and Smith W H F (2001) Bathymetric Estimation. *Satellite Altimetry and Earth Science: A Handbook of Techniques and Applications*, Fu L –L and Cazenave A (Eds.), International Geophysics Series, Volume 69, Academic Press, San Diego, 441–456.

Save H, Bettadpur S and Tapley B D (2016) High-resolution CSR GRACE RL05 mascons. *Journal of Geophysical Research: Solid Earth*, 121 (10): 7547–7569.

Seeber G (1993) *Satellite Geodesy: Foundations, Methods, and Applications*. 1st edition, ISBN: 3-11-017549-5, Walter de Gruyter, Berlin, Germany, 589 pp.

Sezen E (2006) Antalya-I (1935–1977) ve Antalya-II (1985–2005) Mareograf İstasyonlarında Deniz Seviyesi Değişimlerinin Araştırılması. *Master Thesis*, Afyon Kocatepe University, Institute of Science and Technology, Department of Geodesy, Istanbul, 70 pp.

Shmuratko V I (2007) The Post Glacial Transgression of the Black Sea. *The Black Sea Flood Question: Changes in Coastline, Climate and Human Settlement*, Yanko-Hombach V, Gilbert A S, Panin N and Dolukhanov P M (Eds.), ISBN: 978-1-4020-5302-3, Springer, The Netherlands, e-book, 221–250.

Shum C K and Braun A (2004) Satellite Altimetry – Principles and Applications, *Satellite Altimetry and Gravimetry: Theory and Applications*, 21-25 June 2004, Norwegian University of Science and Technology, Trondheim, Norway.

Simav M (2007) Doğu Akdeniz'de Uydu Altimetri Verileri ile Deniz Seviyesi Değişimlerinin Araştırılması. *Master Thesis*, Istanbul Technical University, Graduate School of Natural and Applied Sciences, Department of Geomatics, Istanbul, 91 pp.

Simav M (2012a) Uydu ve Model Verilerine Dayalı Akdeniz Su Kütlesi Değişimleri. *PhD Thesis*, Istanbul Technical University, Graduate School of Natural and Applied Sciences, Department of Geomatics, Istanbul, 84 pp.

Simav Ö (2012b) Deniz Seviyesi Yükselmelerinin Kıyı Alanlarına Olası Etkilerinin Araştırılması. *PhD Thesis*, Istanbul Technical University, Graduate School of Natural and Applied Sciences, Department of Geomatics, Istanbul, 74 pp.

Simav M, Türkezer A, Sezen E, Akyol S, İnam M, Cingöz A, Lenk O ve Kılıçoğlu A (2011) Türkiye Ulusal Deniz Seviyesi İzleme Ağı Veri Kalite Kontrol ve Yönetim Sistemi. *Harita Dergisi*, 145: 15–28.

Simav M, Yıldız H ve Arslan E (2008) Doğu Akdeniz'de Uydu Altimetre Verileri ile Deniz Seviyesi Değişimlerinin Araştırılması. *Harita Dergisi*, 139: 1–31.

Smith W H F (2010) The Marine Geoid and Satellite Altimetry. *Oceanography from Space*, Barale V, Gower J and Alberotanza L (Eds.), Springer, Dordrecht, 181–193.

Sosson M, Kaymakci N, Stephenson R, Bergerat F and Starostenko V (2010) Sedimentary Basin Tectonics from the Black Sea and Caucasus to the Arabian Platform: Introduction. *Geological Society*, London, Special Publications, 340: 1–10.

Stammer D, Cazenave A, Ponte R M and Tamisiea M E (2013) Causes for Contemporary Regional Sea Level Changes. *Annual Review of Marine Science*, 5: 21–46.

Stammer D and Cazenave A (Eds.) (2018) *Satellite Altimetry over Oceans and Land Surfaces*. Earth Observation of Global Changes, ISBN: 9781498743457, CRC Press, Taylor & Francis Group, Boca Raton, 644 pp.

Stanev E V, Le Traon P –Y and Peneva E L (2000) Sea Level Variations and Their Dependency on Meteorological and Hydrological Forcing: Analysis of Altimeter and Surface Data for the Black Sea. *Journal of Geophysical Research: Oceans*, 105 (C7): 17203–17216.

Stanev E V and Peneva E L (2002) Regional Response to Global Climatic Change: Black Sea Examples. *Global and Planetary Changes*, 32: 33–47.

Staneva J V, Stanev E V and Rachev N H (1995) Heat Balance Estimates Using Atmospheric Analysis Data: A Case Study for the Black Sea. *Journal of Geophysical Research Atmospheres*, 100 (C9): 18581–18596.

Steffen K, Thomas R H, Rignot E, Cogley J G, Dyurgerov M B, Raper S C B, Huybrechts P and Hanna E (2010) Cryospheric Contributions to Sea Level Rise and Variability. *Understanding Sea-Level Rise and Variability*, Church J A, Woodworth P, Aarup T and Wilson W S (Eds.), ISBN: 9781444334517, Wiley-Blackwell Publishing, London, UK, 177–225.

Sturges W and Douglas B C (2011) Wind Effects on Estimates of Sea Level Rise. *Journal of Geophysical Research: Oceans*, 116: C06008.

Tamisiea M E, Hughes C W, Williams S D and Bingley R M (2014) Sea Level: Measuring the Bounding Surfaces of the Ocean. *Philosophical Transactions of the Royal Society A: Mathematical, Physical and Engineering Sciences*, 372 (2025): 20130336.

Tapley B D and Kim M C (2001) Applications to Geodesy. *Satellite Altimetry and Earth Science: A Handbook of Techniques and Applications*, Fu L –L and Cazenave A (Eds.), International Geophysics Series, Volume 69, Academic Press, San Diego, 371–403.

Tapley B D, Watkins M M, Flechtner F, Reigber C, Bettadpur S, Rodell M, Sasgen I, Familietti J S, Landerer F W, Chambers D P, Reager J T, Gardner A S, Save H, Ivins E R, Swenson S C, Boening C, Dahle C, Wiese D N, Dobslaw H, Tamisiea M E and Velicogna I (2019) Contributions of GRACE to Understanding Climate Change. *Nature Climate Change*, 9: 358–369.

Tari E, Sahin M, Barka A, Reilinger R, King R W, McClusky S and Prilepin M (2000) Active Tectonics of the Black Sea with GPS. *Earth Planets Space*, 52: 747–751.

Toderascu R and Rusu E (2013) Evaluation of the Circulation Patterns in the Black Sea Using Remotely Sensed and in Situ Measurements. *International Journal of Geosciences*, 4 (7): 1009–1017.

Todorova N, Alyomov S V, Chiotoroiu B C, Fach B, Osadchaya T S, Rangelov M, Salihoglu B and Vasilev V (2018) Black Sea. *World Seas: An Environmental Evaluation, Volume 1: Europe, The Americas and West Africa*, Sheppard C (Ed.), Second Edition, Academic Press, Elsevier, 209-226.

Tol R S J, Klein R J T and Nicholls R J (2008) Towards Successful Adaptation to Sea Level Rise along Europe's Coasts. *Journal of Coastal Research*, 24 (2): 432–442.

Tregoning P and van Dam T (2005) Atmospheric Pressure Loading Corrections Applied to GPS Data at the Observation Level. *Geophysical Research Letters*, 32: L22310.

Tsimplis M N and Baker T F (2000) Sea level drop in the Mediterranean Sea: An indicator of deep water salinity and temperature changes?. *Geophysical Research Letters*, 27 (12), 1731–1734.

Tsimplis M N, Josey S A, Rixen M and Stanev E V (2004) On the Forcing of Sea Level in the Black Sea. *Journal of Geophysical Research*, 109: C08015.

Tsimplis M N and Spencer N E (1997) Collection and Analysis of Monthly Mean Sea Level Data in the Mediterranean and Black Sea. *Journal of Coastal Research*, 13 (2): 534–544.

Tuzhilkin V S (2008a) Thermohaline structure of the Sea. *The Black Sea Environment. The Handbook of Environmental Chemistry*, Kostianoy A and Kosarev A (Eds.), Vol. 5, Part Q, Springer-Verlag, Berlin Heidelberg, 217–254.

Tuzhilkin V S (2008b) General Circulation. *The Black Sea Environment. The Handbook of Environmental Chemistry*, Kostianoy A and Kosarev A (Eds.), Vol. 5, Part Q, Springer-Verlag, Berlin Heidelberg, 159–194.

UNECE (2011) Drainage Basins of the Black Sea. *The Second Assessment of Transboundary Rivers, Lakes and Groundwaters*. United Nations Economic Commission for Europe, 165–252.

Ünlüata Ü, Oguz T, Latif M A and Özsoy E (1990) On the physical oceanography of the Turkish Straits. *The physical oceanography of Sea Straits*, Pratt L J (Ed.), Kluwer Academic Publishing, The Netherlands, 25–60.

Valladeau G, Thibaut P, Picard B, Poisson J C, Tran N, Picot N and Guillot A (2015) Using SARAL/AltiKa to Improve Ka-Band Altimeter Measurements for Coastal Zones, Hydrology and Ice: The PEACHI prototype. *Marine Geodesy*, 38 (sup1): 124–142.

Vergos S G (2002) Sea Surface Topography, Bathymetry and Marine Gravity Field Modelling. *Master Thesis*, University of Calgary, Department of Geomatics Engineering, Calgary, 303 pp.

Vespremeanu E and Golumbeanu M (2018) *The Black Sea. Physical, Environmental and Historical Perspectives*. 1st edition, Volume 69, ISBN: 978-3-319-70853-9, Springer International Publishing, Cham, Switzerland, 150 pp.

Vignudelli S (2016) Satellite Radar Altimetry Applied to Coastal Ocean Studies. *Journal of Marine Science: Research and Development*, 6 (4): 60.

Vignudelli S, Kostianoy A G, Cipollini P and Benveniste J (Eds.) (2011) *Coastal Altimetry*. ISBN: 978-3-642-12795-3, Springer Berlin Heidelberg, 566 pp.

Vignudelli S, Snaith H M, Lyard F, Cipollini P, Venuti F, Birol F, Bouffard J and Roblou L (2006) Satellite Radar Altimetry from Open Ocean to Coasts: Challenges and Perspectives. *Remote Sensing of the Marine Environment*, 6406: 64060L.

Vigo I, Garcia D and Chao B F (2005) Change of Sea Level Trend in the Mediterranean and Black Seas. *Journal of Marine Research*, 63: 1085–1100.

Volkov D L and Landerer F W (2015) Internal and External Forcing of Sea Level Variability in the Black Sea. *Climate Dynamics*, 45 (9–10): 2633–2646.

Wada Y, Reager J T, Chao B F, Wang J, Lo M H, Song C, Li Y and Gardner A S (2017) Recent Changes in Land Water Storage and Its Contribution to Sea Level Variations. *Surveys in Geophysics*, 38 (1): 131–152.

WCRP (2018) Global Sea-Level Budget 1993-Present. *Earth System Science Data*, 10: 1551–1590.

Wong P P, Losada I J, Gattuso J -P, Hinkel J, Khattabi A, McInnes K L, Saito Y and Sallenger A (2014) Coastal Systems and Low-Lying Areas. *Climate Change 2014: Impacts, Adaptation, and Vulnerability. Part A: Global and Sectoral Aspects. Contribution of Working Group II to the Fifth Assessment Report of the Intergovernmental Panel on Climate Change*, Field C B, Barros V R, Dokken D J, Mach K J, Mastrandrea M D, Bilir T E, Chatterjee M, Ebi K L, Estrada Y O, Genova R C, Girma B, Kissel E S, Levy A N, MacCracken S, Mastrandrea P R and White L L (Eds.), Cambridge University Press, Cambridge, United Kingdom and New York, NY, USA, 361–409.

Woodworth P L and Player R (2003) The Permanent Service for Mean Sea Level: An Update to the 21st Century. *Journal of Coastal Research*, 19 (2): 287–295.

Woolf D and Tsimplis M (2002) The Influence of the North Atlantic Oscillation on Sea Level in the Mediterranean and the Black Sea Derived from Satellite Altimetry. *The Second International Conference on Oceanography of the Eastern Mediterranean and Black Sea: Similarities and Differences of Two Interconnected Basins*, 14–18 October, Ankara, Turkey, 145–150.

Wöppelmann G and Marcos M (2012) Coastal Sea Level Rise in Southern Europe and the Nonclimate Contribution of Vertical Land Motion. *Journal of Geophysical Research*, 117: C01007.

Wöppelmann G and Marcos M (2016) Vertical Land Motion as a Key to Understanding Sea Level Change and Variability. *Reviews of Geophysics*, 54: 64–92.

Wunsch C and Stammer D (1997) Atmospheric Loading and the Oceanic "Inverted Barometer" Effect. *Reviews Geophysics*, 35: 79–107.

Yakushev E V, Chasovnikov V K, Murray J W, Pakhomova S V, Podymov O I and Stunzhas P A (2008) Vertical Hydrochemical Structure of the Black Sea. *The Black Sea Environment. The Handbook of Environmental Chemistry*, Kostianoy A and Kosarev A (Eds.), Vol. 5, Part Q, Springer-Verlag, Berlin Heidelberg, 277–307.

Yildiz H, Andersen O B, Kilicoglu, A, Simav M and Lenk O (2008) Sea Level Variations in the Black Sea for 1993–2007 Period from GRACE, Altimetry and Tide-gauge Data. *EGU General Assembly 2008*, 13–18 April, Vienna, Austria.

REFERENCES (continued)

Yildiz H, Andersen O B, Simav M, Aktug B and Ozdemir S (2013) Estimates of Vertical Land Motion along the Southwestern Coasts of Turkey from Coastal Altimetry and Tide-gauge Data. *Advances in Space Research*, 51: 1572–1580.

Yildiz H, Andersen O B, Simav M, Kilicoglu A and Lenk O (2011) Black Sea Annual and Inter Annual Water Mass Variations from Space. *Journal of Geodesy*, 85 (2): 119–127.

Yıldız H, Demir C, Gürdal M A, Akabalı O A, Demirkol E Ö, Ayhan M E ve Türkoğlu Y (2003) Antalya-II, Bodrum-II, Erdek ve Menteş Mareograf İstasyonlarına ait 1984-2002 Yılları Arası Deniz Seviyesi ve Jeodezik Ölçülerin Değerlendirilmesi, *Harita Dergisi*, Özel Sayı 17: 75 s.

Yıldız H ve Deniz R (2006) Mareograf ve Sabit GPS ile Uzun Dönemli Mutlak Deniz Seviyesi Değişimleri. *İtüdergisi/d mühendislik*, 5 (3): 115–125.

Zonenshain L P and Pichon X (1986) Deep basins of the Black Sea and Caspian Sea as remnants of Mesozoic back-arc basins. *Tectonophysics*, 123 (1–4): 181–211.

URL-1 <https://climate.nasa.gov/causes/>, Last Visit: 09.02.2019.

URL-2 <https://www.aviso.altimetry.fr/en>, Last Visit: 25.04.2019.

URL-3 <https://en.wikipedia.org/wiki >, Last Visit: 27.02.2019.

URL-4 <http://www.blacksea-commission.org/_geography.asp>, Last Visit: 14.02.2019.

URL-5 <http://www.blackseascene.net/content/content.asp?menu=0040032_000000>, Last Visit: 14.02.2019.

URL-6 <http://blacksea-education.ru/blacksea.shtml>, Last Visit: 04.03.2019.

URL-7 <http://data.unep-wcmc.org/datasets/41>, Last Visit: 09.03.2019.

URL-8 < https://www.gebco.net>, Last Visit: 16.05.2019.

URL-9 <https://kadirhoca.com/konu-anlatimlari/istanbul-bogazinda-gorulen-alt-dip-ve-ust-yuzey-akintilarin-nedenleri-nelerdir/>, Last Visit: 21.02.2019.

URL-10 <web.worldbank.org>, Last Visit: 23.02.2019.

URL-11 <https://www.noaa.gov/education/resource-collections>, Last Visit: 03.04.2019.

URL-12 <http://www.iasonnet.gr/abstracts/korotaev.html>, Last Visit: 28.02.2019.

URL-13 <https://gro-intelligence.com/insights/black-sea-agricultural-trade-gaining-ground>, Last Visit: 08.03.2019.

URL-14 <https://www.e-education.psu.edu/earth107/node/823>, Last Visit: 14.03.2019.

REFERENCES (continued)

URL-15 <https://www.csiro.au>, Last Visit: 01.06.2019.

URL-16 <https://tudes.harita.gov.tr/tudesportal/AnaEkranEN.aspx>, Last Visit: 13.04.2019.

URL-17 <https://www.gloss-sealevel.org/>, Last Visit: 14.04.2019.

URL-18 <http://eurogoos.eu/>, Last Visit: 14.04.2019.

URL-19 <http://www.psmsl.org/>, Last Visit: 14.04.2019.

URL-20 <http://www.ioc-sealevelmonitoring.org/index.php>, Last Visit: 14.04.2019.

URL-21 <https://uhslc.soest.hawaii.edu/>, Last Visit: 14.04.2019.

URL-22 <https://cnes.fr/en/how-altimetry-works>, Last Visit: 25.04.2019.

URL-23 <https://www.star.nesdis.noaa.gov/socd/lsa/>, Last Visit: 26.05.2019.

URL-24 <http://www.radartutorial.eu/20.airborne/ab12.en.html>, Last Visit: 28.05.2019.

URL-25 <https://duacs.cls.fr/>, Last Visit: 27.04.2019.

URL-26 <https://www.esa.int/spaceinimages/Images/2013/10/Measuring_ocean_currents>, Last Visit: 18.05.2019.

URL-27 <http://marine.copernicus.eu/>, Last Visit: 27.04.2019.

URL-28 <http://rads.tudelft.nl/rads/rads.shtml>, Last Visit: 26.05.2019.

URL-29 <https://openadb.dgfi.tum.de/en/>, Last Visit: 26.05.2019.

URL-30 <https://sealevel.nasa.gov/understanding-sea-level/key-indicators/global-mean-sea-level/>, Last Visit: 26.05.2019.

URL-31 <http://www.esa-sealevel-cci.org/products>, Last Visit: 26.05.2019.

URL-32 <http://sealevel.colorado.edu/>, Last Visit: 26.05.2019.

URL-33 <http://www.cmar.csiro.au/>, Last Visit: 26.05.2019.

URL-34 <http://www.storm-surge.info/coastal-altimetry>, Last Visit: 30.05.2019.

URL-35 <http://www.coastalt.eu/>, Last Visit: 30.05.2019.

URL-36 <http://ctoh.legos.obs-mip.fr/data/coastal-products>, Last Visit: 30.05.2019.

URL-37 <https://oceanexplorer.noaa.gov/facts/unexplored.html>, Last Visit: 04.06.2019.

URL-38 <http://oceanmotion.org/>, Last Visit: 04.06.2019.

REFERENCES (continued)

URL-39 <http://app01.saeon.ac.za/sadcofunstuff/MarineInstrumentation.htm>, Last Visit: 02.06.2019.

URL-40 <https://www.geomar.de/en/research/fb1/fb1-po/observing-systems/>, Last Visit: 02.06.2019.

URL-41 <http://www.argo.ucsd.edu/>, Last Visit: 01.06.2019.

URL-42 <http://www.goosocean.org/>, Last Visit: 01.06.2019.

URL-43 <https://www.aoml.noaa.gov/phod/gdp/>, Last Visit: 02.06.2019.

URL-44 <https://www.ferrybox.org/>, Last Visit: 03.06.2019.

URL-45 <http://www.jcommops.org/board>, Last Visit: 04.06.2019.

URL-46 <https://www.whoi.edu/virtual/oceansites/>, Last Visit: 04.06.2019.

URL-47 <https://www.iode.org/>, Last Visit: 04.06.2019.

URL-48 <https://www.euro-argo.eu/>, Last Visit: 04.06.2019.

URL-49 <https://www.ncei.noaa.gov/>, Last Visit: 05.06.2019.

URL-50 <https://www.ospo.noaa.gov/Products/ocean/index.html>, Last Visit: 04.06.2019.

URL-51 <https://earthdata.nasa.gov>, Last Visit: 04.06.2019.

URL-52 <https://www.jpl.nasa.gov/>, Last Visit: 06.06.2019.

URL-53 <https://www.iha.com.tr/>, Last Visit: 09.06.2019.

URL-54 <http://www2.csr.utexas.edu/grace/RL05_mascons.html>, Last visit: 16.06.2019.

URL-55 <https://www.harita.gov.tr/english/u-13-turkish-national-permanent-rtk-network--tnpgn-active--and-determination-of-the-datum-transformations-parameters.html>, Last visit: 16.06.2019.

URL-56 <http://geodesy.unr.edu/>, Last visit: 19.06.2019.

URL-57 <http://www.igs.org/network>, Last visit: 19.06.2019.

URL-58 <http://www.epncb.oma.be/>, Last visit: 19.06.2019.

BIBLIOGRAPHY

Bondar C (1989) Trends in the Evolution of the Mean Black Sea Level. *Meteorology and Hydrology*, 19 (2): 23–28.

Goryachkin Y N and Ivanov V A (2006) *Black Sea Level: The Past, Present and Future*. MHI NANU, Sevastopol, 210 pp (in Russian).

Sorokin Y I (2002) *The Black Sea: Ecology and Oceanography*. ISBN: 9789057821059, Backhuys Publishers, Amsterdam, 875 pp.

Terziev F S (Ed.) (1991) *Hydrometeorology and Hydrochemistry of the USSR Seas*. Project: Seas of the USSR, Volume IV: The Black Sea, Issue 1: Hydrometeorological conditions, Gidrometeoizdat, St. Petersburg (in Russian).

CURRICULUM VITAE

Nevin Betul Avsar was born in Samsun. She completed her primary education in Eskişehir, and middle and high school in Çankırı. She graduated from the Department of Geodesy and Photogrammetry Engineering (2001), and Department of Mathematics Engineering (2004) of Yıldız Technical University. Afterwards, she worked in the Cybersoft Information Technologies, and Turkish Chamber of Shipping, Karadeniz Ereğli Branch between the years 2004 and 2007, respectively. And then, she became Research Assistant at the Department of Geomatics Engineering in Selcuk University in 2008, and she has received her master's degree at this department in 2009. She started the PhD education in September 2012 at Geomatics Engineering Department of Zonguldak Bülent Ecevit University. Currently, she is working as Research Assistant at this department.

PUBLICATIONS FROM THE THESIS:

Avsar N B, Erol B and Kutoglu H (2014) Investigation of the Sea Level Rise and Its Impacts on the Coastal Areas for Black Sea, *XXIV International Symposium: Modern Technologies, Education and Professional Practice in Geodesy and Related Fields*, 6–7 November 2014, Sofia, Bulgaria.

Avsar N B, Kutoglu H, Erol B and Jin S (2015a) Coastal Risk Analysis of the Black Sea under the Sea Level Rise, *FIG Working Week 2015*, 17–21 May 2015, Sofia, Bulgaria.

Avsar N B, Kutoglu H, Erol B and Jin S (2015b) Sea Level Changes in the Black Sea Using Satellite Altimetry and Tide-gauge Observations, *26th IUGG General Assembly*, 22 June–2 July 2015, Prague, Czechia.

Avsar N B, Kutoglu H, Jin S and Erol B (2015) Investigation of Sea Level Change along the Black Sea Coast from Tide-gauge and Satellite Altimetry, *3rd International Conference on Sensors and Models in Photogrammetry and Remote Sensing (SMPR 2015)*, 23–25 November 2015, Kish Island, Iran, 67–71.

Avsar N B, Jin S, Kutoglu H and Gurbuz G (2016a) Sea Level Change along the Black Sea Coast from Satellite Altimetry, Tide-gauge and GPS Observations. *Geodesy and Geodynamics*, 7 (1): 50–55.

Avsar N B, Jin S, Kutoglu H and Gurbuz G (2016b) Vertical Land Motion along the Black Sea Coast from Tide-gauge, Satellite Altimetry and GPS, *IAG/CPGPS Joint 1st International Conference on GNSS+ (ICG+2016)*, 27–30 July 2016, Shanghai, China.

Avsar N B, Atalay C and Kutoglu S H (2017a) Analysis of Sea Level Rise along the Black Sea Coast Using Open Source GIS, *International Symposium on GIS Applications in Geography and Geosciences (ISGGG 2017)*, 18–21 October 2017, Canakkale, Turkey.

Avsar N B, Jin S, Kutoglu S H and Gurbuz G (2017b) Vertical Land Motion along the Black Sea Coast from Satellite Altimetry, Tide-gauges and GPS. *Advances in Space Research*, 60 (12): 2871–2881.

Avşar N B ve Kutoğlu Ş H (2018a) Karadeniz'de Uzun Dönemli ve Mevsimsel Deniz Seviyesi Değişimleri, *Türkiye Ulusal Jeodezi ve Jeofizik Birliği Bilimsel Kongresi (TUJJB-BK)*, 30 Mayıs–2 Haziran 2018, İzmir, Türkiye, 365–368.

Avsar N B and Kutoglu S H (2018b) An Evaluation of Present-Day Sea Level Change by Considering of Steric and Mass Components, *ESA 11th Coastal Altimetry Workshop*, 12–15 June 2018, Frascati (Roma), Italy.

Avsar N B, Jin S and Kutoglu S H (2018a) Recent Sea Level Changes in the Black Sea from Satellite Gravity and Altimeter Measurements, *Geoinformation for Disaster Management (Gi4DM 2018)*, 18–21 March 2018, Istanbul, Turkey, 83–85.

Avsar N B, Jin S and Kutoglu S H (2018b) Interannual Variations of Sea Surface Temperature in the Black Sea, *IGARSS 2018 - 2018 IEEE International Geoscience and Remote Sensing Symposium*, 22–27 July 2018, Valencia, Spain, 5617–5620.

Avsar N B, Gurbuz G and Kutoglu S H (2018) Vertical Movement Estimates along the Black Sea Coast from GPS and Satellite Altimetry-Tide-gauge, *19th General Assembly of WEGENER*, 10–13 September 2018, Grenoble, France.

Kutoglu S H, Avsar N B and Gurbuz G (2018) Sea Level Rise in the Black Sea and Its Manifestation in Coastal Erosion along the Karasu Coast, *ERA.Net RUS Plus Initiative, BS STEMA – Changes in Storminess and Coastal Erosion Induced by Climate Variability along the Black Sea Coast: Management and Adaptation Workshop*, 14 August 2018, Istanbul, Turkey.

ADDRESS:

Address: Zonguldak Bülent Ecevit University, Faculty of Engineering, Department of Geomatics Engineering, Incivez, 67100, Zonguldak/TURKEY.

Phone: (+90) 372 291 25 78

E-mail: nb_avsar@beun.edu.tr